Nitrogen turnover and N_2O emissions as a function of edaphic and hydrological conditions in subtropical forests of South China

Nitrogen-omsetning og N_2O-utslipp som en funksjon av edafiske og hydrologiske forhold i subtropiske skoger i Sør-Kina

Philosophiae Doctor (PhD) Thesis

Longfei Yu

Department of Environmental Sciences
Faculty of Environmental Science and Technology
Norwegian University of Life Sciences

Ås 2016

Thesis number 2016:81
ISSN 1894-6402
ISBN 978-82-575-1397-9

Ph.D. Supervisors

Prof. Jan Mulder (Main supervisor)
Dept. of Environmental Sciences
Norwegian University of Life Sciences
P.O. Box 5003, N-1432 Ås, Norway
jan.mulder@nmbu.no

Senior Researcher Dr. Peter Dörsch (co-supervisor)
Dept. of Environmental Sciences
Norwegian University of Life Sciences
P.O. Box 5003, N-1432 Ås, Norway
peter.doersch@nmbu.no

Prof. Zhang Xiaoshan (co-supervisor)
Research Center for Eco-Environmental Sciences
Chinese Academy of Sciences
No. 18, Shuangqing Road, 100085 Beijing, China
zhangxsh@rcees.ac.cn

Lecturer Dr. Zhu Jing (co-supervisor)
Department of Environment and Resources
Guangxi Normal University
No. 15, Yucai Road, 541004 Guilin, China
zhu0773@126.com

Thesis Evaluation Committee

Prof. Mo Jiangming (Opponent 1)
South China Botanical Garden
Chinese Academy of Sciences
Xingke Road 723, 510650 Guangzhou, P.R. China
mojm@scib.ac.cn

Senior Researcher PD Dr. Reinhard Well (Opponent 2)
Hanne Schmidt-Przebierala Institute of Climate-Smart Agriculture
Bundesallee 50, 38116 Braunschweig, Germany
reinhard.well@thuenen.de

Assoc. Prof. Line Tau Strand (Coordinator)
Dept. Environmental Sciences
Norwegian University of Life Sciences
P.O. Box 5003, N-1432 Ås, Norway
line.strand@nmbu.no

Table of Contents

Papers I-V (Individual page numbers)

Acknowledgements

This PhD thesis is submitted to the Department of Environmental Sciences, Norwegian University of Life Sciences (NMBU). I gratefully acknowledge funding from the China Scholarship Council (CSC) for my PhD studies in Norway during 2012-2016.

First and foremost I want to express my deeply-felt thanks to my main supervisor, Prof. Jan Mulder, for his valuable guidance, scholarly inputs and consistent supports. It has been a great honor to accomplish a doctoral thesis with him. Jan taught me how to "fish" but did not give me the "fish" itself, guided me to be wise but not bragging, and influenced me not only in academia, but also in life. Through all the years, Jan has become more like a father than a mentor to me. Secondly, I wish to express my sincere gratitude to my co-supervisor Dr. Peter Dörsch. He offered close guidance and great support to me during lab experiments, fieldwork and paper writing. Without his tremendous help, I could never have managed to turn the IRMS into my "new toy" for the PhD study. It's been really educational and fruitful to sit with Peter on all those late evenings, sorting the messy data and revising my writing work. Whenever Peter said "now we are talking!", I knew that this meant a praise from him. Also, I would like to thank the other two co-supervisors, Dr. Zhu Jing and Prof. Zhang Xiaoshan, for their kind and unconditional support. Jing helped me a lot when I started my PhD in Norway. Her determined attitude with work and creativeness in research always inspired me. Xiaoshan was also my supervisor during my master study. Without his help and guidance, it would never have been possible for me to pursue a doctoral degree in Norway. His professional experience and knowledge helped me very much to identify my own research interest and to plan my career.

I would like to thank all my colleagues and friends at the NMBU Nitrogen group and the Soil Science Group. Your support for my research work and your company in everyday life made this PhD thesis possible, and made life through Norwegian winters colorful. I want to thank Prof. Lars Bakken, Prof. Åsa Frostegård and Dr. Peter Dörsch for culturing such a wonderful research environment in the Nitrogen group, thus expanding my knowledge of sciences to wider and deeper dimensions. I am very grateful to Lars Molstad and Trygve Fredriksen for all their technical help with lab experiments and instruments. I want to express my particular gratitude to my office-mate, Alfred Obia, with whom I discussed scientific topics and enjoyed after-work life. I want to thank Pawel Lycus for the countless nights with beer and sport channels on TV, which helped me to

recharge after exhaustion from work. I am also very grateful to Kang Ronghua, Dr. Shahid Nadeem, Dr. Vasileios Tzanakakis, Dr. Vegard Martinsen, Iva Zivanovic from the soil building, and Dr. Liu Binbin, Dr. Qu Zhi, Natalie Lim, Dr. Jan Reent Köster, Dr. Daniel Mania, Daniel Milligan, Dr. Linda Bergaust, Rannei Tjåland, Kedir Woliy Jillo from IKBM. Thank you for your encouragement and help during the last four years, as well as for the memorable time on parties and trips. In addition, I wish to thank Dr. Hanna Silvennoinen and Karl-Andreas Jensen for their tireless help and demonstrations on mass spectrometry. I am also very grateful to Anne-Grethe Kolnes for the IT support, to Mirian Wangen, Anja Nieuwenhuis, Anne-Elisabeth Munkeby and Christel Celine Nguyen for the help with financial and administrative issues, to Irene Dahl, Valentina Zivanovic and Oddny Gimmingsrud for the help with thousands of field samples.

I would like to thank other friends around Ås and Oslo, for their help and care. Thanks to the Chinese friends, Mao Hong, Dr. Zhang Zhibo, Dr. Lu Qiongxian, Wang Yanliang, Yuan Jing, Chi Hai, Duan Chuqing, Xue Yuhang, Gaohong, Xiao Jianfeng, Lin Wenjiao, Meng Yuqiong, Li Xiaoran, Fanqiong for the delicious Chinese food that relieved my homesickness, and for the comforts when I felt lonely and confused. Thanks to friends from all over the world, Armanda Roco, Anna Oleynik, Espen Steinseth Hamborg, Odd Henning Unhjem and all the lovely friends who live(d) at Langbakken 2.

I am also very grateful to all the people who supported me during the three summers of fieldwork in China. Thanks to Dr. Wang Zhangwei, Zhang Yi and Tang Xiong for the lab support at RCEES, to Prof. Duan Lei and Zhang Ting for their generous help in both the lab and field work, to Prof. Wang Yanhui for the help with experimental design and analyses. Thanks to Dr Wang Yihao, Wu Liping, Prof. Jianghong, Prof. Wang Bing, Prof. Qin Pufeng, Xiao Jingsong, Zou Mingquan for their kind help in my field samplings.

Lastly, I am deeply thankful to my beloved parents for their love, care and support. They may not be able to read one page of this book, but I know that they will be so proud of me. This is enough, and makes the last four years meaningful to me. Also, I would like to thank my girlfriend, Gou Yaqing, who supported me and encouraged me with her love throughout all these years.

September 2016

Longfei Yu

Summary

Forests in the Chinese subtropics receive large amounts of nitrogen (N) from the atmosphere, both as ammonium (NH_4^+) and nitrate (NO_3^-). Many of these forests are considered to be "N-saturated", i.e. are not able to take up all added N, but leach significant amounts of NO_3^- to waters or re-emit nitrogen to the atmosphere as gaseous N. The main part of this thesis describes experimental work conducted in the well-studied subtropical forest catchment, "TieShanPing" (TSP). TSP is situated in SW China, on a sandstone ridge close to Chongqing city and is covered by a low-productive, mixed evergreen forest. The forest receives up to 60 kg N ha^{-1} y^{-1} from atmospheric deposition, without showing any sign of improved forest growth. Surprisingly, previous catchment-scale studies at TSP and in other forests in South China, based on input-output budgets, found large apparent retention of atmogenic N in the forest ecosystems, without identifying the responsible mechanisms. This doctoral study focused on N-transformation processes in soils, in an attempt to understand the fate of deposited NH_4^+ and NO_3^- in more detail and to characterize the factors governing retention, removal and loss of reactive nitrogen. A better understanding of transformation, retention and re-emission of reactive N in semi-natural, forested ecosystems is important for regional N budgets, particularly since N deposition is expected to increase in China in the near future.

The turnover of N was studied along hydrological flow paths at TSP and in seven forested headwater catchments across China (**Paper II**), acknowledging that the hydrological connectivity between different landscape elements, such as hillslopes and riparian zones, is likely to play a key role for transformation, transport and removal of deposited N. To characterize N turnover patterns spatially and temporarily, I used natural isotopic signatures of NO_3^- (^{15}N and ^{18}O, **Paper I** and **II**). The analysis of ^{15}N and ^{18}O in NO_3^- was carried out by a modified "denitrifier method", which I helped to develop and implement (**Paper V**). Gross rates of N transformation in hillslope soils were determined by *in situ* ^{15}N tracing (**Paper III**). This experiment also served to explore the origin of N_2O emissions (**Paper III**), which have been reported to be exceptionally large in well-drained hillslope soils of the TSP forest (**Paper IV**). To evaluate whether phosphorous (P) addition could alleviate P limitation and curtail N_2O emissions by stimulating biological N uptake, I started an *in situ* P addition experiment and monitored soil chemistry and N_2O emissions for 1.5 years (**Paper IV**).

The N turnover in five subtropical (southern) and two temperate (northern) forest catchments, as inferred from natural abundance nitrate isotopic signatures (**Paper I** and **II**), revealed a consistent spatial pattern, emphasizing the importance of hydrological connectivity between well-drained oxidative zones and groundwater-influenced, reductive zones. ^{15}N tracing (**Paper III**) revealed that freshly added NH_4^+ is immobilized first into the soil organic N pool, before being released and converted to NO_3^- through nitrification. Experiments with ^{15}N labelled organic substrates (**Paper III**) confirmed that "heterotrophic" nitrification, a poorly constrained biological process, contributes to NH_4^+ oxidation in acid, subtropical soil. Once nitrified, the deposited NH_4^+ leaches as NO_3^- and is transported, together with the deposited NO_3^-, by "interflow" over argic (clay-enriched) B horizons in the commonly found Acrisols to ground water discharge zones situated in valley bottoms and on stream banks. My detailed study of natural abundance isotope signals of NO_3^- along this flow path (**Paper I**) convincingly demonstrated that the groundwater influenced soils are "hot spots" for N removal by microbial denitrification, thus explaining the "missing sink" for N in subtropical forest catchments. Appling the same technique to a range of Chinese forest catchments (**Paper II**), I found that this mechanism is of regional importance for monsoonal South China, but not for North China, where precipitation is too small to develop spatially continuous reductive landscape elements, which are hydrologically connected to oxidative environments upslope. Comparing apparent N-retention in the southern Chinese catchments with annual N deposition rates suggested that N removal in these subtropical catchments can be expected to increase with increasing N input.

Removal of reactive nitrogen by coupled nitrification-denitrification involves nitrous oxide (N_2O) emission. Emission measurements carried out in the context of a phosphorous (P) addition experiment on TSP hillslope soils (**Paper IV**) estimated N_2O emissions of up to 5.3 kg N ha^{-1} yr^{-1}. This is consistent with previous reports, showing that N_2O-N losses equal about 10% of the annually deposited N. This large proportion of N removed as N_2O, is likely a result of rapid microbial N turnover in warm and moist soils during monsoonal summers and the dominance of denitrification as N_2O producing process (**Paper III**). Addition of P caused a strong decrease (50%) in N_2O emission already 1.5 years after the treatment (**Paper IV**). This implies that P addition to the naturally P-limited soils of the Chinese subtropics could enhance biological N uptake and reduce N_2O emissions at the same time.

Overall, this thesis shows that acid, subtropical forest soils in South China support a complex nitrogen cycle that can mediate both net N release and retention, depending on scale and N form studied. While providing a mechanistic framework for the observed strong N attenuation by denitrification at the catchment scale, mitigation options for N_2O emissions remain to be explored.

Sammendrag

Skog i de kinesiske subtropene er utsatt for stor nitrogen (N) nedfall fra atmosfæren, både som ammonium (NH_4^+) og nitrat (NO_3^-). Flere av disse skogene ansees til å være «nitrogen-mettet», dvs. avsatt N blir ikke tatt opp men renner av som NO_3^- til vann eller re-emitteres som N-gas til luft. Hovedparten av denne oppgaven beskriver det eksperimentelle arbeidet jeg har gjennomført i det godt undersøkt subtropisk nedbørsfelt "TieShanPing" (TSP). TSP ligger i sørvest Kina, på en fjellrygg i nærheten av byen Chongqing og har en blandet, eviggrønn skog som er lite produktiv. Nedfall av nitrogen fra atmosfæren er opp til 60 kg N ha^{-1} $år^{-1}$, uten at det har noe synlig effekt på skogens produktivitet. Tidligere studier i TSP og lignende sørkinesiske skog som baserte seg utelukkende på elementbudsjetter, fant at skogen holder igjen overaskende store mengder N, men klarte ikke å identifisere de underliggende mekanismene. Den foreliggende oppgaven setter fokus på omsetting av N i skogsjord for å bedre forstå denne «N-retensjonen» i subtropisk skog. Kunnskap om prosessene og faktorene som bestemmer N-retensjonen og N tap er viktig, for å kunne si noe om skjebnen til de store mengdene avsatt NH_4^+ and NO_3^- på et regional skala. Nedfall av reaktiv nitrogen i kinesiske skog forventes til å øke i nær fremtid, og det trengs mer kunnskap om hvordan N omsettinger i disse skog påvirker regionale N budsjetter.

Jeg undersøkte N omsettinger langs avrenningsveier i nedbørfelt til syv ulike skoger i Kina (**Artikkel II**). De utvalgte felt viste en mer eller mindre utpreget hydrologisk kobling mellom skråning og en grunnvannsinfluert sone ved foten av bakken eller ved elvebredden. De feltene ble valgt slik, fordi koblingen mellom skråning og grunnvannsinfluert sone antas å være nøkkelen til forståelsen av hvordan nitrogen blir omsatt, transportert, fjernet eller holdt tilbake i skogsøkosystemet. Jeg karakteriserte N omsettinger i rom og tid på grunnlag av naturlige variasjoner i forekomsten av de stabile isotopene ^{18}O og ^{15}N i NO_3^- (**Artikkel I** og **II**). For å kunne analysere store mengder prøver med god nøyaktighet, ble det brukt en metode som baserer seg på å omdanne NO_3^- til lystgass (N_2O) gjennom denitrifikasjon. Denne metoden ble modifisert og videreutviklet, noe jeg bidro til (**Artikkel V**). Bruttoratene til N omsettingsprosesser på skråningene ble direkte bestemt i felt ved hjelp av ^{15}N markeringsforsøk (**Artikkel III**). Disse forsøk ble også brukt til å utforske opphavet til lystgass utslipp, som har vist seg å være usedvanlig stort i de godt drenerte skråningene til TSP skogen (**Artikkel III**). For å teste om fosfor (P) tilsetning til utarmet subtropisk jord kunne redusere N_2O utslipp ved

å stimulere N opptak i planter og mikroorganismer, startet jeg et feltforsøk og registrerte forandringer i jordkjemi og N_2O utslipp over halvannet år (**Artikkel IV**).

Nitrogen omsetningene langs hydrologiske avrenningsveier i fem subtropiske (sørlige) skogsfelt og to tempererte (nordlige) felt (**Artikkel I** og **II**) viste et konsistent mønster. Dette bekreftet at kobling mellom oksidative soner i skråningen og reduserende soner ved utløpet eller elvebredden er sentral for N retensjonen. Markeringsforsøk med ^{15}N (**Artikkel III**) avslørte at ferskt tilført NH_4^+ blir først immobilisert i jordens organiske N lager, før den frigjøres og omdannes til NO_3^- gjennom nitrifikasjon. Eksperimenter med ^{15}N markert organisk substrat (**Artikkel III**) bekreftet at "heterotrof nitrifikasjon", en lite forstått biologisk prosess, bidrar vesentlig til NH_4^+ oksidasjon i sur, subtropisk jord. Dette betyr at NH_4^+ fra nedfallet blir nesten kvantitativt oksidert og renner, sammen med avsatt NO_3^-, over et nokså tett leiresjikt ned til grunnvannsinfluerte soner. Slike leiresjikt ar ganske utbredt i subtropisk jord. Mine detaljerte studier av naturlige isotopsignaler i NO_3^- langs slike avrenningsveier (**Artikkel I**) demonstrerte overbevisende at grunnvannsinfluerte soner er "hot spots" for biologisk fjerning av N gjennom denitrifikasjon i det subtropiske skoglandskapet og forklarer således det manglende sluket i N budsjettet til subtropiske skog med høy N nedfall fra atmosfæren. Ved å bruke samme teknikken i en rekke av kinesiske skogsfelt (**Artikkel II**), fant jeg at dette er tilfellet for alle skog påvirket av monsun, men ikke for skog i det nordlige Kina, hvor nedbør er for liten for å skape en hydrologisk forbindelse mellom de ulike landskapselementene. En sammenligning mellom den tilsynelatende N retensjonen og N deposisjonen blant de fem sørlige nedbørsfelt antydet at subtropisk skog tilbakeholder mer N med økende atmosfærisk nedfall. Dermed har mine funn regional betydning for Sør-Kina.

Fjerning av nitrogen gjennom kombinert nitrifikasjon og denitrifikasjon innebærer lystgassutslipp. Anslag av gjennomsnittlig N_2O utslipp fra naturlig jord, basert på mine utslippsmålinger i P eksperimentet på TSP skråningen (**Artikkel IV**), var 5.3 kg N ha^{-1} $år^{-1}$. Slike høye utslippsrater stemmer overens med tidligere observasjoner som fant at N_2O-N tap kan utgjøre opp til 10% av N i nedfallet i TSP. Store N_2O utslipp er med all sannsynlighet resultat av de raske mikrobielle N omsettinger og dominansen av denitrifikasjon blant de N_2O dannende prosessene i et varmt-fuktig subtropisk klima (**Artikkel III**). Tilsetting av P resulterte i en sterk (50%) nedgang av N_2O emisjoner allerede halvannet år etter tiltaket (**Artikkel IV**). Dette medfører at P tilsetting til naturlig

P-utarmet skogsjord i de kinesiske subtropene kunne være en metode til å øke biologisk opptak av N og dermed redusere N_2O utslipp.

Denne oppgaven viser at sur, subtropisk skogsjord i Sør-Kina støtter en kompleks nitrogensyklus, som kan både holde tilbake og frigjøre mineralsk N, avhengig av nitrogenspesies og tidsskalaen den blir studert på. Mine studier tilfører innsikt i de viktigste jordprosessene knyttet til N retensjon og fjerning på skogsfeltskala. Reduksjon av lystgassutslipp fra disse økosystemene forblir viktig for fremtidens forskningsagenda.

List of Papers

Paper I

Longfei Yu, Jing Zhu, Jan Mulder, Peter Dörsch. Multiyear dual nitrate isotope signatures suggest that N-saturated subtropical forested catchments can act as robust N sinks. *Global Change Biology* 2016, doi: 10.1111/gcb.13333.

Paper II

Longfei Yu, Jan Mulder, Jing Zhu, Xiaoshan Zhang, Zhangwei Wang, Peter Dörsch. Denitrification as a major nitrogen sink in forested monsoonal headwater catchments in the sub-tropics: evidence from multi-site dual nitrate isotopes. (Under review in *Environmental Science & Technology*)

Paper III

Longfei Yu, Ronghua Kang, Jing Zhu, Jan Mulder, Peter, Dörsch. Distinct fates of atmogenic NH_4^+ and NO_3^- in subtropical, N-saturated forest soils. (Under review in *Ecology*)

Paper IV

Longfei Yu, Yihao Wang, Xiaoshan Zhang, Peter Dörsch, Jan Mulder. Phosphorus addition mitigates N_2O and CH_4 emissions in N-saturated subtropical forest, SW China. (Manuscript to be submitted to *Biogeosciences*)

Paper V

Jing Zhu, **Longfei Yu**, Lars R. Bakken, Pål Tore Mørkved, Jan Mulder, Peter Dörsch. Controlled induction of denitrification in *Pseudomonas aureofaciens*: a simplified denitrifier method for dual isotope analysis in NO_3^-. (Manuscript)

1. Introduction

Exponential growth of the human population since the 1960s has accelerated the global nitrogen (N) cycle, primarily through N-fixation for food and use of fossil energy (Vitousek *et al.*, 1997; Galloway *et al.*, 2008). Anthropogenic activities have doubled global reactive N (N_r) input, estimated at 420 Tg N yr^{-1}, and this input is likely to increase during the next decades (Galloway *et al.*, 2003; Bodirsky *et al.*, 2014). N_r is essential for life and is re-distributed between ecosystems mainly via atmospheric transport and deposition (Gruber & Galloway, 2008; Fowler *et al.*, 2013). Globally, N input to terrestrial systems, mainly in the form of ammonium (NH_4^+) and nitrate (NO_3^-), has quadrupled from pre-industrial periods to the present (Galloway *et al.*, 2004; Dentener *et al.*, 2006; Bala *et al.*, 2013). Within recent decades, East Asia has become regional hotspots for N pollution, experiencing N deposition rates of up to 80 kg N ha^{-1} yr^{-1} (Xu *et al.*, 2015; Duan *et al.*, 2016).

Emissions of N_r in China have boosted since the 1960s (Cui *et al.*, 2013; Liu *et al.*, 2013), resulting in an average nationwide N deposition rate of 40 kg N ha^{-1} yr^{-1} (Fig. 1.1; Shi *et al.*, 2015; Xu *et al.*, 2015). In subtropical forests of South China, reported inorganic N fluxes in throughfall range from 25 to 70 kg N ha^{-1} yr^{-1} (Chen & Mulder, 2007a; Fang *et al.*, 2008; Huang *et al.*, 2015; Du *et al.*, 2016), far exceeding the threshold of 25 kg N ha^{-1} yr^{-1} for N leaching in temperate forests (Dise & Wright, 1995).

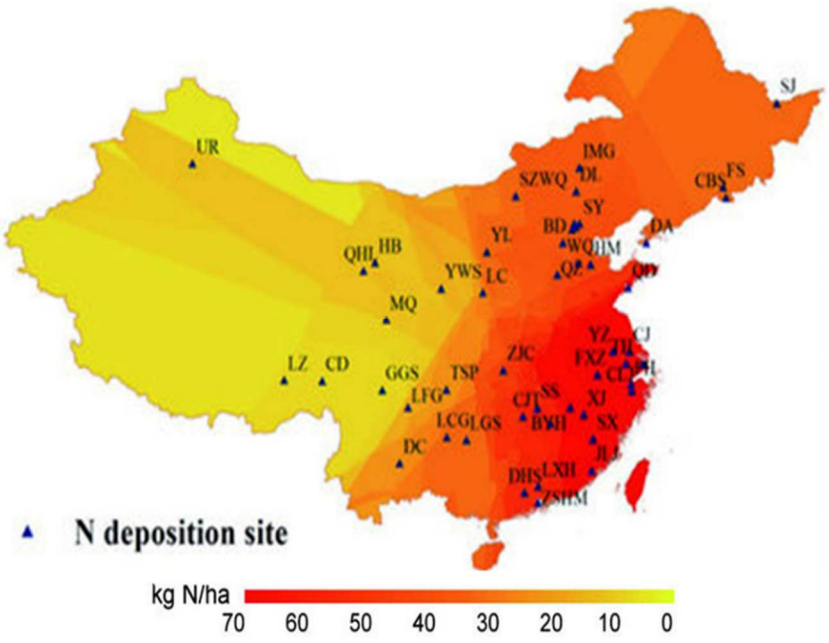

Fig. 1.1 Spatial map of modeled total N deposition rates in China. Sum of wet and dry deposition. Figure from Shi *et al.* (2015).

Elevated N deposition has a number of negative impacts on the terrestrial environment (Vitousek *et al.*, 1997), including reduction in soil fertility due to nutrient leaching (Aber *et al.*, 1989), soil acidification (Zhao *et al.*, 2009; Zhu *et al.*, 2016), eutrophication of aquatic systems (Jaworski *et al.*, 1997) and loss of plant diversity (Clark & Tilman, 2008; Bobbink *et al.*, 2010). In addition, human health is at stake, through pollutions of air and drinking water (Townsend *et al.*, 2003).

Greenhouse gases, such as carbon dioxide (CO_2), methane (CH_4), and nitrous oxide (N_2O), play a key role in global warming (Ciais *et al.*, 2013). However, the impact of rising N pollution on climate change remains under debate. On the positive side, increased N availability enhances growth of plants and thus promotes carbon (C) sequestration, especially in temperate and boreal, N-limited ecosystems (Reay *et al.*, 2008; Butterbach-Bahl *et al.*, 2011). On the other hand, enhanced biogenic N_2O and CH_4 emissions due to increased N deposition may offset the cooling effect of C sequestration, due to N fertilization (Schulze *et al.*, 2009; Tian *et al.*, 2016).

1.1 Efficient transformation of atmogenic N in acid soils of subtropical forests

Unlike temperate forests in Europe (Gundersen *et al.*, 1998a), subtropical Chinese forests generally occur on old, highly-weathered soils (e.g. Acrisols; WRB 2014), characterized by phosphorus (P) deficiency (Liu *et al.*, 2012). Loss of base cations from the soils has been accelerated by extensive NO_3^- leaching (Larssen, 2004), resulting in increased acidification (Seip *et al.*, 1999; Larssen & Carmichael, 2000). Together, acidity and P limitation have resulted in declining forest growth, and thus reduced N uptake by standing biomass (Wang *et al.*, 2007).

Despite the fast growth of NO_x emission in China (Liu *et al.*, 2013), NH_4^+ still dominates (> 50%) the inorganic N deposition (Xu *et al.*, 2015). However, only small amounts of NH_4^+ are found in the soil water of subtropical forests (Chen *et al.*, 2004; Fang *et al.*, 2008). Incoming NH_4^+ seems to be quickly and quantitatively converted to NO_3^- (Larssen *et al.*, 2011). In a seven-year N fertilization experiment in the TieShanPing (TSP) forest (SW, China), Huang *et al.* (2015) found near-quantitative conversion of added NH_4^+ to NO_3^-, even at elevated rates of NH_4^+ input. The apparent efficient turnover of deposited NH_4^+ to NO_3^- and the associated small rate of NH_4^+ leaching suggest microbial

nitrification to be one of the key processes behind forest N loss. Nitrification is important to soil N leaching (Gundersen *et al.*, 1998b), as it transforms the immobile NH_4^+ to highly mobile NO_3^- (Sahrawat, 2008). The ability to nitrify is restricted to small, specialized groups of bacteria, archaea and fungi, of which the latter two seem to be more important in acid soils (Teske *et al.*, 1994; Leininger *et al.*, 2006; Gubry-Rangin *et al.*, 2011). Nitrification activity depends on a number of factors, such as pH, oxygen (O_2) and NH_4^+ availability (Sahrawat, 2008). For instance, enhanced N input has been found to stimulate nitrification rates in a range of soils (Corre *et al.*, 2010; Lu *et al.*, 2011), whereas excessive N addition decreased nitrification activity, likely due to acidification (Venterea *et al.*, 2004; Corre *et al.*, 2007).

Acid soils provide sub-optimal habitats for nitrifiers, since the actual substrate for nitrification, ammonia (NH_3), which is in chemical equilibrium with NH_4^+, is scarce (De Boer & Kowalchuk, 2001). Laboratory ^{15}N tracing studies in acid forest soils found that added NH_4^+ is not directly nitrified, but quickly assimilated into the soil organic N pool (Tahovsk *et al.*, 2013; Gao *et al.*, 2016), before eventually being nitrified. This points at a special role of the soil organic N pool for processing and transforming of deposited NH_4^+ in acid forest soils (Booth *et al.*, 2005; Lu *et al.*, 2011). Previous studies in forest soils of subtropical China reported gross mineralization and nitrification rates, comparable to those found in the tropics (Zhang *et al.*, 2013; Zhu *et al.*, 2013a). This means that atmogenic NH_4^+ may indeed undergo internal cycling in the soil before being recovered as NO_3^-. To explain the conundrum of efficient biological NH_4^+ conversion to NO_3^- in acid soils, "heterotrophic nitrification" (i.e. the co-oxidation of organic N to nitrite during heterotrophic microbial growth) has been invoked, based on circumstantial evidence from *ex situ* ^{15}N labelling studies with a range of subtropical forest soils from China (Zhang *et al.*, 2013; Chen *et al.*, 2015; Gao *et al.*, 2016).

1.2 Understanding denitrification as an N sink at the catchment scale

Subtropical forest soils in China leach significant amounts of N, predominately as NO_3^- (Chen & Mulder, 2007b; Fang *et al.*, 2008). Accordingly, these forests are considered to be 'N-saturated' (Chen & Mulder, 2007b; Koba *et al.*, 2012; Huang *et al.*, 2015). However, based on catchment-scale N fluxes, Larssen *et al.* (2011), while confirming strong NO_3^- leaching from upland hillslope soils, found that most of the

leached NO_3^- does not reach the streams. As forest growth is suppressed by soil acidification and P limitation, net N retention in standing biomass is small (Wang *et al.*, 2007; Huang *et al.*, 2015). Larssen *et al.* (2011) speculated whether NO_3^- is removed by denitrification in riparian soils. Later, Fang *et al.* (2015), studying isotopic signatures in NO_3^- in several tropical forests of China, estimated annual losses of 5.6 to 30.1 kg N ha^{-1} by denitrification, which is in the same order of magnitude as atmogenic N input. However, detailed studies into denitrification at the catchment scale are scarce, due to the lack of methods for direct observation (Groffman, 2012; Duncan *et al.*, 2013; Wexler *et al.*, 2014).

Denitrification is the dissimilatory reduction of NO_3^- to NO_2^-, NO, N_2O and ultimately to dinitrogen gas (N_2), primarily mediated by heterotrophic, facultatively anaerobic bacteria (Focht & Verstraete, 1977; Knowles, 1982). Soil denitrification contributes significantly to N_r dissipation on a global scale (Seitzinger *et al.*, 2006; Bouwman *et al.*, 2013). A range of soil factors, including oxygen (O_2) availability, respirable C, NO_3^- availability, pH and temperature, regulate denitrification activity and the stoichiometry of its gaseous products (Knowles, 1982; Weier *et al.*, 1993; Simek & Cooper, 2002; Zhu *et al.*, 2013b). Denitrification activity strongly depends on anoxia, making soil moisture the most influential factor. Therefore, soil moisture, or drainage status, is often used to identify denitrification hotspots at the landscape scale (Seitzinger *et al.*, 2006). For instance, groundwater-influenced soils of riparian zones show strong denitrification activities (Clément *et al.*, 2003; Billy *et al.*, 2010; Bouwman *et al.*, 2013). However, despite the importance of anoxia for denitrification, highest denitrification activities are not found in the permanently saturated zone below the groundwater table, but rather in the capillary fringe between saturated and unsaturated layers close to the (fluctuating) groundwater table (Duncan *et al.*, 2015; He *et al.*, 2016). Zhu *et al.* (2013a) studied N_2O emissions in a groundwater discharge zone, and summarized that the control of denitrification by the groundwater table likely reflects the tradeoff between decreasing availability of respirable C with depth and increasing anoxia for denitrification (Zhu *et al.*, 2013c), as long as NO_3^- availability is ample (Niu *et al.*, 2016).

If riparian zones are to act as N sink in forest catchments, this raises the question from where the substrate for denitrification (viz. NO_3^-) is derived. Stable isotope studies have shown that NO_3^- being denitrified in riparian soils is not directly from atmogenic deposition, but from soil processes (i.e. nitrification) (Curtis *et al.*, 2011; Rose *et al.*, 2014,

2015; Sabo *et al.*, 2015). Forested catchments can be operationally divided into three landscape elements: well-drained hillslope soils, near-stream or riparian soil environments and stream water, all of which are hydrologically connected (Jencso *et al.*, 2009; Likens, 2013). This means that mobile NO_3^- produced from aerated hillslope soils could be transported to water-saturated riparian soils if there exists a hydrological flow path connecting these elements (Duncan *et al.*, 2015; Griffiths *et al.*, 2016). However, when the system is N-limited, NO_3^- is strongly retained along the hydrological flow path, with little NO_3^- being transported to near-stream environments for denitrification (Rose *et al.*, 2014; Wexler *et al.*, 2014). In this case, N removal would be restricted to coupled nitrification-denitrification in the near-stream soils, which is controlled by seasonally or diurnally fluctuating groundwater tables (Duncan *et al.*, 2015).

Field observations of denitrification often show seasonal patterns, with large fluxes occurring during the warm and humid season (e.g. monsoonal summer in subtropics) (Tang *et al.*, 2006; Zhu *et al.*, 2013c; Morse *et al.*, 2014). During rainstorms, Rose *et al.* (2014) observed high proportions of atmogenic NO_3^- in stream export, suggesting that catchment NO_3^- attenuation also depends on water flow paths and water residence time. In addition, significant, transient denitrification may occur in aerated soils, e.g. in hillslope soils of subtropical forests in China, where Zhu *et al.* (2013c) observed large N_2O emissions from O/A horizons during monsoonal summers, in response to intensive summer rain. Denitrification in upland soils likely occurs in anoxic microsites (e.g. soil aggregates or occluded soil organic matter), which are common in heterogeneous soils (Parkin, 1987; Butterbach-Bahl *et al.*, 2013).

1.3 N_2O emissions from subtropical forests in China

Increased turnover of N in forest soils, triggered by atmogenic N deposition, involves production of N_2O (Ciais *et al.*, 2013), mainly through nitrification and denitrification (Firestone & Davidson, 1989). Among all factors that regulate the contribution of nitrification and denitrification to N_2O production, pH and water-filled pore space (WFPS) appear to be the most important (Bateman & Baggs, 2005; Mathieu *et al.*, 2006; Ju *et al.*, 2011; Cheng *et al.*, 2015). In general, denitrification dominates in near-saturated soils (WFPS > 70%) where it results in large N_2O emission fluxes, while nitrification is the major source for N_2O in unsaturated soils (WFPS < 70%) characterized by smaller

N_2O emission fluxes (Bateman & Baggs, 2005; Mathieu *et al.*, 2006). According to a literature review, N_2O production in low-pH soils tends to be dominated by denitrification (Cheng *et al.*, 2015). In accordance with this, in the acid forest soils of China, denitrification has been identified as the dominant source for N_2O emission (Zhang *et al.*, 2011a; Zhu *et al.*, 2013d).

Acid soils favor the production of N_2O rather than N_2 in denitrification by directly (Liu *et al.*, 2010, 2014) or indirectly (Dörsch *et al.*, 2012; Brenzinger *et al.*, 2015) affecting the enzymatic balance between production and reduction of N_2O. Another mechanism leading to a high proportion of N_2O among denitrification products are frequent shifts between anoxic and oxic conditions. Morley *et al.* (2008) found that fully induced denitrification in soil produces large amounts of N_2O when re-exposed to O_2. Thus, frequent soil moisture changes brought about by monsoonal rainstorms followed by rapid runoff on well-drained hillslopes may result in large N_2O emissions. Indeed, monsoonal-subtropical forests in China with high N deposition and acid soils have been reported to emit 2.0 to 5.4 kg N ha^{-1} of N_2O annually (Tang *et al.*, 2006; Fang *et al.*, 2009; Zhu *et al.*, 2013c), exceeding annual N_2O emission rates in tropical (Werner *et al.*, 2007), and temperate forests (Gundersen *et al.*, 2012). In the TSP forest in SW China, annual N_2O emission of 4.3 to 5.4 kg N ha^{-1} has been reported for well-drained upland soils, accounting for 8 to 10% of the inorganic N deposition (Zhu *et al.*, 2013c). Addition of N to subtropical forests further stimulates N_2O emission (Wang *et al.*, 2014; Chen *et al.*, 2016; Zheng *et al.*, 2016), indicating that these forests are regional hotspots for N_2O emission and will increasingly be so as atmogenic N deposition further rises.

1.4 CH_4 uptake in N-saturated forest soils

Forest ecosystems are commonly regarded as net sinks for atmospheric CH_4, thus contributing to the terrestrial CH_4 balance (Le Mer & Roger, 2010). The CH_4 emission/uptake from soil is determined by the net-effect of CH_4 production by methanogens and CH_4 oxidation by methanotrophs (Smith *et al.*, 2003). CH_4 production requires low redox conditions, which are common in waterlogged environments. CH_4 consumption from the atmosphere, in contrast, is restricted to upper soil layers, where it is controlled by O_2 and CH_4 diffusion from the atmosphere into the soil (Veldkamp *et al.*, 2013). Increased N deposition is believed to inhibit CH_4 uptake in forest soils (Hütsch,

1996; Veldkamp *et al.*, 2001), as NH_4^+ competes with CH_4 for the active site on the central enzyme, methane monooxygenase (Bodelier & Laanbroek, 2004; Zhang *et al.*, 2008a; Veldkamp *et al.*, 2013). Reported CH_4 uptake rates in southern Chinese forests under high N deposition (20-50 kg N ha^{-1} yr^{-1}) are moderate (Tang *et al.*, 2006; Fang *et al.*, 2009; Zhang *et al.*, 2014a) and Zhang *et al.* (2008a) found that a gradual increase in N deposition resulted in a corresponding decrease of CH_4 uptake. Together, this suggests that N deposition to forests of South China may have severely reduced the CH_4 sink strength, probably even resulting in net CH_4 emissions from upland soils.

Addition of P to tropical forests has been found to promote uptake of atmospheric CH_4 in soil (Zhang *et al.*, 2011b, 2014a; Mori *et al.*, 2013b). However, there is ongoing debate on whether P availability affects soil CH_4 uptake directly by stimulating methanotrophic activity or indirectly through changing the soil N status (Veraart *et al.*, 2015). Firstly, since NH_4^+ may compete with CH_4 for the active site on the central enzyme, a reduction of NH_4^+ availability in soil is likely to alleviate N inhibition of CH_4 oxidation (Veldkamp *et al.*, 2001, 2013; Bodelier & Laanbroek, 2004; Zhang *et al.*, 2008a). Secondly, if P addition stimulates plant roots, evapotranspiration from the root zone will increase, resulting in better-aerated soils with more CH_4 diffusion into the soil (Zhang *et al.*, 2011b). A third possibility is that P directly affects CH_4 oxidation activity by stimulating gene transcription of methanotrophic enzymes (Veraart *et al.*, 2015).

1.5 Does P fertilization affect forest N cycling and N_2O emission?

Chronically elevated N deposition in South China and the associated soil acidification have resulted in declining forest growth, characterized by severe defoliation (Wang *et al.*, 2007), loss in biodiversity (Lu *et al.*, 2010) and decrease in plant biomass production (Huang *et al.*, 2015). In the Acrisols from South China, increasing N deposition has aggravated P limitation (Liu *et al.*, 2012; Du *et al.*, 2016). For instance, in the TSP forest in SW China, Huang *et al.* (2015) measured an average N/P ratio of 17 for tree needles, which exceeds the optimum range of 6 to 12 for forest growth (Wang *et al.*, 2007).

Large N_2O emissions have been reported from P-limited forest ecosystems in the tropics upon increasing N deposition experimentally (Hall & Matson, 1999; Zhang *et al.*, 2008b). The large N_2O emission was attributed to the generally small N retention capacity

of these forests. Several studies have specifically addressed the effect of P fertilization on N cycling, both in South China (Zhang *et al.*, 2014b; Chen *et al.*, 2016; Zheng *et al.*, 2016) and in South Ecuador (Martinson *et al.*, 2013; Müller *et al.*, 2015). In both forests, P alone had no significant effect on N_2O emission 1-2 years after addition, whereas N+P treatments showed reduced N_2O emission relative to N fertilization (Martinson *et al.*, 2013; Zheng *et al.*, 2016). However, in the longer term of 3-5 years, P addition significantly decreased N_2O emissions also in the P treatments (Müller *et al.*, 2015; Chen *et al.*, 2016). In both studies, N_2O emission decreased along with inorganic N concentrations in soil, which was attributed to enhanced plant N uptake (Mori *et al.*, 2013a). By contrast, Wang *et al.* (2014) reported that P addition stimulated N_2O emissions in a secondary tropical forest, likely due to increased microbial activity and thus larger nitrification and denitrification rates in the soil (Liu *et al.*, 2012). Therefore, it is likely that the overall effect of P addition on N_2O emission is governed by the trade-off between increased microbial denitrification capacity and increased plant growth, competing with denitrification for N.

1.6 Improving our understanding of forest N cycle with stable isotopes

The N cycle of an ecosystem involves numerous processes and components (Robinson, 2001), some of which are difficult to assess. For instance, it remains difficult to measure *in situ* denitrification, due to the large spatiotemporal variability of denitrification, and the high N_2 background in the atmosphere (Groffman *et al.*, 2006; Duncan *et al.*, 2013). The natural abundance of ^{15}N and ^{18}O in NO_3^- ($\delta^{15}N$ and $\delta^{18}O$) offers a possibility to semi-quantitatively characterize denitrification activity (Kendall *et al.*, 2007). Kinetic fractionation of isotopes occurs during all N transformation processes, by turning over lighter isotopes (^{14}N and ^{16}O) slightly faster than heavier isotopes (^{15}N and ^{18}O) (Fry, 2007). Thus, denitrification enriches both ^{15}N and ^{18}O in its residual substrate, NO_3^-. As the O atoms in NO_3^- are partly exchanged with those in ambient H_2O, the fractionation effect by denitrification for ^{18}O is always smaller than that for ^{15}N in NO_3^- (Knöller *et al.*, 2011; Wunderlich *et al.*, 2013). Therefore, denitrification progressively enriches ^{15}N and ^{18}O in NO_3^- in ratios between 2:1 and 1:1 (Fig. 1.2). In aquatic systems, a ratio of 0.5 for $\delta\ ^{18}O/\delta^{15}N$ is commonly used to identify denitrification (Bottcher *et al.*, 1990). To quantitatively evaluate the kinetic ^{15}N fractionation during denitrification, Mariotti *et al.*

(1981) proposed to calculate an apparent enrichment factor ε, which describes the change of $\delta^{15}N$ versus the change of NO_3^- concentration, between initial and residual NO_3^- in an idealized closed system. Apparent ε values reported for riparian and groundwater studies are in the range of -3.5‰ to -5.9‰ (Mariotti *et al.*, 1988; Spalding *et al.*, 1993; Søvik & Mørkved, 2008; Osaka *et al.*, 2010; Wexler *et al.*, 2014).

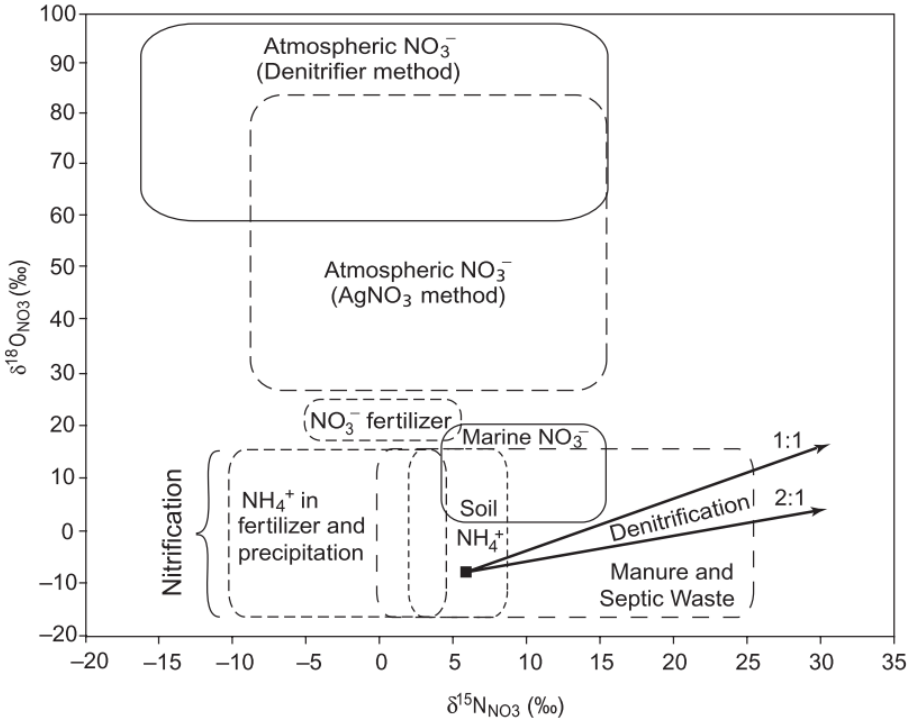

Fig. 1.2 Schematic demonstration of using natural abundance of ^{15}N and ^{18}O isotopes in NO_3^-, for partitioning sources and identifying processes. Figure from Kendall *et al.* (2007).

Nitrification causes ^{15}N depletion in its product (NO_3^-), but the isotopic fractionation effect is usually small, due to substrate limitation of nitrification in soil (Mariotti *et al.*, 1981; Billy *et al.*, 2010). The $\delta^{18}O$ of NO_3^- produced by nitrification is determined by the oxygen sources (O_2 and H_2O) and can be interpreted by mixing of the two end members, $\delta^{18}O$ of H_2O and O_2 in the environment, respectively (Kendall *et al.*, 2007). Thus, the $\delta^{18}O$ values of nitrification-produced NO_3^- is often in the range of -15‰ to +15‰ (Fig. 1.2) (Fang *et al.*, 2012), whereas atmospheric NO_3^- has higher $\delta^{18}O$ values of up to 100‰. This distinction has been used to distinguish atmogenic- and soil-derived NO_3^- (Rose *et al.*, 2015). Very recently, $\delta^{17}O$ of NO_3^- has been used to partition between atmospheric and soil derived NO_3^- in stream waters, based on the strong ^{17}O signal in atmospheric NO_3^-, originating from mass-dependent fractionation during photochemical reaction (Fang *et al.*, 2015; Sabo *et al.*, 2015).

Addition of enriched ^{15}N tracers is another approach for studying N cycling with stable isotopes (Templer *et al.*, 2012). Labeling N pools with small amounts of highly enriched ^{15}N helps to trace N transformations and study the distribution of N to other pools (Hart & Myrold, 1996). Also, net and gross N transformation rates can be estimated based on the net accumulation or dilution of ^{15}N in a product. For instance, Zhu *et al.* (2013b) applied ^{15}N-labeled NO_3^- to hillslope soils in the TSP forest, and measured the ^{15}N in emitted N_2O. They found that emitted N_2O was highly enriched in ^{15}N, with atom% ^{15}N-excess values resembling those of the added NO_3^-. Hence, they concluded that denitrification was the major source of N_2O emission from the hillslope soils.

In order to measure ^{15}N and ^{18}O of NO_3^- by isotope ratio mass spectrometry (IRMS), NO_3^- has to be isolated from solution and converted to a gas that retains information about both ^{15}N and ^{18}O in NO_3^-. Next to conversion to NO (which is very unstable), conversion to N_2O fulfills these criteria. Sigman *et al.* (2001) and Casciotti *et al.* (2002) introduced a bacterial denitrifier method to isolate and convert NO_3^- to N_2O based on *Pseudomonas aureofaciens* (ATCC 13985), a bacterial strain that lacks N_2O reductase (Christensen & Tiedje, 1988; Casciotti *et al.*, 2002). This method has become the most common approach to pretreat NO_3^- samples for isotope analysis. To prevent isotopic fractionation during denitrification (see above), the conversion of NO_3^- has to be complete. Further, the conversion should be rapid to prevent contamination by bacteria contained in the sample that could eventually convert N_2O to N_2. The conventional denitrifier method therefore induces denitrification by preculturing *P. aureofaciens* in the presence of extraneous NO_3^- during a lengthy period (6-10 days), in which the culture grows to high cell numbers, depletes oxygen and switches from oxic to anoxic respiration. However, there are challenges: If the preculturing period is too short, consumption of extraneous NO_3^- will be incomplete and lead to large blank values. On the other hand, if the preculturing period is too long, growing *P. aureofaciens* cells are at risk to run out of electron acceptors, which may lead to a metabolic "arrest" and would impair their "fitness" to convert sample NO_3^- quantitatively to N_2O. In practice, it is difficult to monitor NO_3^- depletion during growth and induction of *P. aureofaciens*. In addition, cells have to be harvested by centrifugation and resuspended in spent medium, from which the N_2O formed by anoxic respiration has to be removed by He or N_2-sparging. Together, this makes the method laborious and difficult to handle. Therefore, a simplified but reliable method is needed to process the large numbers of NO_3^- samples obtained from field experiments.

2. Research Objectives

This thesis follows up previous findings from a range of subtropical forests in South China, which are currently at or near N-saturation. N turnover processes were mainly studied by stable isotope approaches. The response of forest ecosystems (especially soils) to chronically elevated atmogenic N input was the major focus. In addition, I studied soil gas emissions to assess the impact of N-saturation on regional GHG budgets. The specific research objectives of this thesis were:

1. To develop a simplified but reliable "denitrifier method" for the analysis of ^{15}N and ^{18}O isotopes in NO_3^- from natural samples (**Paper V**).

2. To investigate the fate of atmogenic N input in N-saturated subtropical forest soils, and to elucidate the role of soil N turnover for retention and loss of atmogenic N inputs (**Paper III**).

3. To look for "hotspots and hot moments" of N removal by denitrification at the catchment scale (**Paper I**).

4. To study the effects of catchment properties and N deposition on the N sink function of subtropical forests (**Paper I** and **Paper II**).

5. To explore the mechanisms governing N_2O production in acid soils of subtropical forests, and partition the N_2O sources between nitrification and denitrification (**Paper III**).

6. To understand the effect of P addition on N cycling in N-saturated subtropical forests, including its effects on soil-atmosphere exchanges of N_2O and CH_4 (**Paper IV**).

3. Materials and Methods

3.1 Study sites

TieShanPing (TSP; 29°38´N, 106°41´E) is a 16.2-ha subtropical headwater catchment about 25 km Northeast of Chongqing city, South China (Fig. 3.1a). The catchment has a typical monsoonal climate, with an average annual precipitation of 1028 mm and a mean annual temperature of 18.2 ℃ (Zhu *et al.*, 2013c). Most precipitation occurs in summer (April to September). Inorganic N deposition varied between 40 and 65 kg N ha^{-1} yr^{-1} during the last decade, with an increasing trend in recent years (Duan *et al.*, 2013; Huang *et al.*, 2015). The vegetation is a mixed coniferous-broad leaf forest, dominated by Masson pine (*Pinus massoniana*).

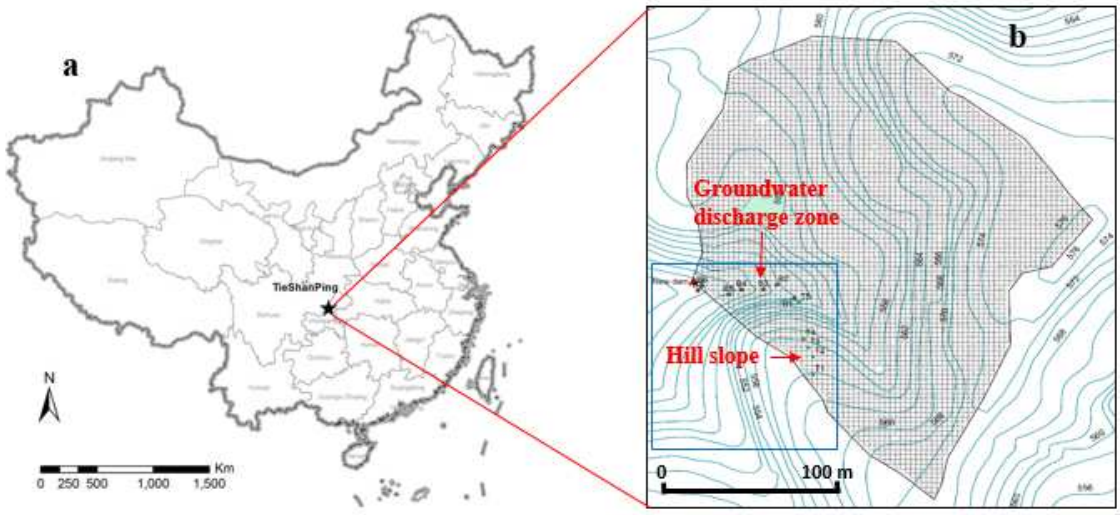

Fig. 3.1 Location of TSP forest **(a)** and digital elevation model (DEM) of the catchment **(b)**, showing the location of two transects, a hillslope (T1-T5) and a groundwater discharge zone (B1-B7). Figure 1 from **Paper I**.

At TSP (**Paper I** and **II**), I selected a 4.2 ha sub-catchment, including two dominant landscape elements: a relatively steep Northeast-facing hill slope (HS), and a hydrologically connected Southeast-Northwest-oriented, terraced groundwater discharge zone (GDZ) (Fig. 3.1b). Soils on HS are acidic (pH = 3.7-4.1), loamy yellow mountain soils (Acrisols; WRB 2014), with a thin O horizon (0-2 cm). Generally, HS soils are well drained, and induce considerable interflow over the argic Bt horizon after rainfall (Sørbotten *et al.*, Accepted). In the GDZ, the soils are developed from colluvium (Cambisol; WRB 2014), derived from the surrounding HS and their hydraulic

conductivity is smaller than that of the surface horizons of HS soils. During summer, drainage from HS may rapidly increase the groundwater level in the GDZ, resulting in temporary water logging (Sørbotten, 2011). The GDZ has an intermittent stream, the outlet of which enters a small pond.

Six additional forest sites in China were included in this thesis (**Paper II**), four in South China and two in North China (see Table 3.1 for site codes and a detailed description). All southern sites have subtropical monsoonal climate similar to that at TSP, with annual precipitation above 1000 mm. Among the northern sites, DLS is located in the warm temperate zone with continental monsoonal climate, while LPS is in the temperate zone with continental climate, only marginally influenced by monsoon. Most precipitation occurs in summer, but mean annual precipitation at the northern sites is markedly smaller (~ 600 mm) than at the southern sites. All catchments have a similar topography as at TSP, characterized by well-drained HS and hydrologically connected GDZ. However, the northern sites have less developed and more discontinuous GDZs along the stream banks, due to the drier conditions.

Table 3.1 Background description of all sites except TSP (soil characteristics mainly refer to hillslope soils; **Paper II**).

Site name	Leigongshan (LGS)	Caijiatang (CJT)	Tianmushan (TMS)	Dagangshan (DGS)	Liupanshan (LPS)	Donglingshan (DLS)
Location	Guizhou	Hunan	Zhejiang	Jiangxi	Ningxia	Beijing
Longitude	108°11′	112°22′	119°26′	114°34′	106°20′	115°26′
Latitude	26°23′	27°50′	30°19′	27°35′	35°15′	39°58′
Mean annual temperature (°C)	15.7	17.5	11.9	15.8	5.8	4.8
Mean annual precipitation (mm)	1120	1250	1581	1591	676	612
Vegetation	*Pinus armandii* dominated, coniferous-broad leaf mixed forest	*Massone pine* dominated, coniferous-broad leaf mixed forest	Broad-leaf forest	Evergreen broad-leaf forest	Mixed deciduous broad-leaf forest; broad-leaf and coniferous forest	Mixed, secondary deciduous broad-leaf forest; coniferous forest
Soil type	Yellow mountain soil	Yellow mountain soil	Red and yellow soils	Red and yellow soils	Gray cinnamon soil	Cinnamon soil
Soil pH[†]	4.4	4.8	6.3	4.9	7.0	6.1
Soil C/N ratio[‡]	12.0	14.2	13.2	14.4	10.4	11.5
Annual throughfall flux (kg N ha^{-1})[θ]	9.8	38.8	19.4	16.0	5.0	11.6

3.2 Experimental design

3.2.1 Isotope analyses (**Paper I-III** and **V**)

^{15}N and ^{18}O of N_2O produced from NO_3^- in natural samples were analyzed with an isotope ratio mass spectrometer coupled to a pre-concentration unit (PreCon-GC-IRMS, Thermo Finnigan MAT). Isotope ratios, such as $^{15}N/^{14}N$ and $^{18}O/^{16}O$, are reported as δ values (‰):

$$\delta = \frac{R_{sample} - R_{standard}}{R_{standard}} \times 1000 \quad (1)$$

where R is the ratio of $^{15}N/^{14}N$ or $^{18}O/^{16}O$. International standards of ^{15}N and ^{18}O refer to atmospheric N_2 and Vienna Standard Mean Water (VSMOW), respectively.

Here, I modified the conventional denitrifier method (Sigman *et al.*, 2001; Casciotti *et al.*, 2002), by preculturing *Pseudomonas aureofaciens* aerobically in a NO_3^--free tryptic soya broth (TSB) and inducing denitrification by repeated helium washing in the presence of µM NO_3^- present in the sample (Fig. 3.2). To remove traces of NO_3^-, the TSB medium was preincubated with *Paracoccus denitrificans* (ATCC 17741), which converts NO_3^- quantitatively to N_2. P. denitrificans was grown aerobically at room temperature under stirring and inoculated at a cell density of 1.9-5.6 × 10^8 cells ml^{-1} to sterile TSB medium. The culture was then incubated for 3-4 days in closed bottles while shaking horizontally, eventually removing all O_2 and NO_3^-. The resulting "NO_3^--free" spent medium was amended with 20 mM NH_4^+ (to compensate for NH_4^+ used during *P. denitrificans* growth), autoclaved and stored frozen for future use. *Pseudomonas aureofaciens* was grown aerobically in the NO_3^--free medium, providing starting and working cultures for the conversion assay (Fig. 3.2). When the working culture reached a cell density of 5.6-9.3 × 10^8 cells ml^{-1}, 2 ml of culture was added to helium-washed, anoxic 120 ml vials containing up to 4 ml of NO_3^- sample or standard. Complete conversion of NO_3^- to N_2O was achieved in less than 10 hours under shaking, after which 0.2 ml of 10 M NaOH was added to stop microbial activity and to trap CO_2.

The $\delta^{18}O$ of converted N_2O differs from that of NO_3^- due to isotopic fractionation associated with the loss of O atom during denitrification and the O exchange with H_2O in the medium (Casciotti *et al.*, 2002; Kool *et al.*, 2011). This fractionation can be assumed to be constant if the conversion is complete and can be corrected by including standards

with known isotopic compositions in each measurement batch (Casciotti *et al.*, 2002; Fry, 2007). Assuming that ^{18}O fractionation, NO_3^- blank of the TSB medium, and O exchange are stable for each batch, I corrected $\delta^{18}O$ values by including two nitrate standards differing in ^{18}O (IAEA N3 and USGS 34), applying the following equation (Casciotti *et al.*, 2002):

$$\delta^{18}O_s = \delta^{18}O_{s1} + \frac{(\delta^{18}O_{s1} - \delta^{18}O_{s2})}{(\delta^{18}O_{m1} - \delta^{18}O_{m2})} (\delta^{18}O_m - \delta^{18}O_{m1}) \quad (2)$$

where $\delta^{18}O_s$, $\delta^{18}O_{s1}$ and $\delta^{18}O_{s2}$ are the mean actual $\delta^{18}O$ values of NO_3^- for sample, standard 1 and standard 2, respectively, whereas $\delta^{18}O_m$, $\delta^{18}O_{m1}$ and $\delta^{18}O_{m2}$ are their mean measured $\delta^{18}O$ values.

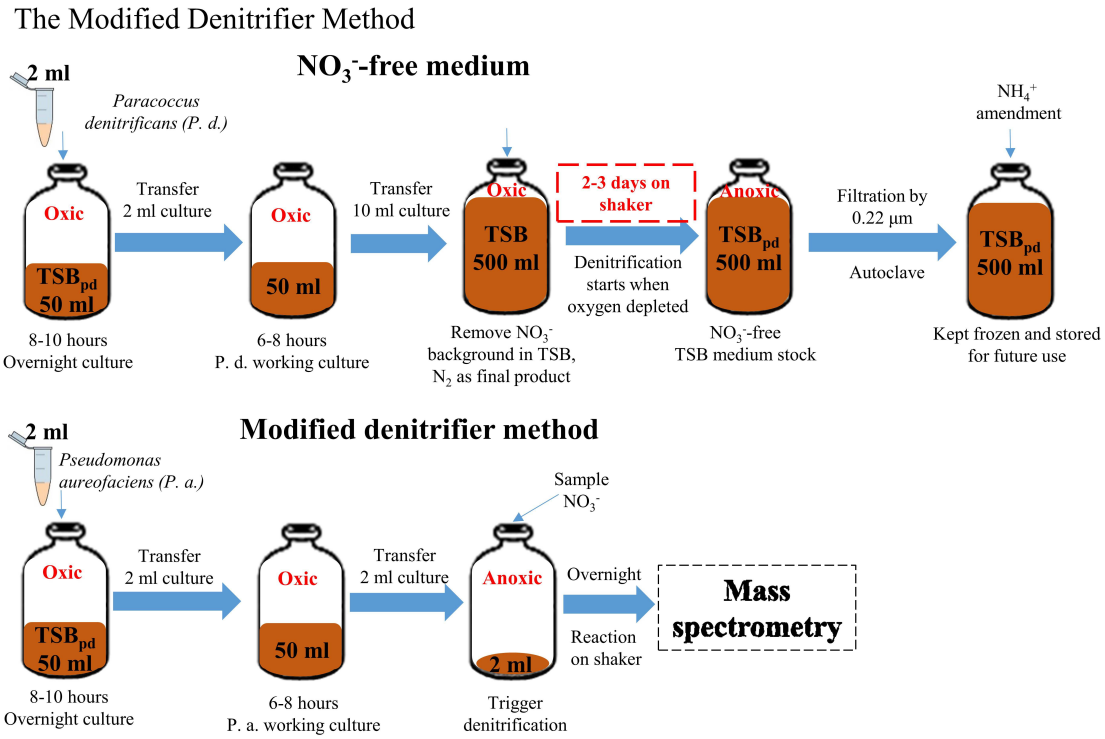

Fig. 3.2 Procedures for converting NO_3^- samples to N_2O by the modified denitrifier method. Figure from **Paper V**.

^{15}N of NH_4^+ in KCl extracts and freshwater samples was analyzed after chemical conversion to N_2O (Zhang *et al.*, 2007). NH_4^+ was first quantitatively converted to NO_2^- by hypobromite (BrO^-) at pH ~ 12, and further reduced to N_2O using a 1:1 mixture of sodium azide and acetic acid. The precision for $\delta^{15}N$ of NH_4^+ was ≤ 0.3‰.

To measure total $\delta^{15}N$, bulk samples (soil and plant) were finely milled and wrapped in tin capsules. Samples were analyzed with an elementary analyzer coupled to an IRMS (Thermo Finnigan, Delta XP). The precision for bulk soil $\delta^{15}N$ was ~ 0.2‰.

3.2.2 Field observations along hydrological continua in seven forest catchments (**Paper I** and **Paper II**)

Soil water was collected along hydrological-connected hillslopes (HS) and groundwater discharge zones (GDZ). See **Paper I** and **Paper II** for a detailed set-up of sampling plots along the hydrological flow paths. Soil pore water was sampled in triplicates at every plot along the flow paths, using either macrorhizon soil moisture samplers (Rhizosphere Research Products) or ceramic suction cup lysimeters (P80; Staatliche Porzellanmanufaktur). Samples were collected by applying vacuum to the lysimeters through a 50 ml syringe for about 12 hours (Fig. 3.3). Throughfall was collected in triplicate in 3-L polyethylene (PET) bottles, equipped with 10.6-cm diameter PET funnels (Fig. 3.3). Stream water was sampled at the weir located at the outlet of the catchment (Fig. 3.3). All water samples were filtered by 0.45 µm syringe-filters (Millex) and frozen before analysis. Bulk soil at the depth of 0-5 cm was sampled using either core rings or a spade, and kept refrigerated (4 ^{o}C) until analysis.

Fig. 3.3 Field sampling of soil water, throughfall and stream runoff (from left to right). Photos: Longfei Yu and Jing Zhu.

After a rainstorm (32 mm; sampled as throughfall) on July 5, 2013 at TSP (**Paper I**), soil water (0-5 cm) and stream water samples were collected once per day for three

consecutive days. An additional sampling was carried out on July 31, after a dry period. The 2013 samples were compared to archived (frozen) water samples (throughfall, soil water and stream water) taken at the same plots in the summers of 2009 (6 different days) and 2010 (10 different days). These samples were collected at four depths in the soils of HS (0-5, 10, 20 and 40 cm) and GDZ (0-5, 30, 60 and 100 cm). All water samples were analyzed for inorganic N concentrations and NO_3^- isotopes. In addition, $\delta^{15}N\text{-}NH_4^+$ was analyzed for a few throughfall samples. Before the rainstorm on July 5, 2013, I took soil samples from the surface horizon (0-5 cm), which were later analyzed for total C, and N contents and $\delta^{15}N$. Precipitation and air temperature at TSP were recorded every 5 minutes using a weather station (WeatherHawk 232) installed on the roof of the local forest bureau, located 1 km south of the catchment. At the outlet of the sub-catchment, water discharge rates were measured by a V-notch weir at 5-minute intervals, using WL705 ultrasonic water level sensor (Global Water, Xylem Inc.).

At the other six sites (**Paper II**), inorganic N concentrations were determined in samples of throughfall, soil water and stream water, collected bi-weekly at all sites from Aug. 2012 to Aug. 2014. For both inorganic N concentration and isotope analyses, I sampled throughfall, soil water (0-5 cm) and stream water (outlet) twice at all sites (only throughfall for DGS) in July and August 2014, respectively. Additional sampling of surface soil, soil water and stream water was conducted in July 2015, only for the southern sites.

The Rayleigh distillation model was used to evaluate denitrification activities quantitatively (Mariotti *et al.*, 1981). For this, I calculated the apparent ^{15}N enrichment factor ε as a proxy for denitrification activity along the water flow path:

$$\varepsilon = \frac{\delta_s - \delta_{s0}}{\ln\left[C(NO_3^-)_s / C(NO_3^-)_{s0}\right]} \quad (3)$$

where $C(NO_3^-)_{s0}$ and, $C(NO_3^-)_s$ are initial and residual NO_3^- concentration, respectively, and δ_{s0} and δ_s are $\delta^{15}N$ of initial and residual NO_3^-. This approach is based on the assumption that the hydrological flow path behaves as a quasi-closed system (Wexler *et al.*, 2014), and that isotopic fractionation is solely due to denitrification.

3.2.3 *In situ* ^{15}N tracing experiment (**Paper III**)

In the TSP forest catchment, I established two experimental sites (upper (P1) and lower (P2); Fig. 1a in **Paper III**) both on the northeast facing hillslope (HS). The two sites were located just below the summit of HS (P1) and at the foot of the hillslope (P2), respectively. ^{15}N tracer was applied on June 23, 2015, in solution as $^{15}NH_4NO_3$ ($^{15}NH_4$, 99 atom% ^{15}N), $NH_4{}^{15}NO_3$ ($^{15}NO_3$, 98 atom% ^{15}N), and ^{15}N-Glutamic acid (^{15}N-Glut, 98 atom% ^{15}N). The reference plots received the same volume of deionized water. At both P1 and P2, three blocks were established; in each block four treatments were randomly assigned to adjacent 1.2 m x 1.2 m plots (Fig. 3.4). The ^{15}N dose for each treatment was the same (0.1 g ^{15}N m^{-2}). ^{15}N tracers were applied in 5 mm deionized water (7.2 L for each plot), using a backpack sprayer (Fig. 3.4). Afterwards, an additional 0.5 mm of deionized water was added to wash off tracer intercepted by vegetation. Tracer application took slightly less than 0.5 hour.

Fig. 3.4 Field sampling during ^{15}N tracing experiments (**Paper III**). Photos: Longfei Yu and Jing Zhu.

Sample collection started immediately following tracer addition (t = 0.5 hr). During a period of about 9 days (219 hours), eight samplings (see **Paper III** for detail) of soil, soil KCl extracts, soil water from lysimeters and emitted N_2O gas were conducted at all plots. Soil samples of the O/A (~ 0-2 cm) and AB (~ 2-15 cm) horizons were randomly taken with a soil auger (Φ = 2.5 cm), and analyzed for total N content and $\delta^{15}N$. Triplicates of soil cores were mixed for each horizon and each plot, before extracting 8 g fresh soil in 40 ml of 1 M KCl (Fig. 3.4). The extracts were filtered and kept frozen prior to measuring concentrations and $\delta^{15}N$ of inorganic N. Soil water was sampled at 0-5 cm depth (O/A

horizon and the upper part of the AB horizon) using lysimeters, and analyzed for inorganic N concentrations and $\delta^{15}N\text{-}NO_3^-$. Gross transformation rates of NH_4^+ and NO_3^- were calculated based on ^{15}N pool dilution and N mass balance (Davidson *et al.*, 1991). When calculating ^{15}N recovery rates, I defined the 'soil residual N' pool, as ^{15}N recovery in total soil N minus that in inorganic (KCl-extractable) soil N.

N_2O emissions were sampled using a static chamber method (Fig. 3.4; Zhu *et al.*, 2013a). In brief, at each plot gas samples were collected from a static chamber in pre-evacuated 120-ml vials 1, 15 and 30 min after chamber deployment. N_2O fluxes were calculated by linear regression of N_2O concentrations versus time. The $\delta^{15}N$ of emitted N_2O was computed using the Keeling plot equation (Yakir & Sternberg, 2000). In addition, I partitioned the N_2O production pathways (nitrification and denitrification) by a two end-member-mixing analysis (Stevens *et al.*, 1997). For every sampling, soil temperature and volumetric moisture contents were measured at 10-cm depth in triplicate at each plot, using a hand-held time-domain reflectometry device (TDR, Hydraprobe). WFPS was calculated using volumetric soil moisture, soil bulk density and assumed soil particle density (2.65 g cm^{-3}; Linn & Doran, 1984).

3.2.4 P application experiment (**Paper IV**)

At TSP, six 20 m x 20 m plots were established in three blocks, each block accommodating two paired plots for P-addition and untreated reference, respectively, separated by a 5 m-wide buffer strip. All three blocks were situated on a gently sloping hillside, with minor differences in elevation and topography. Reference (Ref) and P-treated plots were assigned randomly in each block. On 4 May 2014, P fertilizer was applied once in solid form as $NaH_2PO_4{\cdot}2H_2O$, at a rate of 79.5 kg P ha^{-1} yr^{-1}.

I sampled soil water at 5- and 20-cm depth, bi-monthly in the cool seasons and monthly in the warm seasons, from November 2013 to October 2015. The samples were kept frozen until analyses. Soil samples were taken from the O/A, AB and B horizons near the lysimeter sites in August 2013, and analyzed for pH, organic C, total N and total P as well as ammonium lactate extractable P (P_{AL}). In addition, from the same sites, I collected soil samples in the O/A horizon, once every half year (see **Paper IV** for more detail).

Emitted gases were sampled by static chambers at the same frequency as soil water samples. Fluxes of N_2O and CH_4 were calculated from concentration change over time, as detailed in section 3.2.3. Flux measurements were carried out more frequently around the date of P addition, i.e. once before (2 May) and three times (7, 10 and 12 May) after the P application on 4 May 2014. Monthly litterfall was collected, dried and weighed starting from October 2013. Pine needles were sampled in early Novembers of 2013 and 2014, for analyses of total C, N, P, K, Ca and Mg contents. Also, tree biomass was estimated three times throughout the experimental period (Novembers of 2013, 2014, and February of 2015). See more detail in **Paper IV**.

3.3 Statistics

All statistical analyses presented in this thesis were performed with Minitab 16.2.2. All data were tested for normality (Kolmogorov-Smirnov's test), prior to further analysis. If the data was non-normally distributed, I applied logarithmic transformation to normalize them. Paired t-test was applied to compare temporal changes of concentrations or isotopic signatures (e.g. changes of $\delta^{15}N$ and $\delta^{18}O$ at TSP in 4 days of summer 2013; **Paper I**). One-way ANOVA with post hoc Tukey test was used to determine statistically significant differences in concentrations or isotopic signatures among treatments and sampling plots (e.g. inorganic N concentrations in throughfall, soil water and stream water along the hydrological continua; **Paper II**). Significance levels in this thesis were set at $p < 0.05$, unless specified otherwise.

4. Main Results and Discussion

4.1 Modified denitrifier method for $\delta^{15}N$ and $\delta^{18}O$ analyses in NO_3^-

Using aerobically growing *P. aureofaciens*, conversion efficiency for NO_3^- to N_2O was close to 100%, indicating that denitrification in *P. aurefaciens* does not need to be induced during anaerobic growth with extraneous NO_3^- prior to the conversion assay. We tested our modified denitrifier method with international standards and natural samples (**Paper V**) and found it to be efficient and robust for isolating small amounts of NO_3^- in natural samples as N_2O for subsequent isotope analyses. The method was suitable for samples with low pH (pH = 4) or high salinity (0.25 M KCl). Standard deviations for natural abundance were 0.1-0.3‰ for $\delta^{15}N$ and 0.2-0.7‰ for $\delta^{18}O$.

4.2 N fluxes along hydrological flow paths in seven catchments across China

The seven studied forest catchments in China covered a gradient of N deposition in throughfall, ranging from 5.0 to 48.7 kg N ha^{-1} yr^{-1} (Table 1 in **Paper II**). At most, about half of the N was deposited as NH_4^+-N, with largest values at TSP (56%) and CJT (40%) (Fig. 1 in **Paper II**). At the other sites, inorganic N deposition was dominated by NO_3^--N. On the hill slopes (HS: plots A and B), NH_4^+ concentrations in soil water were generally below 0.1 mg N L^{-1} (except for LPS), and significantly smaller than in throughfall (Fig. 4.1). In contrast, NO_3^- concentrations in soil water on HS were significantly larger than in throughfall (Fig. 4.1). From HS to groundwater discharge zone (GDZ: plots C and D) and stream water, NH_4^+ concentrations remained small, while NO_3^- concentrations significantly decreased.

As an inert solute in the soil, the concentrations of Na^+ along the water flow path could be used as a proxy for evapotranspiration (Huang *et al.*, 2015). I normalized the NO_3^- concentration against the Na^+ concentration, to test whether the change of NO_3^- concentrations along water flow path could be explained by evapotranspiration (Fig. S4 in **Paper II**). The NO_3^-/Na^+ ratios showed a strong increase from throughfall to HS and a pronounced decrease from HS to GDZ and stream. This confirms that the spatial pattern of NO_3^- concentration was not due to evapotranspiration, but indeed resulted from significant source and sink terms in the HS and GDZ, respectively.

In the stream water at all sites, except LGS and LPS, the NO_3^- concentration was somewhat greater than in the soil water of the respective GDZs (Fig. 4.1). This may suggest that the streams also received water directly from surrounding hillslopes, particularly during stormflow conditions (Rose *et al.*, 2014). Our long-term data showed significant N sinks in the GDZs of all catchments. This may further indicate that catchment removal of NO_3^- depends on the GDZ acting as a conduit for water as it passes from HS to the stream.

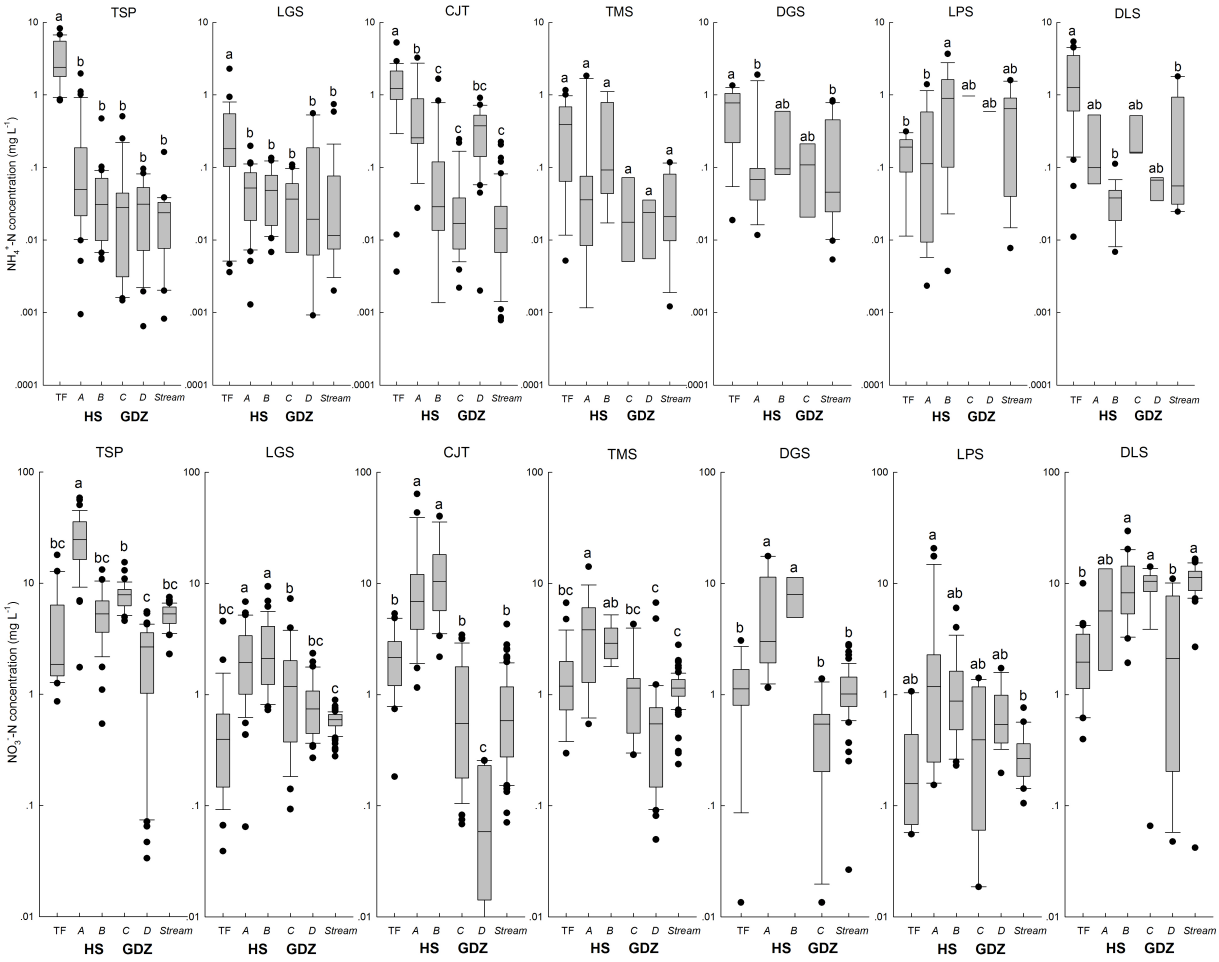

Fig. 4.1 Logarithmic box whisker plot of NH_4^+ (upper) and NO_3^- (lower) concentrations in throughfall (TF), soil water at plots A, B, C, D and stream water in seven forested catchments. Bi-weekly data from Aug. 2012 to Aug. 2014 are presented. Different letters indicate significant differences between sampling points within each site. No data were available for soil water at the D plot, DGS. For site codes, see Table 3.1 in the Materials and Methods section. Figure from **Paper II**.

4.3 Turnover of atmogenic N in upland hillslope soils

Hillslopes are the major landscape element by area in mountainous-forested

catchments (Jencso *et al.*, 2009; Zhu *et al.*, 2013c). Therefore, a ^{15}N tracing experiment was carried out on hillslope soils (upper and lower) at TSP to study short-term N turnover processes (**Paper III**). The majority of added $^{15}NH_4^+$ (> 70%) was quickly retained in the surface soil (Fig 4.2a&d). This could be due to electrostatic bonding of NH_4^+ to negatively charged surface sites of clay minerals or soil organic matter (Nieder *et al.*, 2011). However, large recoveries (40-70%) of $^{15}NH_4^+$ in the soil residual N pools (excluding KCl-extractable inorganic N), points at microbial immobilization rather than chemical fixation (Tahovsk *et al.*, 2013). By contrast, most of the added $^{15}NO_3^-$ was recovered in KCl-extractable NO_3^- in the O/A and AB horizons (Fig. 4.2b&e). The $^{15}NO_3^-$ pool decreased dramatically (90 to 20%) over the 9 days of observation, most likely due to strong NO_3^- loss by leaching (Huang *et al.*, 2015) and/or denitrification. Indeed, the ^{15}N leaching loss estimated for the initial 144 hours explained more than half of the observed ^{15}N loss (Table S1 in **Paper III**). This indicates that in these systems, NO_3^- is to be considered as a mobile anion, showing little or no interaction with the soil.

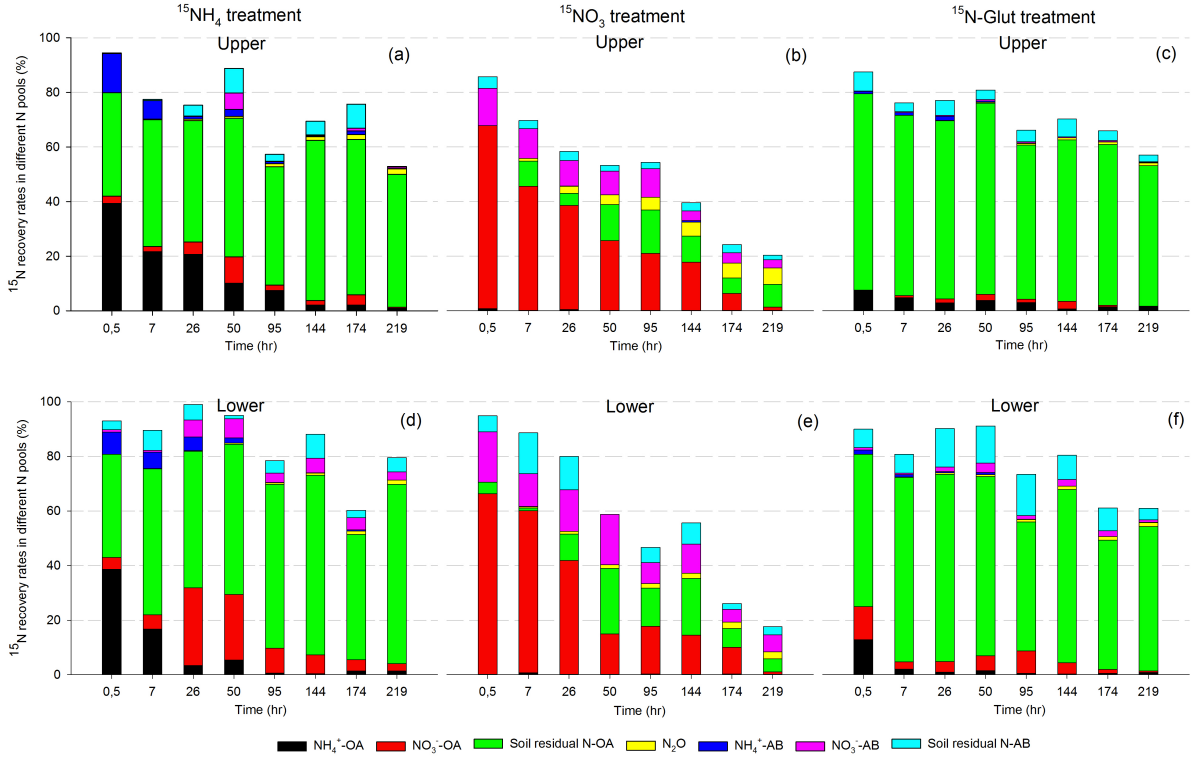

Fig. 4.2 ^{15}N recovery (average of triplicates) in different N pools in $^{15}NH_4$ (a&d), $^{15}NO_3$ (b&e) and ^{15}N-Glut (c&f) treatments. Upper and lower panels refer to P1 (upper site) and P2 (lower site). OA and AB represent the O/A and AB horizons, respectively. The x-axis indicates the time after label application. Figure from **Paper III**.

Immediately after $^{15}NH_4^+$ addition, I observed significant production of $^{15}NO_3^-$, indicating active nitrification (Figs. 4.2 a&d and 4.3 a&d). The gross nitrification rates were in line with those reported in tropical forest soils (Venterea *et al.*, 2004; Templer *et al.*, 2008). However, the scarcity of NH_3 (but not NH_4^+) in acid soil may restrict the first step of nitrification, i.e. ammonia oxidation (De Boer & Kowalchuk, 2001). If NH_4^+ oxidation is the only source of NO_3^-, the ^{15}N enrichment in NO_3^- would never exceed that of NH_4^+ (Hart & Myrold, 1996). Yet, in the $^{15}NH_4$ treatments, ^{15}N atom% in NO_3^- was greater than in NH_4^+ already at the first sampling date (Fig. 4.3 a&d), indicating that ^{15}N-enriched sources other than $^{15}NH_4^+$ contributed to $^{15}NO_3^-$ production. Since added $^{15}NH_4^+$ was largely retained and diluted in the soil residual N pool (with overall small ^{15}N enrichment), I suggest that a more dynamic, labile and ^{15}N-enriched fraction of soil residual N, such as microbial N, must have contributed to $^{15}NO_3^-$ production. Microbial biomass represents the most dynamic N pool in soil, which can rapidly immobilize and release NH_4^+. Once re-mineralized, NH_4^+ is quickly converted to NO_3^- by autotrophic nitrification. A shortcut to NO_3^- production from immobilized NH_4^+ is heterotrophic nitrification, i.e. the direct conversion of organic N to NO_3^- by heterotrophic bacteria or fungi (Zhang *et al.*, 2013; Zhu *et al.*, 2013e). The occurrence of the latter pathway was indirectly confirmed by the ^{15}N-Glut treatment. In this treatment, ^{15}N enrichment in NO_3^- was greater than in NH_4^+ (Fig. 4.3 c&f), demonstrating that $^{15}NO_3^-$ was formed directly from some ^{15}N enriched pool (such as ^{15}N-glutamate), and not from re-mineralized NH_4^+. Heterotrophic nitrification seemed to play a greater role at the lower site (P2), indicating differences in taxonomic composition or activities of nitrifying microbial communities at different topographic positions.

Short-term (9 days) gross NH_4^+ immobilization and mineralization rates in TSP hillslope soils (Table 1 in **Paper III**) were similar to those reported for acid forest soils in southern China (Zhang *et al.*, 2013) and for tropical forest soils (Silver *et al.*, 2001; Sotta *et al.*, 2008; Templer *et al.*, 2008; Arnold *et al.*, 2009). Together, my findings indicate that NH_4^+ conversion to leachable NO_3^- in acid soils relies on dynamic N turnover, with rapid exchange between organic and inorganic N pools, rather than on direct nitrification of deposited NH_4^+. If assuming that the sizes of the N pools do not change over longer periods, this turnover will result in complete conversion of NH_4^+ to NO_3^- and deposited NH_4^+ will leach more or less quantitatively as NO_3^- from the top soils.

This finding is in accordance with a long-term N fertilizer study at TSP, reporting near-quantitative leaching of added NH_4^+ and NO_3^- as NO_3^- (Huang *et al.*, 2015).

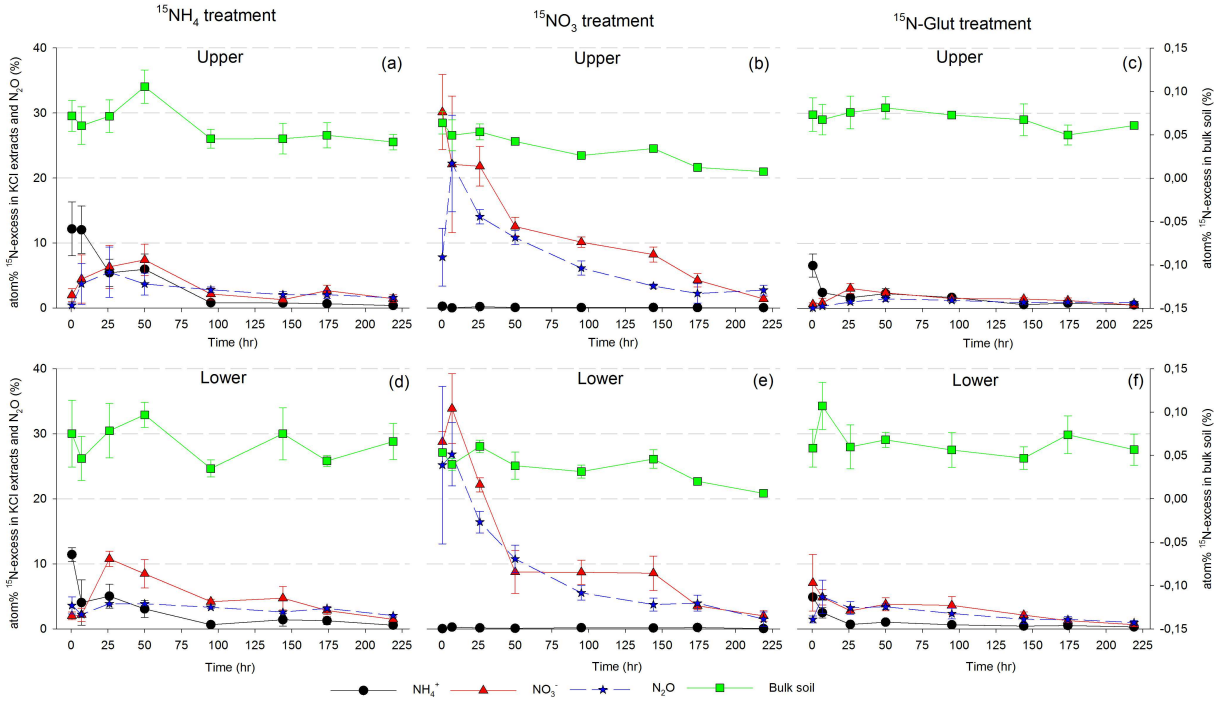

Fig. 4.3 Atom% ^{15}N-excess of NH_4^+ and NO_3^- in KCl extracts (O/A horizon), of total soil N (O/A horizon) and of emitted N_2O for $^{15}NH_4$ (a&d), $^{15}NO_3$ (b&e) and ^{15}N-Glut treatments (c&f). Upper and lower panels refer to P1 (upper) and P2 (lower) sites. Means and standard errors are presented (n = 3). The x-axis indicates the time after label application. Figure from **Paper III**.

4.4 Denitrification in groundwater discharge zones: a major catchment N sink

Natural abundance of ^{15}N and ^{18}O in NO_3^- sampled over three monsoonal summers along the hydrological continuum in the TSP catchment (**Paper I**) revealed characteristic spatial patterns of ^{15}N and ^{18}O depletion and enrichment on HS and GDZ, respectively (Fig. 4.4). The strong decrease of $\delta^{18}O$-NO_3^- in soil water compared to throughfall indicated that NO_3^- in soil water was not exclusively derived from atmogenic deposition, but also from soil N cycling (Rose *et al.*, 2015). In addition, as nitrification produces ^{15}N-depleted NO_3^- relative to its substrate NH_4^+ (Fry, 2007), the relatively smaller $\delta^{15}N$-NO_3^- in soil water than in throughfall confirmed that soil water NO_3^- was mainly from nitrification. By contrast, in the GDZ, increases in both $\delta^{15}N$- and $\delta^{18}O$-NO_3^- suggested pronounced denitrification, as heavier isotopes are enriched during dissimilatory reduction of NO_3^- (Kendall *et al.*, 2007). Therefore, the enrichment in ^{15}N (Fig. 4.4),

associated with decreased concentrations of NO_3^- (Fig. 4.1) confirmed that denitrification in the GDZ is the major N sink for the TSP catchment.

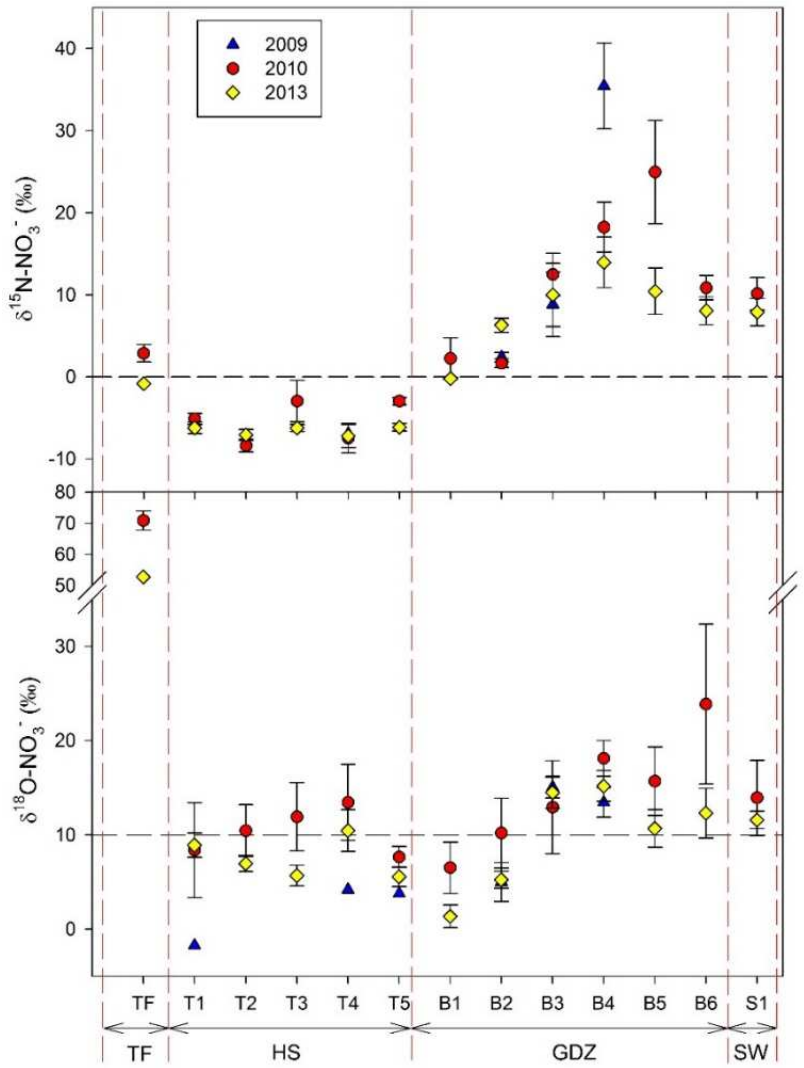

Fig. 4.4 Spatiotemporal variation of $\delta^{15}N\text{-}NO_3^-$ and $\delta^{18}O\text{-}NO_3^-$ in throughfall (TF), and in surface soil water on the hill slope (HS) and in the groundwater discharge zone (GDZ) in the summers of 2009, 2010 and 2013. Means and standard errors are presented. Figure from **Paper I**.

I found similar isotopic patterns in NO_3^- along hydrological flow paths during monsoonal summers in four other subtropical forest catchments in South China (**Paper II**). As at TSP, this pattern was associated with pronounced NO_3^- attenuation (Fig. 4.5). For all southern catchments, including TSP (except DGS because of too few samples), apparent ^{15}N enrichment factors "ε" were estimated to be between -3.0 to 6.0‰ (Fig. S7 in **Paper II**). This is similar to values reported previously for riparian denitrification (Mariotti *et al.*, 1988; Bottcher *et al.*, 1990; Spalding *et al.*, 1993). Hence, my study

suggests that catchment-scale N removal by hydrologically coupled NO_3^- production in aerated hillslope soils and strong denitrification in near-stream saturated soils is a widespread phenomenon across mountainous-monsoonal, subtropical forests in South China.

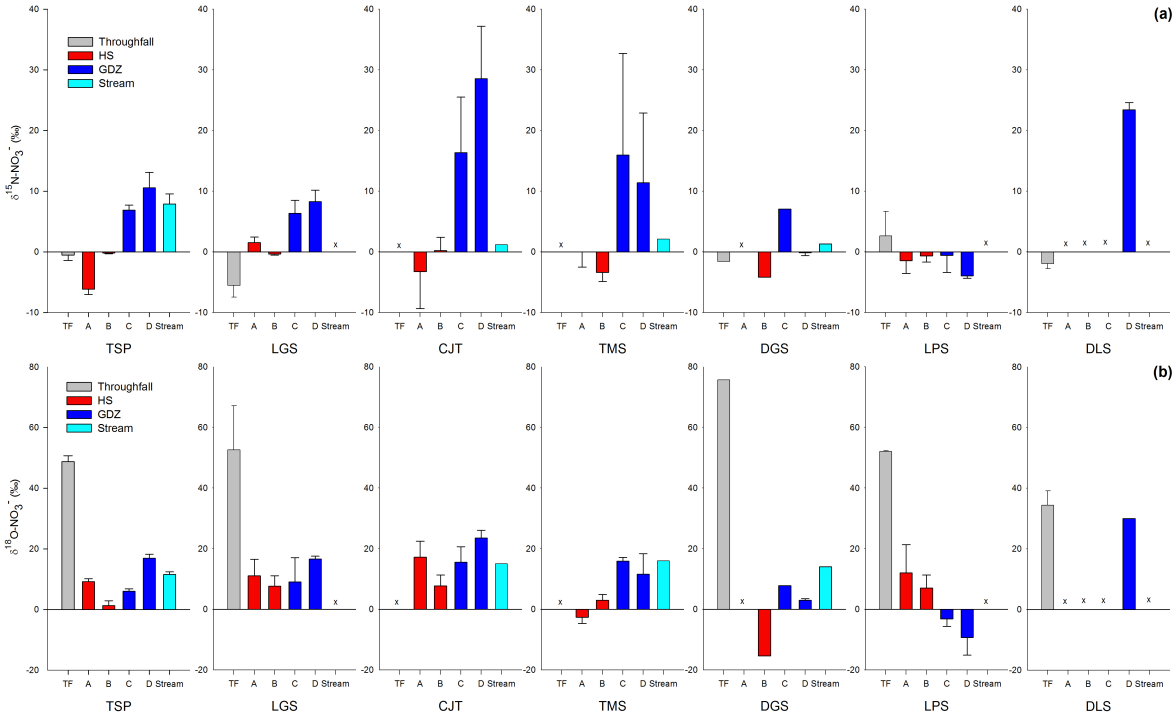

Fig. 4.5 Means and standard errors of $\delta^{15}N_{NO3}$ **(a)** and $\delta^{18}O_{NO3}$ **(b)** in throughfall, soil water and stream water in seven catchments in the summers of 2014 and 2015. 'x' denotes no available data. For site codes, see Table 3.1 in the Materials and Methods section. Figure from **Paper II**.

In contrast, there were clear deviations from this pattern in the two northern forest sites. Isotopic signatures in NO_3^- at the LPS site in NW China indicated that nitrification dominated along the entire flow path (Fig. 4.5). This is likely due to the small N deposition (5 kg ha^{-1} yr^{-1}) at LPS, resulting in stronger assimilation of deposited N than at sites with larger N input (Aber *et al.*, 1998). At the other northern site DLS, near Beijing, I observed strong ^{15}N- and ^{18}O-enrichment in NO_3^- from the GDZ, suggesting that this site has a potential for denitrification. However, catchment N fluxes at DLS showed almost equivalent N input and output (Fig. 4.6a), i.e. there was no or only minor NO_3^- attenuation. Most likely, a substantial part of the drainage water from HS soils bypasses the GDZ at DLS and is little affected by denitrification. The GDZ is less developed at this site, due to the generally drier conditions, so reductive conditions are less common here than in the

southern catchments (Hughes, 2004; Van Gaalen *et al.*, 2013), where annual precipitation is double of that at the northern sites (Table 1 in **Paper II**).

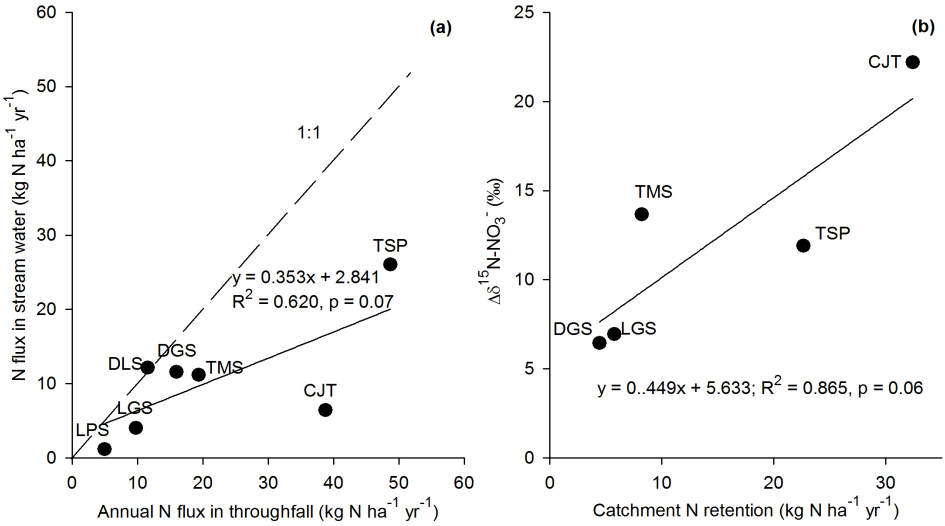

Fig. 4.6a Relationship between annual N flux in throughfall and in stream water from 2012 to 2014. Linear regression lines and equations were presented, as well as the dash line showing 1:1 ratio for x/y values. **4.6b** Relationship of catchment N retention with $\Delta\delta^{15}N_{NO3}$ between HS and GDZ. $\Delta\delta^{15}N_{NO3}$ = (averaged $\delta^{15}N_{NO3}$ in GDZ) - (averaged $\delta^{15}N_{NO3}$ on HS). For site codes of both figures, see Table 3.1 in the Materials and Methods section. Figure from **Paper II**.

At the southern monsoonal sites where GDZs are generally well developed, the relationship between N fluxes in throughfall and stream water indicated that catchment N retention scales roughly linearly with N deposition (Fig. 4.6a). I also compared the overall change of $\delta^{15}N_{NO3}$ between HS to GDZ ($\Delta\delta^{15}N_{NO3}$), a proxy for denitrification strength, with apparent catchment N retention (Fig. 4.6b). The absolute increase in ^{15}N enrichment along the flow paths was positively correlated with catchment N retention, indicating that the denitrification capacity is proportional to N deposition. This may suggest that subtropical-monsoonal forest catchments with well-developed GDZs can adapt to increasing N-loads, without losing their N sink function.

4.5 Hotspots of N_2O emission: the importance of denitrification in hillslope soils in the TSP forest

Mean N_2O fluxes from soils on the hillslope in the TSP forest were in the range of 40 to 120 μg N m^{-2} hr^{-1} from summer 2013 to autumn 2015 (Figs. 2 and 3; **Paper IV**) and similar to N_2O fluxes reported previously for the TSP forest (Zhu *et al.*, 2013c). The N_2O

emission rates at TSP are large compared to other forests in South China, showing average emissions of 15 to 50 μg N m^{-2} hr^{-1} (Tang *et al.*, 2006; Fang *et al.*, 2009). Average cumulative N_2O emission from the hillslope soils at TSP was 5.3 kg N ha^{-1} yr^{-1} (Fig. 4.7), which equals 10% of the N deposited (50 kg N ha^{-1} yr^{-1}). This "emission factor" (N_2O-N emission/N input) is far greater than any factor used for estimating N_2O emission in global models (1% to 5%) (Reay *et al.*, 2012). Interestingly, short-term N_2O flux measurements (**Paper III**) showed larger N_2O emission in the upper, drier hillslope than in the wetter, lower hillslope (Fig. 4.8). This matches long-term field observation at TSP by Zhu *et al.* (2013c), who found larger N_2O emissions on the HS than in the GDZ (the zone of NO_3^- attenuation). They attributed this to the more "flashy" hydrology on hillslopes as opposed to the more permanently saturated conditions in the GDZ, which would promote N_2O reduction to N_2 by denitrification (Morley *et al.*, 2008). My results confirm that well-drained hillslope soils are a hotspot for N_2O emissions in N-saturated, subtropical forests, likely being of regional significance.

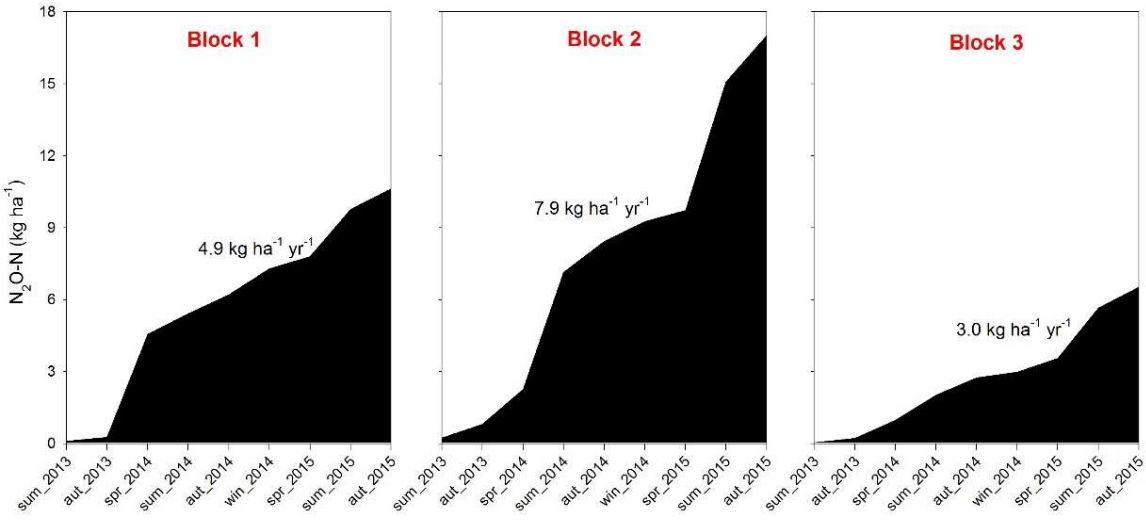

Fig. 4.7 Cumulative N_2O emissions from summer 2013 to autumn 2015 in the hillslope soils of the TSP forest. Block 1 to 3 refer to reference plots in the P fertilization experiment. Numbers in figures are estimated annual N_2O-N emission rates. Figure reproduced from **Paper IV**.

The *in situ* ^{15}N tracing experiment (**Paper III**) showed that cumulative ^{15}N recovery in emitted N_2O during nine days accounted for about 6.0% of added ^{15}N tracer in the upper hillslope soils (Fig. 4.2). End-member mixing analysis demonstrated that the contribution of nitrification and denitrification to N_2O production varied with changing WFPS (Fig. 4.8). Large fluxes occurred at high WFPS values, and could be apportioned

predominantly to denitrification, which matches previous observations by Zhu *et al.* (2013d) at TSP, reporting 71% to 100% of the emitted N_2O from hillslope soils deriving from denitrification. However, the contribution of nitrification to N_2O emission increased when WFPS decreased below 60% at the upper site and below 70% at the lower site (Fig. 4.8). Khalil et al. (2004) and Mathieu et al. (2006) found that N_2O emissions from nitrification dominated (> 60%) in unsaturated agricultural soils. Also, in acid subtropical forest soils of China, Zhang et al. (2011) found 27% to 42% of the N_2O production being due to nitrification, at WFPS values of 40% to 52%. It is likely that nitrification in the aerated hillslope soils of TSP plays an important role for N_2O emissions during dry periods.

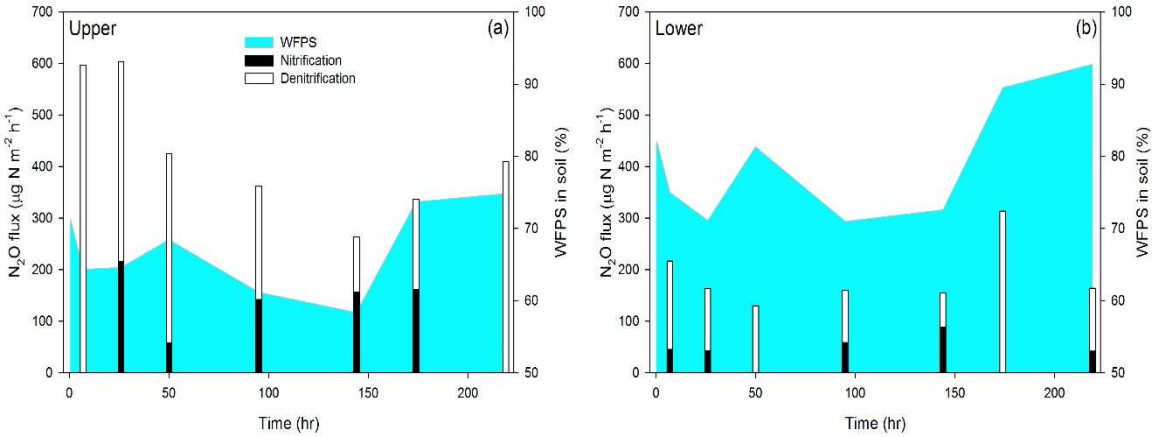

Fig. 4.8 Mean N_2O fluxes attributed to nitrification and denitrification at the upper site (**a**) and the lower site (**b**). The shaded background indicates water filled pore space (WFPS; average values are presented, n =3). Figure from **Paper III**.

4.6 P addition to N-saturated forest: an option to mitigate GHG emissions?

Addition of P to the hillslope of TSP substantially increased plant-available P in soil (Table 2 in **Paper IV**). In 1.5 years following P addition, a significant decline in soil water NO_3^- concentrations (0-5 cm; Fig. 4.9a) was observed, and this decline was associated with a strong decrease of N_2O fluxes by 50% (Fig. 4.9b). This is consistent with a number of other studies, suggesting that decreased mineral N content in soil, likely due to stimulated plant uptake, is responsible for the reduced N_2O emission (Hall & Matson, 1999; Baral *et al.*, 2014; Mori *et al.*, 2014). However, enhanced forest growth was not detected within the study period, in neither tree biomass, litterfall nor needles (Table S1 and Fig. S6 in **Paper IV**). This could be due to the shortness of the observation period (Alvarez-Clare *et al.*, 2013) and overlooked N uptake by understory biomass (Fraterrigo

et al., 2011). Studies in tropical forests of South Ecuador (Martinson *et al.*, 2013) and South China (Zheng *et al.*, 2016) reported no significant effect on N_2O emission within 2 years after P addition, which most likely can be attributed to the significantly smaller mineral N concentrations in these soils as compared with TSP soils (Huang *et al.*, 2015).

Two of three reference plots at TSP showed net CH_4 emission during the two years of observation (Fig. 4.9c). This is in contrast to the commonly reported CH_4 sink function of forested upland soils (Dutaur & Verchot, 2007; Ciais *et al.*, 2013). Addition of P strongly affected CH_4 fluxes, and changed net emission to a small net uptake (Fig. 4.9c). The observed P effect on CH_4 fluxes is consistent with previous studies (Zhang *et al.*, 2011b; Mori *et al.*, 2013b, 2013c). High availability of NH_4^+ has been suggested to inhibit CH_4 uptake in soil (Veldkamp *et al.*, 2001; Bodelier & Laanbroek, 2004). Although I only observed a slight decrease in the soil water NH_4^+ pool (Fig. S2 in **Paper IV**), the significant reduction in soil NO_3^- concentrations (Fig. 4.9a) likely also reflects smaller NH_4^+ concentrations, as NH_4^+ is the substrate for NO_3^- production by nitrification. Therefore, it is likely that the increased CH_4 uptake after P addition is due to an alleviation of NH_4^+ inhibition on CH_4 oxidation (Mori *et al.*, 2013c). Thus, my findings contribute to the ongoing debate on whether P availability affects soil CH_4 uptake directly via stimulation of methanotrophic activity or indirectly by altering N cycling (Veraart *et al.*, 2015).

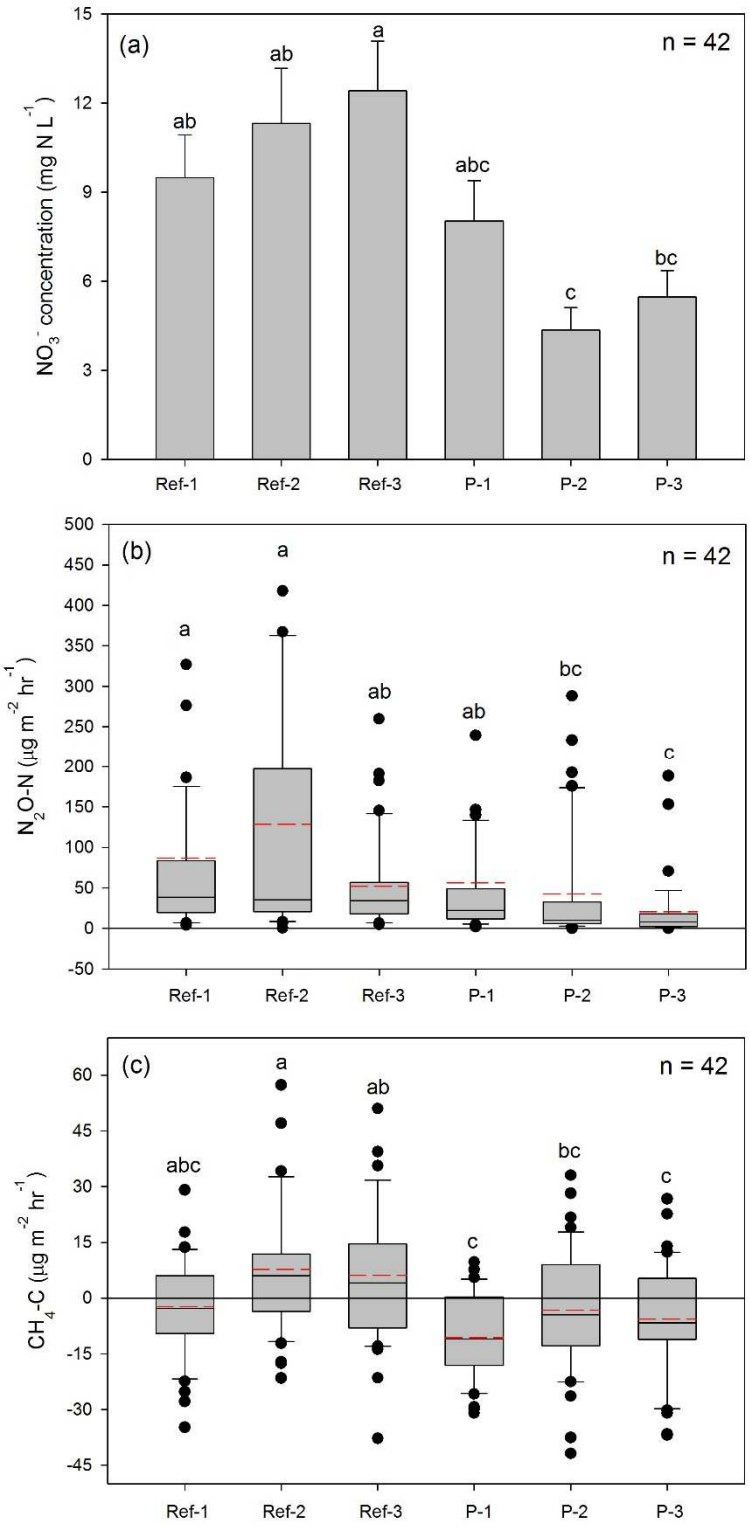

Fig. 4.9 Mean NO_3^- concentrations in soil water (0-5 cm; **a**), and box whisker plots of N_2O fluxes (**b**) and CH_4 fluxes (**c**) for three blocks in reference and P treatments throughout 1.5 years after the P addition; small letters indicate significant differences among treatments and blocks. Ref-1 and P-1 belong to the same block, and the same rule applies to blocks 2 and 3; red dashed lines in box whisker plots indicate mean values. Figure from **Paper IV**.

5. Conclusions

Forests in South China receive increasing loads of reactive N from the atmosphere. In this thesis, I studied transformation processes and fate of atmogenic N deposited as NH_4^+ and NO_3^- on subtropical forest soils in South China. The turnover of N was investigated across multiple spatial (catchment to region) and temporal (short to long term) scales, mainly by field observation. Emissions of N_2O and CH_4 were investigated in an attempt to better understand sources of and mitigation options for these greenhouse gases. In addition, I contributed to the development of a robust but simplified "denitrifier method", which was indispensable for analyzing dual NO_3^- isotopes in large amounts of field samples (throughfall, soil and stream waters). Stable isotopes (^{18}O, ^{15}N) in NO_3^- proved to be a powerful tool for studying N cycling and in particular denitrification, at the catchment scale. Experiments with ^{15}N-labelled substrates (NH_4^+, NO_3^-, glutamate) gave valuable insights into the complex N cycle of acid soils in warm-humid climate. The main conclusions are:

1. Atmogenic N deposited as NO_3^- is not retained in the soil, but leaches near-quantitatively from the topsoil (0-15 cm). This is in line with "N-saturation", ascribed to many South Chinese forests, denoting a critical state characterized by excessive N-leaching. By contrast, atmogenic NH_4^+ is rapidly retained in the soil organic N pool, but eventually transformed to NO_3^-. Obviously, acid soils of N-saturated subtropical forests support efficient microbial nitrification activity, be it through autotrophic nitrification by NH_4^+ oxidation or heterotrophic nitrification, i.e. by direct conversion of organic N to NO_3^-. The latter process seemed to be more important in the wetter soils at TSP. My study adds to the understanding of a dynamic N turnover of NH_4^+ in acid subtropical soils and helps to explain the near-quantitative N leaching (as NO_3^-) of both NH_4^+ and NO_3^- deposited to the system.

2. Across five studied subtropical forest catchments, progressive enrichment in dual NO_3^- isotopes along the hydrological flow paths indicated efficient nitrification on well-drained hillslope soils and strong denitrification in saturated groundwater discharge zones. Hydrological connectivity of oxidative and reductive landscape zones via NO_3^- transport over argic Bt horizons was thus identified as the central mechanism behind the high apparent N retention in these catchments. At the southern monsoonal sites with well-developed groundwater discharge zones, comparison of NO_3^- attenuation across

catchments differing in N input suggested that N removal by denitrification is proportional to N deposition. By contrast, two catchments with less developed groundwater discharge zones in northern China retain little N, most probably because hydrological connectivity between HS soils and groundwater discharge zone is week in a drier climate.

3. Large N_2O emission, summing up to an annual rate of ~ 5.3 kg N ha^{-1} yr^{-1} was observed in hillslope soils at TSP. The amount of N re-emitted to the atmosphere as N_2O equaled about 10% of the annual N deposition at this site. This confirms that the N-saturated TSP forest is a regional hotspot for N_2O. Denitrification is the main source, especially during episodes of large N_2O emission fluxes, whereas the contribution of nitrification to N_2O emission is small.

4. P addition significantly decreased soil water NO_3^- concentration already in the first year after addition, likely due to enhanced plant or microbial N uptake. This was associated with a strong (50%) reduction in N_2O emission. Meanwhile, P addition also reduced net CH_4 emissions and turned the soil into a small, but measurable CH_4 sink. This may be due to decreased NH_4^+ inhibition of CH_4 oxidation, when the mineral N availability decreases in soil. These findings suggest that P application to N-saturated forest soils has the potential to mitigate emissions of both N_2O and CH_4.

References

Aber JD, Nadelhoffer KJ, Steudler P, Melillo JM (1989) Nitrogen Saturation in Northern Forest Ecosystems. *BioScience*, **39**, 378–386.

Aber J, McDowell W, Nadelhoffer K et al. (1998) Nitrogen saturation in temperate forest ecosystems - hypotheses revisited. *Bioscience*, **48**, 921–934.

Alvarez-Clare S, Mack MC, Brooks M (2013) A direct test of nitrogen and phosphorus limitation to net primary productivity in a lowland tropical wet forest. *Ecology*, **94**, 1540–1551.

Arnold J, Corre MD, Veldkamp E (2009) Soil N cycling in old-growth forests across an Andosol toposequence in Ecuador. *Forest Ecology and Management*, **257**, 2079–2087.

Bala G, Devaraju N, Chaturvedi RK, Caldeira K, Nemani R (2013) Nitrogen deposition: How important is it for global terrestrial carbon uptake. *Biogeosciences*, **10**, 7147–7160.

Baral BR, Kuyper TW, Van Groenigen JW (2014) Liebig's law of the minimum applied to a greenhouse gas: Alleviation of P-limitation reduces soil N_2O emission. *Plant and Soil*, **374**, 539–548.

Bateman EJ, Baggs EM (2005) Contributions of nitrification and denitrification to N_2O emissions from soils at different water-filled pore space. *Biology and Fertility of Soils*, **41**, 379–388.

Billy C, Billen G, Sebilo M, Birgand F, Tournebize J (2010) Nitrogen isotopic composition of leached nitrate and soil organic matter as an indicator of denitrification in a sloping drained agricultural plot and adjacent uncultivated riparian buffer strips. *Soil Biology and Biochemistry*, **42**, 108–117.

Bobbink R, Hicks K, Galloway J et al. (2010) Global assessment of nitrogen deposition effects on terrestrial plant diversity. *Ecological Applications*, **20**, 30–59.

Bodelier PLE, Laanbroek HJ (2004) Nitrogen as a regulatory factor of methane oxidation in soils and sediments. *FEMS Microbiology Ecology*, **47**, 265–277.

Bodirsky BL, Popp A, Lotze-Campen H et al. (2014) Reactive nitrogen requirements to feed the world in 2050 and potential to mitigate nitrogen pollution. *Nature communications*, **5**, 3858.

De Boer W, Kowalchuk G (2001) Nitrification in acid soils : micro-organisms and mechanisms. *Soil Biology and Biochemistry*, **33**, 853–866.

Booth MS, Stark JM, Rastetter E (2005) Controls on nitrogen cycling in terrestrial ecosystems: a synthetic analysis of literature data. *Ecological Monographs*, **72**, 139–157.

Bottcher J, Strebel O, Voerkelius S, Schmidt H (1990) Using isotope fractionation of nitrate-nitrogen and nitrate-oxygen for evaluation of microbial denitrification in a sandy aquifer. *Journal of Hydrology*, **114**, 413–424.

Bouwman AF, Beusen AHW, Griffioen J et al. (2013) Global trends and uncertainties in terrestrial denitrification and N_2O emissions. *Philosophical transactions of the Royal Society of London. Series B, Biological sciences*, **368**, 1–11.

Brenzinger K, Dörsch P, Braker G (2015) pH-driven shifts in overall and transcriptionally active denitrifiers control gaseous product stoichiometry in growth experiments with extracted bacteria from soil. *Frontiers in Microbiology*, **6**, 1–11.

Butterbach-Bahl K, Nemitz E, Zaehle S et al. (2011) Chapter 19: Effect of reactive nitrogen on the European greenhouse balance *In: The European Nitrogen Assessment* (ed Sutton MA). Cambridge University Press, 434-462 pp.

Butterbach-Bahl K, Baggs EM, Dannenmann M, Kiese R, Zechmeister-Boltenstern S (2013) Nitrous oxide emissions from soils: how well do we understand the processes and their controls? *Philosophical transactions of the Royal Society of London. Series B, Biological sciences*, **368**, 20130122.

Casciotti KL, Sigman DM, Hastings MG, Böhlke JK, Hilkert A (2002) Measurement of the oxygen isotopic composition of nitrate in seawater and freshwater using the denitrifier method. *Analytical chemistry*, **74**, 4905–12.

Chen XY, Mulder J (2007a) Atmospheric deposition of nitrogen at five subtropical forested sites in South China. *The Science of the total environment*, **378**, 317–30.

Chen X, Mulder J (2007b) Indicators for nitrogen status and leaching in subtropical forest ecosystems, South China. *Biogeochemistry*, **82**, 165–180.

Chen XY, Mulder J, Wang YH, Zhao DW, Xiang RJ (2004) Atmospheric deposition, mineralization and leaching of nitrogen in subtropical forested catchments, South China. *Environmental geochemistry and health*, **26**, 179–86.

Chen Z, Ding W, Xu Y et al. (2015) Importance of heterotrophic nitrification and dissimilatory nitrate reduction to ammonium in a cropland soil: Evidences from a ^{15}N tracing study to literature synthesis. *Soil Biology and Biochemistry*, **91**, 65–75.

Chen H, Gurmesa GA, Zhang W et al. (2016) Nitrogen saturation in humid tropical forests after 6 years of nitrogen and phosphorus addition: Hypothesis testing.

Functional Ecology, **30**, 305–313.

Cheng Y, Zhang JB, Wang J, Cai ZC, Wang SQ (2015) Soil pH is a good predictor of the dominating N_2O production processes under aerobic conditions. *Journal of Plant Nutrition and Soil Science*, **61**. 506-515.

Christensen S, Tiedje JM (1988) Sub-parts-per-billion nitrate method: use of an N_2O producing denitrifier to convert NO_3^- or $^{15}NO_3^-$ to N_2O. *Applied and Environmental Microbiology*, **54**, 1409–1413.

Ciais P, Sabine C, Bala G et al. (2013) Carbon and Other Biogeochemical Cycles *In: Climate Change 2013: The Physical Science Basis.* (eds Stocker, TF, Qin D, Plattner GK, Tignor M, Allen SK, Boschung J, Nauels A, Xia Y, Bex V and Midgley PM). Cambridge University Press, Cambridge, United Kingdom and New York, NY, USA, 465-570 pp.

Cirmo CP, McDonnell JJ (1997) Linking the hydrologic and biogeochemical controls of nitrogen transport in near-stream zones of temperate-forested catchments: A review. *Journal of Hydrology*, **199**, 88–120.

Clark CM, Tilman D (2008) Loss of plant species after chronic low-level nitrogen deposition to prairie grasslands. *Nature*, **451**, 712–5.

Clément J, Holmes R, Peterson B, Pinay G (2003) Isotopic investigation of denitrification in a riparian ecosystem in western France. *Journal of Applied Ecology*, **40**, 1035–1048.

Corre MD, Brumme RR, Veldkamp E, Beese FO (2007) Changes in nitrogen cycling and retention processes in soils under spruce forests along a nitrogen enrichment gradient in Germany. *Global Change Biology*, **13**, 1509–1527.

Corre MD, Veldkamp E, Arnold J, Joseph Wright S (2010) Impact of elevated N input on soil N cycling and losses in old-growth lowland and montane forests in Panama. *Ecology*, **91**, 1715–1729.

Cui S, Shi Y, Groffman PM, Schlesinger WH, Zhu Y-G (2013) Centennial-scale analysis of the creation and fate of reactive nitrogen in China (1910-2010). *Proceedings of the National Academy of Sciences of the United States of America*, **110**, 2052–7.

Curtis CJ, Evans CD, Goodale CL, Heaton THE (2011) What Have Stable Isotope Studies Revealed About the Nature and Mechanisms of N Saturation and Nitrate Leaching from Semi-Natural Catchments? *Ecosystems*, **14**, 1021–1037.

Davidson EA, Hart SC, Shanks CA, Firestone MK (1991) Measuring gross nitrogen

minearlization, immobilization, and nitrification by ^{15}N isotopic pool dilution in intact soil cores. *Journal of Soil Science*, **42**, 335–349.

Dentener F, Drevet J, Lamarque JF et al. (2006) Nitrogen and sulfur deposition on regional and global scales: A multimodel evaluation. *Global Biogeochemical Cycles*, **20**.

Dise NB, Wright RF (1995) Nitrogen leaching from European forests in relation to nitrogen deposition. *Forest Ecology and Management*, **71**, 153–161.

Dörsch P, Braker G, Bakken LR (2012) Community-specific pH response of denitrification: Experiments with cells extracted from organic soils. *FEMS Microbiology Ecology*, **79**, 530–541.

Du E, de Vries W, Han W, Liu X, Yan Z, Jiang Y (2016) Imbalanced phosphorus and nitrogen deposition in China's forests. *Atmospheric Chemistry and Physics*, 1–17.

Duan L, Liu J, Xin Y, Larssen T (2013) Air-pollution emission control in China: Impacts on soil acidification recovery and constraints due to drought. *Science of the Total Environment*, **463**–**464**, 1031–1041.

Duan L, Yu Q, Zhang Q et al. (2016) Acid deposition in Asia: Emissions, deposition, and ecosystem effects. *Atmospheric Environment*. In Press.

Duncan JM, Groffman PM, Band LE (2013) Towards closing the watershed nitrogen budget: Spatial and temporal scaling of denitrification. *Journal of Geophysical Research: Biogeosciences*, **118**, 1105–1119.

Duncan J, Band J, Groffman P, Bernhardt E (2015) Mechanisms driving the seasonality of catchment scale nitrate export: Evidence for riparian ecohydrologil controls. *Water Resources Research*, **51**, 3982-3997.

Dutaur L, Verchot L V. (2007) A global inventory of the soil CH_4 sink. *Global Biogeochemical Cycles*, **21**, GB4013.

Fang YT, Gundersen P, Mo JM, Zhu WX (2008) Input and output of dissolved organic and inorganic nitrogen in subtropical forests of South China under high air pollution. *Biogeosciences*, **5**, 339–352.

Fang Y, Gundersen P, Zhang W et al. (2009) Soil–atmosphere exchange of N_2O, CO_2 and CH_4 along a slope of an evergreen broad-leaved forest in southern China. *Plant and Soil*, **319**, 37–48.

Fang Y, Koba K, Makabe A, Zhu F, Fan S, Liu X, Muneoki Y (2012) Low $\delta^{18}O$ values of nitrate produced from nitrification in temperate forest soils. *Environmental Science & Technology*, **46**, 8723–8730.

Fang Y, Koba K, Makabe A, Takahashi C, Zhu W, Hayashi T (2015) Microbial denitrification dominates nitrate losses from forest ecosystems. *Proceedings of the National Academy of Sciences of the United States of America*, **112**, 1470-1474.

Firestone MK, Davidson EA (1989) Microbiological Basis of NO and N_2O Production and Consumption in Soil *In: Exchange of Tracer Gases between Terrestrial Ecosystems and the Atmosphere.* (eds Andreae MO and Schimel DS). John Wiley & Sons Ltd, New York, 7-21 pp.

Focht DD, Verstraete W (1977) Biochemical ecology of nitrification and denitrification *In: Advance in Microbial Ecology* (ed Alexander M). Plenum Press, New York, 135–214 pp.

Fowler D, Coyle M, Skiba U et al. (2013) The global nitrogen cycle in the twenty- first century. *Philosophical transactions of the Royal Society of London. Series B, Biological sciences*, **368**, 20130112.

Fraterrigo JM, Strickland MS, Keiser AD, Bradford MA (2011) Nitrogen uptake and preference in a forest understory following invasion by an exotic grass. *Oecologia*, **167**, 781–791.

Fry B (2007) *Stable Isotope Ecology*. Springer, New York, 194-270 pp.

Van Gaalen JF, Kruse S, Lafrenz WB, Burroughs SM (2013) Predicting Water Table Response to Rainfall Events, Central Florida. *GroundWater*, **51**, 350–362.

Galloway J, Aber J, Erisman J, Speitzinger S, Howarth R, Cowling E, Cosby A (2003) The nitrogen cascade. *Bioscience*, **53**, 341–356.

Galloway JN, Dentener FJ, Capone DG et al. (2004) *Nitrogen cycles: Past, present, and future*, Vol. 70. 153-226 pp.

Galloway JN, Townsend AR, Erisman JW et al. (2008) Transformation of the nitrogen cycle: recent trends, questions, and potential solutions. *Science*, **320**, 889–92.

Gao W, Kou L, Yang H, Zhang J, Müller C, Li S (2016) Are nitrate production and retention processes in subtropical acidic forest soils responsive to ammonium deposition? *Soil Biology and Biochemistry*, **100**, 102–109.

Griffiths NA, Jackson CR, McDonnell JJ, Klaus J, Du E, Bitew MM (2016) Dual nitrate isotopes clarify the role of biological processing and hydrological flow paths on nitrogen cycling in subtropical low-gradient watersheds. *Journal of Geophysical Research: Biogeosciences*, **121**.

Groffman PM (2012) Terrestrial denitrification: challenges and opportunities. *Ecological Processes*, **1**, 1–11.

Groffman PM, Altabet MA, Böhlke JK et al. (2006) Methods for Measuring Denitrification : Diverse Approaches to a Difficult Problem. *Ecological Application*, **16**, 2091–2122.

Gruber N, Galloway JN (2008) An Earth-system perspective of the global nitrogen cycle. *Nature*, **451**, 293–296.

Gubry-Rangin C, Hai B, Quince C et al. (2011) Niche specialization of terrestrial archaeal ammonia oxidizers.

Gundersen P, Emmett BA, Kjønaas OJ, Koopmans CJ, Tietema A (1998a) Impact of nitrogen deposition on nitrogen cycling in forests: A synthesis of NITREX data. *Forest Ecology and Management*, **101**, 37–55.

Gundersen P, Callesena I, Vriesb W (1998b) Nitrate leaching in forest ecosystems is related to forest floor C/N ratios. *Environmental Pollution*, **102**, 403–407.

Gundersen P, Christiansen JR, Alberti G et al. (2012) The response of methane and nitrous oxide fluxes to forest change in Europe. *Biogeosciences*, **9**, 3999–4012.

Hall SJ, Matson PA (1999) Nitrogen oxide emissions after nitrogen additions in tropical forests. *Nature*, **400**, 152-155.

Hart SC, Myrold DD (1996) ^{15}N tracer studies of soil nitrogen transformations *In: Mass Spectrometry of soils.* (eds Boutton TW and Yamasaki S). Macerl Dekker, inc, New York, 225-245 pp.

He H, Jansson PE, Svensson M, Meyer A, Klemedtsson L, Kasimir Å (2016) Factors controlling nitrous oxide emission from a spruce forest ecosystem on drained organic soil, derived using the CoupModel. *Ecological Modelling*, **321**, 46–63.

Huang Y, Kang R, Mulder J, Zhang T, Duan L (2015) Nitrogen saturation, soil acidification, and ecological effects in a subtropical pine forest on acid soil in southwest China. *Journal of Geophysical Research: Biogeosciences*, **120**, 2457–2472.

Hughes D A (2004) Incorporating groundwater recharge and discharge functions into an existing monthly rainfall–runoff model. *Hydrological Sciences Journal*, **49**, 37–41.

Hütsch BW (1996) Methane oxidation in soils of two long-term fertilization experiments in Germany. *Soil Biology and Biochemistry*, **28**, 773–782.

Jaworski NA, Howarth RW, Hetling LJ (1997) Atmospheric Deposition of Nitrogen Oxides onto the Landscape Contributes to Coastal Eutrophication in the Northeast United States. *Environmental Science & Technology*, **31**, 1995–2004.

Jencso KG, McGlynn BL, Gooseff MN, Wondzell SM, Bencala KE, Marshall LA

(2009) Hydrologic connectivity between landscapes and streams: Transferring reach- and plot-scale understanding to the catchment scale. *Water Resources Research*, **45**, 1–16.

Ju X, Lu X, Gao Z et al. (2011) Processes and factors controlling N_2O production in an intensively managed low carbon calcareous soil under sub-humid monsoon conditions. *Environmental Pollution*, **159**, 1007–1016.

Kendall C, Elliott EM, Wankel SD (2007) Tracing anthropogenic inputs of nitrogen to ecosystems. *In Stable Isotopes in Ecology and Environmental Science, 2nd ed.* (eds Michener, R. H., Lajtha, K.). Blackwell Publishing, New Jersey, USA 375–449 pp.

Khalil K, Mary B, Renault P (2004) Nitrous oxide production by nitrification and denitrification in soil aggregates as affected by O_2 concentration. *Soil Biology and Biochemistry*, **36**, 687–699.

Knöller K, Vogt C, Haupt M, Feisthauer S, Richnow HH (2011) Experimental investigation of nitrogen and oxygen isotope fractionation in nitrate and nitrite during denitrification. *Biogeochemistry*, **103**, 371–384.

Knowles R (1982) Denitrification. *Microbiological Reviews*, **46**, 43–70.

Koba K, Fang Y, Mo J et al. (2012) The ^{15}N natural abundance of the N lost from an N-saturated subtropical forest in southern China. *Journal of Geophysical Research: Biogeosciences*, **117**, 1–13.

Kool DM, Wrage N, Oenema O, Van Kessel C, Van Groenigen JW (2011) Oxygen exchange with water alters the oxygen isotopic signature of nitrate in soil ecosystems. *Soil Biology and Biochemistry*, **43**, 1180–1185.

Larssen T et al. (2004) *Integrated Monitoring Program on Acidification of Chinese Terrestrial Systems-IMPACTS*.

Larssen T, Carmichael GR (2000) Acid rain and acidification in China: The importance of base cation deposition. *Environmental Pollution*, **110**, 89–102.

Larssen T, Duan L, Mulder J (2011) Deposition and leaching of sulfur, nitrogen and calcium in four forested catchments in China: implications for acidification. *Environmental science & technology*, **45**, 1192–8.

Leininger S, Urich T, Schloter M et al. (2006) Archaea predominate among ammonia-oxidizing prokaryotes in soils. *Nature*, **442**, 806–809.

Likens GE (2013) *Biogeochemistry of a forested ecosystem, third edition*. 1-208 pp.

Linn DM, Doran JW (1984) Effect of Water-Filled Pore Space on Carbon Dioxide and Nitrous Oxide Production in Tilled and Nontilled Soils. *Soil Science Society of*

America Journal, **48**, 1267–1272.

Liu B, Mørkved PT, Frostegård A, Bakken LR (2010) Denitrification gene pools, transcription and kinetics of NO, N_2O and N_2 production as affected by soil pH. *FEMS Microbiology Ecology*, **72**, 407–17.

Liu L, Gundersen P, Zhang T, Mo J (2012) Effects of phosphorus addition on soil microbial biomass and community composition in three forest types in tropical China. *Soil Biology and Biochemistry*, **44**, 31–38.

Liu X, Zhang Y, Han W et al. (2013) Enhanced nitrogen deposition over China. *Nature*, **494**, 459–62.

Liu B, Frostegård Å, Bakken L (2014) Impaired reduction of N_2O to N_2 in acid soils is due to a posttranscriptional interference with the expression of nosZ. *mBio*, **5**, 1383–14.

Lovett GM, Goodale CL (2011) A New Conceptual Model of Nitrogen Saturation Based on Experimental Nitrogen Addition to an Oak Forest. *Ecosystems*, **14**, 615–631.

Lu X, Mo J, Gilliam FS, Zhou G, Fang Y (2010) Effects of experimental nitrogen additions on plant diversity in an old-growth tropical forest. *Global Change Biology*, **16**, 2688–2700.

Lu M, Yang Y, Luo Y et al. (2011) Responses of ecosystem nitrogen cycle to nitrogen addition: A meta-analysis. *New Phytologist*, **189**, 1040–1050.

Mariotti A, Germon J, Hubert P, Kaiser P, Letolle R, Tardieux A, Tardieux P (1981) Experimental determination of nitrogen kinetic isotope fractionation: some principles; illustration for the denitrification and nitrification processes. *Plant and Soil*, **62**, 413–430.

Mariotti A, Landreau A, Simon B (1988) ^{15}N isotope biogeochemistry and natural denitrification process in groundwater: Application to the chalk aquifer of northern France. *Geochimica et Cosmochimica Acta*, **52**, 1869–1878.

Martinson GO, Corre MD, Veldkamp E (2013) Responses of nitrous oxide fluxes and soil nitrogen cycling to nutrient additions in montane forests along an elevation gradient in southern Ecuador. *Biogeochemistry*, **112**, 625–636.

Mathieu O, Hénault C, Lévêque J, Baujard E, Milloux MJ, Andreux F (2006) Quantifying the contribution of nitrification and denitrification to the nitrous oxide flux using ^{15}N tracers. *Environmental Pollution*, **144**, 933–940.

Le Mer J, Roger P (2010) Production, oxidation, emission and consumption of methane

by soils: A review. *European Jornal of Soil Biology*, **37**.

Mori T, Ohta S, Ishizuka S, Konda R, Wicaksono A, Heriyanto J, Hardjono A (2013a) Effects of phosphorus addition with and without ammonium, nitrate, or glucose on N_2O and NO emissions from soil sampled under Acacia mangium plantation and incubated at 100% of the water-filled pore space. *Biology and Fertility of Soils*, **49**, 13–21.

Mori T, Ohta S, Ishizuka S, Konda R, Wicaksono A, Heriyanto J (2013b) Effects of phosphorus application on CH_4 fluxes in an Acacia mangium plantation with and without root exclusion. *Tropics*, **22**, 13–17.

Mori T, Ohta S, Ishizuka S et al. (2013c) Soil greenhouse gas fluxes and C stocks as affected by phosphorus addition in a newly established Acacia mangium plantation in Indonesia. *Forest Ecology and Management*, **310**, 643–651.

Mori T, Ohta S, Ishizuka S, Konda R, Wicaksono A, Heriyanto J (2014) Phosphorus application reduces N_2O emissions from tropical leguminous plantation soil when phosphorus uptake is occurring. *Biology and Fertility of Soils*, **50**, 45–51.

Morley N, Baggs EM, Dörsch P, Bakken L (2008) Production of NO, N_2O and N_2 by extracted soil bacteria, regulation by NO_2^- and O_2 concentrations. *FEMS Microbiology Ecology*, **65**, 102–112.

Morse J, Duran J, Beall F, Enanga EM, Creed IF, Fernandez I, Groffman PM (2014) Soil denitrification fluxes from three northeastern North American forests across a range of nitrogen deposition. *Oecologia*, **177**, 17–27.

Mulholland PJ, Helton AM, Poole GC et al. (2008) Stream denitrification across biomes and its response to anthropogenic nitrate loading. *Nature*, **452**, 202–205.

Müller AK, Matson AL, Corre MD, Veldkamp E (2015) Soil N_2O fluxes along an elevation gradient of tropical montane forests under experimental nitrogen and phosphorus addition. *Frontiers in Earth Science*, **3**, 1–12.

Nieder R, Benbi DK, Scherer HW (2011) Fixation and defixation of ammonium in soils: A review. *Biology and Fertility of Soils*, **47**, 1–14.

Niu S, Classen AT, Dukes JS et al. (2016) Global patterns and substrate-based mechanisms of the terrestrial nitrogen cycle. *Ecology Letters*, **19**, 697–709.

Osaka K, Ohte N, Koba K et al. (2010) Hydrological influences on spatiotemporal variations of $\delta^{15}N$ and $\delta^{18}O$ of nitrate in a forested headwater catchment in central Japan: Denitrification plays a critical role in groundwater. *Journal of Geophysical Research*, **115**, G02021.

Parkin TB (1987) Soil microsites as a source of denitrification variability. *Soil Science Society of America Journal*, **51**, 1194–1199.

Reay DS, Dentener F, Smith P, Grace J, Feely RA (2008) Global nitrogen deposition and carbon sinks. *Nature Geoscience*, **1**, 430–437.

Reay DS, Davidson EA, Smith KA, Smith P, Melillo JM, Dentener F, Crutzen PJ (2012) Global agriculture and nitrous oxide emissions. *Nature Climate Change*, **2**, 410–416.

Robinson D (2001) $\delta^{15}N$ as an integrator of the nitrogen. *TRENDS in Ecology & Evolution*, **16**, 153–162.

Rose L, Sebestyen SD, Elliott EM, Koba K (2014) Drivers of atmospheric nitrate processing and export in forested catchments. *Water Resources Research*, **51**, 1333–1352.

Rose LA, Elliott EM, Adams MB (2015) Triple Nitrate Isotopes Indicate Differing Nitrate Source Contributions to Streams Across a Nitrogen Saturation Gradient. *Ecosystems*, **18**, 1209–1223.

Sabo RD, Nelson DM, Eshleman KN (2015) Episodic, seasonal, and annual export of atmospheric and microbial nitrate from a temperate forest. *Geophysical Research Letters*, **43**, 683–691.

Sahrawat KL (2008) Factors Affecting Nitrification in Soils. *Communications in Soil Science and Plant Analysis*, **39**, 1436–1446.

Schulze ED, Luyssaert S, Ciais P et al. (2009) Importance of methane and nitrous oxide for Europe's terrestrial greenhouse-gas balance. *Nature Geoscience*, **2**, 842–850.

Seip HM, Aagaard P, Angell V et al. (1999) Acidification in China: Assessment based on studies at forested sites from Chongqing to Guangzhou. *Ambio*, **28**, 522–528.

Seitzinger S, Harrison J, Bohlke J et al. (2006) Denitrification across landscaes and waterscapes: a synthesis. *Ecological Applications*, **16**, 2064–2090.

Shi Y, Cui S, Ju X, Cai Z, Zhu Y (2015) Impacts of reactive nitrogen on climate change in China. *Scientific Reports*, **5**, 8118.

Sigman DM, Casciotti KL, Andreani M, Barford C, Galanter M, Böhlke JK (2001) A bacterial method for the nitrogen isotopic analysis of nitrate in seawater and freshwater. *Analytical chemistry*, **73**, 4145–53.

Silver WL, Herman DJ, Firestone MK (2001) Dissimilatory nitrate reduction to ammonium in upland tropical forest soils. *Ecology*, **82**, 2410–2416.

Simek M, Cooper JE (2002) The influence of pH on denitrification:Progress towards the

understanding of this interaction over the last fifty years. *European Journal of Soil Science*, **53**, 345–354.

Smith K a., Ball T, Conen F, Dobbie KE, Massheder J, Rey A (2003) Exchange of greenhousegases between soil and atmosphere: interactions of soil physical factors and biological processes. *European Journal of Soil Science*, **54**, 779–791.

Sørbotten L (2011) Hill slope unsaturated flowpaths and soil moisture variability in a forested catchment in southwest China. *Master Thesis, Norwegian Univsity of Life Sciences*.

Sørbotten L, Stolte J, Wang Y, Mulder J (2016) Hydrological Response and Flow Pathways in Acrisols on a Forested Hillslope in Monsoonal Sub-tropical Climate, Chonqing, Southwest. *Pedosphere*, **Accepted**.

Sotta ED, Corre MD, Veldkamp E (2008) Differing N status and N retention processes of soils under old-growth lowland forest in Eastern Amazonia, Caxiuanã, Brazil. *Soil Biology and Biochemistry*, **40**, 740–750.

Søvik AK, Mørkved PT (2008) Use of stable nitrogen isotope fractionation to estimate denitrification in small constructed wetlands treating agricultural runoff. *The Science of the total environment*, **392**, 157–65.

Spalding RF, Exner ME, Martin GE, Snow DD (1993) Effects of sludge disposal on groundwater nitrate concentrations. *Journal of Hydrology*, **142**, 213–228.

Stevens RJ, Laughlin RJ, Burns LC, Arah JRM, Hood RC (1997) Measuring the contributions of nitrification and denitrification to the flux of nitrous oxide from soil. *Soil Biology and Biochemistry*, **29**, 139–151.

Tahovsk K, Kana J, Barta J, Oulehle F, Richter A, Santruckova H (2013) Microbial N immobilization is of great importance in acidified mountain spruce forest soils. *Soil Biology and Biochemistry*, **59**, 58–71.

Tang X, Liu S, Zhou G, Zhang D, Zhou C (2006) Soil-atmospheric exchange of CO_2, CH_4, and N_2O in three subtropical forest ecosystems in southern China. *Global Change Biology*, **12**, 546–560.

Templer PH, Silver WL, Pett-ridge J, Deangelis KM, Firestone MK (2008) Plant and Microbial Controls on Nitrogen Retention and Loss in a Humid Tropical Forest. *Ecology*, **89**, 3030–3040.

Templer PH, Mack MC, Chapin III FS et al. (2012) Sinks for nitrogen inputs in terrestrial ecosystems: a meta-analysis of ^{15}N tracer field studies. **93**, 1816–1829.

Teske A, Alm E, Regan JM, Toze S, Rittmann BE, Stahl DA (1994) Evolutionary

Relationships among Ammonia- and Nitrite-Oxidizing Bacteria. *Journal of Bacteriology*, **176**, 6623–6630.

Tian H, Lu C, Ciais P et al. (2016) The terrestrial biosphere as a net source of greenhouse gases to the atmosphere. *Nature*, **531**, 225–228.

Townsend AR, Howarth RW, Bazzaz FA et al. (2003) Human health effects of a changing global nitrogen cycle. *Frontiers in Ecology and the Environment*, **1**, 240–246.

Veldkamp E, Weitz AM, Keller M (2001) Management effects on methane fluxes in humid tropical pasture soils. *Soil Biology and Biochemistry*, **33**, 1493–1499.

Veldkamp E, Koehler B, Corre MD (2013) Indications of nitrogen-limited methane uptake in tropical forest soils. *Biogeosciences*, **10**, 5367–5379.

Venterea RT, Groffman PM, Verchot LV, Magill AH, Aber JD (2004) Gross nitrogen process rates in temperate forest soils exhibiting symptoms of nitrogen saturation. *Forest Ecology and Management*, **196**, 129–142.

Veraart AJ, Steenbergh AK, Ho A, Kim SY, Bodelier PLE (2015) Beyond nitrogen: The importance of phosphorus for CH4 oxidation in soils and sediments. *Geoderma*, **259**–**260**, 337–346.

Vitousek PM, Aber JD, Howarth RW et al. (1997) Human alteration of the global nitrogen cycle: causes and consequences. *Issues in Ecology*, **7**, 737–750.

Wang Y, Solberg S, Yu P, Myking T, Vogt RD, Du S (2007) Assessments of tree crown condition of two Masson pine forests in the acid rain region in south China. *Forest Ecology and Management*, **242**, 530–540.

Wang F, Li J, Wang X, Zhang W, Zou B, Neher DA, Li Z (2014) Nitrogen and phosphorus addition impact soil N_2O emission in a secondary tropical forest of South China. *Scientific reports*, **4**, 5615.

Weier KL, Doran JW, Power JF, Walters DT (1993) Denitrification and the Dinitrogen/Nitrous Oxide Ratio as Affected by Soil Water, Available Carbon, and Nitrate. *Soil Science Society of America Journal*, **57**, 66.

Weintraub SR, Taylor PG, Porder S, Cleveland CC, Asner GP, Townsend AR (2014) Topographic controls on soil nitrogen availability in a lowland tropical forest. *Ecology*, **96**, 1561–1574.

Werner C, Butterbach-Bahl K, Haas E, Hickler T, Kiese R (2007) A global inventory of N_2O emissions from tropical rainforest soils using a detailed biogeochemical model. *Global Biogeochemical Cycles*, **21**, GB 3010.

Wexler SK, Goodale CL, McGuire KJ, Bailey SW, Groffman PM (2014) Isotopic signals of summer denitrification in a northern hardwood forested catchment. *Proceedings of the National Academy of Sciences of the United States of America*, **111**, 16413-16418.

IUSS Working Group (2014) World Reference Base for Soil Resources 2014 *In: International soil classification system for naming soils and creating legends for soil maps. World Soil Resouces Reports.* FAO, Rome, 1-191 pp.

Wunderlich A, Meckenstock RU, Einsiedl F (2013) A mixture of nitrite-oxidizing and denitrifying microorganisms affects the $\delta^{18}O$ of dissolved nitrate during anaerobic microbial denitrification depending on the $\delta^{18}O$ of ambient water. *Geochimica et Cosmochimica Acta*, **119**, 31–45.

Xu W, Luo XS, Pan YP et al. (2015) Quantifying atmospheric nitrogen deposition through a nationwide monitoring network across China. *Atmospheric Chemistry and Physics*, **15**, 12345–12360.

Yakir D, Sternberg L da S (2000) The use of stable isotopes to study ecosystem gas exchange. *Oecologia*, 297–311.

Zhang L, Altabet M A, Wu T, Hadas O (2007) Sensitive measurement of NH_4^+ $^{15}N/^{14}N$ (delta $^{15}NH_4^+$) at natural abundance levels in fresh and saltwaters. *Analytical chemistry*, **79**, 5297–303.

Zhang W, Mo J, Zhou G et al. (2008a) Methane uptake responses to nitrogen deposition in three tropical forests in southern China. *Journal of Geophysical Research Atmospheres*, **113**, 1–10.

Zhang W, Mo J, Yu G, Fang Y, Li D, Lu X, Wang H (2008b) Emissions of nitrous oxide from three tropical forests in Southern China in response to simulated nitrogen deposition. *Plant and Soil*, **306**, 221–236.

Zhang J, Cai Z, Zhu T (2011a) N_2O production pathways in the subtropical acid forest soils in China. *Environmental Research*, **111**, 643–649.

Zhang T, Zhu W, Mo J, Liu L, Dong S (2011b) Increased phosphorus availability mitigates the inhibition of nitrogen deposition on CH_4 uptake in an old-growth tropical forest, southern China. *Biogeosciences*, **8**, 2805–2813.

Zhang J, Cai Z, Zhu T, Yang W, Müller C (2013) Mechanisms for the retention of inorganic N in acidic forest soils of southern China. *Scientific reports*, **3**, 2342.

Zhang W, Wang K, Luo Y et al. (2014a) Methane uptake in forest soils along an urban-to-rural gradient in Pearl River Delta, South China. *Scientific reports*, **4**, 5120.

Zhang W, Zhu X, Luo Y, Rafique R, Chen H, Huang J, Mo J (2014b) Responses of nitrous oxide emissions to nitrogen and phosphorus additions in two tropical plantations with N-fixing vs. non-N-fixing tree species. *Biogeosciences Discussions*, **11**, 1413–1442.

Zhao Y, Duan L, Xing J, Larssen T, Nielsen C, Hao J (2009) Soil Acidification in China : Is Controlling SO_2 Emissions Enough? *Environmental Science & Technology*, **43**, 8021–8026.

Zheng M, Zhang T, Liu L, Zhu W, Zhang W, Mo J (2016) Effects of nitrogen and phosphorus additions on nitrous oxide emission in a nitrogen-rich and two nitrogen-limited tropical forests. *Biogeosciences*, **13**, 3503–3517.

Zhu T, Meng T, Zhang J, Yin Y, Cai Z, Yang W, Zhong W (2013a) Nitrogen mineralization, immobilization turnover, heterotrophic nitrification, and microbial groups in acid forest soils of subtropical China. *Biology and Fertility of Soils*, **49**, 323–331.

Zhu J, Mulder J, Solheimslid SO, Dörsch P (2013b) Functional traits of denitrification in a subtropical forest catchment in China with high atmogenic N deposition. *Soil Biology and Biochemistry*, **57**, 577–586.

Zhu J, Mulder J, Wu LP, Meng XX, Wang YH, Dörsch P (2013c) Spatial and temporal variability of N_2O emissions in a subtropical forest catchment in China. *Biogeosciences*, **10**, 1309–1321.

Zhu J, Mulder J, Bakken L, Dörsch P (2013d) The importance of denitrification for N_2O emissions from an N-saturated forest in SW China: results from in situ ^{15}N labeling experiments. *Biogeochemistry*, **116**, 103–117.

Zhu T, Meng T, Zhang J, Yin Y, Cai Z, Yang W, Zhong W (2013e) Nitrogen mineralization, immobilization turnover, heterotrophic nitrification, and microbial groups in acid forest soils of subtropical China. *Biology and Fertility of Soils*, **49**, 323–331.

Zhu Q, De Vries W, Liu X et al. (2016) The contribution of atmospheric deposition and forest harvesting to forest soil acidification in China since 1980. *Atmospheric Environment*, In Press.

Paper I

Multiyear dual nitrate isotope signatures suggest that N-saturated subtropical forested catchments can act as robust N sinks

Longfei Yu, Jing Zhu, Jan Mulder and Peter Dörsch

Global Change Biology (2016), doi: 10.1111/gcb.13333

Global Change Biology

Global Change Biology (2016), doi: 10.1111/gcb.13333

Multiyear dual nitrate isotope signatures suggest that N-saturated subtropical forested catchments can act as robust N sinks

LONGFEI YU[1], JING ZHU[1,2], JAN MULDER[1] and PETER DÖRSCH[1]

[1]*Department of Environmental Sciences, Norwegian University of Life Sciences, Postbox 5003, N-1432 Aas, Norway,* [2]*Department of Environment and Resources, Guangxi Normal University, 541004 Guilin, China*

Abstract

In forests of the humid subtropics of China, chronically elevated nitrogen (N) deposition, predominantly as ammonium (NH_4^+), causes significant nitrate (NO_3^-) leaching from well-drained acid forest soils on hill slopes (HS), whereas significant retention of NO_3^- occurs in near-stream environments (groundwater discharge zones, GDZ). To aid our understanding of N transformations on the catchment level, we studied spatial and temporal variabilities of concentration and natural abundance ($\delta^{15}N$ and $\delta^{18}O$) of nitrate (NO_3^-) in soil pore water along a hydrological continuum in the N-saturated Tieshanping (TSP) catchment, southwest China. Our data show that effective removal of atmogenic NH_4^+ and production of NO_3^- in soils on HS were associated with a significant decrease in $\delta^{15}N\text{-}NO_3^-$, suggesting efficient nitrification despite low soil pH. The concentration of NO_3^- declined sharply along the hydrological flow path in the GDZ. This decline was associated with a significant increase in both $\delta^{15}N$ and $\delta^{18}O$ of residual NO_3^-, providing evidence that the GDZ acts as an N sink due to denitrification. The observed apparent ^{15}N enrichment factor (ε) of NO_3^- of about −5‰ in the GDZ is similar to values previously reported for efficient denitrification in riparian and groundwater systems. Episode studies in the summers of 2009, 2010 and 2013 revealed that the spatial pattern of $\delta^{15}N$ and $\delta^{18}O\text{-}NO_3^-$ in soil water was remarkably similar from year to year. The importance of denitrification as a major N sink was also seen at the catchment scale, as largest $\delta^{15}N\text{-}NO_3^-$ values in stream water were observed at lowest discharge, confirming the importance of the relatively small GDZ for N removal under base flow conditions. This study, explicitly recognizing hydrologically connected landscape elements, reveals an overlooked but robust N sink in N-saturated, subtropical forests with important implications for regional N budgets.

Keywords: denitrification, hydrological continuum, nitrification, $\delta^{15}N$, $\delta^{18}O$

Received 29 January 2016 and accepted 2 April 2016

Introduction

In East Asia, emissions of ammonia (NH_3) and nitrogen oxides (NO_x) have increased significantly during recent decades (Li & Lin, 2000; Liu *et al.*, 2013) and large amounts of reactive, atmogenic N enter terrestrial systems through wet and dry depositions (Emmett *et al.*, 1998; Galloway *et al.*, 2003). Numerous studies have documented N contamination of soils, groundwater, and aquatic ecosystems, causing elevated emissions of N_2O (Zhu *et al.*, 2013), a potent greenhouse gas, and ecological degradation, including acidification, eutrophication, and associated changes in biodiversity (Jaworski *et al.*, 1997; Vitousek *et al.*, 1997; Ju *et al.*, 2006; Clark & Tilman, 2008; Galloway *et al.*, 2008). In humid subtropical forests in south China, receiving atmogenic N inputs as large as 60 kg N ha^{-1} yr^{-1} (Chen & Mulder, 2007a; Zhao *et al.*, 2009), N saturation, associated with significant leaching of NO_3^- in well-drained soils, has been reported (Chen & Mulder, 2007b; Larssen *et al.*, 2011; Liu *et al.*, 2011). Leaching of N from soils occurs mainly as NO_3^-, even though atmogenic N inputs predominantly consist of ammonium (NH_4^+) (Chen & Mulder, 2007a). The apparent nitrification seems efficient even in the low-pH forest soils of south China (pH < 4; Zhang *et al.*, 2013). Despite significant NO_3^- leaching from well-drained hill slope (HS) soils, Larssen *et al.* (2011) found only limited export of NO_3^- in stream water and hypothesized that denitrification, but not plant uptake, in groundwater discharge zones (GDZ) of near-stream environments was responsible for the efficient NO_3^- removal. Recently, Zhu *et al.* (2013) confirmed a pronounced decline of NO_3^- in pore water along the water flow path in the GDZ of a headwater catchment at Tieshanping, southwest China. Unfortunately, catchment N budgets are difficult to close, mainly due to our inability to directly measure denitrification in soils (Groffman *et al.*, 2006; Duncan *et al.*, 2013).

Natural abundance of ^{15}N and ^{18}O in NO_3^- has been used to characterize biological N processing in complex

Correspondence: Peter Dörsch, tel. +47 67231836, fax +47 67230691, e-mail: peter.doersch@nmbu.no

landscapes (Kendall *et al*., 2007; Billy *et al*., 2010; Osaka *et al*., 2010; Fang *et al*., 2012, 2015; Rose *et al*., 2014). Kinetic isotopic fractionation occurs during N transformation processes, in which lighter isotopes (^{14}N and ^{16}O) are turned over slightly faster than heavier isotopes (^{15}N and ^{18}O) (Kendall *et al*., 2007; Bai *et al*., 2012). Thus, NO_3^- produced by nitrification is more depleted in ^{15}N than its substrate (NH_4^+), while microbial denitrification enriches both ^{15}N and ^{18}O in residual NO_3^- (Robinson, 2001; Fry, 2007). In aquifer studies, a value of ~0.5 for the $\delta^{18}O/\delta^{15}N$ ratio has been used to identify denitrification (Bottcher *et al*., 1990; Kendall *et al*., 2007). Other processes, such as mineralization, NO_3^- leaching and assimilation, are generally believed to have negligible ^{15}N fractionation (Mariotti *et al*., 1982; Billy *et al*., 2010). NO_3^- isotopes also carry information about source differentiation, in which atmosphere-derived NO_3^- often exhibits greater $\delta^{18}O$-NO_3^- compared to biologically processed NO_3^- (Pardo *et al*., 2004; Kendall *et al*., 2007; Sabo *et al*., 2016).

Understanding turnover processes of excess N at the landscape level in general and identifying zones of N mobilization and dissipation in particular are prerequisites for modeling regional N balances and are important for regional assessments of carbon (C) sequestration (Houlton & Bai, 2009; Bouwman *et al*., 2013; Houlton *et al*., 2015). Mechanisms of N turnover at the catchment scale, as indicated by NO_3^- isotopes, have been little explored, particularly for the subtropics (Osaka *et al*., 2010; Duncan *et al*., 2013; Zhu *et al*., 2013; Rose *et al*., 2014). Rather than studying $\delta^{15}N$-NO_3^- along hydrological continua, most studies have focused on temporal variations in individual landscape elements such as riparian zones, ground waters, seeps, and streams (Barnes *et al*., 2008; Søvik & Mørkved, 2008; Billy *et al*., 2010; Schwarz *et al*., 2011; Koba *et al*., 2012; O'Reilly *et al*., 2012; Riha *et al*., 2014; Wexler *et al*., 2014). For instance, Wexler *et al*. (2014) reported daily variation of $\delta^{15}N$-NO_3^- in ground and stream water in a northern hardwood forest during summer, but did not link this to $\delta^{15}N$-NO_3^- in different edaphic environments. On the other hand, studies focusing on spatial changes of $\delta^{15}N$ signals in NO_3^- along hydrological continua lack temporal resolution (Koba *et al*., 1997, 2012; Osaka *et al*., 2010; Fang *et al*., 2015). Likewise, NO_3^- isotopic signals in response to rain events, and their implications for N cycling in monsoonal regions with high N deposition, are understudied (Zhu *et al*., 2013).

To improve our understanding of N turnover and its spatial and temporal variabilities in N-saturated subtropical forest ecosystems, we investigated the natural abundance of ^{15}N and ^{18}O of NO_3^- in soil pore and stream water throughout three monsoonal summers, along a hydrological continuum in the Tieshanping catchment, Chongqing, SW China. The objectives were (i) to clarify transformation processes and fate of deposited N in a hydrologically connected forest landscape in subtropical China, (ii) to explore short-term responses of watershed N turnover and dissolved inorganic N export to monsoonal rain storms, and (iii) to assess the interannual variation of watershed N turnover in monsoonal summers.

The study was conducted in 2009, 2010, and 2013 in the Tieshanping catchment at Chongqing and involved soil water from well-drained soils on hill slopes and hydrologically connected, poorly drained soils in groundwater discharge zones, respectively, as well as stream water.

Materials and methods

Study site

Tieshanping (TSP; 29° 38′ N, 106° 41′ E) is a 16.2-ha subtropical headwater catchment about 25 km northeast of Chongqing city, south China (Fig. 1a). Having a typical monsoonal climate, the catchment receives an average annual precipitation of 1028 mm and has a mean annual temperature of 18.2 °C (Chen & Mulder, 2007b). About 75% of precipitation occurs in summer (April to September). Annual inorganic N deposition varied between 40 and 65 kg N ha^{-1} during the last decade, with an increasing trend in recent years (Duan *et al*., 2013; Huang *et al*., 2015). Annual stream N export is around 7 kg N ha^{-1} (Larssen *et al*., 2011). The vegetation is a secondary mixed coniferous-broadleaf forest, dominated by Masson pine (*Pinus massoniana*) on hill slopes (HS), and by grasses and shrubs in the GDZ. Under long-term stress of soil acidification and N saturation, net N uptake by standing biomass is believed to be small compared to the N deposition (Huang *et al*., 2015).

For the study, we selected a 4.2-ha subcatchment, including two dominant landscape elements: a relatively steep northeast-facing hill slope (HS), and a hydrologically connected southeast–northwest-oriented, terraced groundwater discharge zone (GDZ) (Fig. 1b) (Zhu *et al*., 2013). Soils on HS are acidic (pH = 3.7–4.1), loamy yellow mountain soils (Acrisols; WRB, 2006), with a thin O horizon (0–3 cm). Generally, HS soils are well drained, with considerable interflow over the B horizon following rainfall (Sørbotten *et al*., Accepted). In the GDZ, the soils are developed from colluvium (Cambisols; WRB, 2006) derived from the surrounding HS and their hydraulic conductivity is smaller than that of the surface horizons of HS soils. During summer, drainage from HS may rapidly increase the groundwater level in the GDZ and result in temporary water logging (Sørbotten, 2011). The GDZ has an intermittent stream, the outlet of which enters a small pond.

Sampling design

Soil water was sampled along two hydrologically connected transects, one established on the HS (plots T1 to T5), and one

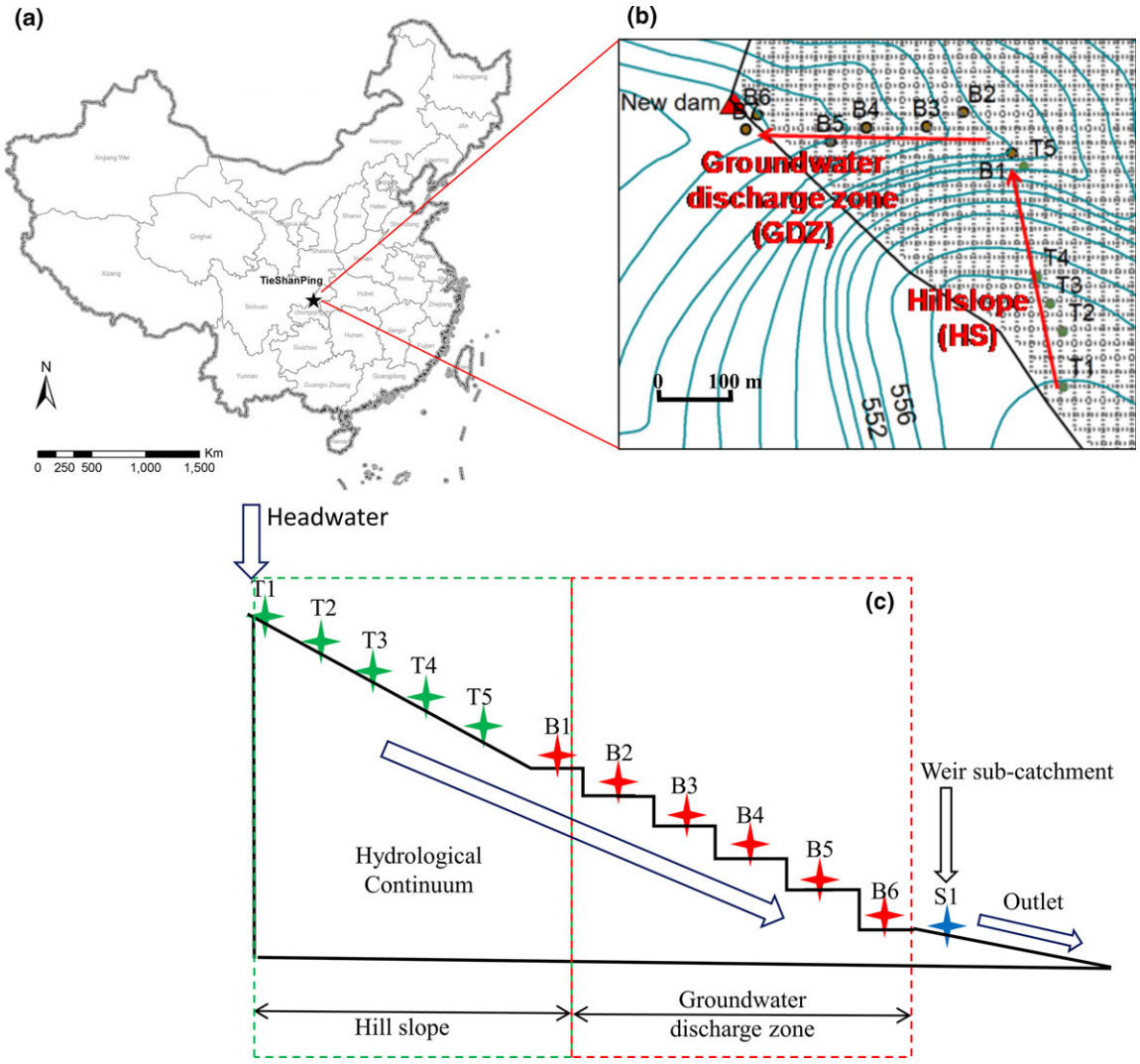

Fig. 1 Site description and observational design.

in the GDZ (plots B1 to B6; Fig. 1), where B1 was situated at the transition from HS to GDZ. Soil pore water was sampled in triplicate from top soils (0–5 cm) at each plot, using macrorhizon soil moisture samplers (Rhizosphere Research Products, the Netherlands). At GDZ plots except B1, samples were also taken from 60 and 100 cm soil depth. Samples were collected by applying vacuum to the lysimeters through a 50-ml syringe for about 12 h. Throughfall was collected in triplicate in 3-L PET bottles, equipped with 10.6-cm-diameter polyethylene (PET) funnels. Stream water was sampled at the weir S1 of the subcatchment in close vicinity to plot B6 (Fig. 1c). All water samples were filtered by 0.45-μm syringe filters (Millex, Millipore Corporation, Billerica, MA, USA) and frozen before analysis. Bulk soil was sampled with 100-cm^3 core rings from 0 to 5 cm depth in triplicate at plots T1, T2, T3, T5, B2, B3, B5 and B6, prior to the initial round of soil water sampling on July 6, 2013. Soil samples were kept refrigerated (4 °C) until analysis.

In summer 2013, soil water and stream water samples were collected on July 6, about 14 h after a rainstorm (32 mm) on July 5. Subsequent sampling took place on July 7 and July 8. No additional precipitation occurred during these days. A final series of soil water samples was collected in the GDZ on July 31, 12 days after a relatively small rainstorm (19 mm). On that day, no soil water samples could be retrieved on HS because the soils were too dry. On July 7, 2013, and July 8, 2013, complete depth profiles of soil water were sampled on plots B2 to B6 (5–100 cm).

Precipitation and air temperature at TSP were recorded every 5 min using a weather station (WeatherHawk 232, USA) installed on the roof of the local Forest Bureau, located 1 km south of the catchment. At the outlet of the subcatchment (Fig. 1c) and of the main catchment, the water discharge rates were measured at a V-notch weir at 5-min intervals, using WL705 ultrasonic water level sensor (Global Water, Xylem Inc., College Station, TX, USA).

Volumetric soil moisture (VM, $cm^3\ cm^{-3}$) at 4 depths (5, 10, 20 and 40 cm) was recorded at plots T3 and B1 at 10-min intervals, using TDR probes (Hydra Probe II). Water-filled pore space (WFPS) was calculated using bulk densities (BD) at 5,

10, 20, and 40 cm depths (Sørbotten, 2011), assuming a soil particle density (PD) of 2.65 g cm^{-3} (Linn & Doran, 1984) as

$$\mathrm{WFPS}(\%) = \frac{\mathrm{VM}}{1 - \frac{\mathrm{BD}}{\mathrm{PD}}} \times 100 \quad (1)$$

In our study, we included archived (frozen) water samples (throughfall, soil water, and stream water) taken at the same plots in the summers of 2009 (sampled at 6 different days) and 2010 (sampled at 10 different days), respectively. In both years, soil water at each HS plot and at the B1 plot of GDZ was sampled at four depths (5, 10, 20, and 40 cm), using ceramic suction cup lysimeters (P80; Staatliche Porzellanmanufaktur, Berlin, Germany). At the other GDZ plots, soil water was sampled at three depths (30, 60, and 100 cm) using macrorhizons. All samples were filtered through 0.22-μm syringe filters (Millex) and frozen directly after sampling.

Analytical procedures

The NH_4^+ concentration in water samples was analyzed with a flow injection analyzer (FIA, Tecator, Sweden), after reaction with alkaline phenol and sodium hypochlorite reagents. The NO_3^- concentration was analyzed by ion chromatography (DX-500; DIONEX; Thermo Fisher Scientific, Dreieich, Germany). Detection limits were 0.001 mg N/L for NH_4^+ and 0.01 mg N/L for NO_3^-.

Soil samples were air-dried and sieved (2 mm mesh size). After milling, the samples were analyzed for total organic carbon (TOC) and total N using a LECO elemental analyzer (TruSpec® CHN, St. Joseph, MI, USA).

^{15}N of NH_4^+ in throughfall was analyzed applying chemical conversion to N_2O (Zhang *et al.*, 2007). NH_4^+ was first quantitatively converted to NO_2^- by hypobromite at pH ~ 12, and further reduced to N_2O using a 1 : 1 sodium azide and acetic acid buffer solution. The precision of $\delta^{15}N$ was better than 0.3‰.

^{15}N and ^{18}O of NO_3^- were analyzed by a modified denitrifier method (Sigman *et al.*, 2001; Casciotti *et al.*, 2002; J. Zhu, L. Yu, L.R. Bakken, P.T. Mørkved, J. Mulder, P. Dörsch, in preparation). *Pseudomonas aureofaciens* (ATCC 13985) was grown aerobically in tryptic soy broth (TSB) medium, which had been pretreated anaerobically with *Paracoccus denitrificans* to remove NO_3^-. At an optical density of 0.3, 2 ml of the aerobically grown *P. aureofaciens* culture was added to He-washed, anoxic 120-ml vials. Then 2 ml sample was injected to the vials and placed overnight on a horizontal shaker. Complete conversion of NO_3^- to N_2O was achieved in less than 10 h, after which 0.2 ml of 10 M NaOH was added to stop microbial activity and to trap CO_2. ^{15}N and ^{18}O of produced N_2O were analyzed with an isotope ratio mass spectrometer coupled with a preconcentration unit (PreCon-GC-IRMS, Thermo Finnigan MAT, Bremen, Germany). In order to obtain constant N_2O peaks for precise analysis, the sample volumes were adjusted to obtain 100 nmol N per vial. International standards, IAEA N3 ($\delta^{15}N$ = 4.7‰ air N2, $\delta^{18}O$ = 25.6‰ VSMOW) and USGS 34 ($\delta^{15}N$ = −1.8‰ air N2, $\delta^{18}O$ = −27.9‰ VSMOW), were included in each batch for data correction. A standard gas with 4.81 ppm N_2O in helium ($\delta^{15}N$ = 1.2‰ air N2, $\delta^{18}O$ = 8.5‰ VSMOW) was used as running standard.

The $\delta^{18}O$ values of N_2O differ from those of NO_3^- due to isotopic fractionation associated with the loss of O atoms from nitrate and O exchange with H_2O in the medium (Casciotti *et al.*, 2002; Kool *et al.*, 2011). The ^{18}O fractionation during nitrate reduction may enrich $\delta^{18}O$ in N_2O, but this fractionation effect is believed to be constant during complete conversion in closed vials and can be corrected by standards with known isotopic compositions (Casciotti *et al.*, 2002; Fry, 2007). The exchange of O with H_2O in our modified denitrifier method ranged from 8% to 15% (J. Zhu, L. Yu, L.R. Bakken, P.T. Mørkved, J. Mulder, P. Dörsch, in preparation) and was determined for every batch using NO_3^- standards together with ^{18}O-enriched water. Assuming that ^{18}O fractionation, the NO_3^- blank of the TSB medium, and O exchange are stable within each analysis batch, we corrected $\delta^{18}O$ values by including two nitrate standards differing in ^{18}O (IAEA N3 and USGS 34) applying the following equation (Casciotti *et al.*, 2002):

$$\delta^{18}O_s = \delta^{18}O_{s1} + \frac{(\delta^{18}O_{s1} - \delta^{18}O_{s2})}{(\delta^{18}O_{m1} - \delta^{18}O_{m2})}(\delta^{18}O_m - \delta^{18}O_{m1}) \quad (2)$$

where $\delta^{18}O_s$, $\delta^{18}O_{s1}$, and $\delta^{18}O_{s2}$ are the mean actual $\delta^{18}O$ values of NO_3^- for sample, standard 1 and standard 2, respectively, whereas $\delta^{18}O_m$, $\delta^{18}O_{m1}$, and $\delta^{18}O_{m2}$ are their mean measured $\delta^{18}O$ values. Overall, the precisions of our method were 0.2‰ and 0.5‰ for ^{15}N and ^{18}O, respectively.

To measure $\delta^{15}N$ of soil organic matter, the bulk soil samples were finely milled and wrapped in tin capsules. Samples were analyzed by EA-IRMS (isotope ratio mass spectrometer coupled with an element analyzer, Thermo Finnigan MAT, Bremen, Germany). IAEA N1 ($\delta^{15}N$ = 4.7‰air N2) and IAEA N3 ($\delta^{15}N$ = 0.4‰air N2) were included as standards in the batch, and the precision of analysis was 0.2‰.

^{15}N enrichment factor

To provide a proxy for denitrification activity in our GDZ relative to other NO_3^- isotopic studies on riparian denitrification, we calculated the apparent ^{15}N enrichment factor ε as a proxy for denitrification activity along the flow path, using the Rayleigh distillation model (Mariotti *et al.*, 1981):

$$\varepsilon = \frac{\delta_S - \delta_{S0}}{\ln[C(NO_3^-)_S / C(NO_3^-)_{S0}]} \quad (3)$$

where $C(NO_3^-)_{S0}$ the concentration of initial substrate NO_3^-, $C(NO_3^-)_S$ the concentration of residual NO_3^-, δ_{S0} the $\delta^{15}N$ values of the initial NO_3^-, and δ_S the $\delta^{15}N$ values of residual NO_3^-. This equation is based on the assumption that the hydrological flow path is a closed system, with no external NO_3^- input (Mariotti *et al.*, 1981). In our study, we observed steady decline of NO_3^- concentrations from T5 to B4 on most sampling dates, and we used these data to calculate the apparent ^{15}N enrichment factor.

End-Member Mixing Analysis (EMMA)

End-member mixing analysis has been applied previously to stream water for estimating the contribution of specific soil

environments (end-members) to stream discharge at S1 (Mulder *et al.*, 1995). The analysis uses solutes, of which the concentration is significantly different between potential end-members and assumes conservative mixing. Here, we used hydrogen ions (H^+) and NO_3^- in soil water of HS (mean concentration for T1 to T5) and of GDZ (mean concentration for B5 to B6) to derive mixing ratios of the two end-members that explain solute concentrations in stream water at different days.

Statistical analysis

Paired t-tests were performed to compare the difference of NH_4^+ and NO_3^- concentrations, as well as $\delta^{15}N$ and $\delta^{18}O$-NO_3^- among different plots and sampling days. All statistical analyses were performed with Minitab 16.2.2 (Minitab Inc., State College, PA, USA). Significance levels in this study were set at $P < 0.05$.

Results

Mineral N after rainstorm in July 2013

After a heavy rainstorm on July 5 (32 mm) and a smaller precipitation event on July 19 (19 mm), no rain episodes occurred until after July 31, the final sampling date in 2013 (Fig. 2a). The WFPS increased instantaneously after both rain events (Fig. 2b), and decreased gradually afterward. The WFPS on HS (plot T3) was generally 10% smaller than at the interface of HS and GDZ (plot B1). At T3, WFPS varied from 35% to 65% with smallest values at 5 cm, and increased with depth. At B1, the WFPS at 10 and 20 cm was greater than at 5 and 40 cm.

From July 6 to July 8, the days following the heavy rain episode on July 5, the concentrations of NH_4^+ and NO_3^- in soil water (0–5 cm) were greatest on HS and decreased sharply along the flow path in the GDZ (Fig. 3, Tables S1 and S2). NH_4^+ concentrations decreased from 2.3 mg N/L in throughfall to less than 0.4 mg N/L in soil water on HS (except for T1 on July 6, when the concentration was 0.8 mg N/L), and remained small in the GDZ. NO_3^- concentrations increased dramatically from throughfall (2.3 mg N/L) to soil water on HS (up to 40 mg N/L), but decreased significantly ($P < 0.01$) to less than 5 mg N/L in soil water in the GDZ. NO_3^- concentrations were significantly ($P < 0.05$) smaller on July 7 than on July 6, while no significant differences of NH_4^+ were found among the first three sampling days (Fig. 3). On July 31, 12 days after moderate rainfall (July 19), when WFPS

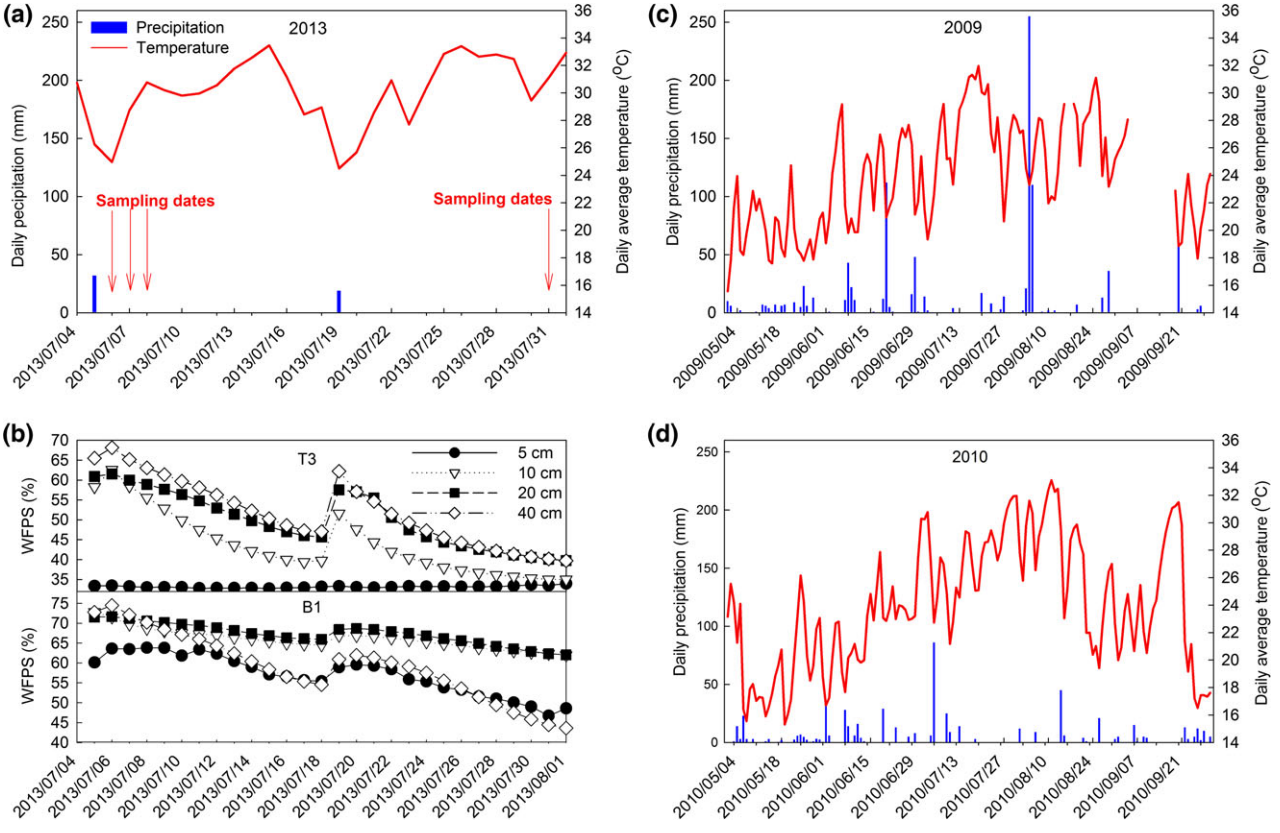

Fig. 2 Daily precipitation and average air temperature in summers of 2013 (a), 2009 (c), and 2010 (d) as well as water-filled pore space (WFPS) of the soil at four depths at plots T3 and B1 in summer 2013 (b). Weather data in 2009 and 2010 were obtained from Zhu *et al.* (2013).

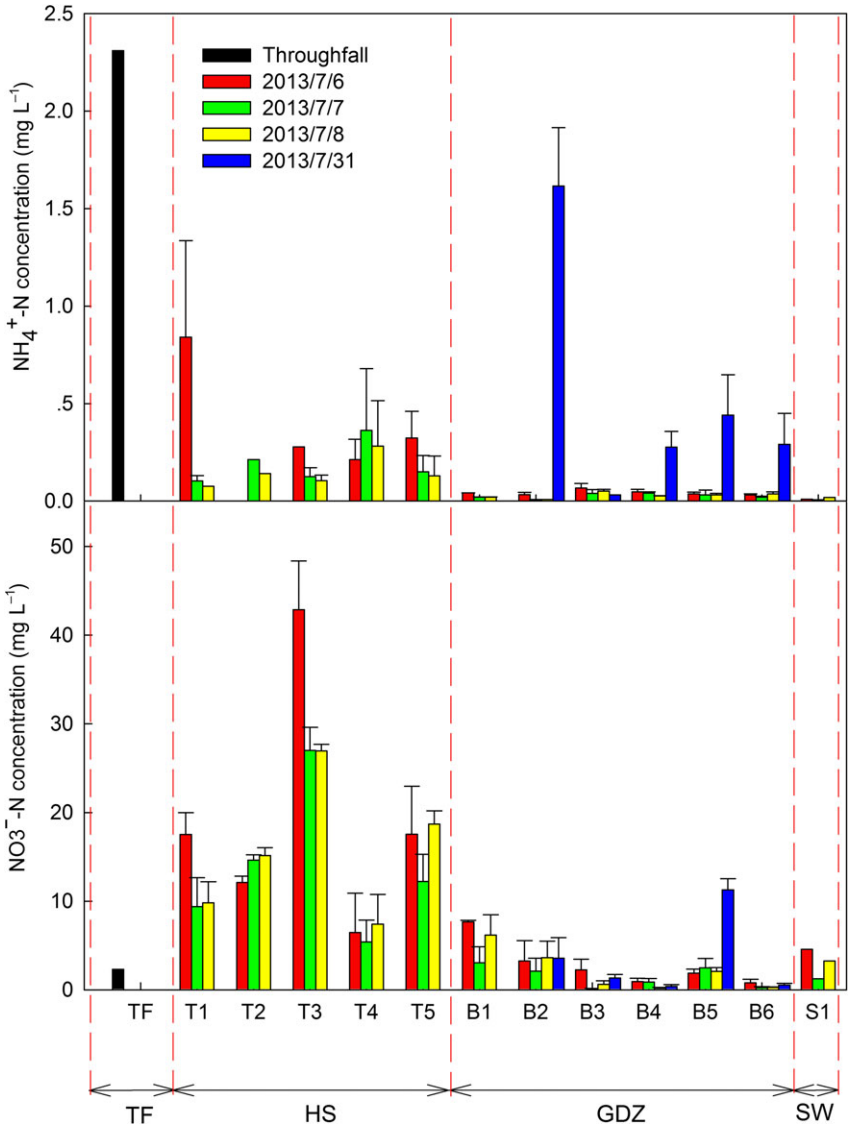

Fig. 3 Spatiotemporal variation of NH_4^+ and NO_3^- concentrations in throughfall (TF), surface soil water (0–5 cm depth interval) on hill slope (HS) and in groundwater discharge zone (GDZ), and stream water (SW) in summer 2013. Values are means and standard errors (n = 3). On July 31, HS and B1 soils were too dry for soil water sampling. For sample codes, see Fig. 1.

values were at their lowest during the 2013 sampling campaign, NH_4^+ and NO_3^- concentrations in GDZ, but not on HS, were larger than on other sampling days. Relatively large NH_4^+ concentrations were observed at B2 (1.5 mg N/L). In stream water, NH_4^+ concentrations were extremely low, even on July 31, while stream water NO_3^- concentrations were similar to those observed in soil water of the GDZ (Table S2 and Fig. 3).

$\delta^{15}N$ and $\delta^{18}O$-NO_3^- after rainstorm in July 2013

The $\delta^{15}N$-NO_3^- and $\delta^{15}N$-NH_4^+ in throughfall collected on July 5 were −0.8‰ and −5.1‰, respectively (Fig. 4). From July 6 to July 8, mean position-specific $\delta^{15}N$-NO_3^- in HS soil water (0–5 cm) varied between −4.5‰ and −10‰, that is was more negative than $\delta^{15}N$-NO_3^- and $\delta^{15}N$-NH_4^+ in throughfall. By contrast, mean $\delta^{15}N$-NO_3^- in GDZ (0–5 cm) and stream water was positive (1–30‰) and greater than the $\delta^{15}N$ of both NH_4^+-N and NO_3^--N in throughfall. Thus, along the hydrological continuum from HS to GDZ, $\delta^{15}N$-NO_3^- decreased from throughfall to soil water in HS plots, but increased significantly ($P < 0.01$) in the GDZ, starting at B1 and reaching a maximum of +30‰ in B4 4 days after the rainstorm (Fig. 4). In soil water of the GDZ and stream water, but not of the HS, $\delta^{15}N$-NO_3^- increased significantly ($P < 0.05$) from July 6 to July 7. On July 31, two weeks after the initial rainstorm, the $\delta^{15}N$-NO_3^- in soil

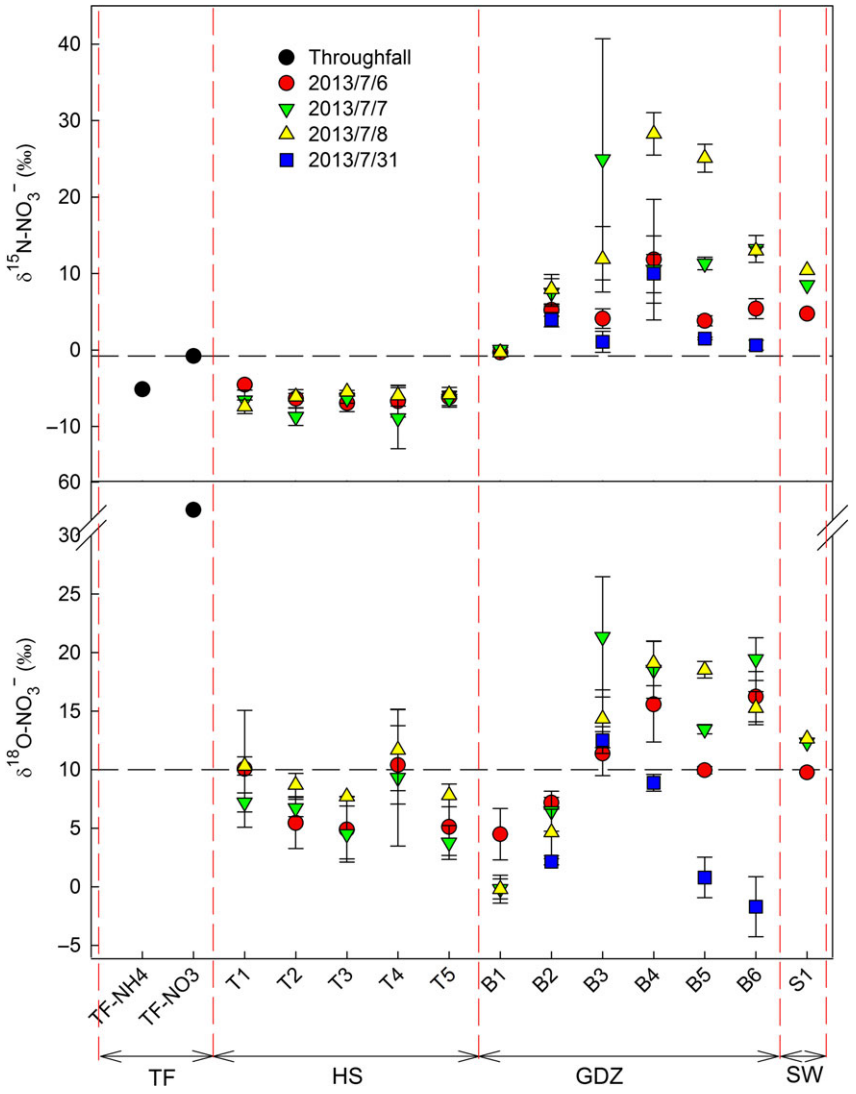

Fig. 4 Spatiotemporal variation of $\delta^{15}N\text{-}NO_3^-$ and $\delta^{18}O\text{-}NO_3^-$ in throughfall (TF), surface soil water (0–5 cm depth interval) on hill slope (HS) and groundwater discharge zone (GDZ), and stream water (SW) in summer 2013. Values are means and standard errors (n = 3). On July 31, HS and B1 soils were too dry for soil water sampling. For sample codes, see Fig. 1. TF-NH4 refers to $\delta^{15}N\text{-}NH_4^+$ in throughfall.

water of the GDZ decreased to values between 2‰ and 10‰.

$\delta^{18}O\text{-}NO_3^-$ in throughfall was larger than +50‰ and much greater than in soil water. The spatial pattern of $\delta^{18}O\text{-}NO_3^-$ in soil water (0–5 cm) paralleled that of $\delta^{15}N$ from July 6 to July 8, increasing from HS to GDZ (Fig. 4). In the GDZ plots B3 to B6, mean $\delta^{18}O\text{-}NO_3^-$ was larger on July 7 and July 8 than on July 6, and declined significantly ($P < 0.01$) on July 31.

$\delta^{15}N$ of bulk soil

Mean $\delta^{15}N$ values of bulk soil N (0–5 cm) sampled in 2013 showed a clear increase from −2.6‰ to +1.5‰ from T1 (top of HS) to B6 (close to the outlet in the GDZ), with negative values on HS and positive values in GDZ (Fig. 5). By contrast, the C/N ratios of these soil layers declined significantly ($P < 0.05$) along the flow path.

N concentrations and isotopic signals in summers 2009 and 2010

Precipitation from May to September, 2009 and 2010, amounted to 1054 and 850 mm, respectively (Fig. 2c, d). Rain episodes were more intense and frequent in 2009, with a pronounced rainstorm event of 250 mm on August 4, 2009 (Fig. 2c). Mean concentration of NO_3^- in surface soil water (5 cm on HS and

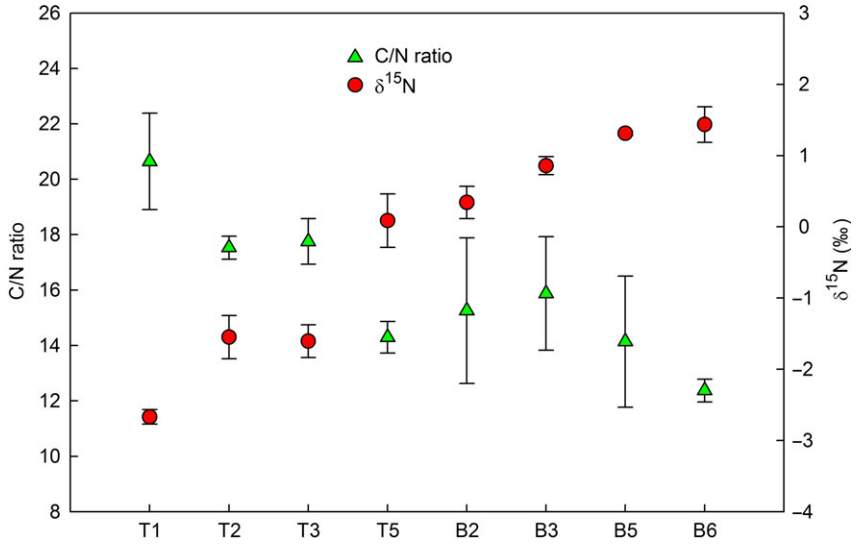

Fig. 5 C/N ratios and $\delta^{15}N$ values of bulk soil (0–5 cm depth) N in summer 2013 (no sample was available at T4, B1, and B4 plots.). Error bars indicate standard errors (n = 3).

30 cm in GDZ) showed a similarly declining pattern along the water flow path as in 2013 (Table S2). As in 2013, the NH_4^+ concentration in soil water was small at all plots (Table S1). The spatial pattern of $\delta^{15}N\text{-}NO_3^-$ and $\delta^{18}O\text{-}NO_3^-$in surface soil water was similar to that in July 2013 (Fig. 6), albeit $\delta^{15}N\text{-}NO_3^-$ in the GDZ tended to be smaller in 2013 than in 2009 and 2010.

Isotopic pattern with soil depth

The NO_3^- concentration did not change with soil depth (Table S2). Although $\delta^{15}N$ and $\delta^{18}O$ of NO_3^- in soil water on HS varied widely at 5 cm depth, the mean values of $\delta^{15}N$ and $\delta^{18}O$ were about 2‰ and 5‰ greater at 5 and 40 cm depth, respectively (Fig. 7). $\delta^{15}N\text{-}NO_3^-$ at B1 was positive and significantly ($P < 0.01$) smaller at 5 cm depth than at other depths, among which no significant difference of $\delta^{15}N$ values was shown. In the other GDZ soils (except B1), mean $\delta^{15}N$ and $\delta^{18}O\text{-}NO_3^-$ decreased in the order 30 cm > 100 cm > 60 cm > 5 cm.

Discussion

Ammonium (NH_4^+) in throughfall, entering HS soils on July 6, 2013, rapidly decreased in concentration in the surface layer (0–5 cm), while NO_3^- concentrations increased simultaneously (Fig. 3). Larssen *et al.* (2011) suggested nitrification to be the main cause and that in the long term (years) this conversion was close to quantitative. Recently, such a near-quantitative conversion was confirmed by Huang *et al.* (2015), based on a 7-year study of N mass balances at the same site. This indicates efficient nitrification, as previously suggested by Chen & Mulder (2007a), and is consistent with the observed decrease in $\delta^{15}N\text{-}NO_3$ of soil water compared with NO_3^- in throughfall (Fig. 4). The importance of nitrification for the NO_3^- concentration in HS soils is also supported by its $\delta^{18}O$ values, which ranged from +2‰ to +14‰. These values are as expected for acidic forest floors (Mayer *et al.*, 2001), assuming that nitrification-derived NO_3^- receives two O atoms from H_2O and one from O_2 in soil (Kendall *et al.*, 2007; Fang *et al.*, 2012), with $\delta^{18}O$ of soil H_2O being generally in the range of −15‰ to 5‰ and that of soil O_2 being similar to those of atmospheric O_2 (23.5‰) (Horibe *et al.*, 1973).

Nitrification produces ^{15}N-depleted NO_3^- relative to its substrate NH_4^+ (Fry, 2007). In the summer of 2013, after a heavy rainfall, ^{15}N depletion in soil water NO_3^- relative to atmogenic NH_4^+ was small and changed little over time (Fig. 4). This may be due to rapid nitrification of NH_4^+, resulting in NH_4^+ exhaustion and thus negligible ^{15}N fractionation (Fig. 3 and Table S1) (Mariotti *et al.*, 1981; Wexler *et al.*, 2014). Alternatively, NH_4^+ other than of atmogenic origin contributed to nitrification on the HS. Mineralization rates of soil organic matter have been reported to produce as much as 18.4 kg N ha^{-1} yr^{-1} in HS soils at Tieshanping (Chen & Mulder, 2007b), likely contributing significant amounts of NH_4^+ for nitrification. As soil N mineralization causes negligible ^{15}N fractionation (Kendall *et al.*, 2007), the mineralization-produced NH_4^+ is expected to inherit $\delta^{15}N$ values from soil organic N on HS (−2.6‰ to 0‰, Fig. 5).

In summer 2013 after a heavy rain storm, a sharp decline in NO_3^- concentration and a significant increase in $\delta^{15}N\text{-}NO_3^-$ ($P < 0.01$) was observed at the transition from HS to GDZ and further along the flow path of the GDZ (Figs 3 and 4, Table S1). As

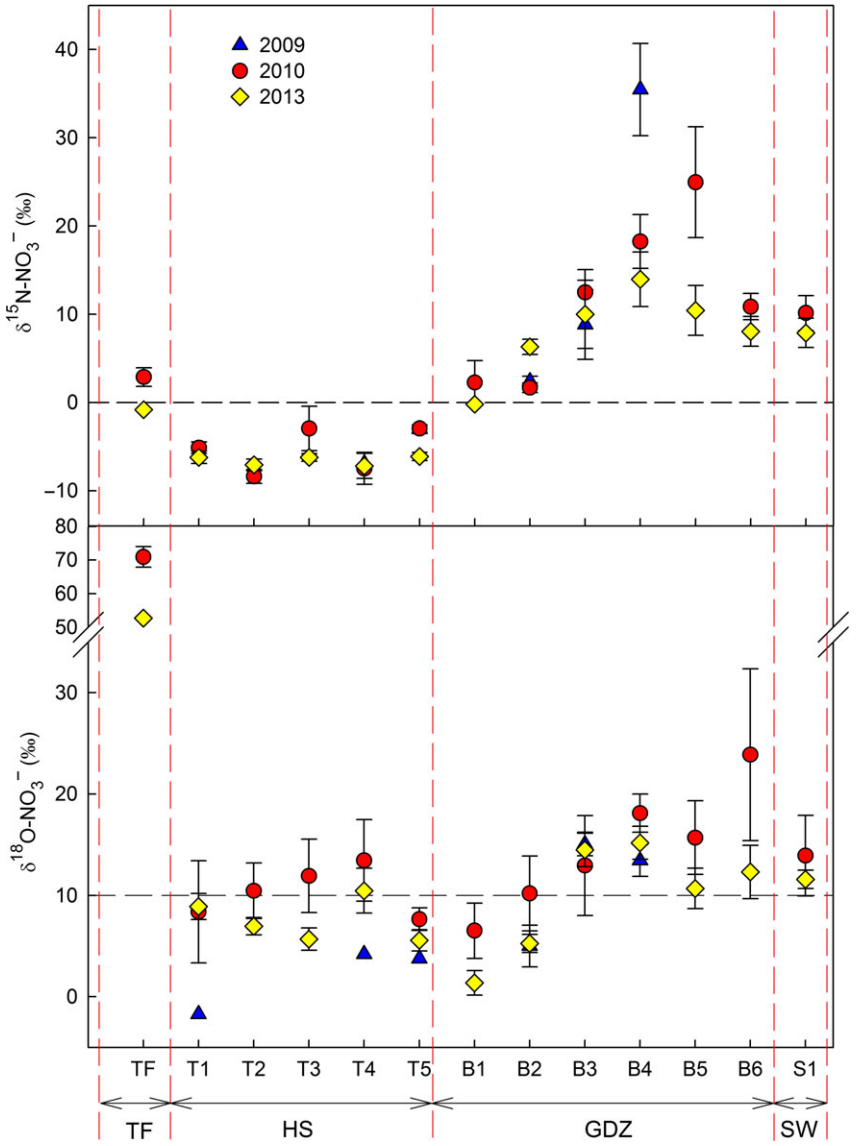

Fig. 6 Spatiotemporal variation of δ^{15}N-NO_3^- and δ^{18}O-NO_3^- in throughfall (TF), and in surface soil water on the hill slope (HS) and in the groundwater discharge zone (GDZ) in the summers of 2009, 2010, and 2013. Values are means and standard errors for all measured samples (for details see Materials and Method section). In 2009 and 2010, soil water was sampled at 5 and 30 cm soil depth in HS and GDZ soils, respectively, except at plot B1, which was sampled as in HS soils at 5 cm depth only. In 2013, all soil water samples were taken at the 0–5 cm depth interval. For sample codes, see Fig. 1.

denitrification, and not assimilation, is known to cause ^{15}N enrichment in NO_3^- (Kendall *et al.*, 2007; Osaka *et al.*, 2010), this indicates significant denitrification in the GDZ. In surface soils, the contrast of δ^{15}N-NO_3^- between HS (negative) and GDZ (positive) (Fig. 4) was consistent with the spatial pattern of δ^{15}N of bulk soil (Fig. 5). This likely reflects the spatial distribution of dissimilatory N processes along the hydrological continuum, as the isotopic signals of NO_3^- were incorporated into the organic N pool during long-term soil N turnover (Robinson, 2001). The dominance of dissimilatory processes in the GDZ does not preclude intermittent nitrification during dry periods, as observed on July 31, when δ^{15}N and δ^{18}O values at B5 dropped close to 0‰ (Fig. 4). However, as judged from the average δ^{15}N values for all 3 years (Fig. 6), these occasions are likely rare and do not invalidate our conclusion that the GDZ acts predominately as N sink.

As δ^{15}N, δ^{18}O-NO_3^- increased along the flow path in the GDZ (Figs 4 and 6). For the 2013 data, the slope of the regression line of δ^{18}O vs. δ^{15}N for all GDZ soil water samples was 0.69 ($R^2 = 0.61$, $P < 0.05$) (Fig. 8), whereas

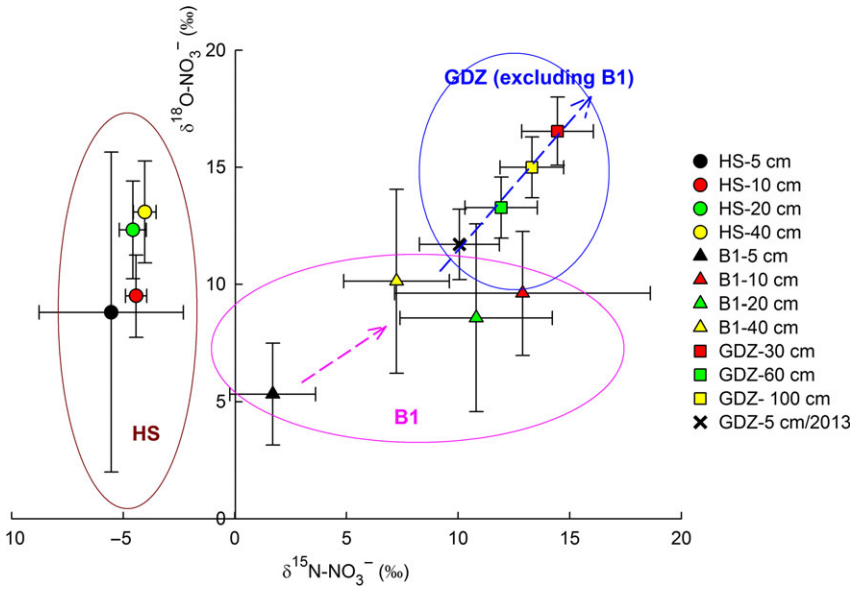

Fig. 7 $\delta^{15}N$ and $\delta^{18}O$ of NO_3^- in soil water at increasing depth on HS (T1 to T5), and in B1 and the remaining GDZ plots (B2 to B7). Means and standard deviations are based on all data from 2009, 2010, and 2013; GDZ-5 cm data refer to summer 2013 data only.

in 2010 this was 0.57, ($R^2 = 0.27$, $P < 0.05$). In 2009, with only few observations, $\delta^{15}N$ was not significantly correlated with $\delta^{18}O$. The slopes for 2010 and 2013 were close to 0.5, which has been taken as an indication of denitrification in aquifers (Bottcher *et al.*, 1990; Lehmann *et al.*, 2003; Wexler *et al.*, 2014; Fang *et al.*, 2015). From the foot of the HS (T5) to B4 in the GDZ, we identified an 'active denitrification zone', where NO_3^--N is effectively removed from soil water and $\delta^{15}N\text{-}NO_3^-$ increases along the water flow path (Figs 3, 4 and 6). The correlation between $\delta^{15}N\text{-}NO_3^-$ and ln (NO_3^-) in the active denitrification zone (T5 to B4) was significantly negative in 2010 and 2013 (Fig. 9). Assuming that this zone may be considered as a quasi-closed system, such a relationship can be described by the ^{15}N enrichment factor ε (Equation 3), based on the Rayleigh distillation model (Mariotti *et al.*, 1981; Wexler *et al.*, 2014). Using linear regression for the active denitrification zone, ε values were $-5.63‰$ and $-4.86‰$ for 2010 and 2013, respectively. The regression for 2009 was not significant. These values fall in the range of reported ε values for riparian and groundwater denitrification ($-3.5‰$ to $-5.9‰$) (Mariotti *et al.*, 1988; Bottcher *et al.*, 1990; Spalding *et al.*, 1993; Søvik & Mørkved, 2008; Osaka *et al.*, 2010). Thus, the GDZ (less than 5% of the catchment area) is an important 'hot spot' for denitrification, constituting the previously hypothesized N sink function in this N-saturated catchment (Larssen *et al.*, 2011).

The pattern of $\delta^{15}N$ and $\delta^{18}O\text{-}NO_3^-$ along the hydrological continuum, with relatively small values in HS soils and relatively large values in the GDZ, was similar for the summers of 2009, 2010, and 2013 (Fig. 6). This indicates a consistent spatial pattern of N transformations irrespective of differences in climatic conditions (Fig. 2a, c, d). This is noteworthy, because monsoonal summers in SE Asia have highly variable amounts and frequency distributions of precipitation (Loo *et al.*, 2014). Such variability would be expected to directly affect site specific N transformation as well as residence times of NO_3^- in different landscape elements (Ohte *et al.*, 2010), both of which would influence dual NO_3^- isotope signatures. Thus, our data suggest that biological processes shaping dual NO_3^- isotope signatures at TSP are controlled predominately by landscape attributes brought about by topographic influences (Anderson *et al.*, 2015) rather than by climatic factors. If such N transformation patterns occur among other N-saturated forested watersheds across the subtropics, the strikingly efficient N removal observed in the Tieshanping catchment may represent a widely underestimated N sink across south China and beyond.

Small enrichment of $^{15}N\text{-}NO_3^-$ and $^{18}O\text{-}NO_3^-$ with soil depth on HS (Fig. 7) suggested that subsoils in upland positions contribute only moderately to N removal by denitrification. Also for B1 (the interface between the two transects), only a modest increase in $\delta^{15}N\text{-}NO_3^-$ and $\delta^{18}O\text{-}NO_3^-$ with depth was observed when pooling all observations (Fig. 7). Enrichment was greatest at 10 and 20 cm soil depth, where WFPS values were largest (Fig. 2b). Among the depth profiles of GDZ plots, $\delta^{15}N\text{-}NO_3^-$ and $\delta^{18}O\text{-}NO_3^-$ values indicated strong denitrification activities ($\delta^{18}O$ vs. $\delta^{15}N \sim 1.0$) over the entire soil profile with a maximum at 30 cm depth. This was expected from groundwater

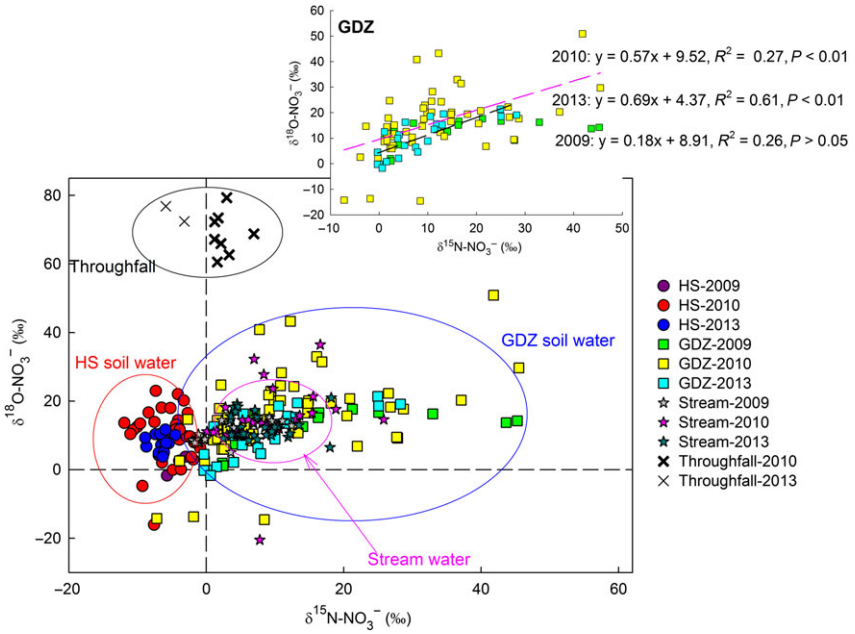

Fig. 8 Relationship between $\delta^{15}N$ and $\delta^{18}O$ of NO_3^- in throughfall, surface soil water, and stream water. The data shown are annual averages for sampling points along the two transects and in stream water. For detailed sampling depths, see Fig. 5. The insert shows the linear regression in GDZ soil water for the 3 years.

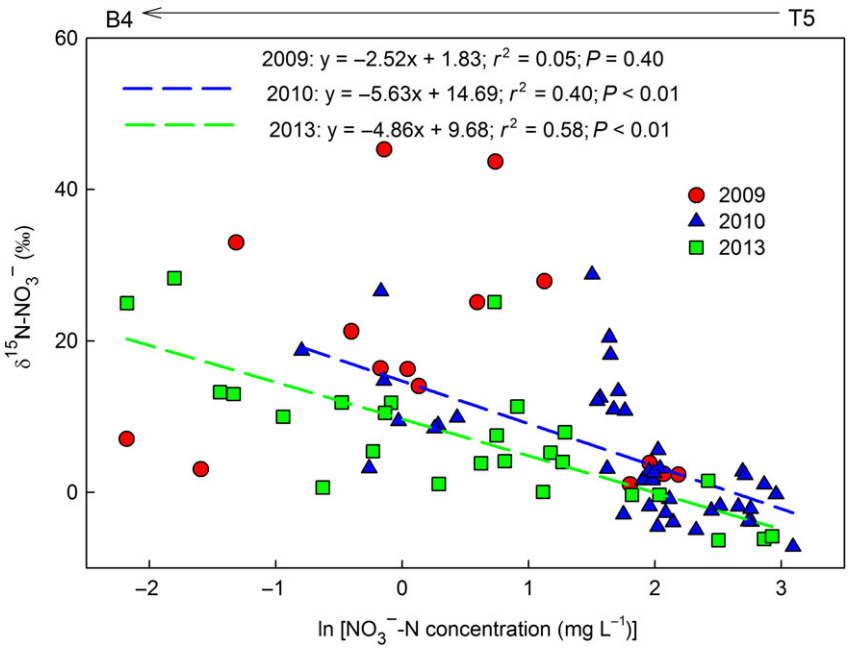

Fig. 9 Relationship between $\delta^{15}N\text{-}NO_3^-$ and NO_3^--N concentrations (in logarithmic scale) in surface soil water (5 cm depth) from plot T5 to B4 over 3 years. Shown are all samples taken in the years 2009, 2010, and 2013 (for details see Materials and Method section). The direction along the flow path is indicated by the arrow above the figure (T5 → B4).

level (GWL) observations at the GDZ in 2009 and 2010 (Zhu *et al.*, 2013) showing that summertime GWL fluctuated between −1.0 and +0.1 m, with a clear top in frequency distribution at −0.3 m. Denitrification would be expected to be greatest at the capillary fringe where abundant NO_3^- meets anoxia (e.g. He *et al.*, 2016).

Several studies in headwater catchments have used NO_3^- isotopic signals in stream water to assess N

turnover (Koba *et al.*, 2012; Riha *et al.*, 2014; Rose *et al.*, 2014; Wexler *et al.*, 2014). As shown in Fig. 8, the stream water in the TSP catchment integrates NO_3^- originating from both HS and GDZ water. End-member mixing analysis, using soil water in HS and GDZ as end-members, and selecting concentrations of H^+ and NO_3^- in 2010 and 2013, suggested that the GDZ, constituting < 5% of the total catchment area, has an important contribution (> 60%) to stream discharge (S1). During large events (runoff > 60 L min^{-1}), the contribution of the GDZ to stream water runoff remains significant, but decreases to about 40% (Fig. S2). The estimated contributions of soil water from HS and GDZ to stream discharge provide reasonable predictions of $\delta^{15}N\text{-}NO_3^-$ in stream water (Fig. S3), thus confirming the importance of the GDZ as N sink at the catchment scale.

As a major nutrient in terrestrial ecosystems, the availability of N is of great importance for modeling primary production and thus carbon sequestration, both at landscape, regional, and global levels (Gruber & Galloway, 2008). As natural isotopic benchmarks are increasingly applied in climate change models, more "ground-truth" is required to validate the models (Houlton *et al.*, 2015). Even though our findings are for one N-saturated headwater catchment only, the Tieshanping catchment is representative for a wide range of forested sites in south China. Larssen *et al.* (2011) reported significant N sinks in groundwater discharge zones of four other forested catchments in south China, all characterized by a similar but typical geomorphology. This suggests that our findings are important for regional N budgets. The surprisingly robust isotopic pattern across climatically different years improves the accuracy of large-scale isotopic models and may also be important to constrain C sequestration models in regions with high N pollution.

Acknowledgements

Longfei Yu thanks the China Scholarship Council (CSC) for his PhD scholarship. Support from the Norwegian Research Council to project 209696/E10 'Forest in South China: an important sink for reactive nitrogen and a regional hotspot for N_2O?' is gratefully acknowledged. We thank Wang Yanhui, Wang Yihao, Duan Lei, and Zhang Xiaoshan for their help during data collection.

References

Anderson TR, Groffman PM, Walter MT (2015) Using a soil topographic index to distribute denitrification fluxes across a northeastern headwater catchment. *Journal of Hydrology*, **522**, 123–134.

Bai E, Houlton BZ, Wang YP (2012) Isotopic identification of nitrogen hotspots across natural terrestrial ecosystems. *Biogeosciences*, **9**, 3287–3304.

Barnes RT, Raymond PA, Casciotti KL (2008) Dual isotope analyses indicate efficient processing of atmospheric nitrate by forested watersheds in the northeastern U.S. *Biogeochemistry*, **90**, 15–27.

Billy C, Billen G, Sebilo M, Birgand F, Tournebize J (2010) Nitrogen isotopic composition of leached nitrate and soil organic matter as an indicator of denitrification in a sloping drained agricultural plot and adjacent uncultivated riparian buffer strips. *Soil Biology and Biochemistry*, **42**, 108–117.

Bottcher J, Strebel O, Voerkelius S, Schmidt H (1990) Using isotope fractionation of nitrate-nitrogen and nitrate-oxygen for evaluation of microbial denitrification in a sandy aquifer. *Journal of Hydrology*, **114**, 413–424.

Bouwman AF, Beusen AHW, Griffioen J *et al.* (2013) Global trends and uncertainties in terrestrial denitrification and N_2O emissions. *Philosophical Transactions of the Royal Society of London. Series B, Biological sciences*, **368**, 1–11.

Casciotti KL, Sigman DM, Hastings MG, Böhlke JK, Hilkert A (2002) Measurement of the oxygen isotopic composition of nitrate in seawater and freshwater using the denitrifier method. *Analytical Chemistry*, **74**, 4905–4912.

Chen X, Mulder J (2007a) Atmospheric deposition of nitrogen at five subtropical forested sites in South China. *The Science of the Total Environment*, **378**, 317–330.

Chen X, Mulder J (2007b) Indicators for nitrogen status and leaching in subtropical forest ecosystems, South China. *Biogeochemistry*, **82**, 165–180.

Clark CM, Tilman D (2008) Loss of plant species after chronic low-level nitrogen deposition to prairie grasslands. *Nature*, **451**, 712–715.

Duan L, Liu J, Xin Y, Larssen T (2013) Air-pollution emission control in China: impacts on soil acidification recovery and constraints due to drought. *Science of the Total Environment*, **463–464**, 1031–1041.

Duncan JM, Groffman PM, Band LE (2013) Towards closing the watershed nitrogen budget: spatial and temporal scaling of denitrification. *Journal of Geophysical Research: Biogeosciences*, **118**, 1105–1119.

Emmett BA, Boxman D, Bredemeier M *et al.* (1998) Predicting the effects of atmospheric nitrogen deposition in conifer stands: evidence from the NITREX ecosystem-scale experiments. *Ecosystems*, **1**, 352–360.

Fang Y, Koba K, Makabe A, Zhu F, Fan S, Liu X, Muneoki Y (2012) Low $\delta^{18}O$ values of nitrate produced from nitrification in temperate forest soils. *Environmental Science & Technology*, **46**, 8723–8730.

Fang Y, Koba K, Makabe A, Takahashi C, Zhu W, Hayashi T (2015) Microbial denitrification dominates nitrate losses from forest ecosystems. *Proceedings of the National Academy of Sciences of the United States of America*, **112**, 1470–1474.

Fry B (2007) Chapter 7. Fraction. In: *Stable Isotope Ecology*, pp. 194–270. Springer, New York, NY, USA

Galloway JN, Aber J, Erisman J, Speitzinger S, Howarth R, Cowling E, Cosby A (2003) The nitrogen cascade. *BioScience*, **53**, 341–356.

Galloway JN, Townsend AR, Erisman JW *et al.* (2008) Transformation of the nitrogen cycle: recent trends, questions, and potential solutions. *Science*, **320**, 889–892.

Groffman PM, Altabet MA, Böhlke JK *et al.* (2006) Methods for measuring denitrification: diverse approaches to a difficult problem. *Ecological Applications*, **16**, 2091–2122.

Gruber N, Galloway JN (2008) An Earth-system perspective of the global nitrogen cycle. *Nature*, **451**, 293–296.

He H, Jansson PE, Svensson M, Meyer A, Klemedtsson L, Kasimir Å (2016) Factors controlling Nitrous Oxide emission from a spruce forest ecosystem on drained organic soil, derived using the CoupModel. *Ecological Modelling*, **321**, 46–63.

Horibe Y, Shigehara K, Takakuwa Y (1973) Isotope separation factor of carbon dioxide-water system and isotopic composition of atmospheric oxygen. *Journal of Geophysical Research*, **78**, 2625–2629.

Houlton BZ, Bai E (2009) Imprint of denitrifying bacteria on the global terrestrial biosphere. *Proceedings of the National Academy of Sciences of the United States of America*, **106**, 21713–21716.

Houlton BZ, Marklein AR, Bai E (2015) Representation of nitrogen in climate change forecasts. *Nature Climate Change*, **5**, 398–401.

Huang Y, Kang R, Mulder J, Zhang T, Duan L (2015) Nitrogen saturation, soil acidification, and ecological effects in a subtropical pine forest on acid soil in southwest China. *Journal of Geophysical Research: Biogeosciences*, **120**, 2457–2472.

Jaworski NA, Howarth RW, Hetling LJ (1997) Atmospheric deposition of nitrogen oxides onto the landscape contributes to coastal eutrophication in the Northeast United States. *Environmental Science & Technology*, **31**, 1995–2004.

Ju X, Kou C, Zhang F, Christie P (2006) Nitrogen balance and groundwater nitrate contamination: comparison among three intensive cropping systems on the North China Plain. *Environmental Pollution*, **143**, 117–125.

Kendall C, Elliott EM, Wankel SD (2007) Tracing anthropogenic inputs of nitrogen to ecosystems. In: *Stable Isotopes in Ecology and Environmental Science*, 2nd edn (eds Michener RH, Lajtha K), pp. 375–449. Blackwell Publishing, Oxford, UK.

Koba K, Tokuchi N, Wada E, Nakajima T, Iwatsubo G (1997) Intermittent denitrification: the application of a ^{15}N natural abundance method to a forested ecosystem. *Geochimica et Cosmochimica Acta*, **61**, 5043–5050.

Koba K, Fang Y, Mo J *et al.* (2012) The ^{15}N natural abundance of the N lost from an N-saturated subtropical forest in southern China. *Journal of Geophysical Research: Biogeosciences*, **117**, 1–13.

Kool DM, Wrage N, Oenema O, Van Kessel C, Van Groenigen JW (2011) Oxygen exchange with water alters the oxygen isotopic signature of nitrate in soil ecosystems. *Soil Biology and Biochemistry*, **43**, 1180–1185.

Larssen T, Duan L, Mulder J (2011) Deposition and leaching of sulfur, nitrogen and calcium in four forested catchments in China: implications for acidification. *Environmental Science & Technology*, **45**, 1192–1198.

Lehmann MF, Reichert P, Bernasconi SM, Barbieri A, McKenzie JA (2003) Modelling nitrogen and oxygen isotope fractionation during denitrification in a lacustrine redox-transition zone. *Geochimica et Cosmochimica Acta*, **67**, 2529–2542.

Li Y, Lin E (2000) Emissions of N_2O, NH_3 and NO_x from fuel combustion, industrial processes and the agricultural sectors in China. *Nutrient Cycling in Agroecosystems*, **57**, 99–106.

Linn DM, Doran JW (1984) Effect of water-filled pore space on carbon dioxide and nitrous oxide production in tilled and nontilled soils. *Soil Science Society of America Journal*, **48**, 1267–1272.

Liu X, Duan L, Mo J *et al.* (2011) Nitrogen deposition and its ecological impact in China: an overview. *Environmental pollution*, **159**, 2251–2264.

Liu X, Zhang Y, Han W *et al.* (2013) Enhanced nitrogen deposition over China. *Nature*, **494**, 459–462.

Loo YY, Billa L, Singh A (2014) Effect of climate change on seasonal monsoon in Asia and its impact on the variability of monsoon rainfall in Southeast Asia. *Geoscience Frontiers*, **6**, 1–7.

Mariotti A, Germon J, Hubert P, Kaiser P, Letolle R, Tardieux A, Tardieux P (1981) Experimental determination of nitrogen kinetic isotope fractionation: some principles; illustration for the denitrification and nitrification processes. *Plant and Soil*, **62**, 413–430.

Mariotti A, Germon JC, Leclerc A (1982) Nitrogen isotope fractionation associated with the $NO_2^- \rightarrow N_2O$ step of denitrification in soils. *Canadian Journal of Soil Science*, **2**, 227–241.

Mariotti A, Landreau A, Simon B (1988) ^{15}N isotope biogeochemistry and natural denitrification process in groundwater: application to the chalk aquifer of northern France. *Geochimica et Cosmochimica Acta*, **52**, 1869–1878.

Mayer B, Bollwerk SM, Mansfeldt T, Hütter B, Veizer J (2001) The oxygen isotope composition of nitrate generated by nitrification in acid forest floors. *Geochimica et Cosmochimica Acta*, **65**, 2743–2756.

Mulder J, Christophersen N, Kopperud K, Fjeldal PH (1995) Water-flow paths and the spatial-distribution of soils as a key to understanding differences in streamwater chemistry between three catchments (Norway). *Water Air and Soil Pollution*, **81**, 67–91.

Ohte N, Tokuchi N, Fujimoto M (2010) Seasonal patterns of nitrate discharge from forested catchments: information derived from Japanses case studies. *Geography Compass*, **4**, 1358–1376.

O'Reilly AM, Chang NB, Wanielista MP (2012) Cyclic biogeochemical processes and nitrogen fate beneath a subtropical stormwater infiltration basin. *Journal of Contaminant Hydrology*, **133**, 53–73.

Osaka K, Ohte N, Koba K *et al.* (2010) Hydrological influences on spatiotemporal variations of $\delta^{15}N$ and $\delta^{18}O$ of nitrate in a forested headwater catchment in central Japan: denitrification plays a critical role in groundwater. *Journal of Geophysical Research*, **115**, G02021.

Pardo LH, Kendall C, Pett-Ridge J, Chang CCY (2004) Evaluating the source of streamwater nitrate using $\delta^{15}N$ and $\delta^{18}O$ in nitrate in two watersheds in New Hampshire, USA. *Hydrological Processes*, **18**, 2699–2712.

Riha KM, Michalski G, Gallo EL, Lohse KA, Brooks PD, Meixner T (2014) High atmospheric nitrate inputs and nitrogen turnover in semi-arid urban catchments. *Ecosystems*, **17**, 1309–1325.

Robinson D (2001) $\delta^{15}N$ as an integrator of the nitrogen. *TRENDS in Ecology & Evolution*, **16**, 153–162.

Rose L, Sebestyen SD, Elliott EM, Koba K (2014) Drivers of atmospheric nitrate processing and export in forested catchments. *Water Resources Research*, **51**, 1333–1352.

Sabo RD, Nelson DM, Eshleman KN (2016) Episodic, seasonal, and annual export of atmospheric and microbial nitrate from a temperate forest. *Geophysical Research Letters*, **43**, 683–691.

Schwarz MT, Oelmann Y, Wilcke W (2011) Stable N isotope composition of nitrate reflects N transformations during the passage of water through a montane rain forest in Ecuador. *Biogeochemistry*, **102**, 195–208.

Sigman DM, Casciotti KL, Andreani M, Barford C, Galanter M, Böhlke JK (2001) A bacterial method for the nitrogen isotopic analysis of nitrate in seawater and freshwater. *Analytical Chemistry*, **73**, 4145–4153.

Sørbotten LE (2011) Hill slope unsaturated flowpaths and soil moisture variability in a forested catchment in southwest China. Master Thesis, Norwegian Univsity of Life Sciences.

Sørbotten LE, Stolte J, Wang Y, Mulder J Hydrological response and flow pathways in acrisols on a forested hillslope in monsoonal sub-tropical climate, Chonqing, Southwest China. *Pedosphere*, Accepted

Søvik AK, Mørkved PT (2008) Use of stable nitrogen isotope fractionation to estimate denitrification in small constructed wetlands treating agricultural runoff. *The Science of the Total Environment*, **392**, 157–165.

Spalding RF, Exner ME, Martin GE, Snow DD (1993) Effects of sludge disposal on groundwater nitrate concentrations. *Journal of Hydrology*, **142**, 213–228.

Vitousek P, Aber J, Howarth R (1997) Issues in Ecology: human alteration of the global nitrogen cycle: Causes and consequences. *Ecological Applications*, **7**, 737–750.

Wexler SK, Goodale CL, McGuire KJ, Bailey SW, Groffman PM (2014) Isotopic signals of summer denitrification in a northern hardwood forested catchment. *Proceedings of the National Academy of Sciences of the United States of America*, **111**, 16413–16418.

WRB (2006) *World reference base for soil resources*, (2006 edn), pp. 67–97. FAO, Rome.

Zhang L, Altabet MA, Wu T, Hadas O (2007) Sensitive measurement of NH_4^+ $^{15}N/^{14}N$ (δ^{15} NH_4^+) at natural abundance levels in fresh and saltwaters. *Analytical Chemistry*, **79**, 5297–5303.

Zhang J, Cai Z, Zhu T, Yang W, Müller C (2013) Mechanisms for the retention of inorganic N in acidic forest soils of southern China. *Scientific Reports*, **3**, 2342.

Zhao Y, Duan L, Xing J, Larssen T, Nielsen C, Hao J (2009) Soil acidification in China: is controlling SO2 emissions enough? *Environmental Science & Technology*, **43**, 8021–8026.

Zhu J, Mulder J, Wu LP, Meng XX, Wang YH, Dörsch P (2013) Spatial and temporal variability of N_2O emissions in a subtropical forest catchment in China. *Biogeosciences*, **10**, 1309–1321.

Supporting Information

Additional Supporting Information may be found in the online version of this article:

Fig. S1 EMMA model results estimating the contribution from HS in stream water (S1) in summer 2010 and 2013, based on water H^+ and NO_3^- concentrations.
Fig. S2 Relationship between $\delta^{15}N$-NO_3^- and NO_3^--N concentrations and flume discharge in stream water (S1) of summer 2010 and 2013.
Fig. S3 Relationship between $\delta^{15}N$-NO_3^- and NO_3^--N concentrations in stream water (S1) across all 3 year.
Table S1 Mean NH_4^+-N concentrations (mg L^{-1}) in throughfall, soil water and stream water in summers of 2009, 2010 and 2013.
Table S2 Mean NO_3^--N concentrations (mg L^{-1}) in throughfall, soil water and stream water in summers of 2009, 2010 and 2013.

Multiyear dual nitrate isotope signatures suggest that N-saturated subtropical forested catchments can act as robust N sinks

Running head: N-saturated catchments act as robust N sinks

Longfei Yu[1], Jing Zhu[2], Jan Mulder[1], Peter Dörsch[1]

[1]Department of Environmental Sciences, Norwegian University of Life Sciences, Postbox 5003, N-1432 Aas, Norway.

[2] Present address: Department of Environment and Resources, Guangxi Normal University, 541004, Guilin, China.

Corresponding author: Peter Dörsch, peter.doersch@nmbu.no, Tel. +47 67231836

Supporting Information

Table S1-S2

Figure S1-S3

Table S1 Mean NH_4^+-N concentrations (mg/ L) in throughfall, soil water and stream water in summers of 2009, 2010 and 2013

		HS					GDZ	Throughfall
		T1	T2	T3	T4	T5	B1	
2009	5 cm	0.10	— [a]	—	0.45	0.03	—	—
	10 cm	0.18	0.17	0.13	0.19	0.03	—	
	20 cm	0.12	0.08	0.02	0.02	0.02	—	
	40 cm	0.14	0.08	4.67	0.08	0.02	—	
2010	5 cm	0.10 (0.04)	0.06 (0.03)	0.17 (0.04)	0.06 (0.02)	0.07 (0.02)	0.15 (0.08)	7.33 (3.27)
	10 cm	0.14 (0.03)	0.24 (0.09)	0.08 (0.04)	0.10 (0.05)	1.33 (1.2)	0.08 (0.02)	
	20 cm	0.11 (0.03)	0.11 (0.03)	0.04	0.07 (0.03)	0.08 (0.03)	0.05 (0.01)	
	40 cm	0.09 (0.02)	0.04 (0.02)	0.06 (0.03)	0.09 (0.04)	0.05 (0.02)	0.05 (0.01)	
2013	5 cm	0.34 (0.25)	0.18 (0.04)	0.17 (0.05)	0.29 (0.04)	0.20 (0.06)	0.03 (0.01)	2.31

		GDZ					Stream
		B2	B3	B4	B5	B6	S1
2009	30 cm	0.02 (0.00)	0.11 (0.01)	0.03 (0.01)	0.23 (0.01)	1.18 (0.06)	—
	60 cm	0.02 (0.00)	—	0.10 (0.02)	0.14 (0.01)	1.27 (0.07)	
	100 cm	0.03 (0.00)	—	0.07 (0.01)	0.02 (0.00)	0.48 (0.02)	
2010	30 cm	0.05 (0.02)	0.02 (0.01)	0.02 (0.01)	0.01 (0.00)	1.10 (0.13)	0.17 (0.07)
	60 cm	0.02 (0.01)	0.07 (0.06)	0.02 (0.01)	0.04 (0.01)	1.18 (0.06)	
	100 cm	0.02 (0.02)	0.01 (0.00)	0.01 (0.01)	0.00 (0.00)	0.49 (0.03)	
2013[b]	5 cm	0.42 (0.40)	0.05 (0.01)	0.10 (0.06)	0.14 (0.10)	0.10 (0.07)	0.01 (0.00)
	60 cm	0.00 (0.00)	0.00 (0.00)	0.01 (0.00)	0.02 (0.01)	0.04 (0.00)	
	100 cm	0.00 (0.00)	—	0.00 (0.00)	0.01 (0.00)	0.49 (0.05)	

[a] not available, [b] soil water samples were only available at 5 cm depth on HS in 2013, 0-5 cm data in 2013 are listed as 5 cm; *standard errors in parentheses*

Table S2 Mean NO_3^--N concentrations (mg/ L) in throughfall, soil water and stream water in summers of 2009, 2010 and 2013

		HS					GDZ	Throughfall
		T1	T2	T3	T4	T5	B1	
2009	5 cm	7.6	— [a]	—	4.0	6.7	—	—
	10 cm	6.2	10.5	13.1	4.4	15.5	—	
	20 cm	6.8	13.3	15.6	7.6	10.1	—	
	40 cm	6.2	12.1	4.4	6.7	11.2	—	
2010	5 cm	14.1 (1.9)	10.9 (2.3)	10.6 (1.8)	12.4 (1.7)	11.0 (1.1)	13.6 (1.7)	3.3 (1.1)
	10 cm	17.0 (3.1)	8.2 (1.7)	6.8 (0.6)	11.1 (1.2)	5.7 (0.3)	9.3 (1.6)	
	20 cm	25.0 (2.8)	6.1 (0.5)	6.3	10.8 (0.6)	4.8 (0.5)	9.8 (0.4)	
	40 cm	26.4 (1.2)	6.9 (0.8)	10.9 (0.1)	10.7 (1.2)	7.1 (0.6)	10.3 (0.8)	
2013[b]	5 cm	12.2 (2.6)	14.0 (0.9)	32.3 (5.3)	6.4 (0.6)	16.2 (2.0)	5.6 (1.4)	2.3

		GDZ					Stream
		B2	B3	B4	B5	B6	S1
2009	30 cm	7.5 (0.6)	0.4 (0.2)	2.0 (0.5)	—	—	—
	60 cm	7.7 (0.5)	—	2.3 (0.5)	—	—	
	100 cm	4.8 (0.5)	—	3.6 (0.3)	0.9 (0.2)	—	
2010	30 cm	6.5 (0.7)	1.0 (0.1)	5.0 (0.2)	0.4 (0.0)	0.3 (0.0)	3.0 (0.5)
	60 cm	7.2 (0.4)	4.6 (0.5)	5.3 (0.2)	1.7 (0.5)	0.1 (0.0)	
	100 cm	6.5 (0.4)	5.9 (0.2)	4.4 (0.3)	2.3 (0.5)	0.1 (0.0)	
2013	5 cm	3.1 (0.4)	1.1 (0.5)	0.6 (0.2)	4.4 (2.3)	0.5 (0.1)	3.0 (1.0)
	60 cm	5.7 (1.3)	4.7 (0.6)	3.4 (0.1)	3.0 (0.6)	0.4 (0.0)	
	100 cm	7.4 (1.4)	—	4.7 (1.3)	2.8 (0.9)	0.0 (0.0)	

[a] not available, [b] soil water samples were only available at 5 cm depth on HS in 2013, 0-5 cm data in 2013 are listed as 5 cm; standard errors in parentheses.

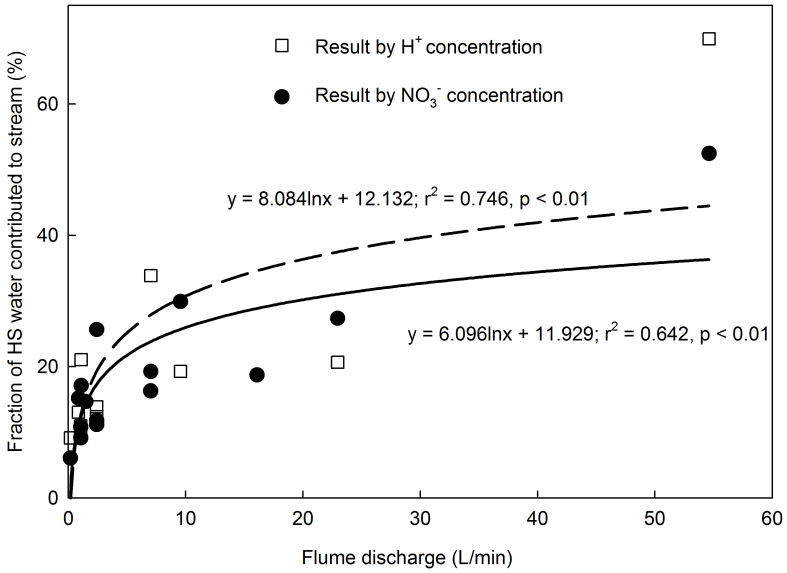

Fig. S1 EMMA model results estimating the contribution from HS in stream water (S1) in summer 2010 and 2013, based on water H^+ and NO_3^- concentrations. Mean concentrations of the two end-members (soil water from the hill slope and the GDZ) were derived from T1 to T5 and B5 to B6, respectively.

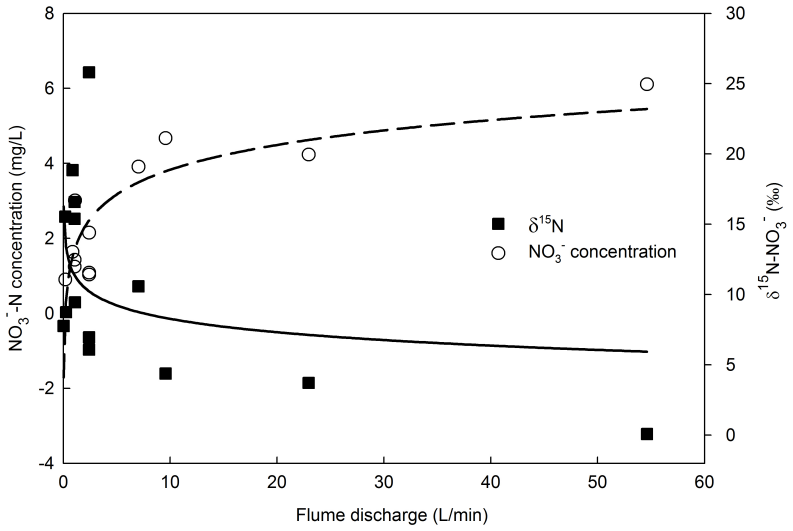

Fig. S2 Relationship between $\delta^{15}N\text{-}NO_3^-$ and NO_3^--N concentrations and flume discharge in stream water (S1) of summer 2010 and 2013

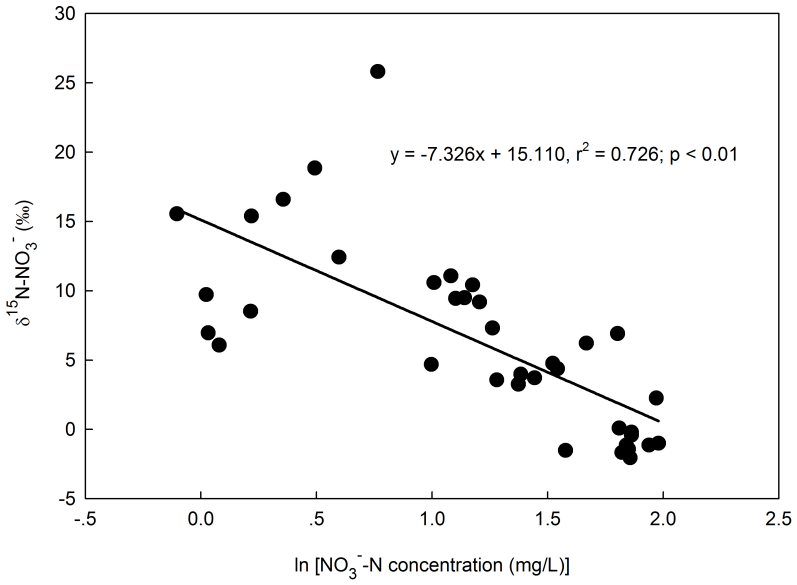

Fig. S3 Relationship between $\delta^{15}N\text{-}NO_3^-$ and NO_3^--N concentrations (in logarithmic scale) in stream water (S1) across all three years

Paper II

Denitrification as a major nitrogen sink in forested monsoonal headwater catchments in the sub-tropics: evidence from multi-site dual nitrate isotopes

Longfei Yu, Jan Mulder, Jing Zhu, Xiaoshan Zhang, Zhangwei Wang, Peter Dörsch

Under review in Environmental Science & Technology

Denitrification as a major nitrogen sink in forested monsoonal headwater catchments in the sub-tropics: evidence from multi-site dual nitrate isotopes

Longfei Yu[1], Jan Mulder[1*], Jing Zhu[1, 2], Xiaoshan Zhang[3], Zhangwei Wang[3], Peter Dörsch[1]

[1]Department of Environmental Sciences, Norwegian University of Life Sciences, Postbox 5003, N-1432 Aas, Norway.

[2]Department of Environment and Resources, Guangxi Normal University, 541004, Guilin, China.

[3]Research Center for Eco-Environmental Sciences, Chinese Academy of Sciences, 100085, Beijing, China

[*]Correspondence: Jan Mulder, tel. +47 67231852, E-mail jan.mulder@nmbu.no

Abstract

Increased nitrogen (N) deposition in many subtropical forests of south China has resulted in N saturation, associated with significant nitrate (NO_3^-) leaching from well-drained soils. At the catchment level, however, strong N retention was reported in groundwater discharge zones (GDZ), hydrologically connected to surrounding hill slopes (HS). Recently, a detailed dual-isotope study of ^{15}N- and ^{18}O-NO_3^- in the subtropical forested headwater catchment at Tieshanping, SW China, confirmed the importance of the GDZ as the prime N-sink and hotspot for denitrification. Here, we test if this finding is representative for a wider range of forest catchments throughout China differing in atmogenic N input and rainfall. In all catchments, inorganic N fluxes indicated efficient conversion of NH_4^+ to NO_3^- on well-drained HS, followed by significant attenuation of NO_3^- in the GDZ. Depletion of ^{15}N- and ^{18}O-NO_3^- in HS soils supports the importance of nitrification, as a source of NO_3^-. In all catchments, except the non-N-saturated northwestern site, NO_3^- attenuation in the GDZ was associated with ^{15}N and ^{18}O enrichment of residual NO_3^-, confirming denitrification. However, only the N-saturated southern catchments had a well-developed, continuous GDZ, hydrologically-connected to HS, which is essential if denitrification is to be a major catchment N-sink.

Key Word: Nitrification, $\delta^{15}N$, $\delta^{18}O$, Water flowpath, Groundwater discharge zone

Introduction

Anthropogenic changes to the global nitrogen (N) cycle affect the environment both regionally and globally [1,2]. Numerous studies report effects related to ecosystem functions [3,4], climatic change [5,6] and human health [7]. While the global inventory of the input of reactive N into the biosphere suggests a doubling in the last century [8,9], the relative contribution of mainland China to global N pollution is growing [10]. In southern Chinese forests, receiving N deposition of up to 60 kg N ha^{-1} yr^{-1} [11], N saturation has been reported with significant nitrate (NO_3^-) leaching from well-drained forest soils [12]. Yet, on the headwater catchment scale, large proportions of dissolved inorganic N are found to be attenuated in riparian soils just before entering streams [13,14].

Biological N sinks in forest ecosystems include assimilation (both in plant and microbial biomass) and NO_3^- removal by denitrification [15]. In the strongly acidic forest soils of South China, N uptake by standing biomass is limited due to slow tree growth [16,17], while net N assimilation into soil organic matter (SOM) is restricted by low carbon availability [18,19]. Several N mass balance studies from subtropical Chinese forest catchments have implicated denitrification, particularly in wet soils near streams, as possible N sink [13,20,21]. Recently, this conjecture was strengthened by stable isotope studies [22]. However, the importance of denitrification at the catchment scale is under-studied, due to the lack of spatially resolved data for soil denitrification [23].

Previous studies in temperate forests have documented significant, but transient denitrification activities in shallow saturated soils [23–26], where the required NO_3^- is derived from soil N cycling rather than from atmogenic sources [25,27,28]. Other studies have proposed spatially and temporally coupled nitrification-denitrification, where production and consumption of NO_3^- occur in the same shallow, fluctuating groundwater body [23,24,29]. This differs fundamentally from observations in

50 southern Chinese forests, where large amounts of NO_3^- are produced in well-drained top soils on
51 hill slopes (HS) without undergoing appreciable denitrification [13,30]. Recently, Yu et al. [31] observed
52 a robust multi-year ^{15}N and ^{18}O pattern in nitrate (NO_3^-) along a water flowpath in a headwater
53 catchment in SW China, suggesting that NH_4^+ is rapidly nitrified to NO_3^- in well-drained HS soils
54 during monsoonal summers. Subsequently, NO_3^- is transported by interflow over the argic Bt
55 horizons of the common Acrisols to a groundwater discharge zone (GDZ), where it is efficiently
56 denitrified. Similar geomorphologically related patterns of N turnover, transport and retention have
57 been reported in temperate and subtropical systems [29,32].

58 Denitrification in soils is difficult to measure directly [33], making dual isotopic signatures of NO_3^-
59 an attractive tool for integrating temporal and spatial variability of N turnover [25,26,29,34–36].
60 Biological transformations fractionate stable isotopes [36,37] and the resulting changes in ^{15}N and ^{18}O
61 signatures of residual NO_3^- can be used to partition NO_3^- sources as well as to elucidate underlying
62 biological processes. For instance, NO_3^- produced through nitrification is often ^{15}N-depleted
63 compared to NH_4^+ and ^{18}O-depleted compared to atmogenic NO_3^-. $\delta^{18}O$ of NO_3^- in precipitation is
64 generally larger than +60‰ [38], and can be used to partition ecosystem NO_3^- from microbial and
65 atmospheric sources [28,39], as soil NO_3^- incorporates oxygen from both ^{18}O-depleted atmospheric
66 O_2 and ^{18}O-enriched H_2O [36]. Microbial denitrification results in an enrichment of both ^{15}N and ^{18}O
67 in residual NO_3^- with a ratio between 1:1 and 2:1. The latter is routinely used to identify
68 denitrification in riparian and aquatic systems [26,34,36].

69 Here, we hypothesize that the geomorphological conditions in headwater catchments of the hilly
70 landscape of South China support N retention at large by combining nitrification and
71 denitrification in spatially distinct, but hydrologically connected landscape elements.
72 Denitrification may be enhanced by the abundance of reactive N [40,41], but it remains unclear how

73 catchment-scale N retention will respond to increasing N deposition loads, given the fact that other
74 factors, such as climatic conditions and soil properties, regulate biological N turnover locally [42,43].
75 To advance our understanding of N retention mechanisms in Chinese forests, we combined a dual
76 NO_3^- isotope study with a two-year monitoring project on N fluxes in seven forested headwater
77 catchments throughout China, differing in climatic and edaphic characteristics and with different
78 N deposition rates.

Materials and Methods

Study sites

Data were collected from five catchments in South China, and two catchments in North China (Figure 1). Some data from the southern Tieshanping (TSP) site were previously published [31] and are included for comparison. Details of site location, mean annual temperature and precipitation, vegetation, soil characteristics and annual N fluxes in throughfall are listed in Table 1. The five southern sites (Tieshanping-TSP, Leigongshan-LGS, Caijiatang-CJT, Tianmushan-TMS and Dagangshan-DGS) are subtropical and have a monsoonal climate [31], with annual precipitation greater than 1000 mm. Among the northern sites, Donglingshan (DLS) is located in the warm temperate zone with continental monsoonal climate, while Liupanshan (LPS) is in the temperate zone with continental climate, only marginally influenced by monsoon. Most precipitation occurs in summer, but mean annual precipitation at the northern sites is markedly smaller (~600 mm) than at the southern sites. All catchments have a similar topography characterized by well-drained hillslopes (HS) and hydrologically connected groundwater discharge zones (GDZ). However, the northern sites have less developed and more discontinuous GDZs along the stream, probably due to the drier conditions.

Soil types on HS at the southern sites are mainly Alisol and Acrisol, while Luvisols dominate at the northern sites [44]. The surface O/A horizon (excluding undecomposed litter) from most southern sites have a pH of about 4.0, except at TMS (6.3). Soil pH of the O/A horizon at the northern sites is 6.1 and 7.0 at DLS and LPS, respectively. C/N ratios of the O/A horizons are similar at all sites, ranging from 10.4 to 14.4. The seven sites represent a gradient of inorganic N in throughfall deposition, ranging from 5.0 to 48.7 kg N ha^{-1} yr^{-1} (Table 1).

Sampling design

In each of the seven catchments, soil and soil water samples were collected along the water flow path, from two permanent sampling plots at HS, two at GDZ and one at the stream outlet (Figure 1). Plots A and B were situated at the top and foot of the HS, respectively, while plots C and D represent the elevational gradient along the GDZ. Samples of throughfall, soil water and stream water were collected bi-weekly at all sites from Aug. 2012 to Aug. 2014. Throughfall samples for each month were pooled for analysis, and the total volumes were recorded. Throughfall was sampled in triplicate in 3 L PET (polyethylene) bottles, equipped with PET funnels with nylon gauze to exclude canopy litter. Soil water was sampled at each plot in triplicate from the surface soil (0-5 cm) with macrorhizon soil moisture samplers (Rhizosphere Research Products, The Netherlands). Vacuum was applied using a 50 ml syringe for 12 hours [31]. Stream water was collected above 'V'-shaped weirs established at the outlet of each catchment. Surface soils (0-3 cm, O/A horizon) were collected in triplicate using a garden spade, while excluding the litter layer (Oi). Water samples were kept frozen at -20^{o}C until analysis, whereas soil samples were stored at 4 ^{o}C.

For stable isotope analysis, we sampled throughfall, soil water and stream water twice at all sites (only throughfall for DGS) in July and August 2014, respectively. As shown by Yu et al. [31], N turnover processes are most intensive, and thus isotopic fractionation most pronounced, during warm and humid summers. Due to drought, no soil pore water could be sampled in the summer months at A, B and C plots at DLS. Additional samples of surface soil, soil water and stream water (at the outlet) were collected during a sampling campaign in July 2015 at four of the southern sites (LGS, CJT, TMS and DGS). During this campaign, little water was sampled at A, B and C of DGS, but pooling of triplicate samples at plots B and C produced enough sample for isotope analysis.

During the 2015 sampling campaign, all soil and water samples from a single site were collected on the same day. Previously published isotope data from the fifth southern site, TSP, obtained in 2013 using the same methods, are included for comparison [31].

Chemical analyses

The concentration of NH_4^+ and NO_3^- in water samples collected for routine analysis were analyzed by ion chromatography (DX-500, DIONEX) at the Research Center of Eco-Environmental Sciences, Chinese Academy of Science (CAS), Beijing. Mineral N concentrations of water samples, comprising NH_4^+-N and NO_3^--N, collected for isotope analysis, were determined spectrophotometrically using a flow injection analyzer (FIA star 5020, Tecator, Sweden) at Norwegian University of Life Sciences. Air-dried soil samples were sieved (2 mm), milled and then analyzed for total organic carbon (C) and total N contents, using a LECO elemental analyzer (TruSpec®CHN, USA). The soil pH was measured in 50 ml water (deionized) suspension with 10 g dry weight soil, using an Orion SA720 electrode pH-meter. All soil analyses were conducted at the Norwegian University of Life Sciences.

$\delta^{15}N$ and $\delta^{18}O$ of NO_3^- ($\delta^{15}N_{NO3}$ and $\delta^{18}O_{NO3}$) were analyzed, using a modified denitrifier method [45,46], at the Norwegian University of Life Sciences. Briefly, tryptic soya broth (TSB) medium was pretreated with *Paracoccus denitrificans* (ATCC 17741) to remove background NO_3^-, prior to culturing *Pseudomonas aureofaciens (P. a.)* (ATCC 13985) aerobically. In order to ensure rapid and successful transition from oxic to anoxic respiration in *P. a.* culture, the medium was amended with NH_4Cl. Aerobically grown *P. a.* culture was then injected into anoxic 120 ml vials (Helium-washed) to trigger conversion of NO_3^- to N_2O. $\delta^{15}N$ and $\delta^{18}O$ of N_2O were measured with an isotope ratio mass spectrometer coupled to a pre-concentration unit (PreCon-GC-IRMS, Thermo Finnigan MAT, Bremen, Germany). International standards (IAEA N3, USGS 32 and 34) were

included in each batch to correct for background and ^{18}O fractionation during conversion. The analytical precision was 0.2‰ for $\delta^{15}N$ and 0.5‰ for $\delta^{18}O$.

$\delta^{15}N$ of bulk soil ($\delta^{15}N_{soil}$) was measured by an EA-Conflow-IRMS system (Thermo Finnigan MAT, Bremen, Germany). Before analysis, air-dried samples were milled and weighed in tin capsules (8*5 mm, Elemental Microanalysis). IAEA standards (N1 and N3) as well as in-house materials (lab-mixed forest soils) were included in each batch. The analytical precision was 0.2‰.

Rayleigh enrichment factor

The Rayleigh distillation model [47]

$$\varepsilon = \frac{\delta_s - \delta_{s0}}{\ln [C(NO_3^-)_s / C(NO_3^-)_{s0}]}$$

where $C(NO_3^-)_{s0}$ and, $C(NO_3^-)_s$ are initial and residual NO_3^- concentration, respectively, and δ_{s0} and δ_s are $\delta^{15}N$ of initial and residual NO_3^-, was used to estimate the apparent ^{15}N enrichment factor for denitrification in the groundwater discharge zone. This approach is based on the assumption that the hydrological flow path behaves as a quasi-closed system [26], and that isotopic fractionation is solely due to denitrification [31].

Estimation of the annual N balance at the catchment-scale

We assumed the annual N flux in throughfall to represent the N input. The annual N flux by stream export was calculated by multiplying the annual mean inorganic N concentration with estimated water discharge. Stream water discharge rates were estimated based on precipitation data and runoff coefficients. For TSP, CJT and LGS, we adopted the runoff coefficients (the ratio of stream discharge to throughfall) given by Larssen et al. [13]. The coefficients for TMS and DGS, sites with similar climatic conditions as the former three, were estimated to be the average of those for TSP,

168 CJT and LGS. For the northern sites, LPS and DLS, assuming annual evapotranspiration to be
169 about 500 mm [48], the runoff coefficients were taken as 0.26 and 0.18, respectively, which is in
170 accordance with data from a large range of northern Chinese catchments [49]. We computed
171 catchment N retention by subtracting the N flux in the stream from the N flux in throughfall.

172 *Statistics*

173 Statistical analyses were performed with Minitab 16.2.2 (Minitab Inc., State College, PA, USA).
174 Significance levels in this study were set at $p < 0.05$, unless specified otherwise. One-way ANOVA
175 with post hoc Tukey test was performed to test differences in NH_4^+ and NO_3^- concentrations, as
176 well as in $\delta^{15}N_{NO3}$, $\delta^{18}O_{NO3}$ and $\delta^{15}N_{Soil}$ among different sampling plots and sites.

Results and Discussion

N sinks revealed by inorganic N fluxes

Nitrogen fluxes in throughfall decreased in the order TSP>CJT>TMS>DGS>DLS>LGS>LPS (Table 1), indicating largest N inputs at the southern sites (except for the background site LGS). At most, about half of the N was deposited as NH_4^+, with largest values at TSP (56%) and CJT (40%) (Figure 1). At the other sites, dissolved N in throughfall was dominated by NO_3^--N. Compared with earlier throughfall data for the period 2001–2004 [50], this suggests that the relative importance of NO_3^--N has increased significantly during the last 10 years. On the hill slopes (HS), NH_4^+ concentrations in soil water were generally below 0.1 mg N L^{-1} (except for LPS, Figure S1) and significantly smaller ($p < 0.05$) than in throughfall, while NO_3^- concentrations were significantly ($p < 0.05$) larger in soil water than in throughfall (Figure 2). From the HS to the groundwater discharge zone (GDZ), the NH_4^+ concentration in soil water remained low, while NO_3^- declined in soil water from HS to GDZ and stream water. The samples collected during the summer campaign for isotope analysis showed NH_4^+ concentrations similar to those of the long-term data (compare Figure S2a with Figures 2 and S1). With the exception of DGS (increase at plot C, GDZ) and LPS (overall low concentrations), also the spatial pattern of NO_3^- concentrations along the water flow path resembled that of the 2-year data set (Figure S2b).

The concentration of Na^+ in throughfall, soil water and stream water (Figure S3), which may be used as a proxy for evapotranspiration, assuming Na^+ is an inert solute in the soil and does not have a source in the catchment [12], showed a general increase along the water flow path (except at CJT). We normalized the NO_3^- concentration against the Na^+ concentration measured along the water flow path, to account for concentration changes due to evapotranspiration. The spatial

pattern of the NO_3^-/Na^+ ratio showed the expected sharp increase from throughfall to HS and a subsequent pronounced decrease from HS to GDZ (Figure S4). This confirms that the spatial pattern of NO_3^- concentration was not due to evapotranspiration, but resulted from significant source (HS) and sink terms (GDZ), respectively.

There were exceptions to the general pattern of NO_3^- concentrations, however. At LPS, N deposition was smallest among all sites (Table 1), and thus NO_3^- leaching from the HS soil was least significant (Figures 2 and S2b), also resulting in no apparent change in NO_3^- concentration along the water flow path. This suggests that LPS is a N-limited system, with N sinks dominated by plant and soil assimilation [4]. At DGS, during summer 2015, there was an increase in NO_3^- concentration from HS to GDZ, followed by decrease in the stream (Figure S2b). Only few samples could be obtained from this site, but it is likely that the elevated NO_3^- concentration in GDZ during summer 2015 was a result of strong evaporation due to drought, similar to observations made by Yu et al. [31] during a drought period in 2013 at TSP. These elevated NO_3^- concentrations play little role for the annual NO_3^- flux, however, as water transport is small.

At all sites, the concentration of NO_3^- in stream water tended to be greater than that in soil water at plot D of the GDZ, except at LGS and LPS (Figure 2), the two sites where N fluxes in throughfall and NO_3^- concentrations in soil water were smallest. Greater NO_3^- concentrations in stream water than in soil water in GDZ may be due to NO_3^- entering the stream directly from surrounding hillslopes, bypassing the GDZ in the valley bottom, particularly during periods of high flow [31]. In addition, NO_3^- may be produced locally by intermittent nitrification in the GDZ or in the stream during low-flow conditions, as previously suggested for temperate systems [24]. Both long- and short-term data sets (Figures 2 and S2, respectively) indicate significant N sinks in all seven catchments (Figure S4), located predominantly in the GDZ. This suggests that the efficiency of

222 the catchment to remove NO_3^- depends on the GDZ acting as a conduit for water as it passes from
223 HS to the stream.

224 ***Within-catchment N turnover gauged by NO_3^- isotope signatures***

225 At all sites, $\delta^{15}N_{NO3}$ in soil water on HS was < 0‰, except for plot A at LGS (Figure 3a). In general,
226 NO_3^- in soil water on HS was more depleted in ^{15}N and ^{18}O than in throughfall (Figure 3),
227 indicating that soil water NO_3^- is mostly derived from nitrification, and to a smaller extent directly
228 from atmogenic deposition [31,37]. Similar findings were reported for a range of forest soils in the
229 northern US [25]. In addition, at all sites, except DGS, soil water on HS had $\delta^{15}N_{NO3}$ and $\delta^{18}O_{NO3}$
230 values in the range -5 to +5‰ and -10 to +10‰, respectively (Figure S5), which has previously
231 been taken as indicative for nitrification-derived NO_3^- [26,31].

232 Nitrification causes only small isotopic fractionation, thus retaining the $\delta^{15}N$ signatures from NH_4^+
233 in NO_3^- [47]. As suggested by the LGS data, which showed greater $\delta^{15}N_{NO3}$ values in soil water than
234 in throughfall (Figure 3a), NO_3^- in soil water on HS is primarily derived from soil organic N (NH_4^+
235 produced by mineralization). Soil organic N at LGS is characterized by relatively large $\delta^{15}N$ values,
236 ranging from +4 to +5‰ (Fig. S6), as often found in nitrogen-rich litter [51], e.g. of *Pinus armandii*,
237 the dominant tree species at LGS. It is beyond the scope of the present study to partition sources
238 of NH_4^+ undergoing nitrification in HS soils, but recent ^{15}N tracing study in subtropical forest soils
239 have suggested that much of the atmogenic NH_4^+ entering the soil is immobilized and undergoes
240 internal N cycling before being nitrified [52,53].

241 Decreasing NO_3^- concentrations along the water flow path from HS to GDZ (Figures 2 and S2b)
242 were associated with a significant ($p < 0.05$) increase of both $\delta^{15}N$ and $\delta^{18}O$ in residual NO_3^-
243 (Figure 3a) at all sites, except LPS. This supports our earlier conclusion that the observed N

retention on the catchment scale relies on denitrification in the stream-near GDZ, similar to what has been reported for agroecosystems [54] and for temperate forest ecosystems [34]. A regression of $\delta^{18}O_{NO3}$ against $\delta^{15}N_{NO3}$ values resulted in slopes between 0.5 and 1 (Figure S5), which is well within the range of ratios considered diagnostic for denitrification [26,36,55,56]. Despite the lack of data for DLS, large $\delta^{15}N_{NO3}$ (23.4 ‰) and $\delta^{18}O_{NO3}$ (30.0‰) values observed in a pooled GDZ soil water sample was in line with strong denitrification in the near-stream environment.

Apparent ^{15}N enrichment factors for LGS, CJT and TMS were estimated by Raleigh fractionation [47] (DGS and DLS were not included due to too little data), based on the progressive NO_3^- consumption and ^{15}N enrichment along the water flow path from HS to GDZ (Figures 2 and 3). The enrichment factors (Figure S7) were between -3.0 to -6.0‰ and are similar to those reported for TSP [31] and for groundwaters [57–59]. Except for the low N deposition site (LPS) in NW China and the central northern site DLS (for which no data could be obtained from the HS), all catchments showed the same spatial pattern of dual NO_3^- isotopes associated with N retention as reported for TSP [31], reflecting efficient N turnover and NO_3^- removal in hydrologically connected landscapes. Our finding of similar patterns in these five sites in South China substantiates the idea that N removal by denitrification in stream-near groundwater discharge zones may be a widespread phenomenon in monsoonal, subtropical forest catchments.

What factors govern the N sink function of forested catchments?

Distinct landscape elements with prevailing oxidative or reductive conditions and NO_3^- transport between these elements appear to be central for the N retention observed at the catchment scale. Argic horizons with restricted hydraulic conductivity are widespread in Ali- and Acrisols of subtropical China and favor the transport of NO_3^- by “interflow” along the hillslopes. This interflow leads to well-developed groundwater discharge zones, where the landscape flattens out.

By contrast, direct seepage of NO_3^- in these soils to the groundwater seems to play a minor role [60]. Others have found a similar connection between topography and dissimilatory N turnover. For instance, Hilton et al. [61]and Weintraub et al. [62] reported a negative correlation between slope angle and $\delta^{15}N$ of bulk soil in subtropical and tropical forests. We found a similar pattern at the southern sites (except in the *Pinus armandii*-dominated LGS, with its more N-rich litter and associated greater $\delta^{15}N_{soil}$), as $\delta^{15}N_{soil}$ gradually increased along the hydrological flowpath (from the steeper A to the less steep D plots, Figure S6). In addition there was a strong ($p < 0.01$) negative correlation between $\delta^{15}N_{soil}$ and the C/N ratio (Figure S8), suggesting that N is increasingly processed along the flowpath [63,64]. In a northeastern catchment in the US, Anderson et al. [32] observed a strong impact of topography on denitrification rates, which was also linked to the distribution of water-saturated zones. Hence, the hilly topography, the monsoonal climate with large amounts of precipitation in summer and the prevalence of Ali- and Acrisols producing interflow are crucial factors for the development of continuous groundwater discharge zones with a significant capacity for denitrification, allowing for the observed N sink function in southern China.

At the northern site DLS, we observed NO_3^--N fluxes in stream water that were similar to the rates of N fluxes in throughfall (Figure 4a). This implies a relatively small annual N-sink, despite the elevated $\delta^{15}N_{NO3}$ values in the GDZ, which suggested a significant hotspot for denitrification (Figure 3). Most likely, a substantial part of the drainage water from HS soils bypasses the GDZ and is little affected by denitrification. In the southern TSP catchment, Yu et al. [31] observed a similar, albeit less extreme tendency of HS water bypassing the GDZ during single, intensive rainstorms. Probably, the GDZ is less developed in the drier, northern DLS, and thus reductive conditions are less common, than in the southern catchments [65,66], where annual precipitation is double that at the northern site (Table 1).

Catchment N retention scaled with N fluxes in throughfall, with an average retention rate of 65% across all sites (Figure 4a). To compare the resulting ^{15}N enrichment by denitrification among the southern catchments, we calculated the overall change of $\delta^{15}N_{NO3}$ from HS to GDZ ($\Delta\delta^{15}N_{NO3}$), which positively correlated with N deposition Retention (Figure 4b). This suggests that the N sink by denitrification could be stimulated by enhanced N deposition [41], on the condition that runoff is channeled through saturated GDZs before reaching the stream, as is the case at the southern sites, but not the northern.

Our study confirms the prevalence of GDZ denitrification in a range of forest catchments across China. The N turnover patterns along the water flowpaths in monsoonal South China were similar to those previously observed at TSP [31] and confirm our hypothesis that N retention by hydrologically coupled nitrification–denitrification is a more widespread phenomenon in humid southern Chinese forest catchments. By contrast, at the northern site, the GDZ, which was less developed due to the drier conditions, is unlikely to constitute an efficient N sink for the catchment.

Acknowledgement

Longfei Yu thanks the China Scholarship Council (CSC) for supporting his PhD study. Support from the Norwegian Research Council to project 209696/E10 ‘Forest in South China: an important sink for reactive nitrogen and a regional hotspot for N_2O?’ is gratefully acknowledged. We thank Yaqing Gou for plotting Figure 1, and Wang Yanhui, Zhang Yi, Cui Juan, Wang Bing, Xiao Jinsong, Qin Pufeng, Jiang Hong, Zou Mingquan for their help during data collection.

Reference

(1) Vitousek, P. M.; Aber, J. D.; Howarth, R. W.; Likens, G. E.; Matson, P. A.; Schindler, D. W.; Schlesinger, W. H.; Tilman, D. M. Human alteration of the global nitrogen cycle: causes and consequences. *Issues Ecol.* **1997**, *7*, 737–750.

(2) Galloway, J.; Aber, J.; Erisman, J.; Speitzinger, S.; Howarth, R.; Cowling, E.; Cosby, A. The nitrogen cascade. *Bioscience* **2003**, *53* (4), 341–356.

(3) Jaworski, N. A.; Howarth, R. W.; Hetling, L. J. Atmospheric Deposition of Nitrogen Oxides onto the Landscape Contributes to Coastal Eutrophication in the Northeast United States. *Environ. Sci. Technol.* **1997**, *31* (7), 1995–2004.

(4) Aber, J.; McDowell, W.; Nadelhoffer, K.; Magill, A.; Berntson, G.; Kamakea, M.; McNulty, S.; Currie, W.; Rustad, L.; Fernandez, I. Nitrogen saturation in temperate forest ecosystems - hypotheses revisited. *Bioscience* **1998**, *48* (11), 921–934.

(5) Shi, Y.; Cui, S.; Ju, X.; Cai, Z.; Zhu, Y. Impacts of reactive nitrogen on climate change in China. *Sci. Rep.* **2015**, *5*, 8118.

(6) Bernal, S.; Hedin, L.; Likens, G.; Gerber, S.; Buso, D. Complex response of the forest nitrogen cycle to climate change. *Proc. Natl. Acad. Sci. U. S. A.* **2012**.

(7) Townsend, A. R.; Howarth, R. W.; Bazzaz, F. A.; Booth, M. S.; Cleveland, C. C.; Collinge, S. K.; Dobson, A. P.; Epstein, P. R.; Holland, E. A.; Keeney, D. R.; et al. Human health effects of a changing global nitrogen cycle. *Front. Ecol. Environ.* **2003**, *1* (5), 240–246.

(8) Cui, S.; Shi, Y.; Groffman, P. M.; Schlesinger, W. H.; Zhu, Y.-G. Centennial-scale analysis of the creation and fate of reactive nitrogen in China (1910-2010). *Proc. Natl. Acad. Sci. U. S. A.* **2013**, *110* (6), 2052–2057.

(9) Gu, B.; Ge, Y.; Ren, Y.; Xu, B.; Luo, W.; Jiang, H.; Gu, B.; Chang, J. Atmospheric reactive nitrogen in china: Sources, recent trends, and damage costs. *Environ. Sci. Technol.* **2012**, *46* (17), 9420–9427.

(10) Liu, X.; Zhang, Y.; Han, W.; Tang, A.; Shen, J.; Cui, Z.; Vitousek, P.; Erisman, J. W.; Goulding, K.; Christie, P.; et al. Enhanced nitrogen deposition over China. *Nature* **2013**, *494* (7438), 459–462.

(11) Xu, W.; Luo, X. S.; Pan, Y. P.; Zhang, L.; Tang, A. H.; Shen, J. L.; Zhang, Y.; Li, K. H.; Wu, Q. H.; Yang, D. W.; et al. Quantifying atmospheric nitrogen deposition through a nationwide monitoring network across China. *Atmos. Chem. Phys.* **2015**, *15* (21), 12345–12360.

(12) Huang, Y.; Kang, R.; Mulder, J.; Zhang, T.; Duan, L. Nitrogen saturation, soil acidification, and ecological effects in a subtropical pine forest on acid soil in southwest China. *J. Geophys. Res. Biogeosciences* **2015**, *120*, 2457–2472.

(13) Larssen, T.; Duan, L.; Mulder, J. Deposition and leaching of sulfur, nitrogen and calcium

in four forested catchments in China: implications for acidification. *Environ. Sci. Technol.* **2011**, *45* (4), 1192–1198.

(14) Duan, L.; Yu, Q.; Zhang, Q.; Wang, Z.; Pan, Y.; Larssen, T.; Tang, J.; Mulder, J. Acid deposition in Asia: Emissions, deposition, and ecosystem effects. *Atmos. Environ.* **2016**.

(15) Yanai, R. D.; Vadeboncoeur, M. A.; Arthur, M. A.; Fuss, C. B.; Driscoll, C. T.; Groffman, P. M.; Siccama, T. G. From missing source to missing sink: Long-term nitrogen dynamics in the northern hardwood forest. *Proc. Natl. Acad. Sci.* **2013**, *47*, 11440–11448.

(16) Li, Z.; Wang, Y.; Liu, Y.; Guo, H.; Li, T.; Li, Z. H.; Shi, G. Long-term effects of liming on health and growth of a Masson pine stand damaged by soil acidification in Chongqing, China. *PLoS One* **2014**, *9* (4), 1–9.

(17) Wang, Y.; Solberg, S.; Yu, P.; Myking, T.; Vogt, R. D.; Du, S. Assessments of tree crown condition of two Masson pine forests in the acid rain region in south China. *For. Ecol. Manage.* **2007**, *242* (2-3), 530–540.

(18) MacDonald, J. A.; Dise, N.; Matzner, E.; Armbruster, M.; Gundersen, P.; Forsius, M. Nitrogen input together with ecosystem nitrogen enrichment predict nitrate leaching from Europen forests. *Glob. Chang. Biol.* **2002**, *8* (10), 1028–1033.

(19) Chen, X.; Mulder, J. Indicators for nitrogen status and leaching in subtropical forest ecosystems, South China. *Biogeochemistry* **2007**, *82* (2), 165–180.

(20) Chen, X. Y.; Mulder, J.; Wang, Y. H.; Zhao, D. W.; Xiang, R. J. Atmospheric deposition, mineralization and leaching of nitrogen in subtropical forested catchments, South China. *Environ. Geochem. Health* **2004**, *26* (2-3), 179–186.

(21) Zhu, J.; Mulder, J.; Wu, L. P.; Meng, X. X.; Wang, Y. H.; Dörsch, P. Spatial and temporal variability of N_2O emissions in a subtropical forest catchment in China. *Biogeosciences* **2013**, *10* (3), 1309–1321.

(22) Fang, Y.; Koba, K.; Makabe, A.; Takahashi, C.; Zhu, W.; Hayashi, T. Microbial denitrification dominates nitrate losses from forest ecosystems. *Proc. Natl. Acad. Sci. U. S. A.* **2015**, 1–5.

(23) Duncan, J. M.; Groffman, P. M.; Band, L. E. Towards closing the watershed nitrogen budget: Spatial and temporal scaling of denitrification. *J. Geophys. Res. Biogeosciences* **2013**, *118* (3), 1105–1119.

(24) Duncan, J.; Band, J.; Groffman, P.; Bernhardt, E. Mechanisms driving the seasonality of catchment scale nitrate export: Evidence for riparian ecohydrologil controls. *Water Resour. Res.* **2015**, 1–16.

(25) Rose, L.; Sebestyen, S. D.; Elliott, E. M.; Koba, K. Drivers of atmospheric nitrate processing and export in forested catchments. *Water Resour. Res.* **2014**, *51*, 1333–1352.

(26) Wexler, S. K.; Goodale, C. L.; McGuire, K. J.; Bailey, S. W.; Groffman, P. M. Isotopic signals of summer denitrification in a northern hardwood forested catchment. *Proc. Natl. Acad. Sci. U. S. A.* **2014**, No. 15, 1–6.

(27) Sabo, R. D.; Nelson, D. M.; Eshleman, K. N. Episodic, seasonal, and annual export of atmospheric and microbial nitrate from a temperate forest. *Geophys. Res. Lett.* **2015**, *43*, 683–691.

(28) Rose, L. A.; Elliott, E. M.; Adams, M. B. Triple Nitrate Isotopes Indicate Differing Nitrate Source Contributions to Streams Across a Nitrogen Saturation Gradient. *Ecosystems* **2015**, *18* (7), 1209–1223.

(29) Griffiths, N. A.; Jackson, C. R.; McDonnell, J. J.; Klaus, J.; Du, E.; Bitew, M. M. Dual nitrate isotopes clarify the role of biological processing and hydrological flow paths on nitrogen cycling in subtropical low-gradient watersheds. *J. Geophys. Res. Biogeosciences* **2016**, *121*.

(30) Fang, Y.; Gundersen, P.; Vogt, R. D.; Koba, K.; Chen, F.; Chen, X. Y.; Yoh, M. Atmospheric deposition and leaching of nitrogen in Chinese forest ecosystems. *J. For. Res.* **2011**, *16* (5), 341–350.

(31) Yu, L.; Zhu, J.; Mulder, J.; Dörsch, P. Multiyear dual nitrate isotope signatures suggest that N-saturated subtropical forested catchments can act as robust N sinks. *Glob. Chang. Biol.* **2016**, *In Press*.

(32) Anderson, T. R.; Groffman, P. M.; Walter, M. T. Using a soil topographic index to distribute denitrification fluxes across a northeastern headwater catchment. *J. Hydrol.* **2015**, *522*, 123–134.

(33) Kulkarni, M. V.; Burgin, A. J.; Groffman, P. M.; Yavitt, J. B. Direct flux and ^{15}N tracer methods for measuring denitrification in forest soils. *Biogeochemistry* **2014**, *117* (2-3), 359–373.

(34) Osaka, K.; Ohte, N.; Koba, K.; Yoshimizu, C.; Katsuyama, M.; Tani, M.; Tayasu, I.; Nagata, T. Hydrological influences on spatiotemporal variations of $\delta^{15}N$ and $\delta^{18}O$ of nitrate in a forested headwater catchment in central Japan: Denitrification plays a critical role in groundwater. *J. Geophys. Res.* **2010**, *115* (G2), G02021.

(35) Schwarz, M. T.; Oelmann, Y.; Wilcke, W. Stable N isotope composition of nitrate reflects N transformations during the passage of water through a montane rain forest in Ecuador. *Biogeochemistry* **2011**, *102* (1-3), 195–208.

(36) Kendall, C.; Elliott, E. M.; Wankel, S. D. Tracing anthropogenic inputs of nitrogen to ecosystems. In Stable Isotopes in Ecology and Environmental Science In Stable Isotopes in Ecology and Environmental Science, 2nd ed.; Michener, R. H., Lajtha, K. Eds. *Blackwell Publ.* **2007**, 375–449.

(37) Fry, B. *Stable Isotope Ecology*; Springer: New York, 2007.

(38) Garten, C. T. Nitrogen isotope composition of ammonium and nitratein bulk precipitation and forest throughfall. *Int. J. Environ. Anal. Chem.* **1992**, *47*, 33–45.

(39) Barnes, R. T.; Raymond, P. A.; Casciotti, K. L. Dual isotope analyses indicate efficient processing of atmospheric nitrate by forested watersheds in the northeastern U.S. *Biogeochemistry* **2008**, *90* (1), 15–27.

(40) Niu, S.; Classen, A. T.; Dukes, J. S.; Kardol, P.; Liu, L.; Luo, Y.; Rustad, L.; Sun, J.; Tang, J.; Templer, P. H.; et al. Global patterns and substrate-based mechanisms of the terrestrial nitrogen cycle. *Ecol. Lett.* **2016**, *19*, 697–709.

(41) Seitzinger, S.; Harrison, J.; Bohlke, J.; Bouwman, A.; Lowrance, R.; Peterson, B.; Tobias, C.; Van Drecht, G. Denitrification across landscaes and waterscapes: a synthesis. *Ecol. Appl.* **2006**, *16* (6), 2064–2090.

(42) Groffman, P. M. Terrestrial denitrification: challenges and opportunities. *Ecol. Process.* **2012**, *1*, 1–11.

(43) Sahrawat, K. L. Factors Affecting Nitrification in Soils. *Commun. Soil Sci. Plant Anal.* **2008**, *39* (9-10), 1436–1446.

(44) *World Reference Base for Soil Resources 2014*; FAO: Rome, 2014.

(45) Sigman, D. M.; Casciotti, K. L.; Andreani, M.; Barford, C.; Galanter, M.; Böhlke, J. K. A bacterial method for the nitrogen isotopic analysis of nitrate in seawater and freshwater. *Anal. Chem.* **2001**, *73* (17), 4145–4153.

(46) Casciotti, K. L.; Sigman, D. M.; Hastings, M. G.; Böhlke, J. K.; Hilkert, A. Measurement of the oxygen isotopic composition of nitrate in seawater and freshwater using the denitrifier method. *Anal. Chem.* **2002**, *74* (19), 4905–4912.

(47) Mariotti, A.; Germon, J.; Hubert, P.; Kaiser, P.; Letolle, R.; Tardieux, A.; Tardieux, P. Experimental determination of nitrogen kinetic isotope fractionation: some principles; illustration for the denitrification and nitrification processes. *Plant Soil* **1981**, *62*, 413–430.

(48) Xu, X.; Yang, D. Analysis of catchment evapotranspiration at different scales using bottom-up and top-down approaches. *Front. Archit. Civ. Eng. China* **2010**, *4* (1), 65–77.

(49) Wang, S.; Fu, B.-J.; He, C.-S.; Sun, G.; Gao, G.-Y. A comparative analysis of forest cover and catchment water yield relationships in northern China. *For. Ecol. Manage.* **2011**, *262* (7), 1189–1198.

(50) Chen, X.; Mulder, J. Atmospheric deposition of nitrogen at five subtropical forested sites in South China. *Sci. Total Environ.* **2007**, *378* (3), 317–330.

(51) Pardo, L. H.; Templer, P. H.; Goodale, C. L.; Duke, S.; Groffman, P. M.; Adams, M. B.; Boeckx, P.; Boggs, J.; Campbell, J.; Colman, B.; et al. Regional Assessment of N Saturation using Foliar and Root $\delta^{15}N$. *Biogeochemistry* **2006**, *80* (2), 143–171.

(52) Zhang, J.; Cai, Z.; Zhu, T.; Yang, W.; Müller, C. Mechanisms for the retention of inorganic N in acidic forest soils of southern China. *Sci. Rep.* **2013**, *3* (3), 2342.

(53) Gao, W.; Kou, L.; Yang, H.; Zhang, J.; Müller, C.; Li, S. Are nitrate production and retention processes in subtropical acidic forest soils responsive to ammonium deposition? *Soil Biol. Biochem.* **2016**, *100*, 102–109.

(54) Billy, C.; Billen, G.; Sebilo, M.; Birgand, F.; Tournebize, J. Nitrogen isotopic composition of leached nitrate and soil organic matter as an indicator of denitrification in a sloping

drained agricultural plot and adjacent uncultivated riparian buffer strips. *Soil Biol. Biochem.* **2010**, *42* (1), 108–117.

(55) Lehmann, M. F.; Reichert, P.; Bernasconi, S. M.; Barbieri, A.; McKenzie, J. A. Modelling nitrogen and oxygen isotope fractionation during denitrification in a lacustrine redox-transition zone. *Geochim. Cosmochim. Acta* **2003**, *67* (14), 2529–2542.

(56) Mayer, B.; Boyer, E. W.; Goodale, C.; Jaworski, N. A.; Van Breemen, N.; Howarth, R. W.; Seitzinger, S.; Billen, G.; Lajtha, K.; Nadelhoffer, K.; et al. Sources of nitrate in rivers draining sixteen watersheds in the northeastern U.S.: Isotopic constraints. *Biogeochemistry* **2002**, *57-58*, 171–197.

(57) Mariotti, A.; Landreau, A.; Simon, B. ^{15}N isotope biogeochemistry and natural denitrification process in groundwater: Application to the chalk aquifer of northern France. *Geochim. Cosmochim. Acta* **1988**, *52* (7), 1869–1878.

(58) Bottcher, J.; Strebel, O.; Voerkelius, S.; Schmidt, H. Using isotope fractionation of nitrate-nitrogen and nitrate-oxygen for evaluation of microbial denitrification in a sandy aquifer. *J. Hydrol.* **1990**, *114*, 413–424.

(59) Spalding, R. F.; Exner, M. E.; Martin, G. E.; Snow, D. D. Effects of sludge disposal on groundwater nitrate concentrations. *J. Hydrol.* **1993**, *142*, 213–228.

(60) Sørbotten, L.; Stolte, J.; Wang, Y.; Mulder, J. Hydrological Response and Flow Pathways in Acrisols on a Forested Hillslope in Monsoonal Sub-tropical Climate, Chonqing, Southwest. *Pedosphere* **2016**, *Accepted*.

(61) Hilton, R. G.; Galy, A.; West, A. J.; Hovius, N.; Roberts, G. G. Geomorphic control on the $\delta^{15}N$ of mountain forests. *Biogeosciences* **2013**, *10* (3), 1693–1705.

(62) Weintraub, S. R.; Taylor, P. G.; Porder, S.; Cleveland, C. C.; Asner, G. P.; Townsend, A. R. Topographic controls on soil nitrogen availability in a lowland tropical forest. *Ecology* **2014**, *96* (6), 1561–1574.

(63) Billings, S. A.; Richter, D. D. Changes in stable isotopic signatures of soil nitrogen and carbon during 40 years of forest development. *Oecologia* **2006**, *148* (2), 325–333.

(64) Dijkstra, P.; Laviolette, C. M.; Coyle, J. S.; Doucett, R. R.; Schwartz, E.; Hart, S. C.; Hungate, B. A. ^{15}N enrichment as an integrator of the effects of C and N on microbial metabolism and ecosystem function. *Ecol. Lett.* **2008**, *11* (4), 389–397.

(65) Van Gaalen, J. F.; Kruse, S.; Lafrenz, W. B.; Burroughs, S. M. Predicting Water Table Response to Rainfall Events, Central Florida. *GroundWater* **2013**, *51* (3), 350–362.

(66) Hughes, D. A. Incorporating groundwater recharge and discharge functions into an existing monthly rainfall–runoff model. *Hydrol. Sci. J.* **2004**, *49* (2), 37–41.

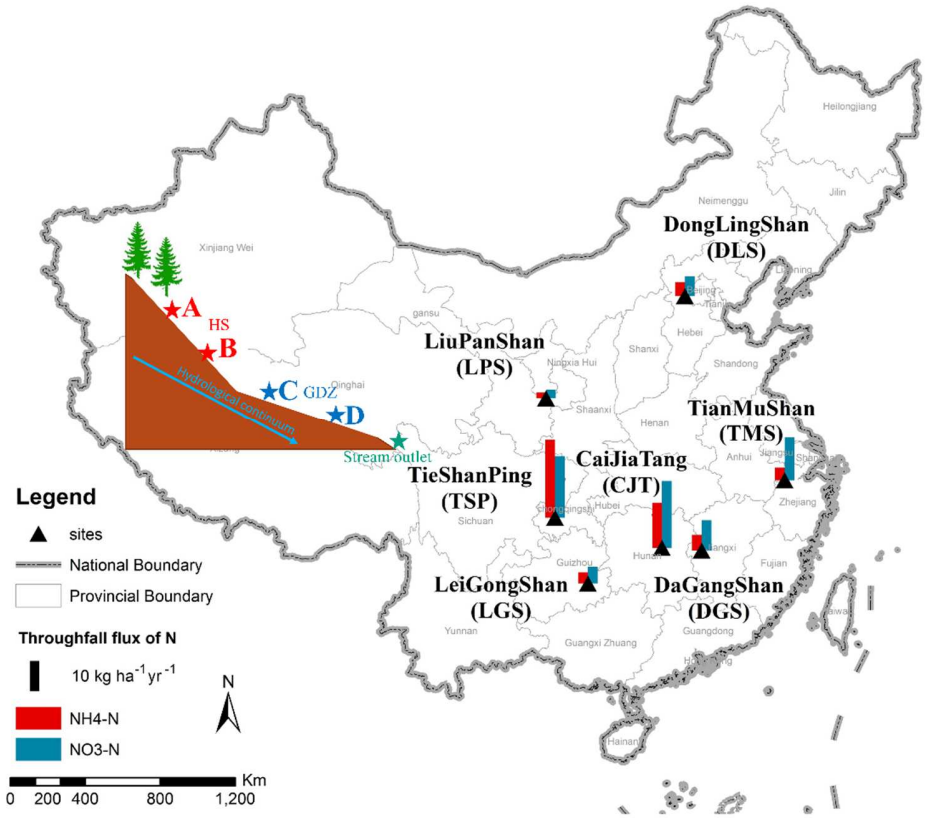

Figure 1. Overview of sampling sites and N fluxes in throughfall. Bars are average annual fluxes of NH_4^+- and NO_3^--N fluxes in throughfall from August 2012 to August 2014. Inserted is a schematic representation of the hydrological continuum, including the sampling plots along the water flowpath, as found in all catchments.

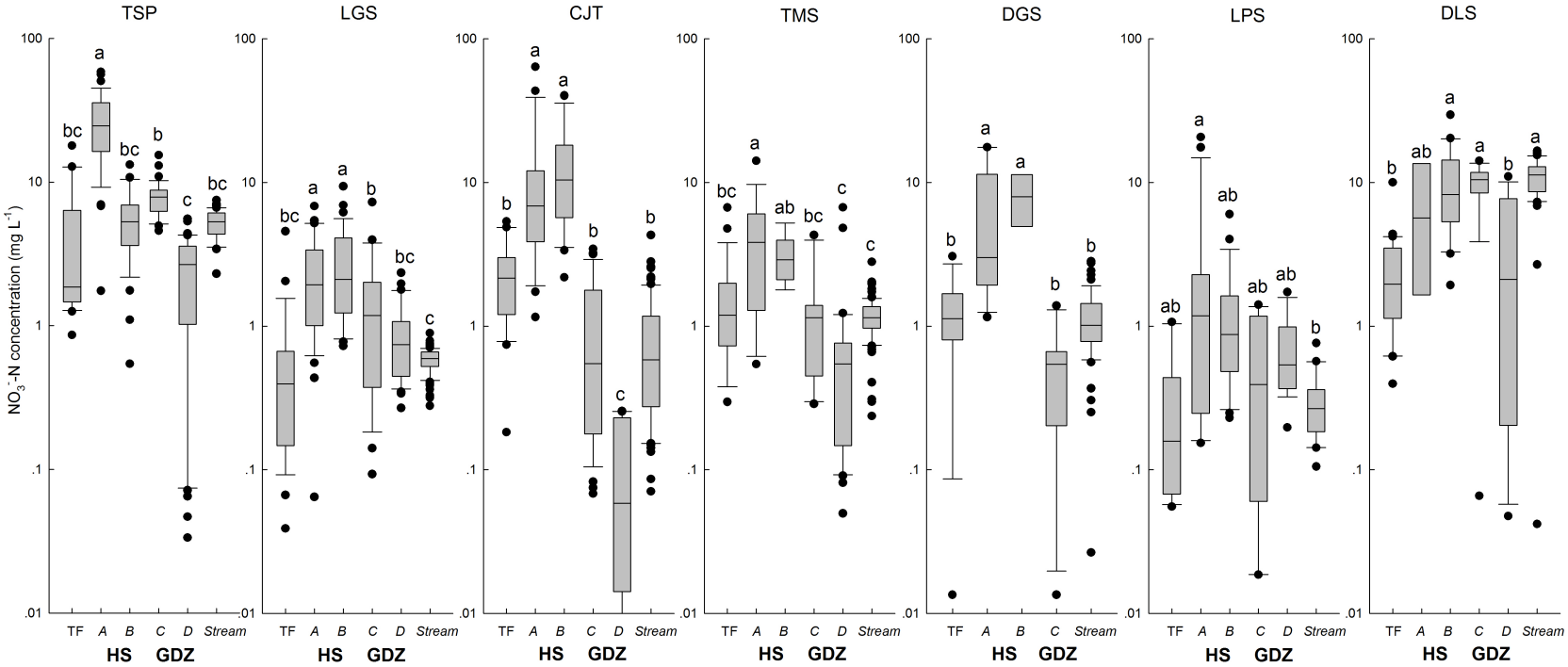

Figure 2 Logarithmic box whisker plot of NO_3^- concentrations in throughfall (TF), soil water at plots A, B, C, D and stream water in seven forested catchments. Bi-weekly data from Aug. 2012 to Aug. 2014 is presented. Different letters indicate significant differences within each site. No data is available for soil water at D plot, DGS. Site codes are as in Figure 1.

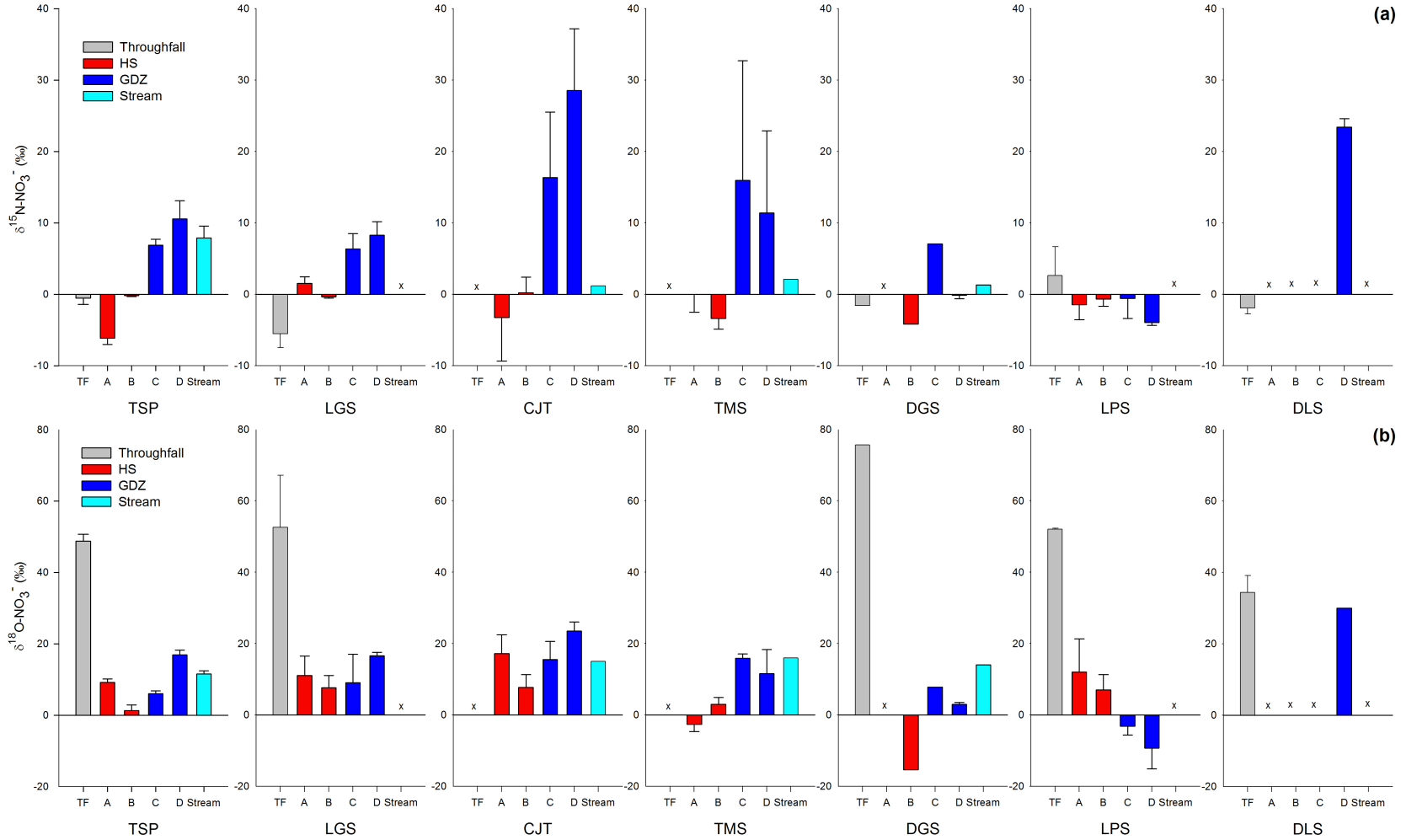

Figure 3 Means and standard errors of $\delta^{15}N_{NO3}$ **(a)** and $\delta^{18}O_{NO3}$ **(b)** in throughfall, soil water and stream water in seven catchments in the summers of 2014 and 2015. Data for TSP are data in summer 2013 from Yu et al. [31]. 'x' denotes no available data. Sites codes are as in Figure 1.

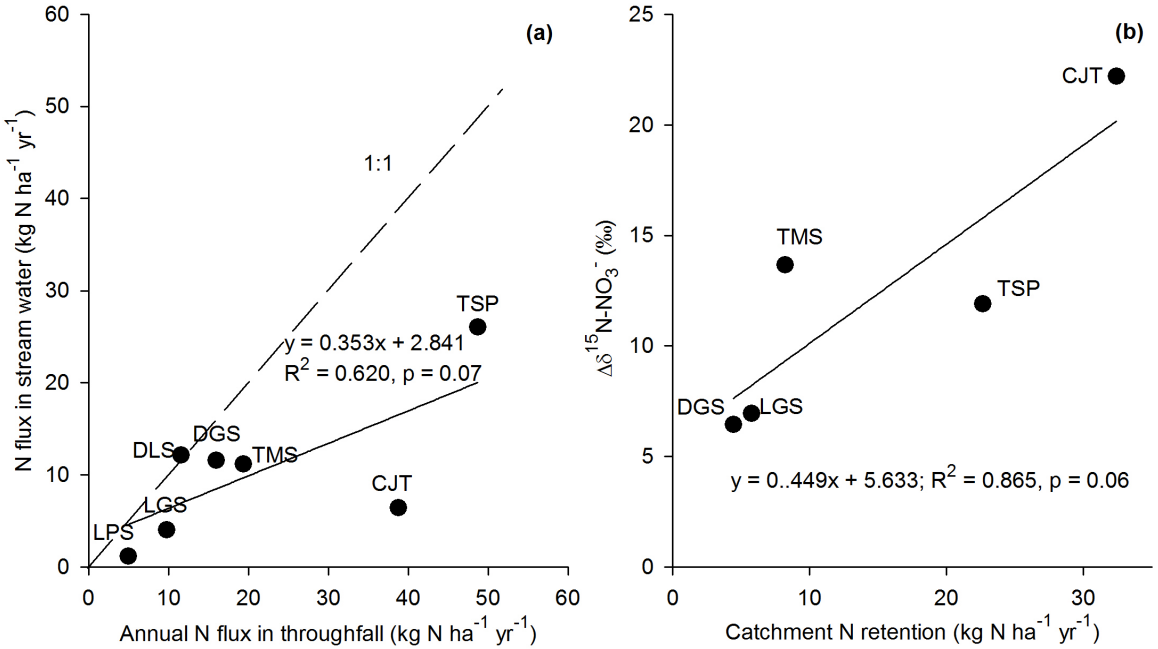

Figure 4a Relationship between annual N flux in throughfall and in stream water from 2012 to 2014. Linear regression lines and equations were shown. N fluxes in stream water are computed as explained in Materials and Methods, and detailed results are presented in Table S2 (supplementary materials).

4b Relationship between catchment N retention and $\Delta\delta^{15}N_{NO3}$ between HS and GDZ. $\Delta\delta^{15}N_{NO3}$ = (averaged $\delta^{15}N_{NO3}$ in GDZ) - (averaged $\delta^{15}N_{NO3}$ on HS).

Table 1. Background descriptions of all sites

Site name	Tieshanping (TSP)*	Leigongshan (LGS)	Caijiatang (CJT)	Tianmushan (TMS)	Dagangshan (DGS)	Liupanshan (LPS)	Donglinshan (DLS)
Location	Chongqing	Guizhou	Hunan	Zhejiang	Jiangxi	Ningxia	Beijing
Longitude	106°41′	108°11′	112°22′	119°26′	114°34′	106°20′	115°26′
Latitude	29°38′	26°23′	27°50′	30°19′	27°35′	35°15′	39°58′
Mean annual temperature (^{o}C)	18.2	15.7	17.5	11.9	15.8	5.8	4.8
Mean annual precipitation (mm)	1028	1120	1250	1581	1591	676	612
Vegetation	Massone pine-dominated, coniferous-broad leaf mixed forest	Pinus armandii dominated, coniferous-broad leaf mixed forest	Massone pine dominated, coniferous-broad leaf mixed forest	Broad-leaf forest	Evergreen broad-leaf forest	Mixed deciduous broad-leaf forest; broad-leaf and coniferous forest	Mixed, secondary deciduous broad-leaf forest; coniferous forest
Soil type	Loamy yellow mountain soil (Haplic Acrisol)	Yellow mountain soil (Alisol and Acrisol)	Yellow mountain soil (Acrisol)	Red and yellow soils (Alisol and Acrisol)	Red and yellow soils (Alisol and Acrisol)	Gray cinnamon soil (Luvisol)	Cinnamon soil (Luvisol)
Soil pH†	4.2	4.4	4.8	6.3	4.9	7.0	6.1
Soil C/N ratio‡	14.0	12.0	14.2	13.2	14.4	10.4	11.5
Annual throughfall flux (kg N ha^{-1})θ	48.7	9.8	38.8	19.4	16.0	5.0	11.6

* Data of Tieshanping site from Yu et al. [31] is included for comparison.

† Soil pH_{H2O} at the surface soil (0-5 cm).

‡ Soil C/N ratio at the O/A soil (0-5 cm).

θ Data refers to the average values for 2013 and 2014.

Denitrification as a major nitrogen sink in forested monsoonal headwater catchments in the sub-tropics: evidence from multi-site dual nitrate isotopes

Longfei Yu[1], Jan Mulder[1*], Jing Zhu[1, 2], Xiaoshan Zhang[3], Zhangwei Wang[3], Peter Dörsch[1]

[1]Department of Environmental Sciences, Norwegian University of Life Sciences, Postbox 5003, N-1432 Aas, Norway.

[2]Department of Environment and Resources, Guangxi Normal University, 541004, Guilin, China.

[3]Research Center for Eco-Environmental Sciences, Chinese Academy of Sciences, 100085, Beijing, China

[*]Correspondence: Jan Mulder, tel. +47 67231852, E-mail jan.mulder@nmbu.no

Supplementary Materials

Table S1-S2

Figure S1-S8

Table S1 Total C, N contents, C/N ratios and pH of O/A horizons[§] (0-3 cm) from all sites

Site name		Tieshanping (TSP)[+]		Leigongshan (LGS)[†]	Caijiatang (CJT)		Tianmushan (TMS)		Dagangshan (DGS)		Liupanshan (LPS)	Donglingshan (DLS)
		Avg.*	Stdv.	Avg.	Avg.	Stdv.	Avg.	Stdv.	Avg.	Stdv.	Avg.	Avg.
C content (%)	A	10.9	5.10	14.1	14.2	5.64	16.9	12.1	4.90	0.92	4.01	3.23
	B	4.91	1.52	9.89	10.0	2.07	4.70	0.83	7.10	0.92	2.77	6.80
	C	3.74	1.51	7.10	3.50	0.72	3.51	0.54	3.90	0.16	4.00	5.52
	D	3.54	0.88	7.43	2.66	0.96	11.4	2.74	6.35	3.60	4.47	8.14
N content (%)	A	0.63	0.01	0.99	0.80	0.28	1.24	0.84	0.31	0.05	0.37	0.26
	B	0.35	0.12	0.81	0.74	0.13	0.37	0.07	0.48	0.07	0.29	0.62
	C	0.28	0.14	0.65	0.28	0.07	0.29	0.05	0.27	0.01	0.38	0.49
	D	0.29	0.08	0.70	0.19	0.05	0.76	0.16	0.49	0.27	0.41	0.71
C/N ratio	A	17.5	0.59	14.3	17.4	1.08	13.3	0.76	15.7	0.45	10.9	12.2
	B	14.3	0.81	12.2	13.5	0.50	12.6	0.29	14.9	0.80	9.5	11.0
	C	15.3	3.71	10.9	12.6	0.66	12.0	0.35	14.2	0.28	10.5	11.2
	D	12.4	0.58	10.6	13.4	2.42	15.0	0.70	12.6	0.81	10.8	11.5
pH	A	3.91	0.20	3.82	3.88	0.10	6.41	0.30	4.22	0.14	6.64	5.59
	B	3.73	0.11	4.03	4.63	0.18	5.55	0.06	4.24	0.03	6.93	7.15
	C	4.72	0.05	5.19	5.18	0.07	6.30	0.23	5.51	0.26	6.46	6.03
	D	4.58	0.10	4.72	5.49	0.04	6.82	0.04	5.70	0.38	8.07	5.53

[§] O/A horizon does not include undecomposed litter (Oi).

* n = 3.

[+] Data obtained from Yu et al. [31].

[†] Replicates were not available.

Table S2 N mass balance and $\Delta^{15}N$ enrichment (GDZ - HS) for all catchments*

Site names	Annual N flux in TF kg N ha^{-1} yr^{-1}	Annual precipitation mm yr^{-1}	Avg Stream NH_4^+-N concentration mg N L^{-1}	Stream NO_3^--N concentration mg N L^{-1}	HS NO_3^--N concentration mg N L^{-1}	Annual N flux in stream water kg N ha^{-1} yr^{-1}	Annual retention kg N ha^{-1} yr^{-1}	$\Delta\delta^{15}N$ enrichment (GDZ - HS) ‰
TSP	48.7	1028	0.01	5.2	15.8	26.0	22.7	11.9
CJT	38.8	1250	0.02	0.8	13.1	6.4	32.4	22.2
TMS	19.4	1581	0.01	1.2	3.9	11.2	8.2	13.7
LGS	9.8	1120	0.02	0.6	2.6	4.0	5.8	6.9
DGS	16.0	1591	0.07	1.1	6.8	11.6	4.4	6.4
LPS	5.0	676	0.37	0.3	2.1	1.2	3.8	-1.2
DLS	11.6	612	0.20	10.8	9.5	12.2	-0.5^{θ}	-†

* The annual N flux by stream runoff was estimated based on the runoff coefficient (the ratio of stream discharge to throughfall). For details see Materials and Methods. N flux in stream refers to dissolved inorganic N export ($NH_4^+ + NO_3^-$). $\Delta\delta^{15}N_{NO3}$= (averaged $\delta^{15}N_{NO3}$ in GDZ) - (averaged $\delta^{15}N_{NO3}$ on HS).

$^{\theta}$ NO_3^- concentration in stream runoff from DLS was unexpectedly high, thus making the annual N retention negative.

† Data not available.

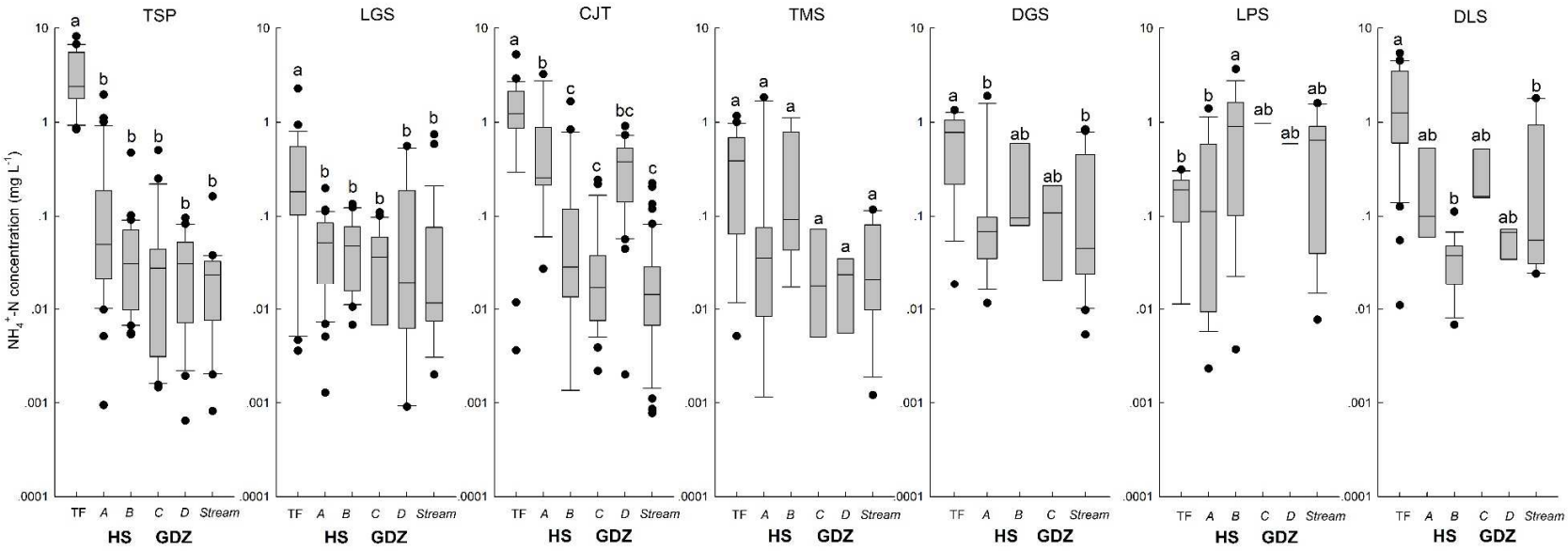

Fig. S1 Logarithmic box whisker plot of NH_4^+ concentrations in throughfall (TF), soil water at plots A, B, C, D and stream water in seven forested catchments. Bi-weekly data from Aug. 2012 to Aug. 2014 is presented. Different letters indicate significant differences within each site. No data is available for soil water at D plot, DGS. Site codes are as in Fig. 1.

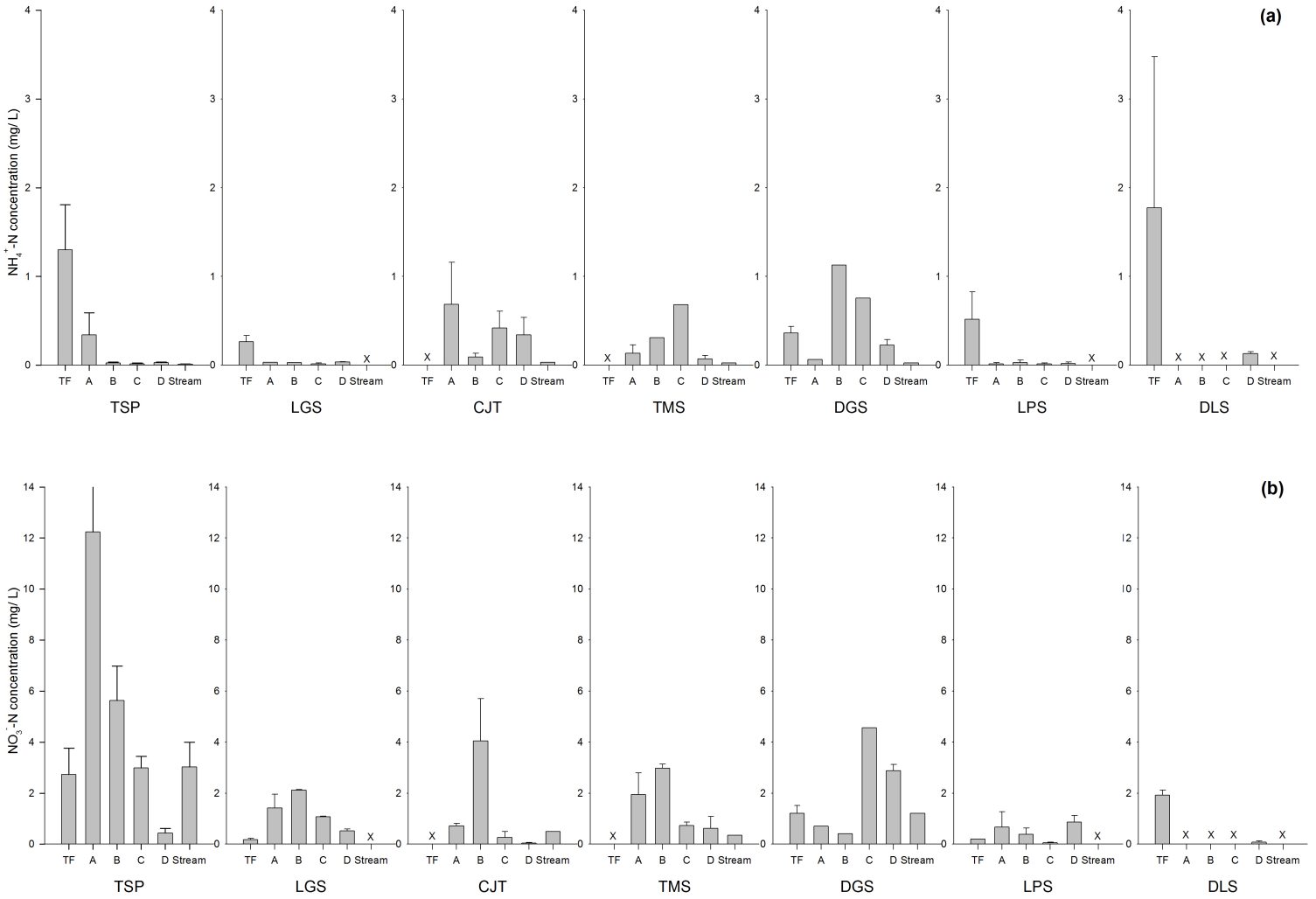

Fig. S2 NH_4^+ **(a)** and NO_3^- **(b)** concentrations of throughfall (TF) and soil pore water along the hydrological flow paths (Fig. 1) at seven sites. Values are means and standard errors of samples obtained in summer 2014 and 2015 for stable isotope analysis. Values at TSP are for summer 2013 taken from Yu et al. [31]. 'x' denotes no available data.

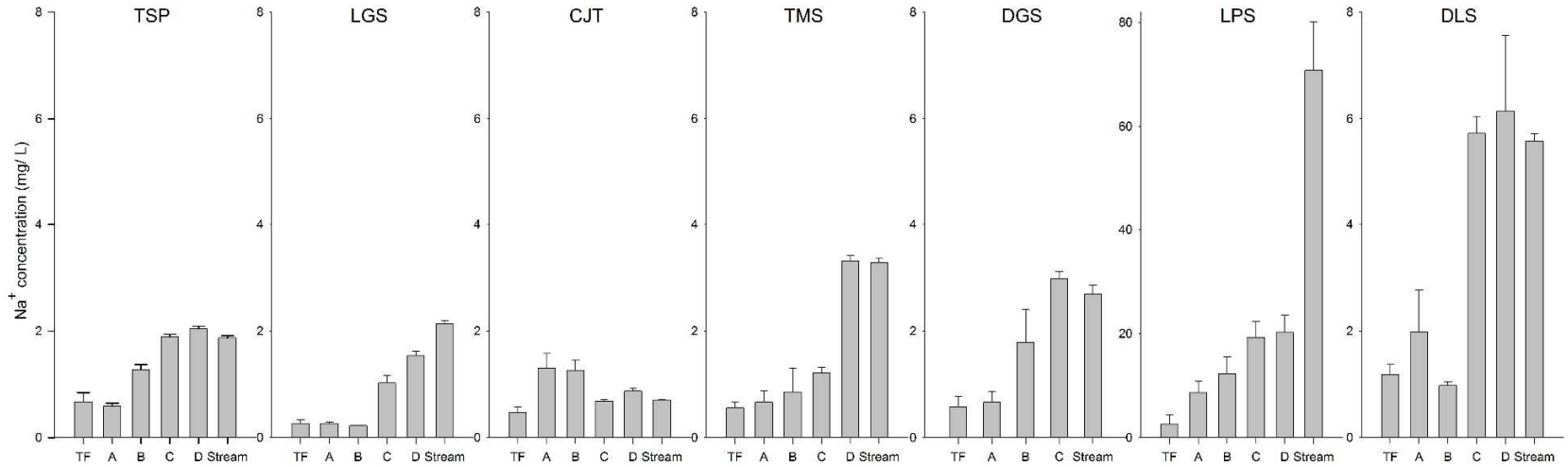

Fig. S3 Na^+ concentration along hydrological continuum among all the headwater catchments. Bi-weekly data from Aug. 2012 to Aug. 2014 is presented, with means and standard errors shown in the figure. Note the different scale for the y-axis for LPS due to larger data range.

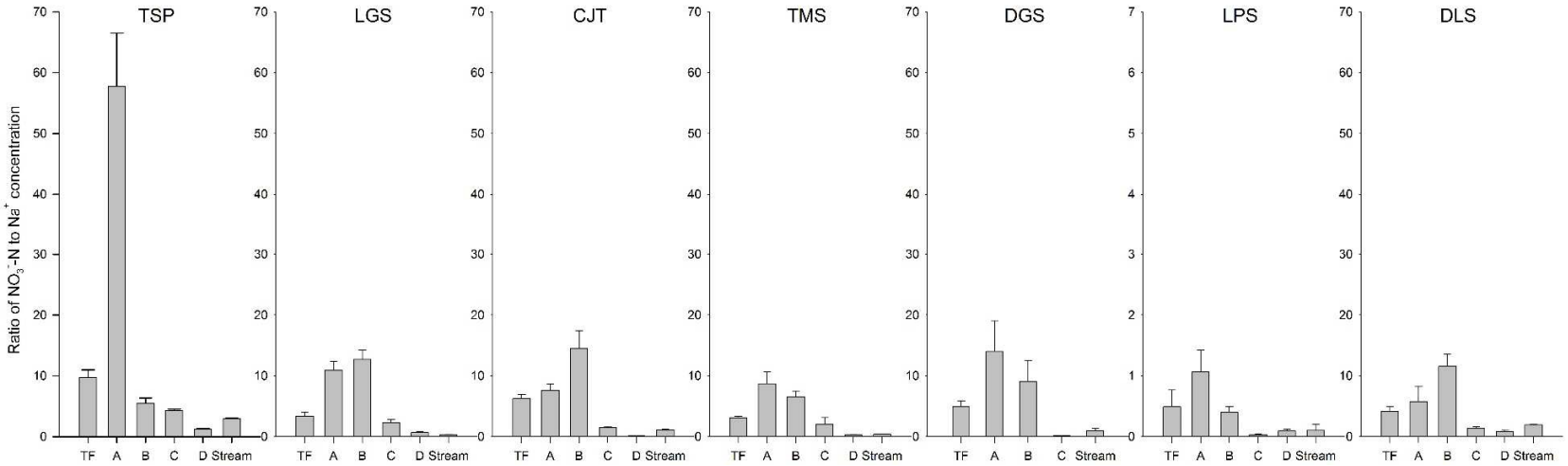

Fig. S4 Ratio of NO_3^- to Na^+ concentration along the hydrological continuum in seven headwater catchments. Bi-weekly data from Aug. 2012 to Aug. 2014 is presented, with means and standard errors shown in the figure. A different scale for y axis is applied only for LPS due to large data range.

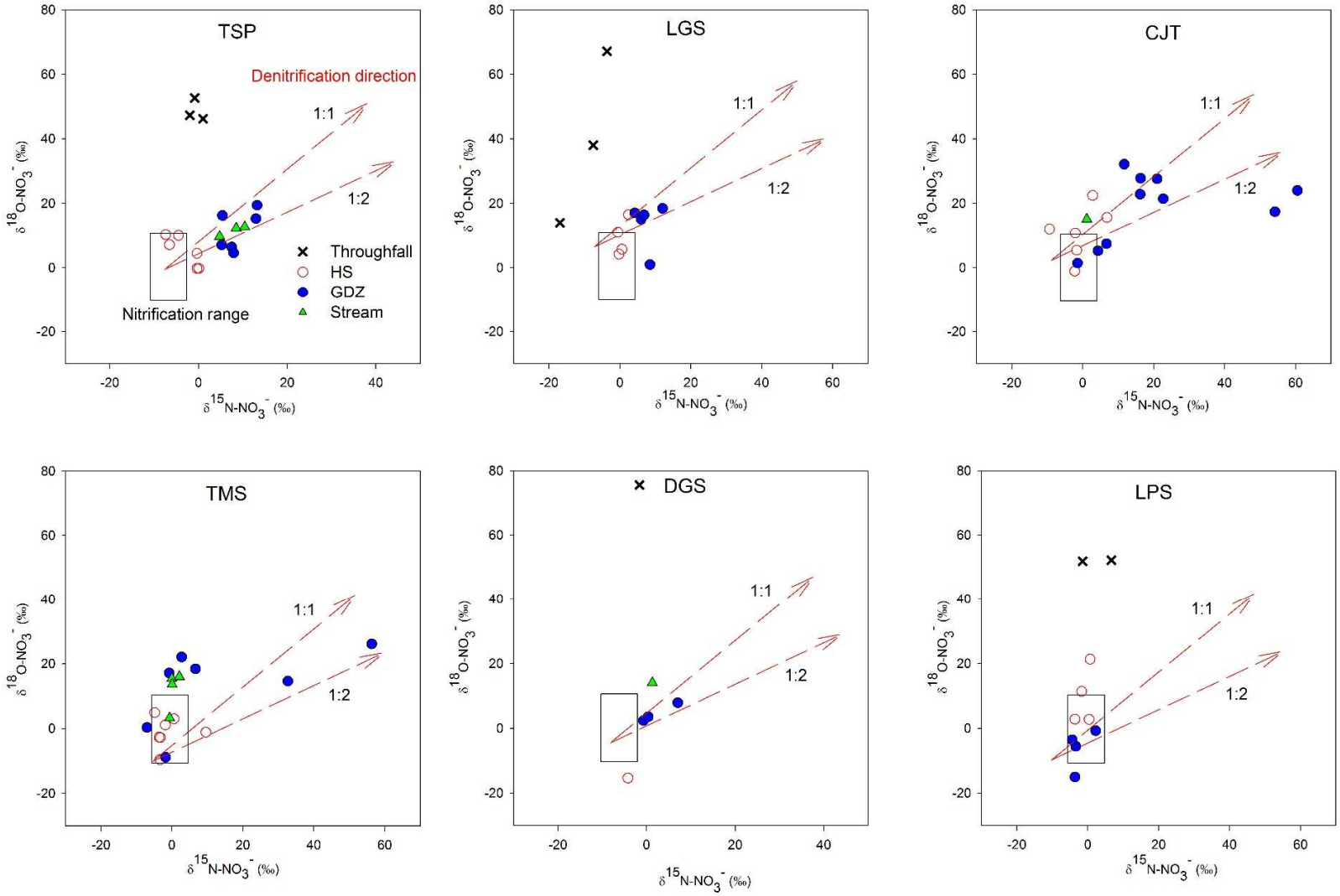

Fig. S5 Relationship between $\delta^{15}N_{NO3}$ and $\delta^{18}O_{NO3}$ at all sites except DLS (little data). Data from TSP sites were values in summer 2013 from Yu et al. [31].

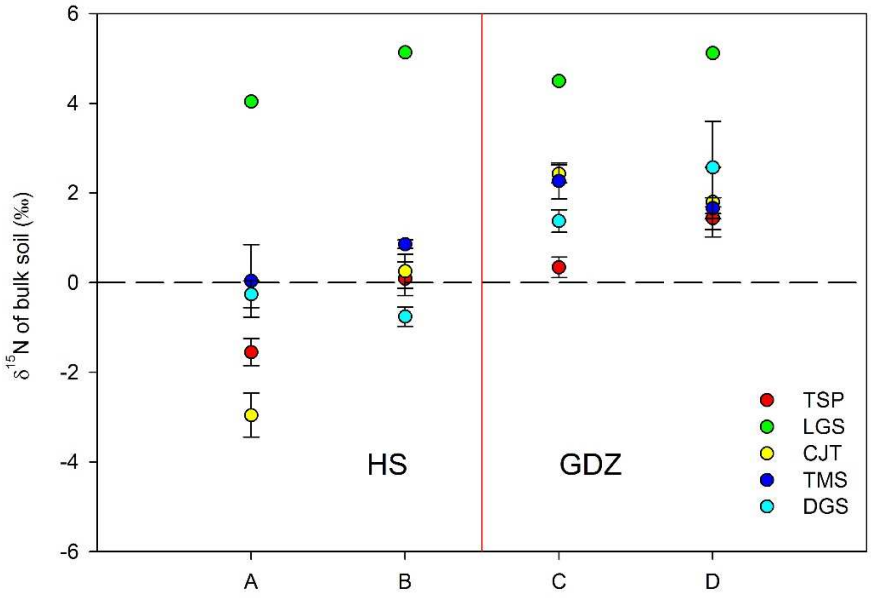

Fig. S6 Means and standard errors of $\delta^{15}N$ of bulk soil (0-3 cm) in A, B, C and D plots from TSP, LGS, CJT, TMS and DGS sites. Data from TSP site were in summer 2013 from Yu et al. [31]. No data were available for LPS and DLS.

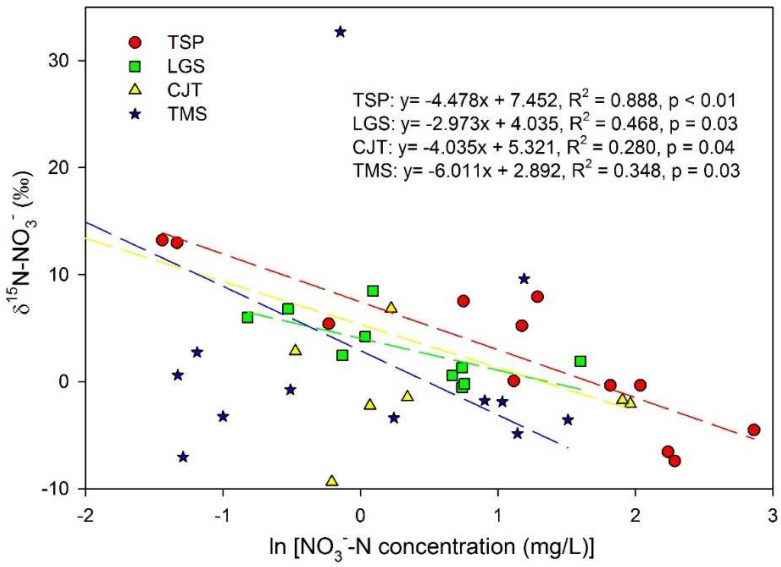

Fig. S7 Relationship between $\delta^{15}N_{NO3}$ and NO_3^- concentration (logarithmic) in soil water (data from both HS and GDZ) at TSP, LGS, CJT and TMS sites (DGS and DLS were not included due to little data). Data from TSP site were in summer 2013 from Yu et al. [31].

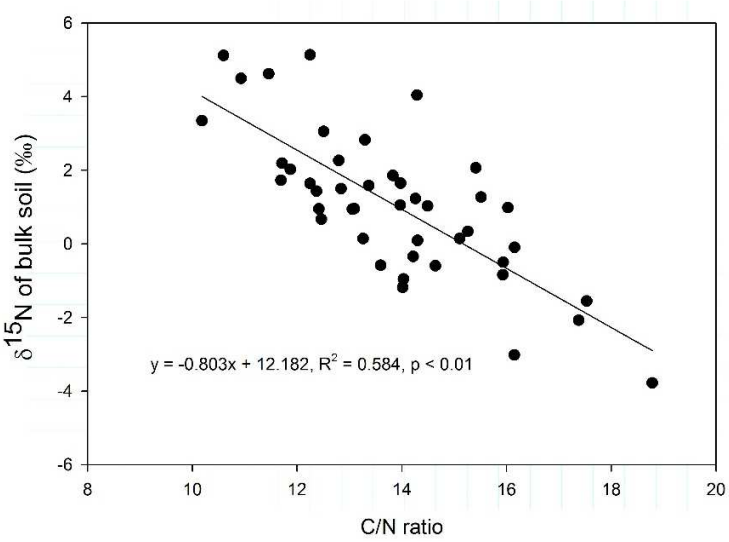

Fig. S8 Relationship between C/N ratio and $\delta^{15}N$ of bulk soils (0-3 cm) in TSP, LGS, CJT, TMS and DGS. Data from all replicates are presented. Data from TSP site are values from summer 2013 obtained from Yu et al. [31].

Paper III

Distinct fates of atmogenic NH_4^+ and NO_3^- in subtropical, N-saturated forest soils

Longfei Yu, Ronghua Kang, Jan Mulder, Jing Zhu, Peter Dörsch

Under review in Ecology

Running head: N turnover in acid forest soils

Distinct fates of atmogenic NH_4^+ and NO_3^- in subtropical, N-saturated forest soils

Longfei Yu[1], Ronghua Kang[1], Jan Mulder[1], Jing Zhu [1,2], Peter Dörsch[1†]

[1]Department of Environmental Sciences, Norwegian University of Life Sciences, Postbox 5003, N-1432 Aas, Norway.

[2]Department of Environment and Resources, Guangxi Normal University, 541004, Guilin, China.

[†]Correspondence: Peter Dörsch, tel. +47 67231836, e-mail: peter.doersch@nmbu.no

Article type**:** Original Article

Abstract

Subtropical forests receive increasing amounts of atmogenic nitrogen (N), both as ammonium (NH_4^+) and nitrate (NO_3^-). Previous long-term studies indicate efficient turnover of atmogenic NH_4^+ to NO_3^- in weathered, acidic soils of the subtropics, leading to excessive NO_3^- leaching. To clarify the mechanism governing the fate of atmogenic inputs in these soils, we conducted an *in situ* ^{15}N tracing experiment in the TieShanPing (TSP) forested catchment, SW China. $^{15}NH_4NO_3$, $NH_4{}^{15}NO_3$ and ^{15}N-glutamic acid were applied to an upland hillslope soil and inorganic N, total soil N and nitrous oxide (N_2O) were monitored for nine days. Incorporation of $^{15}NO_3^-$ into soil organic N was negligible and 80% of the applied label was lost from the top soil (0-15 cm) primarily by leaching within 9 days. In contrast, $^{15}NH_4^+$ was largely retained in soil organic N. However, instant production of $^{15}NO_3^-$ in the $^{15}NH_4^+$ treatment suggested active nitrification. Excess ^{15}N in the NO_3^- pool was greater than in the NH_4^+ pool, suggesting that a sizable proportion of the produced $^{15}NO_3^-$ was derived from ^{15}N immobilized in organic matter without passing through the NH_4^+ pool (heterotrophic nitrification). This was confirmed by persistently greater excess ^{15}N in NO_3^- than in NH_4^+ in the ^{15}N-glutamic acid treatment. The cumulative recovery of ^{15}N in N_2O after 9 days ranged from 2.5 to 6.0% in the $^{15}NO_3^-$ treatment, confirming the previously reported significant denitrification capacity of these soils. Yet, source partitioning of $^{15}N_2O$ demonstrated a measurable contribution of nitrification to N_2O emissions, particularly at low soil moistures. Our study emphasizes the role of a fast-cycling organic N pool (including microbial N) for retention and transformation of atmogenic NH_4^+ in subtropical, acid forest soils. It thus explains the near-quantitative leaching of deposited N (as NO_3^+ and NH_4^+) common to subtropical forest soils with chronic, elevated atmogenic N inputs by i) negligible retention of NO_3^- in the soil and

ii) rapid immobilization-mineralization of NH_4^+ followed by nitrification (autotrophic and heterotrophic).

Key words: N deposition, ^{15}N tracer, gross N transformation, nitrification, denitrification, nitrate leaching, N_2O emission

Introduction

Rapid growth of agriculture and industry has dramatically increased the anthropogenic emission of reactive N (Galloway et al. 2008, Liu et al. 2013). In central China, for example, current N deposition amounts to 30-65 kg N ha^{-1} yr^{-1} (Shi et al. 2015, Xu et al. 2015). Enhanced N deposition causes concerns about negative environmental effects, such as soil acidification (Guo et al. 2010), eutrophication (Galloway et al. 2003), biodiversity loss (Bobbink et al. 2010), nitrous oxide (N_2O) emissions (Zhu et al. 2013c) and threats to human health (Townsend et al. 2003). Elevated N deposition has been reported to cause N saturation in subtropical forests of South China, characterized by strong nitrate (NO_3^-) leaching from soils (Fang et al. 2011, Larssen et al. 2011, Huang et al. 2015). Yet, there is limited understanding of the turnover mechanisms and the fate of reactive N inputs, both with respect to input rate and input form (ammonium (NH_4^+), and NO_3^-).

The concept of N saturation suggests that soil nitrification activity and NO_3^- leaching increase significantly, when N input exceeds N uptake by the forest (Aber et al. 1998, Lovett and Goodale 2011). In a 7-year field experiment in the subtropical Chinese forest "TieShanPing" (TSP), extreme N saturation with N input (NH_4^+-N + NO_3^--N) equaling N output (NO_3^--N) was found in acid soils, even at elevated rates of NH_4^+ input (Huang et al. 2015). The apparent efficient turnover of deposited NH_4^+ to NO_3^- and the associated small rate of NH_4^+ leaching suggest microbial nitrification as the key process behind forest N loss, even though ammonia (NH_3), the substrate of nitrification, is scarce in acid soils (De Boer and Kowalchuk 2001). Possible explanations put forward were production of NH_3 (by mineralization) and consumption of NH_3 (by nitrification) in physically-connected microorganisms (Allison and Prosser 1993), or within the same mixotrophic cell (De Boer et al. 1989, Burton and Prosser 2001). The notion of how NH_4^+ is turned over in acid forest soils changed fundamentally with the discovery of ammonia oxidizing archaea (AOA;

Leininger et al. 2006) and the finding that AOA dominates over ammonium oxidizing bacteria (AOB) in acid soils (Gubry-Rangin et al. 2011), but the question about the actual substrate of nitrification in acid soils remained unresolved. For instance, Levičnik-Höfferle et al. (2012) observed stimulation of thaumarchaeal NH_3 oxidation by addition of organic N but not by NH_4^+. Also, NH_4^+ added to acid forest soil has been found to be quickly assimilated into the microbial N pool (Tahovsk et al. 2013, Gao et al. 2016), which points at a possible role of the soil organic N pool for processing and transformation of deposited NH_4^+ (Booth et al. 2005, Lu et al. 2011). Recent studies based on ^{15}N modeling (Müller et al. 2007) attributed efficient NO_3^- production in acid soils to heterotrophic nitrification, i.e. the co-oxidation of organic N to nitrite during heterotrophic microbial growth (Zhang et al. 2013, Chen et al. 2015). Thus, the pathways involved in transforming N deposited as NH_4^+ to NO_3^- are elusive, raising the question whether NO_3^- is directly produced from organic N or from mineralization-derived NH_4^+.

Stable isotope studies have indicated that denitrification is a quantitatively important sink for NO_3^- in N-saturated forests, particularly in saturated near-stream soils (Fang et al. 2015, Yu et al. 2016). While N_2 is the main product of denitrification, some N_2O, an intermediate product, is emitted (Tiedje 1988). Large N_2O emissions have been reported from the well-drained hillslopes of the TSP catchment, SW China, accounting for 8-10% of the annual N deposition (Zhu et al. 2013c). Acid soils favor the production of N_2O rather than N_2 in the denitrification process (Liu et al. 2010) and frequent soil moisture changes on the well-drained hillslope may favor N_2O production by denitrification relative to N_2O reduction to N_2, as the N_2O reduction enzyme is more easily repressed by oxygen than the other denitrification enzymes (Morley et al. 2008). Accordingly, in the TSP forest, Zhu et al. (2013c) attributed observed large N_2O emissions to intermittent denitrification, triggered by monsoonal rainfalls and confirmed up to 100% contribution of

denitrification by *in situ* $^{15}NO_3^-$ labeling (Zhu et al. 2013a). However, given the unclear role of NH_4^+ transformations for the forest N-budget, also nitrification could be a significant source of N_2O, particularly under relatively dry conditions (Khalil et al. 2004). In a soil core study, Zhang *et al.* (2011) found that nitrification was responsible for up to 42% of the emitted N_2O in four acid, subtropical soils from China incubated at intermediate soil moisture (40-52% WFPS). So far, there are no *in situ* studies that have apportioned N_2O emissions in acid forest soils of South China to different N-transformation pathways under fluctuating soil moisture conditions.

^{15}N tracers have been widely used to investigate the fate and gross transformation of atmogenic N in forest ecosystems (Curtis et al. 2011, Templer et al. 2012). Sheng *et al.* (2014) and Gurmesa *et al.* (2016) measured high retention of ^{15}N tracers ($^{15}NH_4^+ > {}^{15}NO_3^-$) in broadleaf forests of the Chinese tropics, and recovered ^{15}N in both soil and plant biomass one year after addition. However, observed annual N deposition and soil leaching in these forests indicated much greater loss of atmogenic N than predicted by ^{15}N tracing (Gurmesa et al. 2016). This suggests that "freshly" deposited N is retained and cycled internally in the soil prior to being released to leachates, while "old" N is simultaneously mobilized. This is in line with findings from short-term incubation experiments with soils cores from a range of South Chinese forest soils, reporting large gross N immobilization and mineralization rates (Zhang et al. 2013, Gao et al. 2016). Hence, it is likely that efficient turnover of soil organic N is central for the retention of "fresh" atmogenic N and the return of "old" organic N to the inorganic N pool, which would reconcile large N retention with strong NO_3^- leaching.

In the TSP forest in SW China, where N retention by forest growth is limited due to soil acidification (Li et al. 2014) and phosphorus limitation (Wang et al. 2007), soil N turnover can be expected to govern the fate of atmogenic N inputs. To elucidate this, we conducted *in situ* ^{15}N

tracing in well-drained soils of the forested hillslope. ^{15}N label was added in three forms, viz. NH_4^+, NO_3^- and glutamic acid, and N dynamics and ^{15}N distribution in soil pools (extractable and solute NH_4 and NO_3, residual soil N) and in emitted N_2O were monitored frequently during the initial two weeks following ^{15}N application. The objectives of our study were: i) to study the transformation of atmogenic NH_4^+ to NO_3^- in the acid forest soil, ii) to improve our understandings of mechanisms governing nitrification through the partitioning of nitrate production pathways (ammonification followed by autotrophic or heterotrophic nitrification), iii) to unravel the fate of NO_3^- in the well-drained forest soil and iv) to source-partition the N_2O emission to nitrification and denitrification.

Material and Method

Site description

The study was conducted at Tieshanping (TSP), a 16.3 ha headwater catchment located in a forest park, about 25 km northeast of Chongqing, SW China (106° 41′E, 29° 38′N) (Fig. 1a). The catchment has a subtropical monsoonal climate, with a mean annual precipitation of 1028 mm and a mean annual temperature of 18.2 ^{o}C (Chen and Mulder 2007). The vegetation is a Masson pine dominated mixed forest. The TSP catchment consists primarily of steep hillslopes with ground water discharge zones at the foot of the slopes. Hillslope soils are well-drained loamy yellow mountain soils (Haplic Acrisol), with an argic Bt horizon. Soils are acidic, with pH_{H2O} increasing from 3.8 in the O/A horizon to 4.0 in the Bt. Due to fast turnover of organic matter, Acrisols have thin organic horizons (0–2 cm) (Chen and Mulder 2007). Annual N deposition (~ 60% as NH_4^+-N) reported to be 40-60 kg N ha^{-1} yr^{-1} during 2005–2011, is leached nearly quantitatively as NO_3^--N from the root zone (Huang et al., 2015). Soil C/N ratios in the O/A horizons are 14 to 18 (Zhu et al. 2013a, Yu et al. 2016).

Within a 4.6 ha sub-catchment, we established two experimental sites, one just below the hilltop (upper; P1) and one in a foot slope position (lower; P2, Fig. 1a) on a northeast facing hillslope (HS). For a more detailed description of the soil characteristics at TSP, see Zhu *et al.* (2013b) and Sørbotten et al. (accepted). Following rain events, considerable interflow over the Bt horizon occurs along the HS, resulting in larger soil moisture content in P2 than P1 (Sørbotten et al. accepted).

Experimental design and sample collection

At each of the locations, P1 and P2, three blocks were established, each with four adjacent 1.2 m x 1.2 m plots to which labeling treatments were randomly assigned (Fig. 1b). The treatment plots were situated in between trees, and contained a shrubby ground vegetation. Adjacent plots were separated by plywood boards inserted 10 cm into the soil to prevent ^{15}N cross contamination of the plots.

^{15}N tracer was applied on 23 June, 2015 as either $^{15}NH_4NO_3$ ($^{15}NH_4$, 99 atom% ^{15}N), $NH_4{}^{15}NO_3$ ($^{15}NO_3$, 98 atom% ^{15}N), or ^{15}N-Glutamic acid (^{15}N-Glut, 98 atom% ^{15}N), leaving the fourth plot as a reference plot, which received clean water only. ^{15}N-Glut treatment was included to investigate the production pathway of NO_3^- using labile organic N as a substrate. All labeling treatments received 1 kg ^{15}N ha^{-1}. The total N dose was 1 kg N ha^{-1} for the ^{15}N-Glut treatment and 2 kg N ha^{-1} for the $^{15}NH_4$ and $^{15}NO_3$ treatments. The N addition levels amounted to less than 5% of the annually deposited atmogenic N at TSP (40–65 kg N ha^{-1}), thus keeping the fertilization effect to a minimum. ^{15}N tracers were applied in 5 mm deionized water (7.2 L per plot), using backpack sprayers. After the addition of ^{15}N tracer (or 5 mm deionized water at the reference plots), 0.72 L deionized water (0.5 mm) was added to wash off any tracer intercepted by shrubs or plant remnants. The addition of the solutions took slightly less than 0.5 hr, and spraying was done evenly, with the nozzle below the ground vegetation layer, as close as possible to the soil surface.

Sample collection started immediately following the ^{15}N tracer addition (t = 0.5 hr). No rain occurred from two days prior to tracer addition until 7 days after (the 6th sampling; Fig. 2a). During a period of 9 days (219 hours), eight samplings of soil, soil water and emitted N_2O gas were conducted in all plots. N_2O emission fluxes were estimated from changes in N_2O concentration in a static chamber (30 cm in diameter, and 11 cm in height), following the method described by Zhu *et al.* (2013b). On every sampling date, the chamber was deployed at the same position in each

plot, and gas samples were collected in pre-evacuated 120-ml flasks at 1, 15 and 30 min. Gas samples were analyzed for concentration and atom% ^{15}N of N_2O. Soil samples of the O/A (~ 0-5 cm) and AB (~ 5-15 cm) horizons were randomly taken with a soil auger (ϕ = 2.5 cm), avoiding the position assigned to N_2O flux measurements. Sampling holes were refilled with clay plugs. Triplicate cores were mixed manually for each horizon and 8 g soil was extracted on site in 40 ml of 1 M KCl, immediately following sampling. After shaking for 1 hr, the KCl extracts were filtered (30-50 μm). Soil water was sampled at each plot from 0-5 cm depth (including O/A horizon and the upper part of the AB) by means of a pre-installed MacroRhizon soil moisture sampler (Rhizosphere Research Products, the Netherlands). Vacuum was applied for 6-7 hrs by a 50 ml syringe. The KCl extracts and soil solutions were placed on ice in a foam box and transported to a freezer where they were stored at -20 ^{o}C. Fresh soil samples were weighed and oven-dried (50^{o}C) at the day of sampling at the forestry bureau of TSP. After determination of soil moisture, the oven-dried soil samples were stored in sealed polyethylene bags. All samples, including gas, water, KCl-extracts and dried soil were shipped the Norwegian University of Life Sciences for further analyses.

During each sampling, soil temperature and volumetric moisture content were measured at 10 cm depth at three random positions within each plot, using a hand-held TDR (Hydraprobe; Stevens Water Monitoring Systems, USA). From 1 June to 4 July, air temperature and precipitation were monitored hourly by a weather station on the roof of the nearby (~ 1.5 km) forest bureau (WeatherHawk 232, USA).

Sample analysis

The concentrations of NH_4^+ and NO_3^- in KCl extracts and in soil water samples were analyzed with a flow injection analyzer (FIA star 5020, Tecator, Sweden), according to NS 4745&4746

183 (NSF 1975a&b). Dried soil samples were sieved (2 mm mesh size) and milled, before being
184 analyzed for total N using an elemental analyzer (FLASH 2000, ThermoFisher Scientific,
185 Germany). The N_2O concentration in the gas samples was determined by automated gas
186 chromatography (GC Model 7890A, Agilent, USA) as described earlier (Zhu et al. 2013a).

187 The ^{15}N abundance in soil N and N_2O was determined by EA-IRMS and PreCon-GC-IRMS,
188 respectively (Thermo Finnigan MAT, Germany), with a precision of 0.2‰. The ^{15}N abundance in
189 NH_4^+ and NO_3^- in both KCl-extracts and soil water were determined after conversion to N_2O.
190 Ammonium was converted quantitatively to N_2O by first oxidizing it to NO_2^- using hypobromite
191 at pH ~ 12, before reducing NO_2^- to N_2O in an acid-buffered azide solution (Zhang et al. 2007).
192 For ^{15}N-NO_3^-, a bacterial denitrifier method was applied to convert NO_3^- to N_2O (Sigman et al.
193 2001). International standards (IAEA N1&N3, USGS 32&34) were included in each batch for
194 internal calibration. For further details on the conversion assays for NH_4^+ and NO_3^- and the ^{15}N
195 analysis see Yu *et al.* (2016).

196 *Calculations*

197 Water filled pore space (WFPS) was calculated using volumetric soil moisture (VM, $cm^3\ cm^{-3}$),
198 soil bulk density (BD, $g\ cm^{-3}$) and assumed soil particle density (PD, 2.65 $g\ cm^{-3}$) (Linn and Doran
199 1984) as

200 $$WFPS\ (\%) = VM / (1 - BD/PD) \times 100 \qquad (1)$$

201 The tracer application greatly enriches the various N pools, making the ^{15}N distribution in N_2O
202 non-random (Stevens et al. 1997). Thus, both ion currents of m/z (mass-to-charge ratio) 45 and 46
203 need to be considered for the determination of ^{15}N atom% in N_2O. We adopted the equations from
204 Stevens *et al.* (1997) for calculating atom% of ^{15}N in N_2O:

atom% ^{15}N-N_2O = 100 (^{45}R + 2 * ^{46}R- ^{17}R - 2 * ^{18}R) / (2 + 2 * ^{45}R + 2 * ^{46}R) (2)

where ^{45}R refers to the ratio between the peak areas of m/z 45 and 44, ^{46}R to the ratio between the peak areas of m/z 46 and 44, while ^{17}R is set to $3.8861*10^{-4}$ and ^{18}R to $2.0947*10^{-3}$ (Kaiser et al. 2003).

Emission rates of N_2O (μg N m^{-2} hr^{-1}) were calculated by linear regression of N_2O concentrations over time. The atom% ^{15}N of emitted N_2O was calculated using atom% ^{15}N and concentration data of N_2O at three time points, based on the 'Keeling plot' approach (Yakir and Sternberg 2000):

$C_E\delta_E = C_a\delta_a + C_s\delta_s$ (3)

where C_E, C_a, and C_s represent the N_2O concentrations in the ecosystem (collected by static chamber), in the atmosphere, and that of emission sources, respectively; δ_E, δ_a and δ_s represent the atom% ^{15}N of N_2O in the ecosystem, in the atmosphere, and that of emission sources, respectively.

Atom% ^{15}N-excess was calculated for the NH_4^+, NO_3^- and total soil N pool and for emitted N_2O by subtracting the atom% ^{15}N in the corresponding reference treatment at each sampling. If not specified otherwise, atom% ^{15}N-excess values are abbreviated in the text as 'atom% $^{15}N_{NH4}$', 'atom% $^{15}N_{NO3}$', 'atom% $^{15}N_{Soil}$' and 'atom% $^{15}N_{N2O}$', respectively. The soil residual N pool was defined as 'total soil N minus mineral N'. The ^{15}N recoveries (%) in NH_4^+, NO_3^- and soil residual N at each sampling were calculated as:

^{15}N recovery (%) = 100 (m_t * atom% ^{15}N-excess) / m_{added} (4)

where m_t represents the N pool size (concentration) at each sampling and m_{added} the absolute amount of added ^{15}N for each specific treatment. For N_2O emission, we calculated cumulative ^{15}N recovery in N_2O by linear interpolation between adjacent time points.

Gross rates of production (m) and consumption (i) of NH_4^+ were calculated based on ^{15}N pool dilution and N mass balance in the $^{15}NH_4$ treatment (Davidson et al. 1991). The equations used in this study were derived from Kirkham and Bartholomew (1954):

$$m = [(M_0 - M) / t] * [\log (H_0M / HM_0) / \log (M_0 / M)], m \neq i \quad (5)$$

$$i = [(M_0 - M) / t] * [\log (H_0 / M_0) / \log (M_0 / M)], m \neq i \quad (6)$$

where t represents time (d), M_0 and M the sizes of the $^{14+15}N$ pool at t = 0 and t, respectively (mg N g^{-1} dry soil), and H_0 and H the size of the ^{15}N pool at t = 0 and t, respectively (mg N g^{-1} dry soil). Here, the gross production of NH_4^+ equals mineralization, and the gross consumption of NH_4^+ is equivalent to the sum of immobilization and nitrification (Davidson et al. 1992).

When calculating the gross production (m) and consumption (i) rates of NO_3^-, the above equations needed to be modified as the concentration of NO_3^- did not change significantly with time (m = i; i.e. steady state). Therefore, another equation was applied (Kirkham and Bartholomew 1954):

$$m = i = (M_0 / t) * \log (H_0 / H) \quad (7)$$

Here, the gross production of NO_3^- denotes nitrification, and the gross consumption of NO_3^- is the sum of immobilization, denitrification and dissimilatory reduction to ammonium (DNRA) (Davidson et al. 1992).

The net rates of N_2O emission and DNRA were estimated based on the cumulative $^{15}N_{N2O}$ in $^{15}NH_4$ and $^{15}NO_3$ treatments and $^{15}N_{NH4}$ in $^{15}NO_3$ treatment, respectively.

Partitioning of N_2O production pathways

Assuming that N_2O is only produced through either nitrification or denitrification (Firestone and Davidson 1989), we used a two end-member mixing analysis to apportion N_2O to the two processes (Stevens et al. 1997, Zhu et al. 2013a):

$$a_m = d * a_d + (1 - d) * a_n \quad (8)$$

where a_m is the atom% ^{15}N of N_2O, a_n the atom% ^{15}N of NH_4^+, a_d the atom% ^{15}N for NO_3^- and d the fraction of N_2O that is derived from denitrification. In this study, atom% ^{15}N data from the $^{15}NO_3$ treatment was selected for end-member mixing analysis, as the NO_3^- pool has atom% ^{15}N distinct from the NH_4^+ pool. Note that our partitioning does not distinguish between autotrophic and heterotrophic nitrification, as ^{15}N enrichment in N_2O produced by both pathways was at the same natural abundance level.

Statistics

Statistical analyses were performed with Minitab 16.2.2 (Minitab Inc., USA). Significant differences in N concentrations, atom% ^{15}N and ^{15}N recovery along the time series within each site or treatment were examined by One-way ANOVA with post hoc Tukey test. The differences in N concentrations, atom% ^{15}N and ^{15}N recovery among sites and treatments were tested with repeated ANOVA. Significance levels were set at $p < 0.05$, unless specified elsewhere.

Results

Climatic conditions, soil temperature and moisture

A total of 173 mm rain occurred from June 1 to June 23, the day the label was applied (Fig. 2a). Therefore, soils had large WFPS values, about 70% and 80% at the upper and lower sites, respectively, at the beginning of the experiment (Fig. 2b). In the 7-day period from sampling 1 to 6, no rain occurred and WFPS gradually decreased by about 10% (Figs. 2a and 2b). From sampling 7 (30 June) onwards, rain episodes (> 10 mm hr^{-1}) increased the WFPS to about 75% (upper site) and 90% (lower site). WFPS was significantly larger at the lower than at the upper site (on average 79% and 67%, respectively).

N concentrations of different N pools

The NH_4^+ and NO_3^- concentrations in KCl extracts and soil water, total N contents in soil and N_2O emissions were not significantly different among treatments (including the Reference; Fig. 3 and Figs. S1 and S2). In soil water, the NH_4^+ concentration was extremely small compared to NO_3^-. Both mineral N (the sum of KCl extractable NH_4^+ and NO_3^-) and total N in soil (Figs. 3 and S1) were smaller in the AB horizon (< 10 μg N g dry $soil^{-1}$ and ~ 1.5 g N kg dry $soil^{-1}$, respectively) than in the O/A (~ 20 μg N g dry $soil^{-1}$ and ~ 5 g N kg dry $soil^{-1}$, respectively). In general, NH_4^+ prevailed over NO_3^- in extractable mineral N in both O/A and AB horizons at the upper (P1), but not at the lower site (P2) (Fig. 3). In all treatments except the ^{15}N-Glut treatment, the N_2O fluxes at the lower site were significantly smaller than those at the upper site, during the first six sampling dates (viz. prior to new rainfall).

NH_4^+ concentrations in KCl extracts decreased significantly from sampling 1 to 6 at both sites, while those for NO_3^- remained stable (Fig. 3). A spike of N_2O emission (up to 1000 μg N m^{-2} hr^{-1})

283 was observed ~7 hr after label application. After 50 hr, emission rates stabilized and increased
284 again after 174 hr, when new rain episodes caused a sharp increase in WFPS (Figs. 4 and 2b).
285 Total mineral N and bulk soil N fluctuated in time, but differences within the same treatment were
286 not significant among samplings after the 2nd day of the experiment.

287 *Atom% ^{15}N-excess in various N pools*

288 In the O/A horizon, the initial atom% $^{15}N_{NH4}$ of KCl extracts in the $^{15}NH_4$ treatment was about 10%
289 at both the upper (P1) and lower site (P2) and decreased gradually with time (Figs. 4a and d).
290 Simultaneously, atom% $^{15}N_{NO3}$ increased to 7-10% within the first 50 hr, and then decreased with
291 time. This temporal dynamic was faster at the lower site, with larger atom% $^{15}N_{NO3}$ than atom%
292 $^{15}N_{NH4}$ after 25 hr. The atom% $^{15}N_{Soil}$ was fairly constant with time. In general, the atom% $^{15}N_{N2O}$
293 was below 5%, and its temporal dynamics followed that of NO_3^-.

294 In the $^{15}NO_3$ treatment at both sites, atom% $^{15}N_{NO3}$ declined significantly with time, from about
295 30% to near 0% (Figs. 4b&e). Although significantly correlated, atom% $^{15}N_{N2O}$ was smaller than
296 atom% $^{15}N_{NO3}$. Atom% $^{15}N_{NH4}$ in the $^{15}NO_3$ treatment was close to zero throughout the experiment
297 and atom% $^{15}N_{Soil}$ was unaffected by $^{15}NO_3$ application.

298 For the ^{15}N-Glut treatment (Figs. 4 c&f), the temporal patterns of atom% $^{15}N_{NH4}$, atom% $^{15}N_{NO3}$
299 and atom% $^{15}N_{N2O}$ resembled those of the $^{15}NH_4$ treatment, although the atom% $^{15}N_{Soil}$ during the
300 final samplings was significantly larger than in the $^{15}NH_4$ treatment. After ^{15}N-Glut addition at the
301 lower (P2) site, atom% $^{15}N_{NH4}$, atom% $^{15}N_{NO3}$ and atom% $^{15}N_{Soil}$ increased instantaneously (after
302 0.5 hr), earlier than for the other treatments.

In the AB horizon, the atom% ^{15}N dynamics of the different N pools were similar to those in the O/A horizon, albeit less pronounced (Fig. S3). However, the values of atom% $^{15}N_{NO3}$ fluctuated strongly in time and values were highly variable among replicates.

^{15}N recoveries in different N pools

In the $^{15}NH_4$ treatment at the upper site (P1, Fig. 5a), initial recovery rates were > 90%, but decreased with time to about 53%, 219 hr after tracer addition. Recoveries in the NH_4^+ pool declined quickly during the initial 50 hr, while the recovery of ^{15}N in the NO_3^- pool increased. The recovery rates of ^{15}N in mineral N (sum of NH_4^+ and NO_3^-) in the O/A horizon showed an overall decrease from 42% to 1.3% throughout the experiment at both sites, with an intermittent plateau between 26 and 50 hr. Already 0.5 hr after $^{15}NH_4$ addition, 39% of the added tracer was found in the soil residual N pool of the O/A horizon. The recovery of ^{15}N in the residual N pool increased further until reaching about 59% at 144 hr. The AB horizon of the soil contributed less than 18% to the total ^{15}N recovery in the $^{15}NH_4$ treatment, mainly as NO_3^- and soil residual N. The N_2O emitted from the $^{15}NH_4$ plots throughout the entire observation period accounted for < 2% of the added ^{15}N.

At the lower site (P2, Fig. 5d), the ^{15}N distribution pattern in the $^{15}NH_4$ treatment generally resembled that of the upper site. However, the ^{15}N recovery in NO_3^- was significantly larger in both soil horizons than at the upper site. Also the recovery of ^{15}N from the added $^{15}NH_4^+$ in $^{15}NO_3^-$ was faster at the lower site (P2) than at the upper site (P1) (Figs. 5a and d).

In the $^{15}NO_3$ treatment at both upper and lower site (Figs. 5b and e), ^{15}N recovery was greatest in the NO_3^- pool. Total recoveries decreased more quickly than in the $^{15}NH_4$ treatment and at the last two samplings of the experiment, the non-recovered ^{15}N amounted to > 80%. The ^{15}N recovery in

325 NO_3^- decreased from about 65% to 1.0% in the O/A horizon and from about 15% to 5.0% in the
326 AB. The soil residual N in the O/A horizon contributed significantly less to the ^{15}N recovery than
327 in the $^{15}NH_4$ treatment. Cumulative ^{15}N recoveries in N_2O after 219 h were larger than in the $^{15}NH_4$
328 treatment, accounting for about 6.0% and 2.5% of the added ^{15}N at the upper (P1) and lower site
329 (P2), respectively.

330 In the ^{15}N-Glut treatment (Figs. 5c and f), more than 70% of ^{15}N was recovered in the soil residual
331 N pool (about 65% in the O/A and 7% in the AB horizon). Mineral N contributed less to ^{15}N
332 recovery than in the other treatments. Nevertheless, ^{15}N recovery in NO_3^- from the O/A horizon
333 0.5 hr after ^{15}N-Glut application was larger (12%) at the lower than the upper site, and larger than
334 at both sites in the $^{15}NH_4$ treatment. Total ^{15}N recoveries declined to about 60% after 219 h, similar
335 to those in the $^{15}NH_4$ treatment.

336 *Gross N transformation rates in the O/A horizon*

337 Gross NH_4^+ mineralization rates averaged 3.27 (±1.66) and 3.08 (±0.45) μg g^{-1} d^{-1} for the upper
338 (P1) and lower (P2) site, respectively, while gross NH_4^+ immobilization rates averaged 4.39 (±3.67)
339 and 3.84 (±1.88) μg g^{-1} d^{-1} (Table 1). Gross nitrification rates were 1.10 (±0.52) and 1.28 (±0.57)
340 μg g^{-1} d^{-1} for the upper and lower sites, respectively. The gross transformation rates were not
341 significantly different between the upper and the lower site. The average cumulative N_2O loss
342 throughout 219 hr was 0.13 μg N g^{-1} d^{-1} at the upper site, which was significantly larger than 0.05
343 μg g^{-1} d^{-1} at the lower site. DNRA rates were small and indistinguishable between sites (0.03 μg g^{-1} d^{-1}).

Discussion

Fate of atmogenic NO_3^- in soil

Initial recovery (after 0.5 hr) of ^{15}N in the $^{15}NO_3$ treatment was large, and dominated by $^{15}NO_3^-$. However, the total recovery (in O/A and AB horizons) decreased strongly with time to values below 20% after 9 days (Figs. 5b and e). Previous studies in the TSP catchment indicated strong NO_3^- leaching from soils on the hillslope (Chen and Mulder 2007, Larssen et al. 2011, Huang et al. 2015), suggesting that loss by leaching, not transformation, is the dominant fate of deposited NO_3^-. In our $^{15}NO_3$ treatment at both sites, leaching of unprocessed NO_3^- was supported by the recovery of ^{15}N in the deeper AB horizon, where the ^{15}N recovery in KCl-extractable NO_3^- was significantly greater than in the other two treatments (Figs. 5 and S3).

We roughly estimated the contribution of NO_3^- leaching to non-recovered ^{15}N based on water flux and NO_3^- concentrations in soil water for the initial 6 samplings, and found that 21% to 28% of the applied ^{15}N was lost by leaching (Table S1). This would explain more than half of the missing ^{15}N (40% of added ^{15}N). However, we calculated the water flux from the net change of volumetric soil moisture throughout the initial 144 hr, which probably underestimates the gross water flux due to water replenishment from upper hillslopes (Sørbotten et al. accepted). Initially, the ^{15}N recovery in the residual soil N pool (which excluded KCl-extractable inorganic N) was small (a few %) at both sites, but increased to maximum values of about 20% after 50 to 95 hr. This suggests that the residual soil N pool has a dynamic character mediating short-term, temporary $^{15}NO_3^-$ retention, followed by ^{15}N release.

Fate of atmogenic NH_4^+ in soil

In the $^{15}NH_4$ treatment, recovery of ^{15}N was greater than in the $^{15}NO_3^-$ treatment, reaching values

between 50 and 80% after 9 days, at the upper and lower site, respectively (219 hr; Figs.5a and d). This decline in recovery with time was less pronounced than in the $^{15}NO_3$ treatment. Most of the added $^{15}NH_4^+$ was recovered in the residual soil N pool, indicating strong retention of added NH_4^+. This is in accordance with previous short-term tracer studies, reporting high N retention in temperate and tropical forest soils (Perakis et al. 2005, Templer et al. 2008, 2012). High retention of NH_4^+ may be attributed to clay fixation (Nieder et al. 2011). However, more likely, this reflects the dominance of microbial immobilization in NH_4^+ retention (Tahovsk et al. 2013).

Re-mineralization with subsequent nitrification, i.e. the release of NH_4^+ from organically retained N and its biological conversion to NO_3^- has been acknowledged as an important pathway for indirect NO_3^- leaching from forest ecosystems (Curtis et al. 2011). Traditionally, the nitrification process was believed to be inhibited in acid forest soils due to the limited availability of NH_3 for ammonia oxidizing bacteria (De Boer and Kowalchuk 2001). However, we observed ^{15}N-enriched NO_3^- immediately after the addition of $^{15}NH_4^+$ (Figs. 4 and 5), indicating rapid nitrification. The gross nitrification rates, which did not differ significantly between the upper and lower sites (Table 1), were smaller than rates reported for the organic layer of temperate forest soil (Tahovsk et al. 2013), but comparable to those reported in surface mineral soils (0-5 cm) from subtropical and tropical forest soils (Templer et al. 2008, Zhang et al. 2013, Rütting et al. 2015).

If NH_4^+ oxidation is the only source of NO_3^-, the ^{15}N enrichment of NO_3^- would never exceed that of NH_4^+ at any given time point (Hart and Myrold 1996). Yet, from the second sampling of our study onwards, (Figs. 4a and d) we found larger ^{15}N enrichment in NO_3^- than in NH_4^+, especially at the lower site. This indicates that NO_3^- was not only produced from ^{15}N-enriched NH_4^+, but also from other ^{15}N-enriched sources. Regarding that the total soil residual N pool was little enriched in ^{15}N (Figs. 4a and d), a more dynamic, labile, and ^{15}N-enriched fraction of it must have

390 contributed to $^{15}NO_3^-$ production. We did not measure ^{15}N uptake into the soil microbial biomass,
391 but the microbial N pool is the fastest turning over organic N pool in soil (Stark and Hart 1997),
392 likely accumulating ^{15}N through immobilization. Our finding of ^{15}N in NO_3^- exceeding that in
393 NH_4^+ in the $^{15}NH_4$ treatment could thus be explained by re-mineralization of immobilized ^{15}N
394 followed by autotrophic nitrification and/or direct conversion of organic N to NO_3^- by
395 heterotrophic nitrification. The latter pathway was supported by greater ^{15}N enrichment in NO_3^-
396 than in NH_4^+ in the ^{15}N-Glut treatment (Figs. 4 and 5c and f). This effect was more pronounced at
397 the lower (P2) site, where significantly larger ^{15}N enrichment in NO_3^- than in NH_4^+ was observed
398 already from the first sampling onwards (0.5 hr), indicating greater importance of heterotrophic
399 nitrification there. Since fungal communities, which are abundant in acid soils, tolerate lower
400 oxygen tensions than bacteria (Stroo et al. 1986), fungal driven heterotrophic nitrification may
401 offer an explanation for the enhanced heterotrophic nitrification activity observed at this site (Zhu
402 et al. 2014). To the best of our knowledge, this is the first *in situ* observation supporting
403 heterotrophic nitrification activity in acid subtropical forest soils (Zhang et al. 2013, 2015).

404 In a previous study on natural abundance of NO_3^- isotopic signatures in the TSP catchment, we
405 found greatly dampened $\delta^{18}O$ signals in soil water NO_3^- compared to throughfall NO_3^-, indicating
406 that the soil NO_3^- was mostly derived from soil process (Yu et al. 2016). This seems to contradict
407 our finding based on $^{15}NO_3^-$ tracing (Figs. 5b and d), which suggested direct leaching (Curtis et al.
408 2011) without appreciable processing. However, since more than 60% of the atmogenic N
409 deposition at TSP consists of NH_4^+-N, soil NO_3^- is likely a mixture of atmospheric and
410 nitrification-derived NO_3^- as has been found by others (Rose et al. 2015). More importantly, this
411 implies that, currently at TSP, nitrification of atmogenic NH_4^+ is quantitatively more important
412 than NO_3^- deposition for overall soil NO_3^- leaching.

N_2O emissions in response to atmogenic N inputs

End-member mixing analysis showed that the contribution of nitrification and denitrification to N_2O production varied with changing WFPS (Fig. 6). Large fluxes occurring at high WFPS values, could all be apportioned to denitrification. This matches findings by (Zhu et al. 2013a), who reported 71% to 100% of the emitted N_2O to be due to denitrification in the same hillslope soils. In our study, the importance of nitrification for N_2O emission increased when WFPS decreased below 60% at the upper site and below 70% at the lower site (Fig. 6). Khalil et al. (2004) and Mathieu et al. (2006) observed nitrification to contribute more than 60% to N_2O production in unsaturated soils in agricultural soils. Also, in acid subtropical forest soils of China, Zhang et al. (2011) attributed 27% to 42% of the N_2O production to nitrification at WFPS values between 40% to 52%. Long-term observations at TSP have shown that the WFPS in hillslope soil is below 60% outside the rainy season (Zhu et al. 2013c). Therefore, it is likely that nitrification contributes significantly to the small N_2O emissions at our site during the dry season, whereas larger N_2O fluxes during wet conditions primarily derive from denitrification. The N_2O fluxes were significantly smaller at the lower site, despite its higher WFPS (Figs. 6b and S4a). This may be due to increasing N_2O reduction to N_2 under high anoxia (Zhu et al. 2013d), which is supported by the fact that N_2O fluxes decreased at higher WFPS (~ 90%), at the lower site.

The cumulative ^{15}N recovery in N_2O throughout nine days was largest in the $^{15}NO_3$ treatment, amounting to 6.0% and 2.5% at the upper and lower sites, respectively. Such large recoveries of added N as N_2O in a short-term experiment are surprising, as they by far exceed those observed in ^{15}N tracer experiments in temperate forest soil (1 year, < 1%; Eickenscheidt et al. 2011) and tropical forest soil (24 hr, 0.05%; Templer et al. 2008). Earlier, Zhu et al. (2013c) estimated N_2O emissions amounting to 8% to 10% of annual N deposition at TSP. In a six-day ^{15}N tracing

experiment on the hillslope at TSP, 1.3% to 3.2% of added $^{15}NO_3^-$ were recovered in emitted N_2O (Zhu et al. 2013a). Despite the relatively wet condition during our sampling period (60-80% at the upper site and 70-90% at the lower site), our findings are in line with previous studies, confirming significant N_2O losses in response to atmogenic N input during monsoonal summers.

To estimate N_2 loss, we assumed an N_2O/N_2 ratio of 1.5, for denitrification in TSP soils, based on data from an *ex situ* denitrification study (Zhu et al. 2013b). Assuming that 100% of N_2O is derived from denitrification, N_2 emissions would account for 4.0% and 1.7% of the total ^{15}N loss at the upper and lower sites, respectively. This indicates that the contribution of N_2 emission to unrecovered ^{15}N loss on the hill slope was far less important than that of N leaching.

Gross N turnover in N-saturated soils

Gross NH_4^+ immobilization and mineralization rates for TSP soils (Table 1) were slightly greater than those reported from incubation experiments with acid forest soils from southern China (Zhang et al. 2013), and in the low range of those found in tropical forests (Silver et al. 2001, Sotta et al. 2008, Templer et al. 2008, Arnold et al. 2009). In our study, gross turnover of NH_4^+ (~ 3.5 μg g^{-1} d^{-1}) was significantly greater than gross nitrification (~ 1.1 μg g^{-1} d^{-1}), which is similar to the observation by Sotta et al. (2008), who attributed this to a greater importance of NH_4^+ cycling than NO_3^- cycling through the microbial biomass in soil. This results in a dynamic soil N cycle, in which soil microbial immobilization/mineralization dictates the pace at which NH_4^+ is released and nitrified to NO_3^- before being leached. However, assuming the pool sizes do not change in a long term, soil N turnover will result in near-quantitative conversion of added NH_4^+ to NO_3^-, as suggested by the observation of closed input-output balances in subtropical forests on an annual basis (Huang et al. 2015).

458 ^{15}N tracing studies have demonstrated less $^{15}NO_3^-$ than $^{15}NH_4^+$ retention in temperate (Tietema et
459 al. 1998, Corre et al. 2007) and tropical forests (Sotta et al. 2008, Templer et al. 2008). On a weekly
460 scale, Corre et al. (2007) and Sotta et al. (2008) found 70% to 100% of added $^{15}NO_3^-$ to be retained
461 in soil. In our study, we did not recover more than 20% of the added $^{15}NO_3^-$ nine days after addition
462 (Figs. 5b and e) which also is markedly less than the 40% recovered four months after addition to
463 an N-saturated tropical forest soil by Sheng et al. (2014). This suggests that under conditions of
464 extreme N saturation, like at TSP (Huang et al. 2015), deposited NO_3^- is leached directly without
465 further processing. Since the atmogenic deposition of oxidized N (NO_x) is predicted to increase
466 faster than that of NH_4^+ in China (Xu et al. 2015, Liu et al. 2016), N-saturated subtropical forest
467 soils are to be expected to show rapid increases in NO_3^- leaching with little net-retention, thus
468 aggravating N pollution of fresh waters in China.

469

470

471 ## Acknowledgement

472 LY thanks the China Scholarship Council (CSC) for supporting his PhD study. Support from the
473 Norwegian Research Council to project 209696/E10 'Forest in South China: an important sink for
474 reactive nitrogen and a regional hotspot for N2O?' is gratefully acknowledged. We thank Prof.
475 Duan Lei, Dr. Wang Yihao, Wang Jiaqi, Zhang Ting, Yang Hanyue, Wu Liping, Kai Xuan and
476 Zou Mingquan for their help with the data collection throughout the field experiment.

References

Aber, J., W. McDowell, K. Nadelhoffer, A. Magill, G. Berntson, M. Kamakea, S. McNulty, W. Currie, L. Rustad, and I. Fernandez. 1998. Nitrogen saturation in temperate forest ecosystems - hypotheses revisited. Bioscience 48:921–934.

Allison, S. M., and J. I. Prosser. 1993. Ammonia oxidation at low pH by attached populations of nitrifying bacteria. Soil Biology & Biochemistry 25:935–941.

Arnold, J., M. D. Corre, and E. Veldkamp. 2009. Soil N cycling in old-growth forests across an Andosol toposequence in Ecuador. Forest Ecology and Management 257:2079–2087.

Bobbink, R., K. Hicks, J. Galloway, T. Spranger, R. Alkemade, M. Ashmore, S. Cinderby, E. Davidson, F. Dentener, B. Emmett, J. Erisman, M. Fenn, A. Nordin, L. Pardo, W. De Vries, K. Hicks, J. Galloway, R. Bobbink, E. Davidson, F. Dentener, S. Cinderby, T. Spranger, and M. Bustamante. 2010. Global assessment of nitrogen deposition effects on terrestrial plant diversity. Ecological Applications 20:30–59.

De Boer, W., P. J. A. K. Gunnewiek, S. R. Troelstra, and H. J. Laanbroek. 1989. Two types of chemolithotrophic nitrification in acid heathland humus. Plant and Soil 119:229–235.

De Boer, W., and G. Kowalchuk. 2001. Nitrification in acid soils : micro-organisms and mechanisms. Soil Biology and Biochemistry 33:853–866.

Booth, M. S., J. M. Stark, and E. Rastetter. 2005. Controls on nitrogen cycling in terrestrial ecosystems: a synthetic analysis of literature data. Ecological Monographs 72:139–157.

Burton, S. A. Q., and J. I. Prosser. 2001. Autotrophic ammonia oxidation at low pH through urea hydrolysis. Applied and Environmental Microbiology 67:2952–2957.

Chen, X., and J. Mulder. 2007. Indicators for nitrogen status and leaching in subtropical forest ecosystems, South China. Biogeochemistry 82:165–180.

Chen, Z., W. Ding, Y. Xu, C. Müller, T. Rütting, H. Yu, J. Fan, J. Zhang, and T. Zhu. 2015. Importance of heterotrophic nitrification and dissimilatory nitrate reduction to ammonium in a cropland soil: Evidences from a ^{15}N tracing study to literature synthesis. Soil Biology and Biochemistry 91:65–75.

Corre, M. D., R. R. Brumme, E. Veldkamp, and F. O. Beese. 2007. Changes in nitrogen cycling and retention processes in soils under spruce forests along a nitrogen enrichment gradient in Germany. Global Change Biology 13:1509–1527.

Curtis, C. J., C. D. Evans, C. L. Goodale, and T. H. E. Heaton. 2011. What Have Stable Isotope Studies Revealed About the Nature and Mechanisms of N Saturation and Nitrate Leaching from Semi-Natural Catchments? Ecosystems 14:1021–1037.

Davidson, E. A., S. C. Hart, and M. K. Firestone. 1992. Internal Cycling of Nitrate in Soils of a Mature Coniferous Forest. Ecology 73:1148–1156.

Davidson, E. A., S. C. Hart, C. A. Shanks, and M. K. Firestone. 1991. Measuring gross nitrogen minearlization, immobilization, and nitrification by ^{15}N isotopic pool dilution in intact soil cores. Journal of Soil Science 42:335–349.

Eickenscheidt, N., R. Brumme, and E. Veldkamp. 2011. Direct contribution of nitrogen deposition to nitrous oxide emissions in a temperate beech and spruce forest - A ^{15}N tracer study. Biogeosciences 8:621–635.

Fang, Y., P. Gundersen, R. D. Vogt, K. Koba, F. Chen, X. Y. Chen, and M. Yoh. 2011. Atmospheric deposition and leaching of nitrogen in Chinese forest ecosystems. Journal of Forest Research 16:341–350.

Fang, Y., K. Koba, A. Makabe, C. Takahashi, W. Zhu, and T. Hayashi. 2015. Microbial denitrification dominates nitrate losses from forest ecosystems. Proceedings of the National Academy of Sciences of the United States of America 112:1470-1474.

Firestone, M. K., and E. A. Davidson. 1989. Microbiological Basis of NO and N_2O Production and Consumption in Soil. Pages 7-21 *in* M. O. Andreae, D. S. Schimel and G. P. Robertson, editors. Exchange of trace gases between terrestrial ecosystems and the atmosphere. John Wiley & Sons Ltd, Berlin.

Galloway, J., J. Aber, J. Erisman, S. Speitzinger, R. Howarth, E. Cowling, and A. Cosby. 2003. The nitrogen cascade. Bioscience 53:341–356.

Galloway, J. N., A. R. Townsend, J. W. Erisman, M. Bekunda, Z. Cai, J. R. Freney, L. A. Martinelli, S. P. Seitzinger, and M. A. Sutton. 2008. Transformation of the nitrogen cycle: recent trends, questions, and potential solutions. Science 320:889–92.

Gao, W., L. Kou, H. Yang, J. Zhang, C. Müller, and S. Li. 2016. Are nitrate production and retention processes in subtropical acidic forest soils responsive to ammonium deposition? Soil Biology and Biochemistry 100:102–109.

Gubry-Rangin, C., B. Hai, C. Quince, M. Engel, B. C. Thomson, P. James, M. Schloter, R. I. Griffiths, J. I. Prosser, and G. W. Nicol. 2011. Niche specialization of terrestrial archaeal ammonia oxidizers. Proceedings of the National Academy of Sciences of the United States of America 108:21206-21211.

Guo, J. H., X. J. Liu, Y. Zhang, J. L. Shen, W. X. Han, W. F. Zhang, P. Christie, K. W. T. Goulding, P. M. Vitousek, and F. S. Zhang. 2010. Significant acidification in major Chinese croplands. Science 327:1008–1010.

Gurmesa, G. A., X. Lu, P. Gundersen, Q. Mao, K. Zhou, Y. Fang, and J. Mo. 2016. High retention of ^{15}N-labeled nitrogen deposition in a nitrogen saturated old-growth tropical forest. Global Change Biology In Press. doi:10.1111/gcb.13327.

Hart, S. C., and D. D. Myrold. 1996. ^{15}N tracer studies of soil nitrogen transformations. Pages 225-245 *in* Boutton, T.W. and Yamasaki, S.I., editors. Mass spectrometry of soils. Marcel Dekker, Inc., New York.

Huang, Y., R. Kang, J. Mulder, T. Zhang, and L. Duan. 2015. Nitrogen saturation, soil acidification, and ecological effects in a subtropical pine forest on acid soil in southwest China. Journal of Geophysical Research: Biogeosciences 120:2457–2472.

Kaiser, J., T. Rockmann, and C. A. M. Brenninkmeijer. 2003. Complete and accurate mass spectrometric isotope analysis of tropospheric nitrous oxide. Journal of Geophysical Research 108:1–17.

555 Khalil, K., B. Mary, and P. Renault. 2004. Nitrous oxide production by nitrification and
556 denitrification in soil aggregates as affected by O_2 concentration. Soil Biology and
557 Biochemistry 36:687–699.

558 Kirkham, D., and W. V Bartholomew. 1954. Equations for following nutrient transformations in
559 soil, utilizing tracer data: II. Soil Science Society of America Journal 19:189–192.

560 Larssen, T., L. Duan, and J. Mulder. 2011. Deposition and leaching of sulfur, nitrogen and
561 calcium in four forested catchments in China: implications for acidification. Environmental
562 Science & Technology 45:1192–8.

563 Leininger, S., T. Urich, M. Schloter, L. Schwark, J. Qi, G. W. Nicol, J. I. Prosser, S. C. Schuster,
564 and C. Schleper. 2006. Archaea predominate among ammonia-oxidizing prokaryotes in
565 soils. Nature 442:806–809.

566 Levičnik-Höfferle, Š., G. W. Nicol, L. Ausec, I. Mandić-Mulec, and J. I. Prosser. 2012.
567 Stimulation of thaumarchaeal ammonia oxidation by ammonia derived from organic
568 nitrogen but not added inorganic nitrogen. FEMS Microbiology Ecology 80:114–123.

569 Li, Z., Y. Wang, Y. Liu, H. Guo, T. Li, Z. H. Li, and G. Shi. 2014. Long-term effects of liming
570 on health and growth of a Masson pine stand damaged by soil acidification in Chongqing,
571 China. PLoS One 9:1–9.

572 Linn, D. M., and J. W. Doran. 1984. Effect of Water-Filled Pore Space on Carbon Dioxide and
573 Nitrous Oxide Production in Tilled and Nontilled Soils. Soil Science Society of America
574 Journal 48:1267–1272.

575 Liu, B., P. T. Mørkved, A. Frostegård, and L. R. Bakken. 2010. Denitrification gene pools,
576 transcription and kinetics of NO, N_2O and N_2 production as affected by soil pH. FEMS
577 Microbiology Ecology 72:407–17.

578 Liu, X., W. Xu, E. Du, Y. Pan, and K. Goulding. 2016. Reduced nitrogen dominated nitrogen
579 deposition in the United States, but its contribution to nitrogen deposition in China
580 decreased. Proceedings of the National Academy of Sciences 113: E3590–E3591.

581 Liu, X., Y. Zhang, W. Han, A. Tang, J. Shen, Z. Cui, P. Vitousek, J. W. Erisman, K. Goulding,
582 P. Christie, A. Fangmeier, and F. Zhang. 2013. Enhanced nitrogen deposition over China.
583 Nature 494:459–62.

584 Lovett, G. M., and C. L. Goodale. 2011. A New Conceptual Model of Nitrogen Saturation Based
585 on Experimental Nitrogen Addition to an Oak Forest. Ecosystems 14:615–631.

586 Lu, M., Y. Yang, Y. Luo, C. Fang, X. Zhou, J. Chen, X. Yang, and B. Li. 2011. Responses of
587 ecosystem nitrogen cycle to nitrogen addition: A meta-analysis. New Phytologist 189:1040–
588 1050.

589 Mathieu, O., C. Hénault, J. Lévêque, E. Baujard, M. J. Milloux, and F. Andreux. 2006.
590 Quantifying the contribution of nitrification and denitrification to the nitrous oxide flux
591 using ^{15}N tracers. Environmental Pollution 144:933–940.

592 Morley, N., E. M. Baggs, P. Dörsch, and L. Bakken. 2008. Production of NO, N_2O and N_2 by
593 extracted soil bacteria, regulation by NO_2^- and O_2 concentrations. FEMS Microbiology

Ecology 65:102–112.

Müller, C., T. Rutting, J. Kattge, R. J. Laughlin, and R. J. Stevens. 2007. Estimation of parameters in complex ^{15}N tracing models by Monte Carlo sampling. Soil Biology and Biochemistry 39:715–726.

Nieder, R., D. K. Benbi, and H. W. Scherer. 2011. Fixation and defixation of ammonium in soils: A review. Biology and Fertility of Soils 47:1–14.

NSF. (1975a). Water analysis (Determination of the sum of nitrite- and nitrate-nitrogen. NS 4745). Oslo, Norway.

NSF. (1975b). Water analysis (Determination of ammonium-nitrogen. NS 4746). Oslo, Norway.

Perakis, S. S., J. E. Compton, and L. O. Hedin. 2005. N Additions To an Unpolluted Temperate Forest Soil in Chile. Ecology 86:96–105.

Rose, L. A., E. M. Elliott, and M. B. Adams. 2015. Triple Nitrate Isotopes Indicate Differing Nitrate Source Contributions to Streams Across a Nitrogen Saturation Gradient. Ecosystems 18:1209–1223.

Rütting, T., L. C. Ntaboba, D. Roobroeck, M. Bauters, D. Huygens, and P. Boeckx. 2015. Leaky nitrogen cycle in pristine African montane rainforest soil. Global Biogeochemical Cycles 29:1754–1762.

Sheng, W., G. Yu, H. Fang, C. Jiang, J. Yan, and M. Zhou. 2014. Sinks for inorganic nitrogen deposition in forest ecosystems with low and high nitrogen deposition in China. PLoS One 9:e89322.

Shi, Y., S. Cui, X. Ju, Z. Cai, and Y. Zhu. 2015. Impacts of reactive nitrogen on climate change in China. Scientific Reports 5:8118.

Sigman, D. M., K. L. Casciotti, M. Andreani, C. Barford, M. Galanter, and J. K. Böhlke. 2001. A bacterial method for the nitrogen isotopic analysis of nitrate in seawater and freshwater. Analytical Chemistry 73:4145–53.

Silver, W., D. Herman, and M. Firestone. 2001. Dissimilatory nitrate reduction to ammonium in upland tropical forest soils. Ecology 82:2410–2416.

Sørbotten, L., J. Stolte, Y. Wang, and J. Mulder. 2016. Hydrological Response and Flow Pathways in Acrisols on a Forested Hillslope in Monsoonal Sub-tropical Climate, Chonqing, Southwest. Pedosphere Accepted.

Sotta, E. D., M. D. Corre, and E. Veldkamp. 2008. Differing N status and N retention processes of soils under old-growth lowland forest in Eastern Amazonia, Caxiuanã, Brazil. Soil Biology and Biochemistry 40:740–750.

Stark, J. M., and S. C. Hart. 1997. High rates of nitrification and nitrate turnover in undisturbed coniferous forests. Nature 385:810–813.

Stevens, R. J., R. J. Laughlin, L. C. Burns, J. R. M. Arah, and R. C. Hood. 1997. Measuring the contributions of nitrification and denitrification to the flux of nitrous oxide from soil. Soil Biology and Biochemistry 29:139–151.

Stroo, H. F., T. M. Klein, and M. Alexander. 1986. Heterotrophic nitrification in an Acid forest soil and by an Acid-tolerant fungus. Applied and Environmental Microbiology 52:1107–1111.

Tahovsk, K., J. Kana, J. Barta, F. Oulehle, A. Richter, and H. Santruckova. 2013. Microbial N immobilization is of great importance in acidified mountain spruce forest soils. Soil Biology and Biochemistry 59:58–71.

Templer, P. H., M. C. Mack, F. S. Chapin III, L. M. Christenson, J. E. Compton, H. D. Crook, W. S. Currie, C. J. Curtis, D. B. Dail, C. M. D'antonio, B. A. Emmett, H. E. Epstein, C. L. Goodale, P. Gundersen, S. E. Hobbie, K. Holland, D. U. Hooper, B. A. Hungate, S. Lamontagne, K. J. Nadelhoffer, C. W. Osenberg, S. S. Perakis, P. Schleppi, J. Schimel, I. K. Schmidt, M. Sommerkorn, J. Spoelstra, A. Tietema, W. W. Wessel and D. R. Zak. 2012. Sinks for nitrogen inputs in terrestrial ecosystems: a meta-analysis of ^{15}N tracer field studies. Ecology 93:1816–1829.

Templer, P. H., W. L. Silver, J. Pett-ridge, K. M. Deangelis, and M. K. Firestone. 2008. Plant and Microbial Controls on Nitrogen Retention and Loss in a Humid Tropical Forest. Ecology 89:3030–3040.

Tiedje, J. M. 1988. Ecology of denitrification and dissimilatory nitrate reduction to ammonium. Pages 179-244 *in* A. J. B. Zehnder, editor. Environmental Microbiology of Anaerobes. John Wiley & Sons, New York.

Tietema, A., B. A. . Emmett, P. Gundersen, O. J. Kjønaas, and C. J. Koopmans. 1998. The fate of ^{15}N-labelled nitrogen deposition in coniferous forest ecosystems. Forest Ecology and Management 101:19–27.

Townsend, A. R., R. W. Howarth, F. A. Bazzaz, M. S. Booth, C. C. Cleveland, S. K. Collinge, A. P. Dobson, P. R. Epstein, E. A. Holland, D. R. Keeney, M. A. Mallin, C. A. Rogers, P. Wayne, and A. H. Wolfe. 2003. Human health effects of a changing global nitrogen cycle. Frontiers in Ecology and the Environment 1:240–246.

Wang, Y., S. Solberg, P. Yu, T. Myking, R. D. Vogt, and S. Du. 2007. Assessments of tree crown condition of two Masson pine forests in the acid rain region in south China. Forest Ecology and Management 242:530–540.

Xu, W., X. S. Luo, Y. P. Pan, L. Zhang, A. H. Tang, J. L. Shen, Y. Zhang, K. H. Li, Q. H. Wu, D. W. Yang, Y. Y. Zhang, J. Xue, W. Q. Li, Q. Q. Li, L. Tang, S. H. Lu, T. Liang, Y. A. Tong, P. Liu, Q. Zhang, Z. Q. Xiong, X. J. Shi, L. H. Wu, W. Q. Shi, K. Tian, X. H. Zhong, K. Shi, Q. Y. Tang, L. J. Zhang, J. L. Huang, C. E. He, F. H. Kuang, B. Zhu, H. Liu, X. Jin, Y. J. Xin, X. K. Shi, E. Z. Du, A. J. Dore, S. Tang, J. L. Collett, K. Goulding, Y. X. Sun, J. Ren, F. S. Zhang, and X. J. Liu. 2015. Quantifying atmospheric nitrogen deposition through a nationwide monitoring network across China. Atmospheric Chemistry and Physics 15:12345–12360.

Yakir, D., and L. da S. L. Sternberg. 2000. The use of stable isotopes to study ecosystem gas exchange. Oecologia 123:297–311.

Yu, L., J. Zhu, J. Mulder, and P. Dörsch. 2016. Multiyear dual nitrate isotope signatures suggest that N-saturated subtropical forested catchments can act as robust N sinks. Global Change

673 Biology In Press. doi:10.1111/gcb.13333.

674 Zhang, J., Z. Cai, and T. Zhu. 2011. N_2O production pathways in the subtropical acid forest soils
675 in China. Environmental Research 111:643–649.

676 Zhang, J., Z. Cai, T. Zhu, W. Yang, and C. Müller. 2013. Mechanisms for the retention of
677 inorganic N in acidic forest soils of southern China. Scientific Reports 3:2342.

678 Zhang, J., C. Müller, and Z. Cai. 2015. Heterotrophic nitrification of organic N and its
679 contribution to nitrous oxide emissions in soils. Soil Biology and Biochemistry 84:199–209.

680 Zhang, L., M. A. Altabet, T. Wu, and O. Hadas. 2007. Sensitive measurement of NH_4^+ $^{15}N/^{14}N$
681 ($\delta^{15}NH_4^+$) at natural abundance levels in fresh and saltwaters. Analytical Chemistry
682 79:5297–303.

683 Zhu, J., J. Mulder, L. Bakken, and P. Dörsch. 2013a. The importance of denitrification for N_2O
684 emissions from an N-saturated forest in SW China: results from in situ ^{15}N labeling
685 experiments. Biogeochemistry 116:103–117.

686 Zhu, J., J. Mulder, S. O. Solheimslid, and P. Dörsch. 2013b. Functional traits of denitrification in
687 a subtropical forest catchment in China with high atmogenic N deposition. Soil Biology and
688 Biochemistry 57:577–586.

689 Zhu, J., J. Mulder, L. P. Wu, X. X. Meng, Y. H. Wang, and P. Dörsch. 2013c. Spatial and
690 temporal variability of N_2O emissions in a subtropical forest catchment in China.
691 Biogeosciences 10:1309–1321.

692 Zhu, T., T. Meng, J. Zhang, Y. Yin, Z. Cai, W. Yang, and W. Zhong. 2013d. Nitrogen
693 mineralization, immobilization turnover, heterotrophic nitrification, and microbial groups in
694 acid forest soils of subtropical China. Biology and Fertility of Soils 49:323–331.

695 Zhu, T., T. Meng, J. Zhang, W. Zhong, C. Müller, and Z. Cai. 2014. Fungi-dominant
696 heterotrophic nitrification in a subtropical forest soil of China. Journal of Soils and
697 Sediments.

Table 1 Gross N transformation rates of NH_4^+ and NO_3^- in the O/A horizon estimated by the ^{15}N pool dilution method[†]

		Upper site		Lower site	
		Avg.	Stdv.	Avg.	Stdv.
Gross rates ($\mu g\ N\ g\ dry\ soil^{-1}\ d^{-1}$)	NH_4^+ immobilization[§]	4.39	2.67	3.84	1.88
	Mineralization	3.27	1.66	3.08	0.45
	Nitrification	1.10	0.52	1.28	0.57
	N_2O emission[*]	0.13	0.07	0.05	0.03
	DNRA[*]	0.03	0.00	0.03	0.00

[†] Due to the rain episode occurring a few hours prior to the 7th sampling (174 hours after tracer addition), the gross transformation rates were calculated with data for the first 6 samplings only (0-144 hr after tracer addition).

[§] Gross NH_4^+ immobilization rate, calculated by subtracting gross nitrification rate from gross NH_4^+ consumption rate. This rate may be an underestimation due to the contribution of heterotrophic nitrification to gross nitrification.

[*] Net rates estimated from cumulative production.

Figure Legends

Fig. 1a Location of the two experimental sites (P1 and P2) on a Northeast facing hill slope of the Tieshanping (TSP) catchment, Chongqing, SW China. P1 is situated near the summit and P2 at the foot of the hillslope.
1b Set-up of experimental plots at sites P1 and P2. Both sites accommodated three blocks with four randomly distributed treatments. Treatment codes are: A= $^{15}NH_4NO_3$, B= $NH_4{}^{15}NO_3$, C= ^{15}N-Glutamic acid, D= Reference.

Fig. 2a Hourly air temperature and precipitation from 1 June to 4 July, 2015. The eight sampling time points are indicated in red. Label addition was done on 23 June, 2015, 0.5 hr prior to the first sampling (sampling 1).
2b Averages and standard deviations (n = 12) of soil temperature (open circles) and water filled pore space (WFPS; vertical bars) for sites P1 (upper site) and P2 (lower site). The x-axis indicates the time after label application.

Fig. 3 Concentration of NH_4^+ and NO_3^- in KCl extracts, total N content in bulk soil (both in O/A horizon) and N_2O emission flux for the Reference (panels a and e), $^{15}NH_4$ (panels b and f), $^{15}NO_3$ (panels c and g) and ^{15}N-Glut (panels d and h) treatments. Upper and lower panels refer to P1 (upper site) and P2 (lower site). Values are means and standard errors (n = 3). The x-axis indicates the time after label application.

Fig. 4 Atom% ^{15}N-excess of NH_4^+ and NO_3^- in KCl extracts, total soil N (in the O/A horizon) and emitted N_2O for the $^{15}NH_4$ (panels a and d), $^{15}NO_3$ (panels b and e) and ^{15}N-Glut (panels c and f) treatments. Upper and lower panels refer to P1 (upper site) and P2 (lower site). Values are means and standard errors (n = 3). The x-axis indicates the time after label application.

Fig. 5 Average ^{15}N recovery (n=3) in different N pools in $^{15}NH_4$ (panels a and d), $^{15}NO_3$ (panels b and e) and ^{15}N-Glut (panels c and f) treatments. Upper and lower panels refer to P1 (upper site)

and P2 (lower site). OA and AB represent the O/A and AB horizons, respectively. The x-axis indicates the time after label application.

Fig. 6 Mean partitioning of N_2O fluxes to nitrification and denitrification at the upper (P1) site (panel a) and the lower (P2) site (panel b). The shaded background indicates water filled pore space (WFPS; average values are presented, n =3). Fluxes could not be not partitioned for the first sampling date (0.5 hr), since the atom% ^{15}N in N_2O decreased during the initial hours after label application.

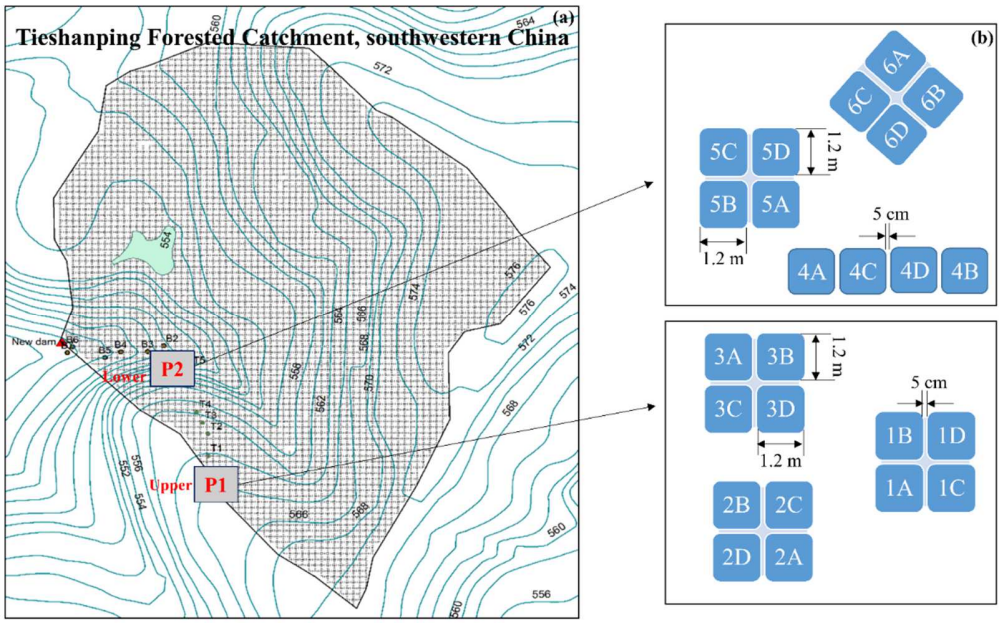
Tieshanping Forested Catchment, southwestern China
(a)
(b)
New dam
Lower
P2
Upper
P1
6A
6B
6C
6D
5C
5D
5B
5A
4A
4C
4D
4B
3A
3B
3C
3D
2B
2C
2D
2A
1B
1D
1A
1C
1.2 m
5 cm

Fig. 1a and **1b**

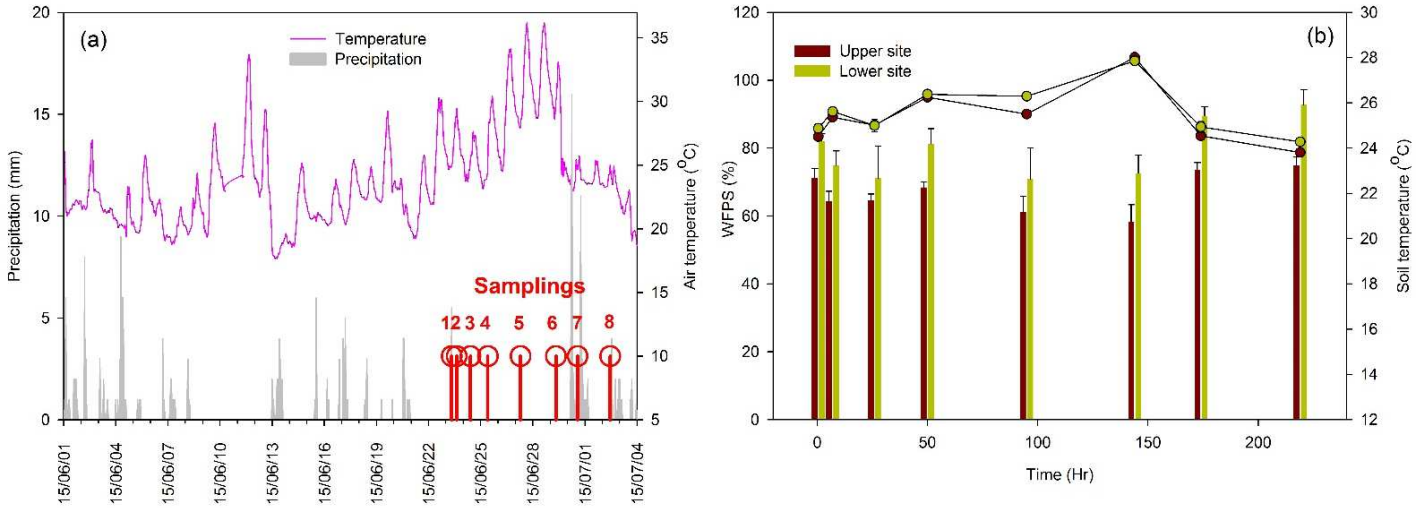
(a)
Temperature
Precipitation
Samplings
1 2 3 4 5 6 7 8
Precipitation (mm)
Air temperature (°C)
15/06/01
15/06/04
15/06/07
15/06/10
15/06/13
15/06/16
15/06/19
15/06/22
15/06/25
15/06/28
15/07/01
15/07/04
(b)
Upper site
Lower site
WFPS (%)
Soil temperature (°C)
Time (Hr)

Fig. 2a and **2b**

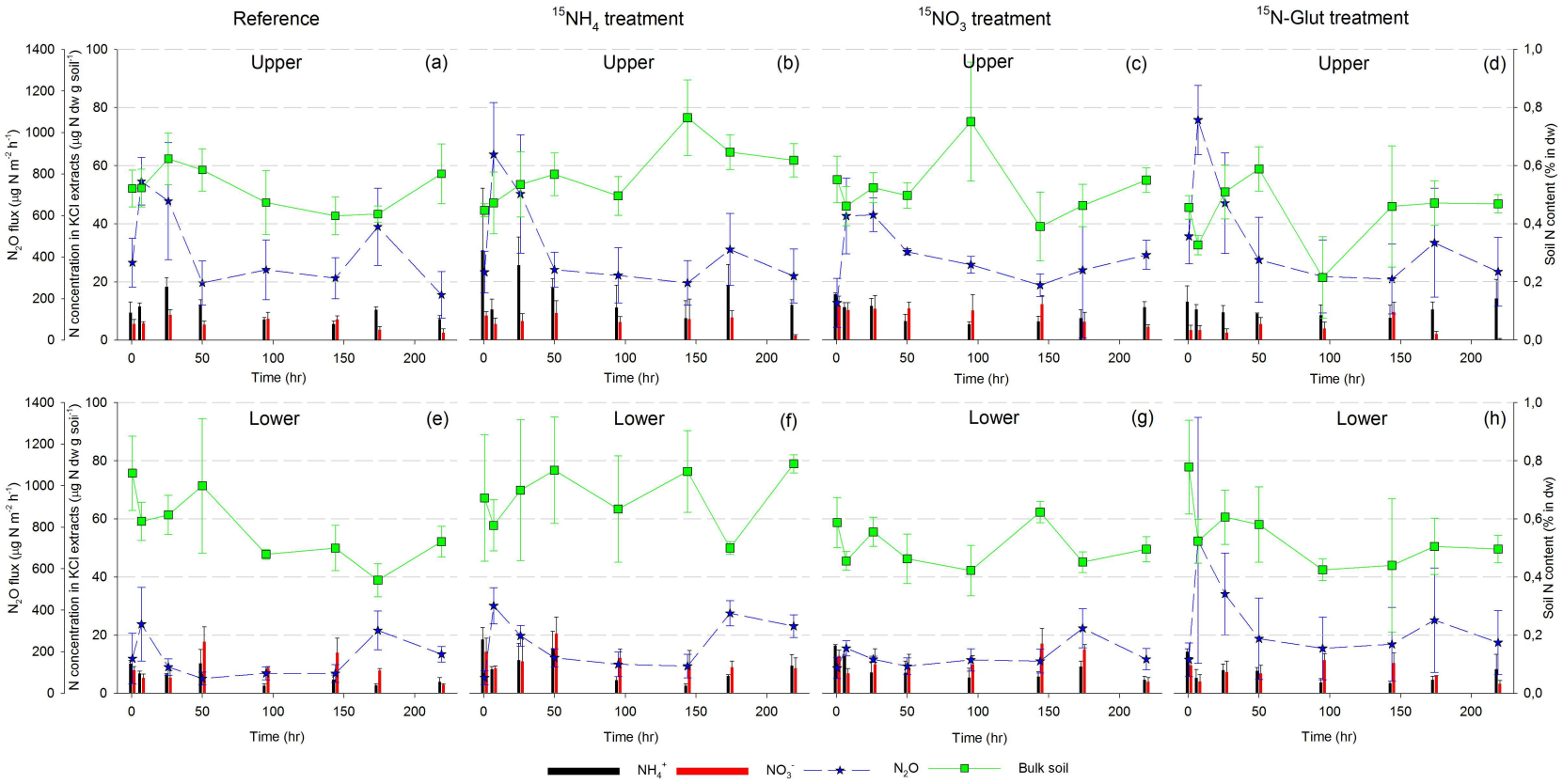

Fig. 3 (panels a to h)

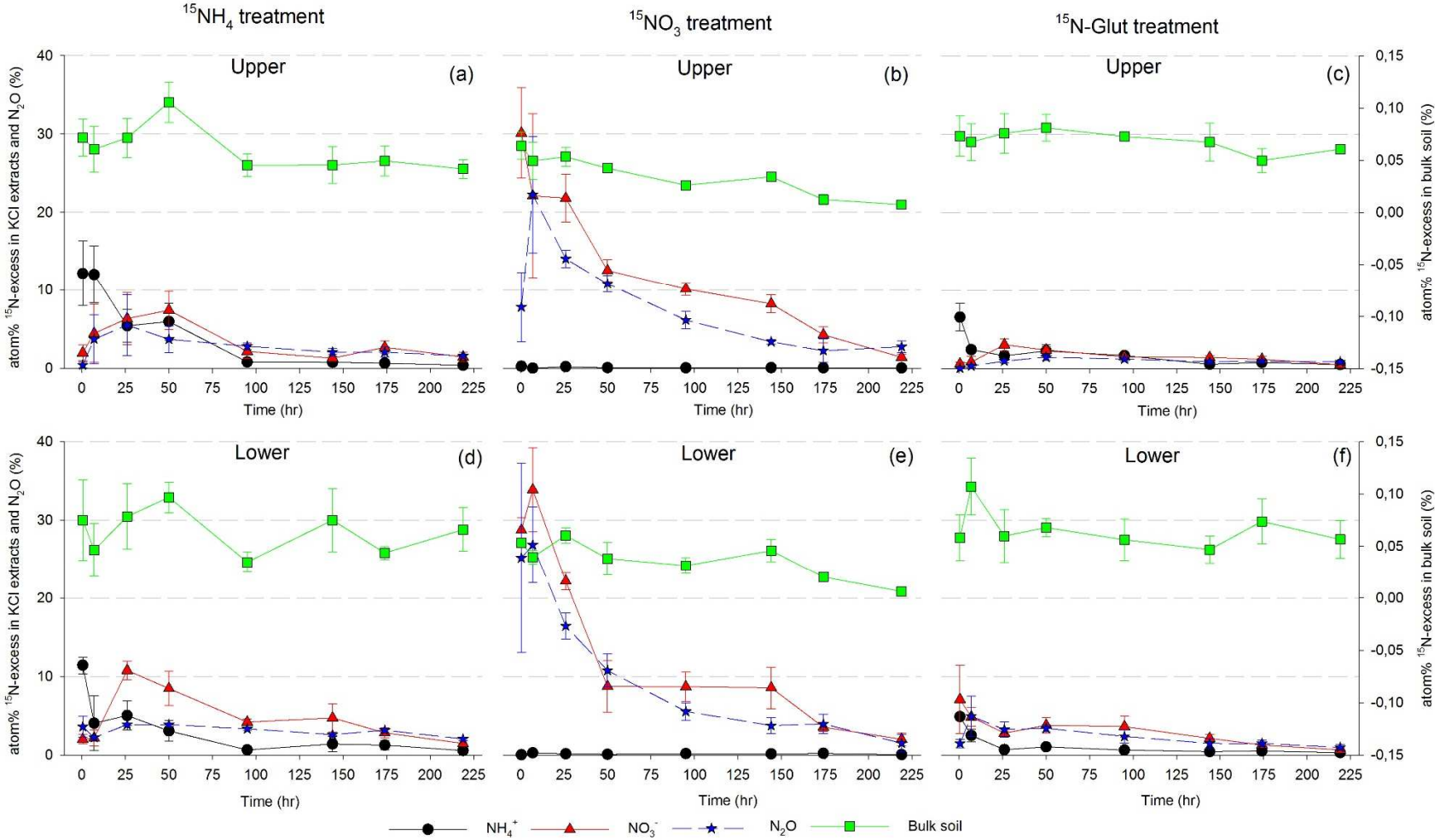

Fig. 4 (panels a to f)

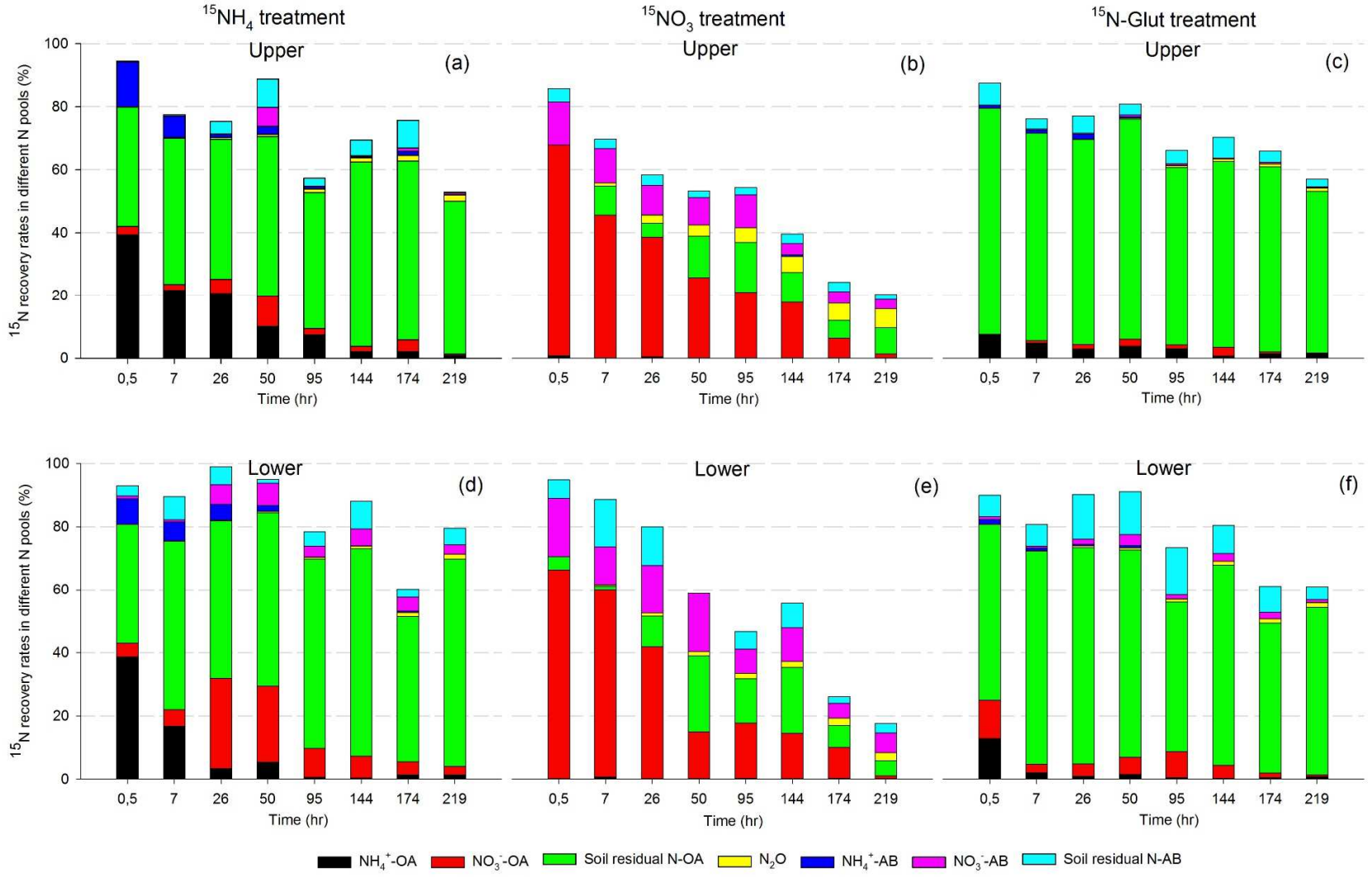

Fig. 5 (panels a to f)

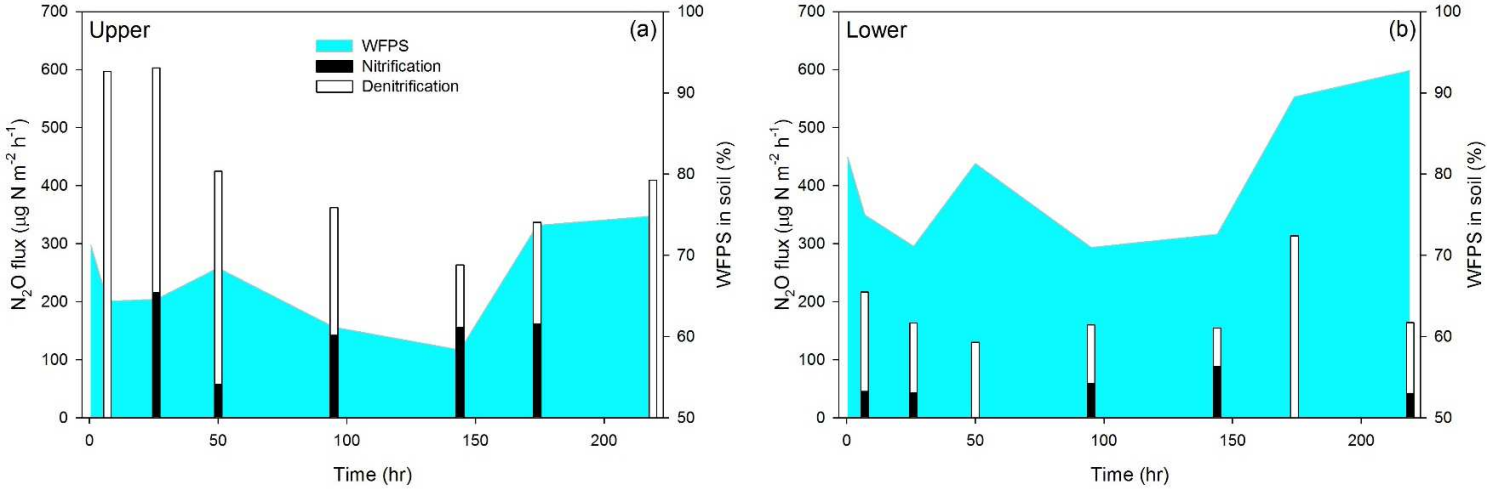
Upper
(a)
WFPS
Nitrification
Denitrification
N2O flux (µg N m-2 h-1)
WFPS in soil (%)
Time (hr)
Lower
(b)
N2O flux (µg N m-2 h-1)
WFPS in soil (%)
Time (hr)

Fig. 6a and **6b**

Distinct fates of atmogenic NH_4^+ and NO_3^- in subtropical, N-saturated forest soils

Longfei Yu[1], Ronghua Kang[1], Jan Mulder[1], Zhu Jing[1,2], Peter Dörsch[1†]

[1]Department of Environmental Sciences, Norwegian University of Life Sciences, Postbox 5003, N-1432 Aas, Norway.

[2]Department of Environment and Resources, Guangxi Normal University, 541004, Guilin, China.

[†]Correspondence: Peter Dörsch, tel. +47 67231836, e-mail: peter.doersch@nmbu.no

Article type**:** Original Article

Supplementary Material

Table S1

Figure S1-S4

Table S1 Comparison of estimated ^{15}N loss by NO_3^- leaching from the upper 0-15 cm of the soil to non-recovered ^{15}N in the $^{15}NO_3$ treatment during 144 hr. ^{15}N loss by NO_3^- leaching was estimated as $^{15}NO_3^-$ leaching (%) = atom% $^{15}N_{NO3}$ leached * NO_3^- concentration (mg L^{-1}) * water flux (L) / 1000 / amount of added ^{15}N (g). The atom% $^{15}N_{NO3}$ leached was estimated as the average atom% $^{15}N_{NO3}$ in the soil KCl extracts measured in the top O/A layer (0-5 cm), assuming that NO_3^- leached to the AB layer (5-15 cm) had the same atom% $^{15}N_{NO3}$ than the NO_3^- in the top layer. The average was calculated from measured values between 7 and 26 hr, as the dilution of ^{15}N signals in NO_3^- followed a non-linear curve (Figs. 4b&e). Concentrations of NO_3^- in the leachate were assumed to be stable in time (Fig. S2). The leachate volume was estimated from the change in volumetric soil moisture (10 cm) recorded between 0 and 144 hr, during which no rain (or new N input) occurred (Fig. 2b).

	P1, Upper site	P2, Lower site
Non-recovered ^{15}N (% of added ^{15}N)	45.0	40.0
Cumulative leached $^{15}NO_3^-$ (% of added ^{15}N)	27.8	21.2
Estimated atom% ^{15}N-excess of the leached NO_3^- (%)	25.0	28.0
Average NO_3^--N concentration in soil water (mg L^{-1})	10.7	11.5
Water loss by leaching and evapotranspiration (L)	14.9	9.50

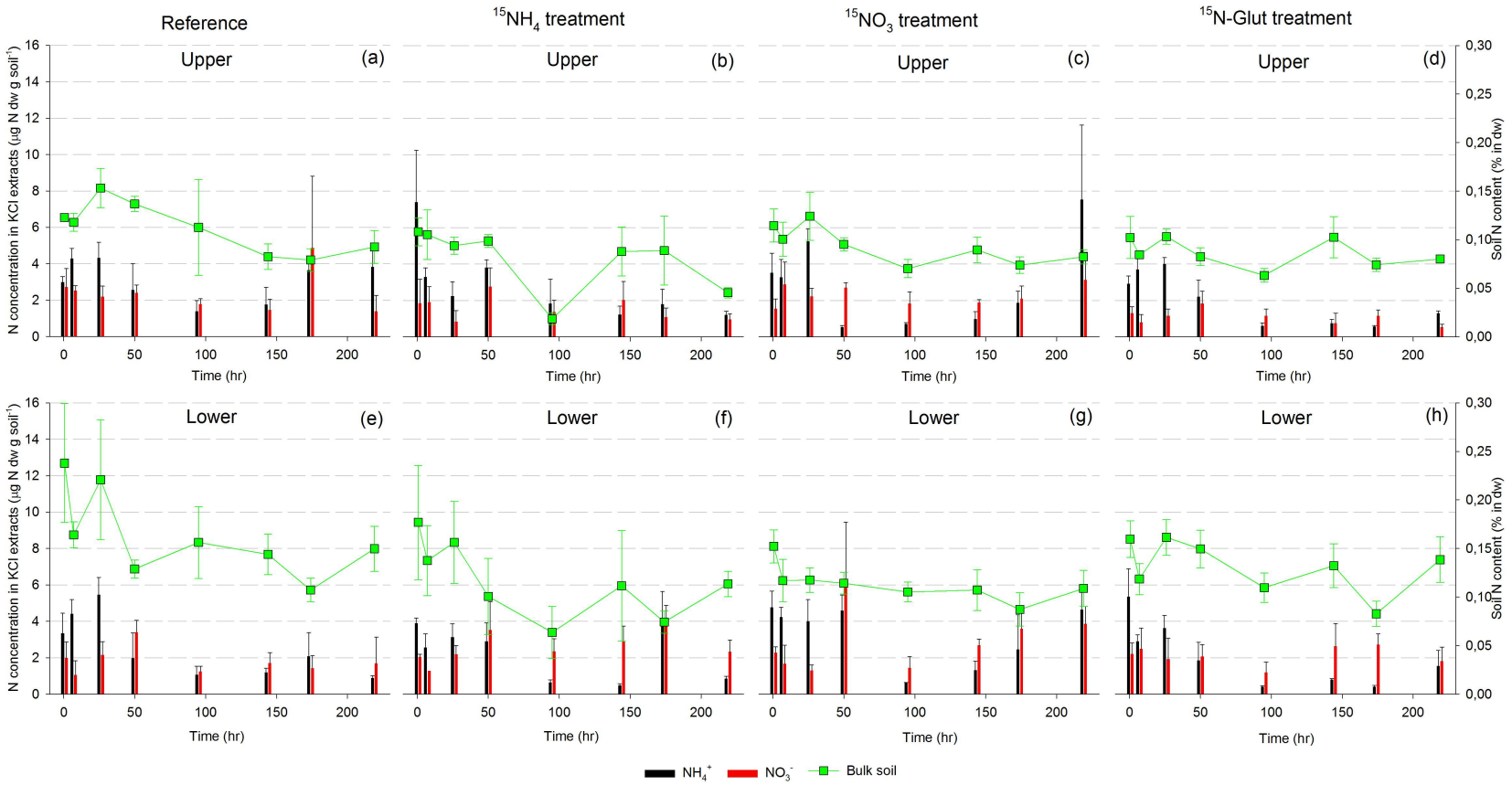

Fig. S1 Concentration of NH_4^+ and NO_3^- in KCl extracts (AB horizon) and total N content in bulk soil (AB horizon) for the Reference (panels a and e), $^{15}NH_4$ (panels b and f), $^{15}NO_3$ (panels c and g) and ^{15}N-Glut (panels d and h) treatments. Upper and lower panels refer to P1 (upper site) and P2 (lower site). Values are averages and standard errors (n = 3). The x-axis indicates the time after label application.

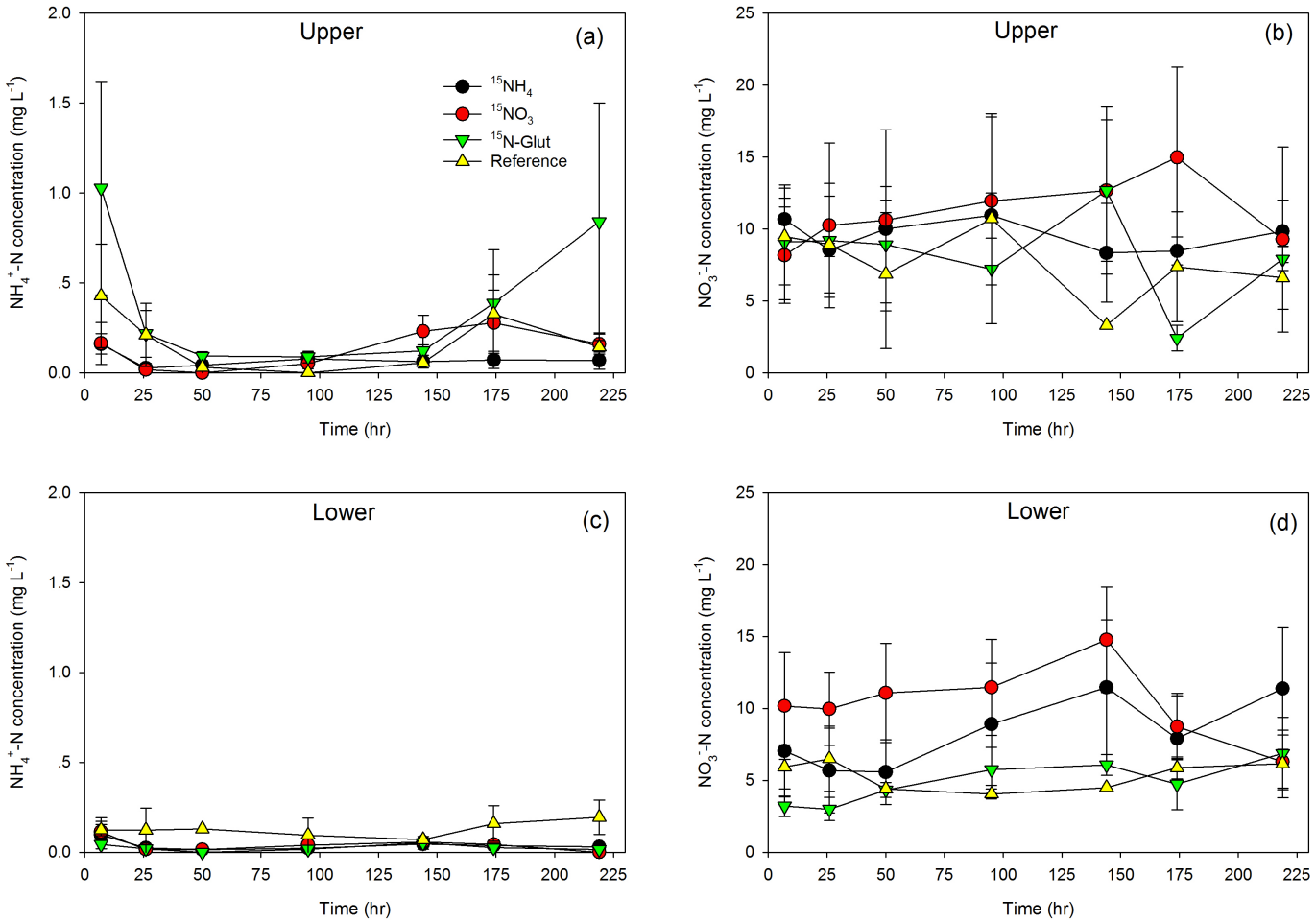

Fig. S2 Concentration of NH_4^+ (panels a and c) and NO_3^- (panels b and d) in lysimeter water from the O/A horizon at the upper (P1) and the lower (P2) site. Values are averages and standard errors (n = 3). The x-axis indicates the time after label application.

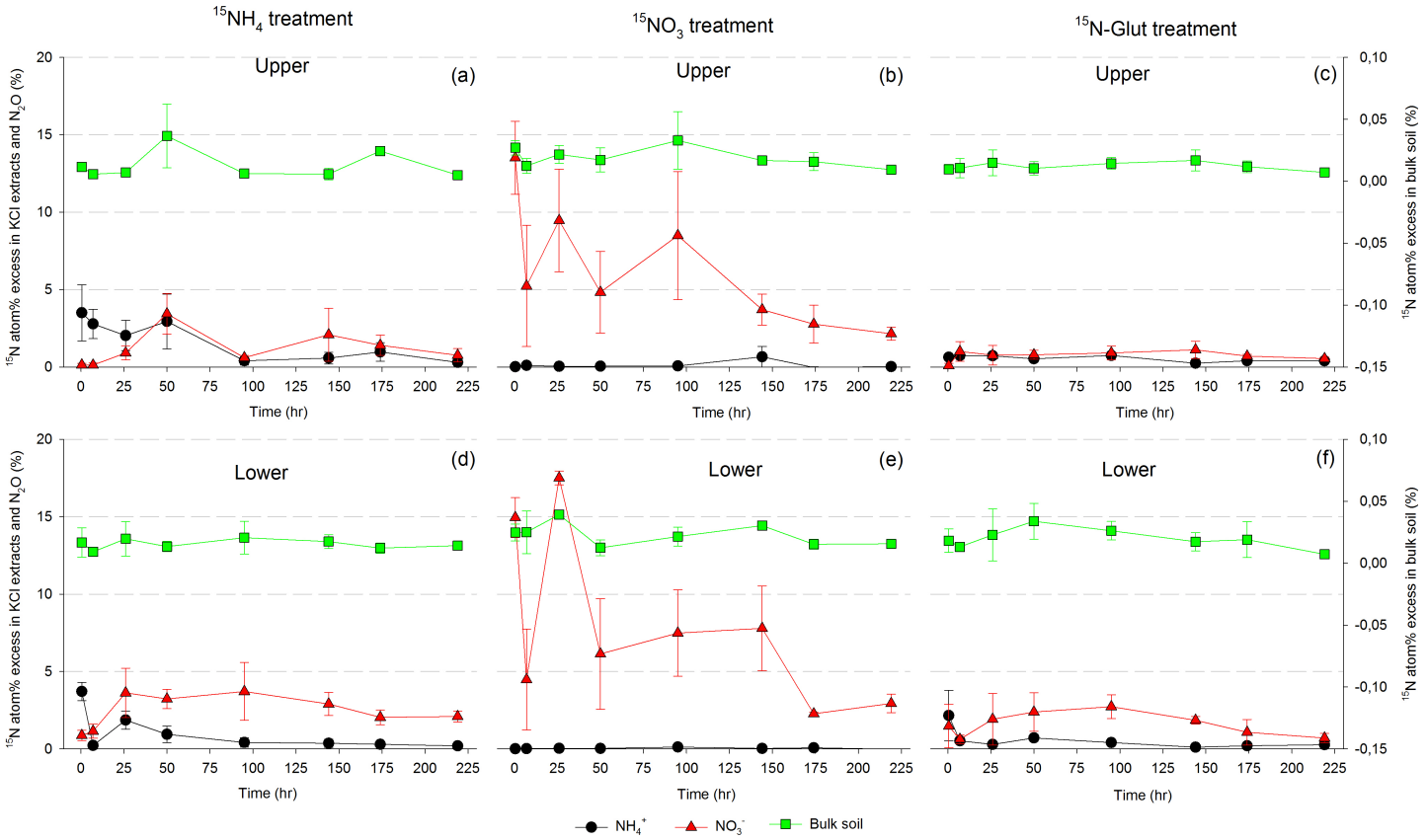

Fig. S3 Atom% ^{15}N-excess of NH_4^+ and NO_3^- in KCl extracts (AB horizon), and of total soil N (AB horizon) for the treatments $^{15}NH_4$ (panels a and d), $^{15}NO_3$ (panels b and e) and ^{15}N-Glut (panels c and f). Upper and lower panels refer to P1 (upper site) and P2 (lower site). Values are means and standard errors (n = 3). The x-axis indicates the time after label application.

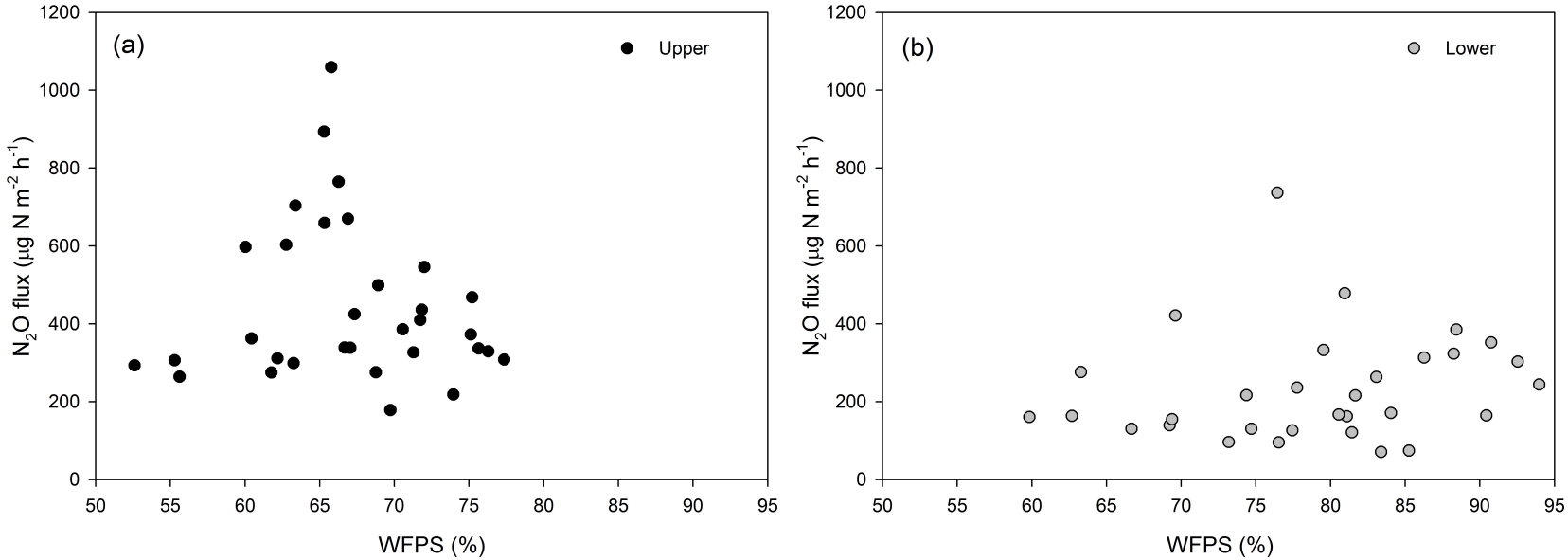

Fig. S4 Relationship between water filled pore space (WFPS) in soil and N_2O fluxes at the upper P1 site (panel a) and the lower P2 site (panel b). Values are means for 3 samplings per treatment.

Paper IV

Phosphorus addition mitigates N_2O and CH_4 emissions in N-saturated subtropical forest, SW China

Longfei Yu, Yihao Wang, Xiaoshan Zhang, Peter Dörsch, Jan Mulder

Manuscript to be submitted to Biogeosciences

Phosphorus addition mitigates N_2O and CH_4 emissions in N-saturated subtropical forest, SW China

Longfei Yu[1*], Yihao Wang[2, 3], Xiaoshan Zhang[3], Peter Dörsch[1], Jan Mulder[1]

[1]Department of Environmental Sciences, Norwegian University of Life Sciences, Postbox 5003, N-1432 Aas, Norway.

[2]Chongqing Academy of Forestry, 400036, Chongqing, China.

[3]Research Center for Eco-Environmental Sciences, Chinese Academy of Sciences, 100085, Beijing, China

[*]Correspondence: Longfei Yu, tel. +47 67231868, E-mail longfei.yu@nmbu.no

Abstract

Chronically elevated nitrogen (N) deposition has led to severe nutrient imbalance in forest soils. Particularly in tropical and subtropical forest ecosystems, increasing N loading has aggravated phosphorus (P) limitation of biomass production, and has resulted in elevated emission of nitrous oxide (N_2O) and reduced uptake of methane (CH_4), both of which are important greenhouse gases. Yet, the interactions of N and P and their effects on GHG emissions remain understudied. Here, we report N_2O and CH_4 emissions together with soil chemistry data for the a period of 18 months following P addition (79 kg P ha^{-1} yr^{-1}, applied as NaH_2PO_4 powder) to a N-saturated, Masson pine-dominated forest at TieShanPing (TSP), Chongqing, SW China. We observed a significant decline both in NO_3^- concentrations in soil water (at 5- and 20-cm depths) and in N_2O emissions, the latter by 3 kg N ha^{-1} yr^{-1}. We hypothesize that enhanced N uptake by plants and soil microbes in response to P addition, results in less available NO_3^- for denitrification. By contrast to most other forest ecosystems, TSP is a net source of CH_4. As for N_2O, P addition significantly decreased CH_4 emissions, turning the soil into a net sink. Based on our data and previous studies in South America and China, we believe that P addition relieves N-inhibition of CH_4 oxidation. Within the 1.5 years after P addition, no significant increase of forest growth was observed at TSP, but we cannot exclude that understory vegetation increased. Our study suggests that P fertilization of acid forest soils could mitigate GHG emissions in addition to alleviate nutrient imbalances and reduce losses of nitrogen through NO_3^- leaching and N_2O emission.

Key Word: N_2O and CH_4 emission, N saturation, Phosphate fertilization, soil CH_4 uptake, acid forest soil.

Introduction

Anthropogenic activities have transformed the terrestrial biosphere into a net source of CH_4, N_2O and CO_2, leading to increased radiative forcing (Montzka et al., 2011; Tian et al., 2016). During the last decade, atmospheric concentrations of CO_2, CH_4, N_2O have increased at rates of 1.9 ppm yr^{-1}, 4.8 and 0.8 ppb yr^{-1}, respectively (Hartmann et al., 2013). In China, the exponential increase of reactive nitrogen (N) input into the biosphere since the 1970s has likely led to more carbon (C) being sequestered in the biosphere (Cui et al., 2013; Shi et al., 2015). However, enhanced emissions of N_2O and CH_4 due to chronic N pollution potentially offset the cooling effect by C sequestration (Liu and Greaver, 2009; Tian et al., 2011).

Microbial nitrification and denitrification in soils account for about 60% of N_2O emissions globally (Ciais et al., 2013; Hu et al., 2015). Although, microbial activity is often restricted in low pH soils of unproductive forests, surprisingly large N_2O emissions have been reported from acid, upland forest soils in South China (Zhu et al., 2013b). Reported average N_2O fluxes in humid, subtropical forests range from 2.0 to 5.4 kg ha^{-1} yr^{-1} (Fang et al., 2009; Tang et al., 2006; Zhu et al., 2013b), which by far exceeds global averages for temperate or tropical forest ecosystems (Werner et al., 2007; Zhuang et al., 2012). This has been attributed to frequently shifting aeration conditions during monsoonal summers, promoting both nitrification and denitrification (Zhu et al., 2013b) and to large soil NO_3^- concentrations due to efficient cycling of deposited N in acid subtropical soils (Yu et al., 2016).

Chronically elevated rates of N deposition (30-65 kg ha^{-1} yr^{-1}; Xu et al., 2015) have resulted in strong nutrient imbalances in southern Chinese forests, aggravating phosphorus (P) limitation (Du et al., 2016). Phosphorous deficiency in N-saturated forests restricts forest growth and thus

53 constrains its capability to retain N (Huang et al., 2015; Li et al., 2016), resulting in ample amounts
54 of mineral N (NH_4^+ and NO_3^-) being present in the soil solution. Accordingly, Hall & Matson
55 (1999) observed larger N_2O emission in P-limited than in N-limited tropical forests after 1 year of
56 repeated N addition. Likewise, previous N manipulation studies in forests of South China reported
57 pronounced stimulation of N_2O emissions by N addition (Chen et al., 2016; Wang et al., 2014;
58 Zheng et al., 2016), supporting the idea that P limitation causes forests to be more susceptible to
59 N saturation and N_2O-N loss. In an N-limited tropical montane forest in southern Ecuador, P
60 addition alone (10 kg P ha^{-1} yr^{-1}) had no effect on N_2O emissions during the first two years.
61 However, N_2O emission was smaller when P was added together with N (50 kg N ha^{-1} yr^{-1}) than
62 treatments with N addition alone (Martinson et al., 2013). After continued fertilization for three
63 years, also P addition alone reduced N_2O emissions at these sites (Müller et al., 2015). In tropical
64 China, with high N deposition (~ 36 kg ha^{-1} yr^{-1}; Mo et al., 2008), P addition (150 kg P ha^{-1} yr^{-1})
65 to an old-growth forest revealed a similar pattern, with no initial effect on N_2O emissions (0-2
66 years) but a significant longer term effect (3 to 5 years) (Chen et al., 2016; Zheng et al., 2016). In
67 a secondary tropical forests in South China, Wang et al. (2014) found no effect on N_2O emissions
68 of P alone (100 kg P ha^{-1} yr^{-1}), and in treatments combining P with N (100 kg N ha^{-1} yr^{-1}), N_2O
69 emissions even increased during the wet season. Meanwhile, they observed a significant increase
70 in soil microbial biomass after P addition, which is in line with previous findings in tropical forest
71 soils of South China (Liu et al., 2012). Thus, they attributed the stimulating effect of P addition on
72 N_2O emissions to the larger nitrification and denitrification potential of the increased soil microbial
73 biomass. This was also proposed by Mori et al. (2014), based on results from a short-term
74 incubation study with P addition, excluding plant roots.

As the sole biogenic sink for CH_4, upland soils play an important role in balancing terrestrial CH_4 emissions (Ciais et al., 2013; Dutaur and Verchot, 2007). Atmospheric CH_4 uptake in soil is mediated by the activity of methanotrophic bacteria, which oxidize CH_4 to CO_2 to gain energy for growth. Well-drained forest and grassland soils are dominated by yet uncultured, high-affinity methanotrophs residing in the upper soil layers (Le Mer and Roger, 2010). In addition to edaphic factors (pH and nutrients), other parameters affecting the diffusion of CH_4 into the soil (soil structure, moisture, temperature) are believed to be the major controllers for CH_4 uptake (Smith et al., 2003). A number of studies have shown that excess N affects CH_4 fluxes in forest soils (Liu and Greaver, 2009; Veldkamp et al., 2013; Zhang et al., 2008b). In general, N addition promotes CH_4 uptake in N-limited soils by enhancing growth and activity of methanotrophs, whereas excessive N input and N saturation inhibit CH_4 oxidation on an enzymatic level (Aronson and Helliker, 2010; Bodelier and Laanbroek, 2004). P addition experiments in N-enriched soils have shown positive effects on CH_4 uptake (Mori et al., 2013a; Zhang et al., 2011), but the underlying mechanisms, i.e. whether P addition affects the methanotrophic community in soils directly or alleviates the N-inhibition effect on CH_4 oxidation through enhanced N uptake (Mori et al., 2013b; Veraart et al., 2015), remain unresolved.

Subtropical forests in South China show strong signs of N saturation, with exceedingly high NO_3^- concentrations in soil water (Larssen et al., 2011; Zhu et al., 2013b). Little is known about how P addition affects N cycling and N_2O emission in these acidic, nutrient-poor soils. Likewise, the importance of increased mineral N concentrations for soil-atmosphere exchange of CH_4, and how this is affected by P fertilization remain to be elucidated for soils of the subtropics. Here, we assessed N_2O and CH_4 fluxes in an N saturated subtropical forest in SW China under ambient N deposition and studied the effect of P addition on emission rates, nutrient availability and tree

98 growth. The objectives were i) to quantify ambient N_2O and CH_4 emissions, ii) to test whether P
99 affects N cycling in a highly N-saturated forest and iii) to investigate the effect of P addition on
100 N_2O and CH_4 emission.

Materials and Methods

Site description

The study site "TieShanPing" (TSP) is a 16.2 ha subtropical forest (29° 380 N, 106° 410 E; 450 m a.s.l.), about 25 km northeast of Chongqing, SW China. TSP is a naturally regenerated, secondary mixed coniferous-broadleaf forest, which developed after clear cutting in 1962 (Larssen et al., 2011). The forest stand is dominated by Masson pine (*Pinus massoniana*) and has a density of about 800 stems ha^{-1} (Huang et al., 2015). Having a monsoonal climate, TSP has a mean annual precipitation of 1028 mm, and a mean annual temperature of 18.2 ^{o}C (Chen and Mulder, 2007). Most of precipitation (> 70%) occurs during the summer period (April to September). The soil is a loamy yellow mountain soil, classified as Haplic Acrisol (WRB 2014), with a thin O horizon (< 2 cm). In the O/A horizon, soil pH is around 3.7, and the mean C/N and N/P ratios are 17 and 16, respectively. In the AB horizon, which has a slightly higher pH, mean C/N is well above 20. More details on soil properties are presented in Table 1.

Annual N deposition at TSP measured in throughfall varies between 40 to 65 kg ha^{-1} and is dominated by NH_4^+ (Yu et al., 2016). According to regional data, annual P deposition via throughfall is < 0.40 kg ha^{-1} (Du et al., 2016). Strong soil acidification at TSP has resulted in severe decline in forest growth (Li et al., 2014; Wang et al., 2007), and in abundance and diversity of ground vegetation (Huang et al., 2015). Pronounced N saturation with strong NO_3^- leaching from the top soil has aggravated P deficiency (Huang et al., 2015). The total P content in the O/A horizon is ~ 300 mg kg^{-1}, while P_{Al} is smaller than 5 mg kg^{-1} (Table 1).

Experimental Design

Three blocks, each having two 20 m * 20 m plots, were established near a hilltop on a gently sloping hillside. A 5-m buffer strip separated the two plots in each block. In each block, plots were assigned ad random to a reference (Ref) and a P treatment. On 4 May 2014, a single dose of P fertilizer was applied as solid $NaH_2PO_4{\cdot}2H_2O$, at a rate of 79.5 kg P ha^{-1}. The amount of P added was estimated from P adsorption isotherms (Supplementary Materials, Table S1 and Figure S1), to ensure significantly increased available P in TSP soil. To apply P fertilizer evenly, we divided each plot into a 5 m * 5 m grid and broadcasted the powdered fertilizer by hand in each grid cell. The P dose applied at TSP was intermediate as compared to the 10 kg P ha^{-1} yr^{-1} applied by Müller et al. (2015) to a mountain forest in Ecuador and the 150 kg P ha^{-1} yr^{-1} applied by Zheng et al. (2016) to a subtropical forest in South China.

Sample collection and analyses

Within each plot, triplicates of ceramic lysimeters (P80; Staatliche Porzellanmanufaktur, Berlin) were installed at 5- and 20-cm soil depths in August 2013. To obtain water samples, 350-ml glass bottles with rubber stoppers were pre-evacuated, using a paddle pump, and connected to the lysimeters for overnight sampling. Between November 2013 and October 2015, we sampled soil pore water bi-monthly in the winter season and monthly during the growing season. All water samples were kept frozen during storage and transport. Concentrations of NH_4^+, NO_3^-, potassium (K^+), calcium (Ca^{2+}), and magnesium (Mg^{2+}) in soil water were measured at the Research Center for Eco-Environmental Sciences (RCEES), Chinese Academy of Sciences, Beijing, using ion chromatography (DX-120 for cations and DX-500 for anions).

In August 2013, soils from the O/A (0- 3 cm), AB (3-8 cm) and B (8-20 cm) horizons were sampled near the lysimeters for soil analysis. Total P and plant-available P contents were monitored in

144 samples collected from the O/A horizons every six months, starting two days before P addition.
145 Soil samples were kept cold (< 4 ^{o}C) during transport and storage. Before analysis, soil samples
146 were air dried and sieved (2 mm). Soil pH was measured in soil suspensions (10 g dry soil and 50
147 ml deionized water) using a pH meter (PHB-4, Leici, China). Total soil C and N contents were
148 determined on dried and milled samples, using a LECO elemental analyzer (TruSpec$^{@}$CHN, USA).
149 To measure total P, 1 g dry soil was digested with 5 ml of 6 M H_2SO_4 (Singh et al., 2005) and
150 measured as ortho-phosphate by the molybdenum blue method (Murphy and Riley, 1962).
151 Ammonium lactate (0.01 M)-extractable P and H_2O-extractable P (P_{Al} and P_{H2O}, respectively) were
152 measured as ortho-phosphate after extraction (1.5 g dry soil in 50 ml solution) (Singh et al., 2005).
153 Ammonium oxalate (0.2 M)-extractable Fe, Al and P were measured by inductive coupled plasma
154 (7500; Agilent) after extraction (1.5 g dry soil in 50 ml solution).

155 From August 2013 onwards, we measured N_2O and CH_4 emissions in triplicate in micro-plots
156 close to the lysimeters, using static chambers (Zhu et al., 2013b). To investigate the immediate
157 effect of P addition on N_2O emissions, we sampled the gas emissions once before (2 May) and
158 three times (7, 10 and 12 May) after the P application. Gas samples (20 ml) were taken 1, 5, 15
159 and 30 minutes after chamber deployment and injected into pre-evacuated glass vials (12 ml)
160 crimp-sealed with butyl septa (Chromacol, UK), maintaining overpressure to avoid contamination
161 during sample transport. Mixing ratios of N_2O, CO_2 and CH_4 were analyzed using a gas
162 chromatograph (Model 7890A, Agilent, US) at RCEES, equipped with an ECD for detection of
163 N_2O (at 375 ^{o}C with 25 ml min^{-1} Ar/CH_4 as make up gas), a FID for CH_4 (250 ^{o}C; 20 ml min^{-1} N_2
164 as make-up gas) and a TCD for CO_2. Exchange rates between soil and atmosphere
165 (emission/uptake) were calculated from measured concentration change in the chambers over time,

applying linear or polynomial fits to the concentration data. Cumulative N_2O emissions over time were estimated by linear interpolation between measurement dates (Zhu et al., 2013b).

From October 2013 onwards, litterfall was collected during the first week of every month in five replicates per plot. Litterfall collectors were made of 1 m^2 nylon nets (1 mm mesh size), held in place by four wooden poles 0.8 m above the ground. Fresh litter was dried at 65^{o}C. In early November 2013 and 2014 (at the end of the growing season), we collected current-year pine needles from several branches of three trees in each plot. The collected needles were dried at 65 ^{o}C and the dry weight of 500 needles was determined. A subsample was dried at 80 ^{o}C and finely milled prior to chemical analysis at the Chinese Academy of Forestry. Total C and N were measured using an elemental analyzer (FLASH 2000; Thermo Scientific; USA). The contents of K, Ca, Mg and P in the needles were determined by ICP-AES (IRIS Intrepid II; Thermo Scientific; USA) after digesting 0.25 g dry weight samples with 5 ml of ultra-pure nitric acid. In November 2013, and 2014, and in February of 2015, we measured the height and the diameter at breast height (DBH) of 6 to 10 Masson pines (only those with DBH > 5 cm) at each plot. These data were used to estimate the standing biomass of Masson pines based on standard allometric equations (Li et al., 2011; Zeng et al., 2008).

Daily average air temperature and sum of precipitation were monitored by a weather station (WeatherHawk 232, USA) placed on the roof at the local forest bureau, in about 1 km distance from the sampling site (Yu et al., 2016).

Statistical analyses

Statistical analyses were performed with Minitab 16.2.2 (Minitab Inc., USA). All data were tested for normality (Kolmogorov-Smirnov's test) and homoscedasticity (Levene's test) before further

188 analysis. If not normally distributed, the data were then normalized by logarithmic transformation.
189 Due to heterogeneity between blocks, data on gas fluxes and mineral N concentrations are
190 presented separately for each block. One-way ANOVA was used to evaluate differences in gas
191 fluxes, as well as nutrient concentrations in soil, soil water and plants between treatments and
192 blocks. Significance levels were set to $p < 0.05$, if not specified otherwise.

193

Results

Nutrient concentrations in soil and soil water

Addition of P resulted in a significant increase in soil P content in the O/A horizon, both as P_{Al} and total P (Table 2). However, after 15 months, only P_{AL} indicated an enhanced P status, while total soil P did not differ significantly from background values at the reference sites. P addition had no significant effect on soil pH, or soil C and N content. The NO_3^- concentration in soil water collected at 5 cm depth varied seasonally, with significantly greater values (30-40 mg N L^{-1}) towards the start of the growing season (April, Fig. S2) in 2015, but not in 2014, likely due to dilution by abundant precipitation in February to March 2014. Addition of P resulted in significantly smaller NO_3^- concentrations in soil water at 5 and 20 cm depth in blocks 2 and 3 but not in block 1 (Fig. 1). In general, the concentration of NH_4^+ in soil water was small (< 0.6 mg L^{-1}) and not affected by P addition (Fig. S3). At both depths, mean soil water concentrations of Mg^{2+} and Ca^{2+} were significantly smaller in the P-treated than the reference plots, and the sum of charge of base cations declined significantly in response to P addition (Fig. S4).

N_2O and CH_4 fluxes: effects of P addition

During the experimental period, N_2O fluxes varied seasonally (Fig. 2), showing a significant relationship with daily precipitation (Fig. S5a), but not with daily mean temperature (Fig. S4b). In the reference plots, mean N_2O fluxes were generally below 50 μg N m^{-2} hr^{-1} in the dry, cool season, but reached up to 600 μg N m^{-2} hr^{-1} in the growing season (Fig. 2). Average and cumulative fluxes of N_2O differed greatly between the three blocks (Figs. 3 and 4, respectively), with the greatest annual emission observed in the reference plot (7.9 kg N ha^{-1}) of block 2. Mean N_2O fluxes during the 1.5 years after P addition were smaller in the P treatments than in the references, the differences

being significant in blocks 2 and 3 (Fig. 3). Cumulative N_2O emissions showed that P addition resulted in a decrease in N_2O emission by about 3 kg N ha^{-1} yr^{-1}, which is a 57% reduction on average (Fig. 4). No immediate effects (within days) of P addition on N_2O emission were observed (Fig. S6).

CH_4 fluxes varied greatly between blocks (Fig. 5). Net-emissions of CH_4 was observed in summer 2013 (~ 80 μg C m^{-2} hr^{-1}) in blocks 1 and 2, whereas block 3 showed CH_4 uptake. From spring 2014 until October 2015, CH_4 fluxes were less variable in all blocks, with values fluctuating around zero. A longer period of net-emission was observed in block 3 during the dry season 2014. The fluxes did not correlate with either precipitation or air temperature (Fig. S5c&d). In the 1.5 years following P addition, mean CH_4 fluxes indicated net CH_4 emission (~ +3.8 μg C m^{-2} hr^{-1}) in the reference plots (except for block 1), whereas net CH_4 uptake (~ -6.5 μg C m^{-2} hr^{-1}) was observed in all P- treated plots (Fig. 6). The suppressing effect of P addition on CH_4 emission was significant in blocks 2 and 3, similar to what was found for NO_3^- concentrations and N_2O fluxes.

The effect to P addition on tree growth

Throughout the 2-year experimental period, we observed no change in tree biomass (138 t ha^{-1}) in response to P addition (Table S2). Likewise, there was no effect of P treatment on the 500-needle weight (13 g on average). Between the two samplings in 2013 and 2014, we found differences in chemical composition of the pine needles, but this effect was not linked to P addition. Also, the C/N and N/P ratios of the needles (40 and 16, respectively) were hardly affected by P addition. Monthly litterfall varied seasonally (Fig. S7), but no significant difference was found between the reference and the P treated plots.

Discussion

Background N_2O emission rates in the reference plots were relatively large, with mean values of 40 to 120 μg N m^{-2} hr^{-1} (Fig. 3). This is within the range previously reported for well-drained hillslope soils at TSP (Zhu et al., 2013b), but greater than the rates reported for other forests in South China. For instance, N_2O emission rates averaged 37 μg N m^{-2} hr^{-1} in unmanaged sites at Dinghushan (Fang et al., 2009; Tang et al., 2006) and up to 50 μg N m^{-2} hr^{-1} in N-fertilized sites (Zhang et al., 2008a). TSP reference plots emitted on average 5.3 kg N ha^{-1} yr^{-1} (Fig. 4), which is about 10% of the annual N deposition (50 kg ha^{-1} yr^{-1}) (Huang et al., 2015). These fluxes were well above average fluxes reported for tropical rainforests (Werner et al., 2007). High N_2O emissions at TSP are likely due to the large N deposition rates (Huang et al. 2015), as suggested by the similar trends indicated by data from a wide range of ecosystems (Liu et al., 2009). Also, warm-humid conditions during monsoonal summers may stimulate N_2O emissions (Ju et al., 2011), as monsoonal rainstorms triggered peak fluxes (Fig. S5a) (Pan et al., 2003). The positive correlation between precipitation and N_2O emission peaks may indicate the importance of denitrification as the dominant N_2O source. This is supported by recent ^{15}N tracing experiments at TSP (Zhu et al., 2013a; Yu et al., submitted).

Addition of P caused a significant decline in soil mineral N (predominantly NO_3^-) in two of three blocks (Fig. 2), particularly during summers, when NO_3^- concentrations were relatively high (Fig. S2). At the same time, annual N_2O emissions decreased by more than 50% (Figs. 3 and 4). These findings are consistent with a number of previous studies (Baral et al., 2014; Hall and Matson, 1999; Mori et al., 2014). The reduction of N_2O emissions in P treated soils was attributed to decreased mineral N content, most likely due to stimulated plant uptake and/or microbial

assimilation. It is noteworthy, however, that there was no significant correlation between N_2O emission rates and soil water NO_3^- concentration in our study (Figs. 2 and S2), suggesting that the suppressing effect of P on N_2O emissions was indirect, probably by affecting the competition for mineral N between plant roots and microbes (Zhu et al., 2016). In contrast to our study, P-addition experiments in South Ecuador (Martinson et al., 2013) and South China (at Dinghushan Biosphere Reserve (DHSBR); Zheng et al., 2016) found no effect of a single P addition on N_2O emission during the first two years after application. However, significant reduction in N_2O emission was observed after three to five years with continuous P addition, both at the Ecuadorian and the Chinese site (Chen et al., 2016; Müller et al., 2015). For the montane forest site in Ecuador, the observed delay in N_2O emission response to P addition may be explained by the moderate amount of P added (10 kg P ha^{-1} yr^{-1}; Martinson et al., 2013). Moreover, the experiments were conducted in a forest with low ambient N deposition (~ 10 kg N ha^{-1} yr^{-1}) and N_2O fluxes (~ 0.36 kg N ha^{-1} yr^{-1} in the reference plot) (Martinson et al., 2013; Müller et al., 2015). By contrast, the DHSBR site in South China receives 36 kg of atmogenic N ha^{-1} yr^{-1}, which is only slightly smaller than the N deposition at our site (Huang et al., 2015), and showed larger N_2O emission rate than the Ecuadorian site (~ 0.88 kg N ha^{-1} yr^{-1} in the reference plot; Zheng et al., 2016). However, forests do not always display a straightforward relationship between N deposition and N_2O emissions. Manipulation experiments in the European NITREX project, for instance, revealed a much stronger correlation of N_2O emissions with soil NO_3^- leaching than with N deposition (Gundersen et al., 2012). Indeed, KCl-extractable mineral N at the DHSBR site (~ 40 mg kg^{-1}; Zheng et al., 2016) were several-fold smaller than at our site (> 100 mg kg^{-1}; Zhu et al., 2013b), indicating that DHSBR is less N-saturated than TSP. This suggests that the response of N_2O emission to P addition might depend on the N status of the soil. The fact that numerous studies found apparent

suppression of N_2O emission in short-term experiments (< 2 years) in N + P treatments, but not in treatments with P alone, supports this idea (Müller et al., 2015; Zhang et al., 2014b; Zheng et al., 2016).

Other studies have observed increased N_2O emissions upon P addition (Mori et al., 2013c; Wang et al., 2014). In an *Acacia mangium* plantation, fertilized with P, Mori et al. (2013b&c) found that N_2O emissions were stimulated in the short-term but reduced in the long-term. While suppression of N_2O emission by P has been attributed to increased plant N uptake (Mori et al., 2014), increased N_2O emission are generally explained by enhanced microbial biomass (Liu et al., 2012) and denitrification activities (Ehlers et al., 2010; He and Dijkstra, 2015). N_2O emissions measured frequently after P addition at our site in May 2014 were not different from fluxes in untreated reference plots (Fig. S5). This may indicate that plant uptake at TSP is more important for the effect of P addition on N_2O emissions than changes in microbial activity, which are expected to occur more rapidly.

Two of three reference plots at TSP showed net CH_4 emission for extended periods of the year (Figs. 5 and 6). Also, long-term CH_4 fluxes sampled between 2012 and 2014 on TSP hillslopes near-by (Fig. S8; Zhu et al., unpublished data) showed net CH_4 emission. This is in contrast to the generally reported CH_4 sink function of forested upland soils (Ciais et al., 2013; Dutaur and Verchot, 2007). For example, CH_4 uptake rates reported for South Chinese forest soils range from 30 to 60 μg C m^{-2} hr^{-1} (Fang et al., 2009; Tang et al., 2006; Zhang et al., 2014a). As CH_4 fluxes at our sites were not correlated with climatic factors (Fig. S5c and d), CH_4 emissions cannot be explained by transitory wet conditions. One reason for the net-CH_4 emission observed at TSP could be inhibition of CH_4 oxidation activity by NH_4^+, as reported previously (Bodelier and Laanbroek, 2004; Zhang et al., 2014a). The concentration of NH_4^+ in the soil water was rather small (< 0.5 g

306 L^{-1}; Fig. S3), which does not preclude, however, that NH_4^+ availability from the soil exchangeable
307 pool is high. Zhu et al. (2013b) found extraordinarily high KCL-extractable NH_4^+ in TSP surface
308 soils, likely reflecting the large atmogenic NH_4^+ input at our site (Huang et al., 2015).

309 P addition had a significant impact on CH_4 fluxes, changing the soil from a net source to a net sink
310 on an annual basis (Fig. 6). However, the uptake rates of CH_4 in the P treatments remained smaller
311 than those reported for forest soils in tropical China (Tang et al., 2006; Zhang et al., 2008b). The
312 stimulating effect of P addition on CH_4 uptake is consistent with previous studies (Mori et al.,
313 2013a, 2013b; Zhang et al., 2011), and has been attributed to lessening the NH_4^+ inhibition of
314 methane oxidation. Unfortunately, we did not measure KCl-extractable NH_4^+ in our study, but a
315 decline of available NH_4^+, which is the substrate for nitrification, is likely as NO_3^- concentrations
316 in soil water were significantly smaller with in the P-treatments (Fig. 2). P addition may also result
317 in a change of the taxonomic composition of the methane oxidizing community (Mori et al., 2013a;
318 Veraart et al., 2015). Alternatively, CH_4 oxidation may be stimulated by increased CH_4 diffusion
319 into the soil, due to enhanced root growth and increased transpiration in P-amended plots (Zhang
320 et al., 2011). Given the high degree of N saturation of TSP forest (Huang et al., 2015), it is likely
321 that the reason for the observed reduction in CH_4 emissions in response to P fertilization was due
322 to alleviating the NH_4^+ inhibition of the methane monooxygenase enzyme (Veldkamp et al., 2013),
323 rather than a direct P-stimulation of methanotrophic activity (Veraart et al., 2015).

324 P application significantly increased plant-available P in the P-limited TSP soil (Table 2).
325 Meanwhile, concentrations of leachable base cations (K^+, Mg^{2+}, Ca^{2+}) in soil water decreased (Fig.
326 S4), as expected from the reduction of NO_3^- concentrations in the P-treatments (Mochoge and
327 Beese, 1986). We observed no sign of stimulated forest growth or increased N uptake by plants
328 within the relatively short period of our study (Table S2 and Fig. S7), which makes it difficult to

329 link the observed reduction in mineral N in the soil solution to plant growth (Fig. 2). When
330 interpreting the observed P effect on NO_3^- concentrations in soil water, several aspects need to be
331 considered. Firstly, two years of observation may be too short to detect any significant NO_3^- uptake
332 by plants, given the commonly large variabilities in tree biomass estimates (Alvarez-Clare et al.,
333 2013; Huang et al., 2015). Secondly, we might have overlooked the contribution to N uptake by
334 understory biomass, which has previously been reported to quickly respond to P addition
335 (Fraterrigo et al., 2011). Thirdly, as long-term N saturation and acidification at TSP has reduced
336 the forest health (Lu et al., 2010; Wang et al., 2007), we may not expect immediate response of
337 forest growth to P addition. Large needle N/P ratios (17-22, Table S2) indicated that P limitation
338 for tree growth was not relieved 1.5 years after P addition (Li et al., 2016). Therefore, enhanced N
339 uptake by understory growth and/or soil microbial biomass may have been the main mechanisms
340 responsible for observed NO_3^- decline in the P-treated soil (Hall & Matson 1999).

341 Overall, our study demonstrates that chronically high N deposition has transformed TSP soils to a
342 regional hotspot for N_2O and CH_4 emission. Within the short experimental period of 1.5 years,
343 P fertilization was shown to significantly decrease NO_3^- concentrations in soil water and to reduce
344 both N_2O and CH_4 emissions. These findings provide a promising starting point for improving
345 forest management towards GHG abatement targets, taking into account the P and N status of
346 impoverished subtropical soils in the region.

Acknowledgement

Longfei Yu thanks the China Scholarship Council (CSC) for supporting his PhD study. Support from the Norwegian Research Council to project 209696/E10 'Forest in South China: an important sink for reactive nitrogen and a regional hotspot for N_2O?' is gratefully acknowledged. We thank Prof. Wang Yanhui, Prof. Duan Lei, Dr. Wang Zhangwei, Zhang Yi, Zhang Ting, Zou Mingquan for their help during sample collection and data analysis. Dr. Zhu Jing is gratefully acknowledged for unpublished data on long-term CH_4 fluxes in the TSP catchment.

Reference

Alvarez-Clare, S., Mack, M. C. and Brooks, M.: A direct test of nitrogen and phosphorus limitation to net primary productivity in a lowland tropical wet forest, Ecology, 94(7), 1540–1551, 2013.

Anon: World Reference Base for Soil Resources 2014, FAO, Rome., 2014.

Aronson, E. L. and Helliker, B. R.: Methane flux in non-wetland soils in response to nitrogen addition: A meta-analysis, Ecology, 91(11), 3242–3251, doi:10.1890/09-2185.1, 2010.

Baral, B. R., Kuyper, T. W. and Van Groenigen, J. W.: Liebig's law of the minimum applied to a greenhouse gas: Alleviation of P-limitation reduces soil N_2O emission, Plant Soil, 374(1–2), 539–548, doi:10.1007/s11104-013-1913-8, 2014.

Bodelier, P. L. E. and Laanbroek, H. J.: Nitrogen as a regulatory factor of methane oxidation in soils and sediments, FEMS Microbiol. Ecol., 47(3), 265–277, doi:10.1016/S0168-6496(03)00304-0, 2004.

Chen, H., Gurmesa, G. A., Zhang, W., Zhu, X., Zheng, M., Mao, Q., Zhang, T. and Mo, J.: Nitrogen saturation in humid tropical forests after 6 years of nitrogen and phosphorus addition: Hypothesis testing, Funct. Ecol., 30(2), 305–313, doi:10.1111/1365-2435.12475, 2016.

Chen, X. and Mulder, J.: Indicators for nitrogen status and leaching in subtropical forest ecosystems, South China, Biogeochemistry, 82(2), 165–180, doi:10.1007/s10533-006-9061-3, 2007.

Ciais, P., Sabine, C., Bala, G., Bopp, L., Brovkin, V., Canadell, J., Chhabra, A., DeFries, R., Galloway, J., Heimann, M., Jones, C., Quéré, C. Le, Myneni, R. B., Piao, S. and Thornton, P.: Carbon and Other Biogeochemical Cycles. In: Climate Change 2013: The Physical Science Basis., edited by T.F., D. Qin, G.-K. Plattner, M. Tignor, S.K. Allen, J. Boschung, A. Nauels, Y. Xia, V. B. and P. M. M. Stocker, Cambridge University Press, Cambridge, United Kingdom and New York, NY, USA., 2013.

Cui, S., Shi, Y., Groffman, P. M., Schlesinger, W. H. and Zhu, Y.-G.: Centennial-scale analysis of the creation and fate of reactive nitrogen in China (1910-2010), Proc. Natl. Acad. Sci. U. S. A., 110(6), 2052–7, doi:10.1073/pnas.1221638110, 2013.

Du, E., de Vries, W., Han, W., Liu, X., Yan, Z. and Jiang, Y.: Imbalanced phosphorus and nitrogen deposition in China's forests, Atmos. Chem. Phys., (16), 8571–8579, doi:10.5194/acp-2015-984, 2016.

Dutaur, L. and Verchot, L. V.: A global inventory of the soil CH_4 sink, Global Biogeochem. Cycles, 21(4), 1–9, doi:10.1029/2006GB002734, 2007.

Ehlers, K., Bakken, L. R., Frostegård, Å., Frossard, E. and Bünemann, E. K.: Phosphorus limitation in a Ferralsol: Impact on microbial activity and cell internal P pools, Soil Biol. Biochem., 42, 558–566, doi:10.1016/j.soilbio.2009.11.025, 2010.

Fang, Y., Gundersen, P., Zhang, W., Zhou, G., Christiansen, J. R., Mo, J., Dong, S. and Zhang,

391 T.: Soil–atmosphere exchange of N_2O, CO_2 and CH_4 along a slope of an evergreen broad-leaved
392 forest in southern China, Plant Soil, 319(1–2), 37–48, doi:10.1007/s11104-008-9847-2, 2009.

393 Fraterrigo, J. M., Strickland, M. S., Keiser, A. D. and Bradford, M. A.: Nitrogen uptake and
394 preference in a forest understory following invasion by an exotic grass, Oecologia, 167(3), 781–
395 791, doi:10.1007/s00442-011-2030-0, 2011.

396 Gundersen, P., Christiansen, J. R., Alberti, G., Brüggemann, N., Castaldi, S., Gasche, R., Kitzler,
397 B., Klemedtsson, L., Lobo-Do-Vale, R., Moldan, F., Rütting, T., Schleppi, P., Weslien, P. and
398 Zechmeister-Boltenstern, S.: The response of methane and nitrous oxide fluxes to forest change
399 in Europe, Biogeosciences, 9(10), 3999–4012, doi:10.5194/bg-9-3999-2012, 2012.

400 Hall, S. J. and Matson, P. A.: Nitrogen oxide emissions after nitrogen additions in tropical
401 forests, Nature, 400(July), 152, doi:10.1038/22094, 1999.

402 Hartmann, D. J., Klein Tank, A. M. G., Rusticucci, M., Alexander, L. V, Brönnimann, S.,
403 Charabi, Y. A.-R., Dentener, F. J., Dlugokencky, E. J., Easterling, D. R., Kaplan, A., Soden, B.
404 J., Thorne, P. W., Wild, M. and Zhai, P.: Observations: Atmosphere and Surface, In: Climate
405 Change 2013: The Physical Science Basis., edited by T.F., D. Qin, G.-K. Plattner, M. Tignor,
406 S.K. Allen, J. Boschung, A. Nauels, Y. Xia, V. B. and P. M. M. Stocker, Cambridge University
407 Press, Cambridge, United Kingdom and New York, NY, USA., 2013.

408 He, M. and Dijkstra, F. A.: Phosphorus addition enhances loss of nitrogen in a phosphorus-poor
409 soil, Soil Biol. Biochem., 82, 99–106, doi:10.1016/j.soilbio.2014.12.015, 2015.

410 Hu, H. W., Chen, D. and He, J. Z.: Microbial regulation of terrestrial nitrous oxide formation:
411 Understanding the biological pathways for prediction of emission rates, FEMS Microbiol. Rev.,
412 39(5), 729–749, doi:10.1093/femsre/fuv021, 2015.

413 Huang, Y., Kang, R., Mulder, J., Zhang, T. and Duan, L.: Nitrogen saturation, soil acidification,
414 and ecological effects in a subtropical pine forest on acid soil in southwest China, J. Geophys.
415 Res. Biogeosciences, 120, 2457–2472, doi:10.1002/2015JG003048.Received, 2015.

416 Ju, X., Lu, X., Gao, Z., Chen, X., Su, F., Kogge, M., Römheld, V., Christie, P. and Zhang, F.:
417 Processes and factors controlling N_2O production in an intensively managed low carbon
418 calcareous soil under sub-humid monsoon conditions, Environ. Pollut., 159(4), 1007–1016,
419 doi:10.1016/j.envpol.2010.10.040, 2011.

420 Larssen, T., Duan, L. and Mulder, J.: Deposition and leaching of sulfur, nitrogen and calcium in
421 four forested catchments in China: implications for acidification, Environ. Sci. Technol., 45(4),
422 1192–8, doi:10.1021/es103426p, 2011.

423 Li, Y., Niu, S. and Yu, G.: Aggravated phosphorus limitation on biomass production under
424 increasing nitrogen loading: A meta-analysis, Glob. Chang. Biol., 22(2), 934–943,
425 doi:10.1111/gcb.13125, 2016.

426 Li, Z., Wang, Y., Liu, Y., Guo, H., Li, T., Li, Z. H. and Shi, G.: Long-term effects of liming on
427 health and growth of a Masson pine stand damaged by soil acidification in Chongqing, China,
428 PLoS One, 9(4), 1–9, doi:10.1371/journal.pone.0094230, 2014.

429 Li, Z., Yu, P., Y., W., Li, Z., Y., W. and Du, A.: Charcters of Litter-Fall in Damaged Pinus
430 massoniana Forests and Its Responses to Environmental Factors in the Acid Rain Region of

Chongqing, China, Sci. Silvae Sin., 47(8), 19–24, 2011.

Liu, L. and Greaver, T. L.: A review of nitrogen enrichment effects on three biogenic GHGs: The CO_2 sink may be largely offset by stimulated N_2O and CH_4 emission, Ecol. Lett., 12(10), 1103–1117, doi:10.1111/j.1461-0248.2009.01351.x, 2009.

Liu, L., Gundersen, P., Zhang, T. and Mo, J.: Effects of phosphorus addition on soil microbial biomass and community composition in three forest types in tropical China, Soil Biol. Biochem., 44(1), 31–38, doi:10.1016/j.soilbio.2011.08.017, 2012.

Lu, X., Mo, J., Gilliam, F. S., Zhou, G. and Fang, Y.: Effects of experimental nitrogen additions on plant diversity in an old-growth tropical forest, Glob. Chang. Biol., 16(10), 2688–2700, doi:10.1111/j.1365-2486.2010.02174.x, 2010.

Martinson, G. O., Corre, M. D. and Veldkamp, E.: Responses of nitrous oxide fluxes and soil nitrogen cycling to nutrient additions in montane forests along an elevation gradient in southern Ecuador, Biogeochemistry, 112(1–3), 625–636, doi:10.1007/s10533-012-9753-9, 2013.

Le Mer, J. and Roger, P.: Production, oxidation, emission and consumption of methane by soils: A review, Eur. J. Soil Biol., 37(2001), 2010.

Mo, J., Li, D. and Gundersen, P.: Seedling growth response of two tropical tree species to nitrogen deposition in southern China, Eur. J. For. Res., 127(4), 275–283, doi:10.1007/s10342-008-0203-0, 2008.

Mochoge, B. O. and Beese, F.: Leaching of plant nutrients from an acid forest soil after nitrogen fertilizer application Audies on the leaching o f plant nutrients from soils after nitrogen, 91, 17–29, 1986.

Montzka, S. A., Dlugokencky, E. J. and Butler, J. H.: Non-CO_2 greenhouse gases and climate change, Nature, 476(7358), 43–50, doi:10.1038/nature10322, 2011.

Mori, T., Ohta, S., Ishizuka, S., Konda, R., Wicaksono, A. and Heriyanto, J.: Effects of phosphorus application on CH_4 fluxes in an Acacia mangium plantation with and without root exclusion, Tropics, 22(1), 13–17, 2013a.

Mori, T., Ohta, S., Ishizuka, S., Konda, R., Wicaksono, A. and Heriyanto, J.: Phosphorus application reduces N_2O emissions from tropical leguminous plantation soil when phosphorus uptake is occurring, Biol. Fertil. Soils, 50(1), 45–51, doi:10.1007/s00374-013-0824-4, 2014.

Mori, T., Ohta, S., Ishizuka, S., Konda, R., Wicaksono, A., Heriyanto, J., Hamotani, Y., Gobara, Y., Kawabata, C., Kuwashima, K., Nakayama, Y. and Hardjono, A.: Soil greenhouse gas fluxes and C stocks as affected by phosphorus addition in a newly established Acacia mangium plantation in Indonesia, For. Ecol. Manage., 310, 643–651, doi:10.1016/j.foreco.2013.08.010, 2013b.

Mori, T., Ohta, S., Ishizuka, S., Konda, R., Wicaksono, A., Heriyanto, J. and Hardjono, A.: Effects of phosphorus addition with and without ammonium, nitrate, or glucose on N_2O and NO emissions from soil sampled under Acacia mangium plantation and incubated at 100 % of the water-filled pore space, Biol. Fertil. Soils, 49(1), 13–21, doi:10.1007/s00374-012-0690-5, 2013c.

Müller, A. K., Matson, A. L., Corre, M. D. and Veldkamp, E.: Soil N_2O fluxes along an

elevation gradient of tropical montane forests under experimental nitrogen and phosphorus addition, Front. Earth Sci., 3(October), 1–12, doi:10.3389/feart.2015.00066, 2015.

Murphy, J. and Riley, J. P.: A modified single method for the determination of phosphate in natural waters, Anal. Chim. Acta, 27(27), 31–36, doi:10.1016/S0003-2670(00)88444-5, 1962.

Pan, F., Peters-Lidard, C. D. and Sale, M. J.: An analytical method for predicting surface soil moisture from rainfall observations, Water Resour. Res., 39(11), 1314, doi:10.1029/2003WR002142, 2003.

Shi, Y., Cui, S., Ju, X., Cai, Z. and Zhu, Y.: Impacts of reactive nitrogen on climate change in China, Sci. Rep., 5, 8118, doi:10.1038/srep08118, 2015.

Singh, B. R., Krogstad, T., Shivay, Y. S., Shivakumar, B. G. and Bakkegard, M.: Phosphorus fractionation and sorption in P-enriched soils of Norway, Nutr. Cycl. Agroecosystems, 73(2–3), 245–256, doi:10.1007/s10705-005-2650-z, 2005.

Smith, K. a., Ball, T., Conen, F., Dobbie, K. E., Massheder, J. and Rey, A.: Exchange of greenhousegases between soil and atmosphere: interactions of soil physical factors and biological processes, Eur. J. Soil Sci., 54(December), 779–791, doi:10.1046/j.1365-2389.2003.00567.x, 2003.

Tang, X., Liu, S., Zhou, G., Zhang, D. and Zhou, C.: Soil-atmospheric exchange of CO_2, CH_4, and N_2O in three subtropical forest ecosystems in southern China, Glob. Chang. Biol., 12(3), 546–560, doi:10.1111/j.1365-2486.2006.01109.x, 2006.

Tian, H., Lu, C., Ciais, P., Michalak, A. M., Canadell, J. G., Saikawa, E., Huntzinger, D. N., Gurney, K. R., Sitch, S., Zhang, B., Yang, J., Bousquet, P., Bruhwiler, L., Chen, G., Dlugokencky, E., Friedlingstein, P., Melillo, J., Pan, S., Poulter, B., Prinn, R., Saunois, M., Schwalm, C. R. and Wofsy, S. C.: The terrestrial biosphere as a net source of greenhouse gases to the atmosphere, Nature, 531(7593), 225–228, doi:10.1038/nature16946, 2016.

Tian, H., Xu, X., Lu, C., Liu, M., Ren, W., Chen, G., Melillo, J. and Liu, J.: Net exchanges of CO_2, CH_4, and N_2O between China's terrestrial ecosystems and the atmosphere and their contributions to global climate warming, J. Geophys. Res. Biogeosciences, 116(2), 1–13, doi:10.1029/2010JG001393, 2011.

Veldkamp, E., Koehler, B. and Corre, M. D.: Indications of nitrogen-limited methane uptake in tropical forest soils, Biogeosciences, 10(8), 5367–5379, doi:10.5194/bg-10-5367-2013, 2013.

Veraart, A. J., Steenbergh, A. K., Ho, A., Kim, S. Y. and Bodelier, P. L. E.: Beyond nitrogen: The importance of phosphorus for CH_4 oxidation in soils and sediments, Geoderma, 259–260, 337–346, doi:10.1016/j.geoderma.2015.03.025, 2015.

Wang, F., Li, J., Wang, X., Zhang, W., Zou, B., Neher, D. a and Li, Z.: Nitrogen and phosphorus addition impact soil N_2O emission in a secondary tropical forest of South China., Sci. Rep., 4, 5615, doi:10.1038/srep05615, 2014.

Wang, Y., Solberg, S., Yu, P., Myking, T., Vogt, R. D. and Du, S.: Assessments of tree crown condition of two Masson pine forests in the acid rain region in south China, For. Ecol. Manage., 242(2–3), 530–540, doi:10.1016/j.foreco.2007.01.065, 2007.

509 Werner, C., Butterbach-Bahl, K., Haas, E., Hickler, T. and Kiese, R.: A global inventory of N_2O
510 emissions from tropical rainforest soils using a detailed biogeochemical model, Global
511 Biogeochem. Cycles, 21(3), doi:10.1029/2006GB002909, 2007.

512 Xu, W., Luo, X. S., Pan, Y. P., Zhang, L., Tang, A. H., Shen, J. L., Zhang, Y., Li, K. H., Wu, Q.
513 H., Yang, D. W., Zhang, Y. Y., Xue, J., Li, W. Q., Li, Q. Q., Tang, L., Lu, S. H., Liang, T.,
514 Tong, Y. A., Liu, P., Zhang, Q., Xiong, Z. Q., Shi, X. J., Wu, L. H., Shi, W. Q., Tian, K., Zhong,
515 X. H., Shi, K., Tang, Q. Y., Zhang, L. J., Huang, J. L., He, C. E., Kuang, F. H., Zhu, B., Liu, H.,
516 Jin, X., Xin, Y. J., Shi, X. K., Du, E. Z., Dore, A. J., Tang, S., Collett, J. L., Goulding, K., Sun,
517 Y. X., Ren, J., Zhang, F. S. and Liu, X. J.: Quantifying atmospheric nitrogen deposition through
518 a nationwide monitoring network across China, Atmos. Chem. Phys., 15(21), 12345–12360,
519 doi:10.5194/acp-15-12345-2015, 2015.

520 Yu, L., Zhu, J., Mulder, J. and Dörsch, P.: Multiyear dual nitrate isotope signatures suggest that
521 N-saturated subtropical forested catchments can act as robust N sinks, Glob. Chang. Biol., In
522 Press, doi:10.1111/gcb.13333, 2016.

523 Zeng, L., Wang, P., Xiao, W., Wan, R., Huang, Z. and Pan, L.: Allocation of Biomass and
524 Productivity of Main Vegetations in Three Gorges Reservoir Region, Sci. Silvae Sin., 44(8), 16–
525 22, 2008.

526 Zhang, T., Zhu, W., Mo, J., Liu, L. and Dong, S.: Increased phosphorus availability mitigates the
527 inhibition of nitrogen deposition on CH 4 uptake in an old-growth tropical forest, southern
528 China, Biogeosciences, 8(9), 2805–2813, doi:10.5194/bg-8-2805-2011, 2011.

529 Zhang, W., Mo, J., Yu, G., Fang, Y., Li, D., Lu, X. and Wang, H.: Emissions of nitrous oxide
530 from three tropical forests in Southern China in response to simulated nitrogen deposition, Plant
531 Soil, 306(1–2), 221–236, doi:10.1007/s11104-008-9575-7, 2008a.

532 Zhang, W., Mo, J., Zhou, G., Gundersen, P., Fang, Y., Lu, X., Zhang, T. and Dong, S.: Methane
533 uptake responses to nitrogen deposition in three tropical forests in southern China, J. Geophys.
534 Res. Atmos., 113(11), 1–10, doi:10.1029/2007JD009195, 2008b.

535 Zhang, W., Wang, K., Luo, Y., Fang, Y., Yan, J., Zhang, T., Zhu, X., Chen, H., Wang, W. and
536 Mo, J.: Methane uptake in forest soils along an urban-to-rural gradient in Pearl River Delta,
537 South China., Sci. Rep., 4, 5120, doi:10.1038/srep05120, 2014a.

538 Zhang, W., Zhu, X., Luo, Y., Rafique, R., Chen, H., Huang, J. and Mo, J.: Responses of nitrous
539 oxide emissions to nitrogen and phosphorus additions in two tropical plantations with N-fixing
540 vs. non-N-fixing tree species, Biogeosciences Discuss., 11(1), 1413–1442, doi:10.5194/bgd-11-
541 1413-2014, 2014b.

542 Zheng, M., Zhang, T., Liu, L., Zhu, W., Zhang, W. and Mo, J.: Effects of nitrogen and
543 phosphorus additions on nitrous oxide emission in a nitrogen-rich and two nitrogen-limited
544 tropical forests, Biogeosciences, 13, 3503–3517, doi:10.5194/bg-2015-552, 2016.

545 Zhu, Q., Riley, W.J., Tang, J., Koven, C.D.: Multiple soil nutrient competition between plants,
546 microbes, and mineral surfaces: model development, parameterization, and example applications
547 in several tropical forests, Biogeosciences 13, 341-36, doi:10.5194/bg-13-341-2016, 2016.

548 Zhu, J., Mulder, J., Bakken, L. and Dörsch, P.: The importance of denitrification for N_2O

emissions from an N-saturated forest in SW China: results from in situ ^{15}N labeling experiments, Biogeochemistry, 116(1–3), 103–117, doi:10.1007/s10533-013-9883-8, 2013a.

Zhu, J., Mulder, J., Wu, L. P., Meng, X. X., Wang, Y. H. and Dörsch, P.: Spatial and temporal variability of N_2O emissions in a subtropical forest catchment in China, Biogeosciences, 10(3), 1309–1321, doi:10.5194/bg-10-1309-2013, 2013b.

Zhuang, Q., Lu, Y. and Chen, M.: An inventory of global N_2O emissions from the soils of natural terrestrial ecosystems, Atmos. Environ., 47, 66–75, doi:10.1016/j.atmosenv.2011.11.036, 2012.

Table 1 Background soil properties of the experimental plots at Tieshanping (TSP). Values are means and standard deviations, in parenthesis (n = 6)[†].

	Soil Layer	pH	Total C	Total N	Total P	C/N	N/P
			g kg^{-1}	g kg^{-1}	mg kg^{-1}		
	O/A (0-3 cm)	3.7 (0.1)	80.7 (32.3)	4.8 (1.7)	308 (57)	17.0 (2.5)	15.5 (5.7)
Block 1	AB (3-8 cm)	3.8 (0.0)	23.9 (9.3)	1.3 (0.6)	-[*]	20.0 (3.0)	-
	B (8-20 cm)	3.9 (0.2)	8.6 (1.2)	< 0.05	-	-	-
	O/A (0-3 cm)	3.6 (0.1)	77.6 (13.4)	4.7 (0.8)	297 (44)	16.7 (1.3)	15.7 (2.8)
Block 2	AB (3-8 cm)	3.7 (0.1)	20.2 (5.3)	1.0 (0.3)	-	21.4 (3.3)	-
	B (8-20 cm)	3.9 (0.1)	7.1 (1.6)	< 0.05	-	-	-
	O/A (0-3 cm)	3.6 (0.1)	67.0 (15.5)	3.8 (0.8)	223 (45)	17.4 (0.6)	17.2 (3.7)
Block 3	AB (3-8 cm)	3.6 (0.1)	21.0 (7.9)	1.1 (0.5)	-	24.5 (4.6)	-
	B (8-20 cm)	3.8 (0.1)	7.2 (1.5)	< 0.05	-	-	-
	Soil Layer	P_{H2O}	P_{Al}	Al_{ox}	Fe_{ox}	P_{ox}	P_{ox} /
		mg kg^{-1}	mg kg^{-1}	mg kg^{-1}	mg kg^{-1}	mg kg^{-1}	(Al_{ox} + Fe_{ox})
	O/A (0-3 cm)	< 5.0	5.8 (1.4)	1700 (513)	1933 (350)	85.8 (22.6)	0.025 (0.008)
Block 1	AB (3-8 cm)	< 5.0	2.1 (0.6)	1217 (243)	1692 (493)	47.1 (22.0)	0.016 (0.007)
	B (8-20 cm)	< 5.0	< 1.0	1083 (90)	1158 (249)	29.3 (28.6)	0.012 (0.011)
	O/A (0-3 cm)	< 5.0	5.9 (1.0)	1500 (238)	1792 (215)	79.2 (21.5)	0.024 (0.007)
Block 2	AB (3-8 cm)	< 5.0	1.6 (0.4)	925 (149)	1517 (320)	37.2 (10.7)	0.016 (0.006)
	B (8-20 cm)	< 5.0	< 1.0	892 (209)	1033 (413)	16.1 (10.5)	0.009 (0.007)
	O/A (0-3 cm)	< 5.0	4.1 (0.9)	1367 (180)	1667 (168)	50.7 (10.9)	0.017 (0.003)
Block 3	AB (3-8 cm)	< 5.0	4.4 (4.0)	1075 (128)	1350 (150)	24.8 (8.3)	0.010 (0.002)
	B (8-20 cm)	< 5.0	< 1.0	992 (130)	875 (138)	8.0 (2.0)	0.004 (0.001)

P_{H2O} = Water extractable P, P_{Al} = Ammonium extractable P,

Al_{ox} = Oxalate extractable Al, Fe_{ox} = Oxalate extractable Fe, P_{ox} = Oxalate extractable P.

[†] Soils were sampled in August 2013.

[*] Data not available

Table 2 Soil pH, C, N and P contents in the O/A horizon (0-3 cm) in Reference and phosphate (P) treatments. Values are means and standard deviations (in brackets), (n = 9).

		pH	Total C	Total N	C/N	P_{Al}	Total P
			g kg^{-1}	g kg^{-1}		mg kg^{-1}	mg kg^{-1}
13/08/02	Ref	3.7 (0.1)^{bc†}	8.3 (2.3)^{ab}	0.5 (0.1)^{bcd}	16.9 (1.1)^{bcd}	5.4 (1.4)^{c}	292 (46)^{bc}
	P	3.6 (0.1)^{c}	6.7 (2.0)^{b}	0.4 (0.1)^{bd}	17.1 (2.1)^{bc}	5.1 (1.3)^{c}	260 (70)^{c}
14/05/02	Ref	3.7 (0.1)^{abc}	12.2 (4.2)^{a}	0.9 (0.3)^{a}	13.7 (1.5)^{e}	19.0 (8.0)^{c}	336 (65)^{bc}
	P	3.8 (0.2)^{abc}	9.0 (3.5)^{ab}	0.7 (0.2)^{abc}	14.2 (2.8)^{de}	13.7 (5.2)^{c}	270 (72)^{bc}
14/05/10	Ref	3.8 (0.1)^{abc}	9.9 (2.1)^{ab}	0.7 (0.2)^{ab}	14.0 (0.7)^{e}	15.4 (7.0)^{c}	304 (49)^{bc}
	P	3.9 (0.3)^{ab}	8.0 (1.9)^{ab}	0.6 (0.1)^{bcd}	14.3 (1.3)^{cde}	174 (114)^{a}	572 (242)^{a}
14/12/02	Ref	3.8 (0.1)^{abc}	10.5 (3.6)^{ab}	0.7 (0.3)^{ab}	14.5 (1.3)^{cde}	14.2 (7.4)^{c}	328 (102)^{bc}
	P	3.9 (0.2)^{abc}	9.5 (2.1)^{ab}	0.7 (0.1)^{abc}	14.0 (0.8)^{e}	66 (24)^{ab}	442 (106)^{ab}
15/08/02	Ref	3.9 (0.2)^{ab}	8.3 (2.2)^{ab}	0.4 (0.1)^{cd}	20.5 (2.5)^{a}	13.4 (6.2)^{c}	291 (61)^{bc}
	P	4.0 (0.2)^{a}	6.5 (1.9)^{b}	0.3 (0.1)^{d}	19.7 (2.2)^{ab}	57 (36)^{ab}	383 (136)^{bc}

$^{\theta}$ P addition was conducted on 14/05/04, after the first two sampling dates.

† different letters indicate significance in difference.

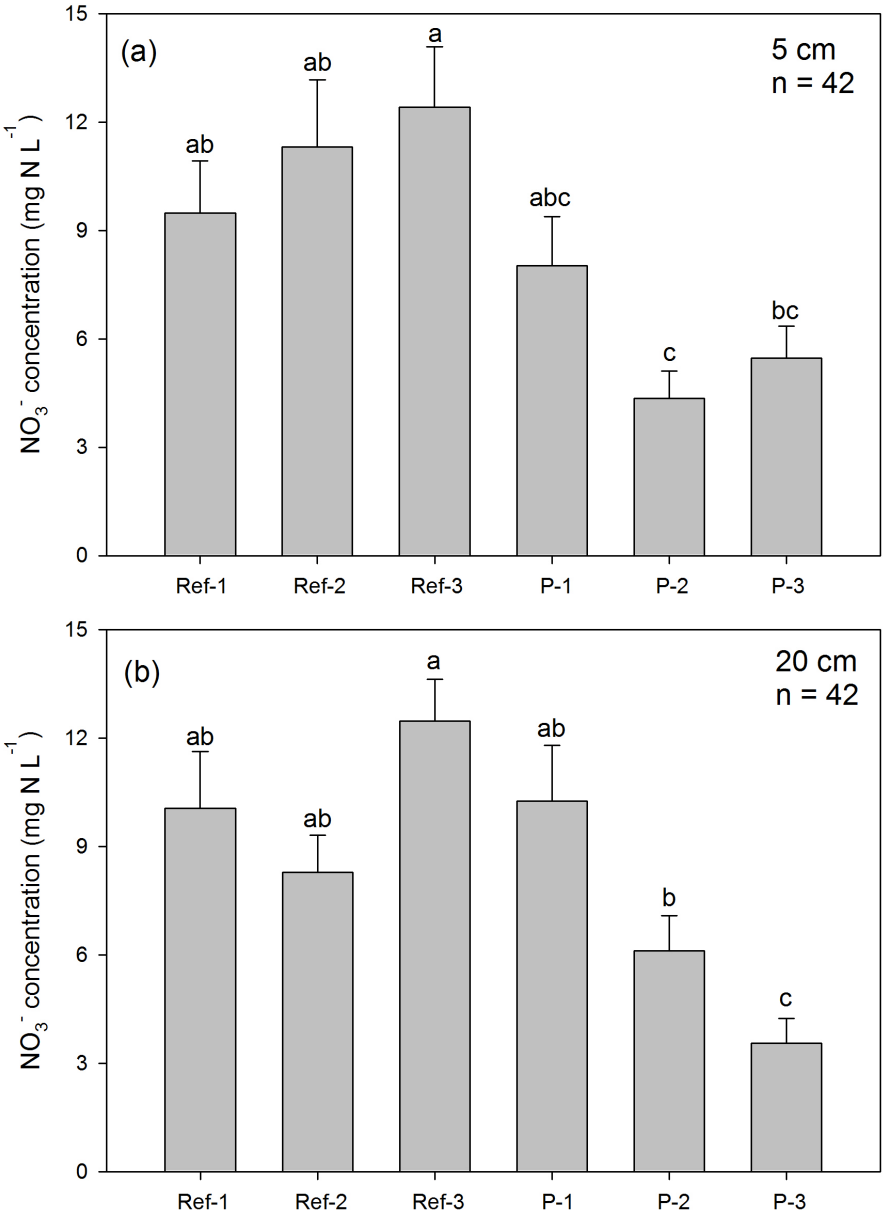

Fig. 1 Mean NO_3^- concentrations in soil water at 5 (a) and 20 (b) cm depths from three blocks with Reference and P treatment, 1.5 years after P addition; different letters indicate significant differences between the treatments and blocks

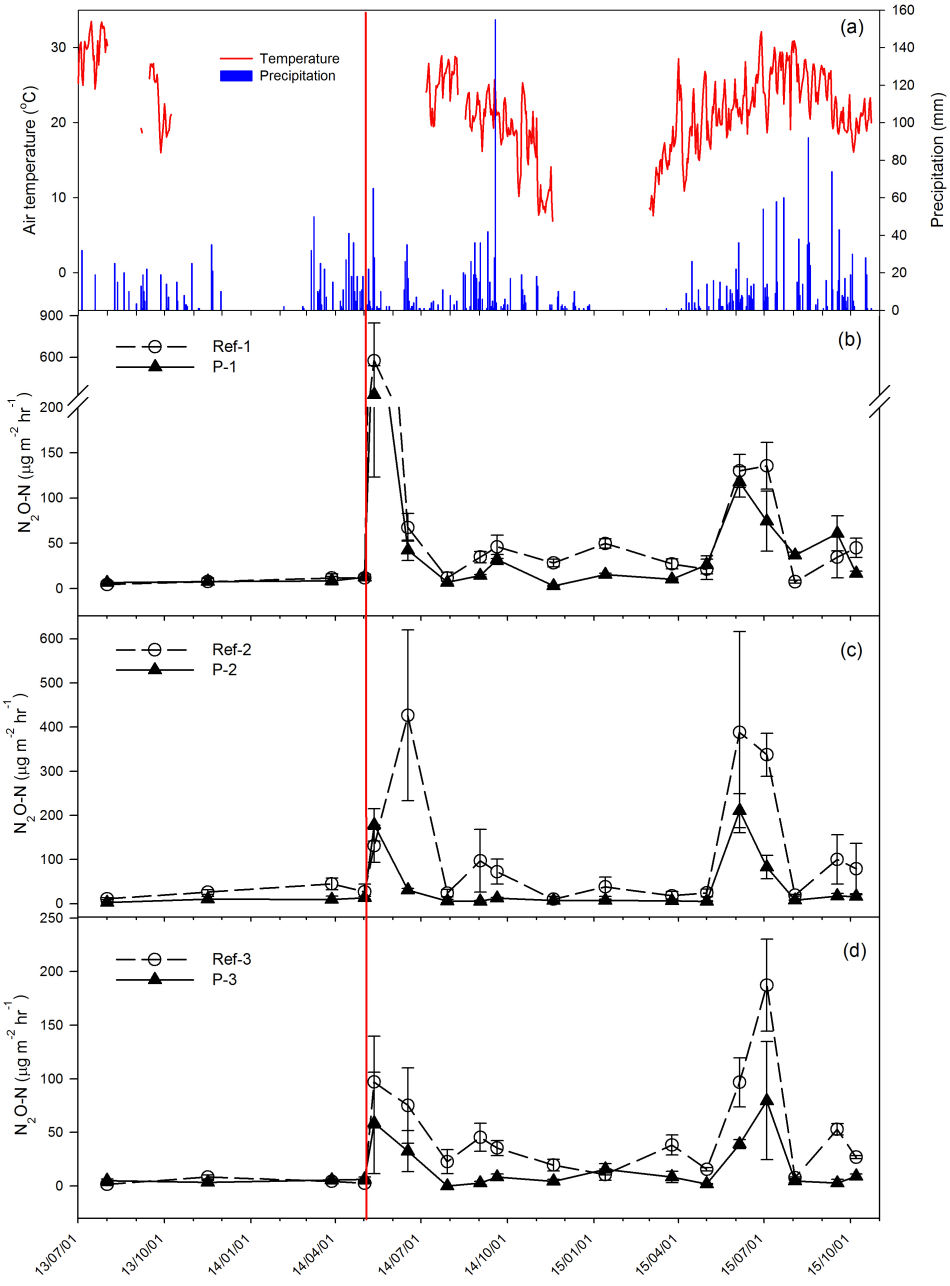

Fig. 2 Daily mean air temperature and precipitation (a), and monthly mean N_2O fluxes in Reference and P treatments in each of the three blocks (b-d); the red line gives the date of P addition.

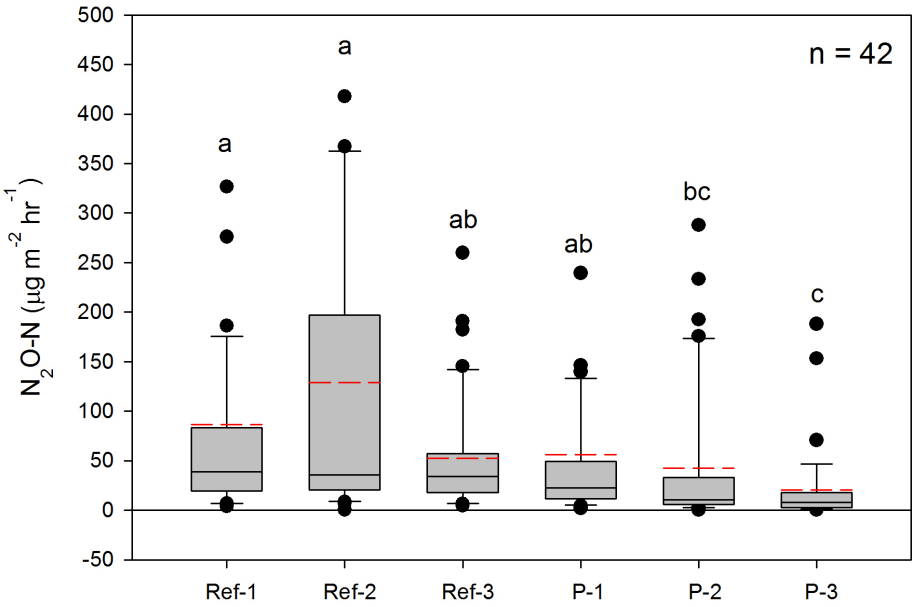

Fig. 3 Box whisker plots for N_2O fluxes in three blocks with Reference and P treatments throughout 1.5 years after the P addition; red dash lines indicate mean values; different letters indicate significant differences between treatments and blocks.

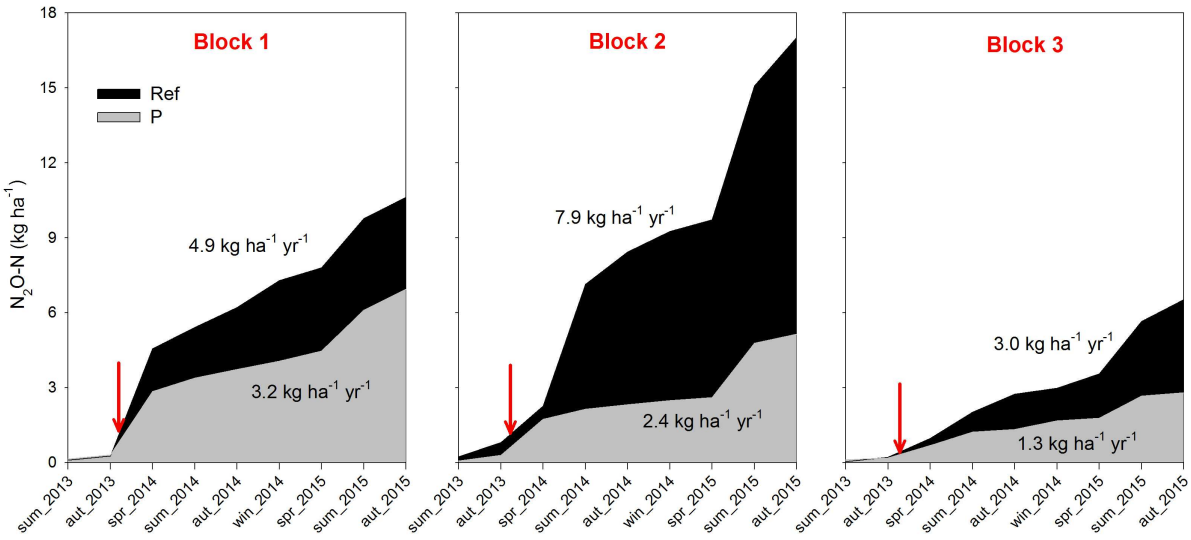

Fig. 4 Cumulative N_2O emissions for three blocks with Reference and P treatments during two years; the red arrows refer to the date when P addition was conducted.

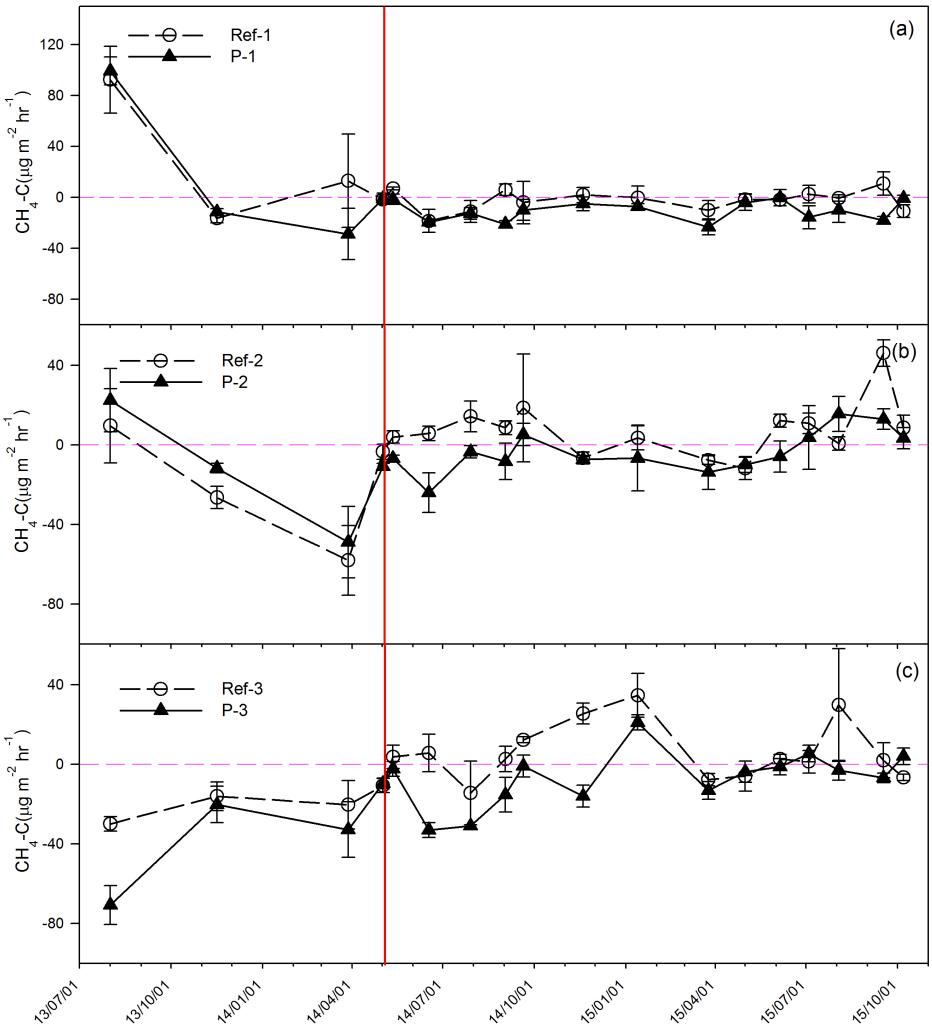

Fig. 5 Monthly mean CH_4 fluxes for three blocks (a-c) with Reference and P treatments during two years; the horizontal broken line indicates zero flux the red line refers to the date of P addition.

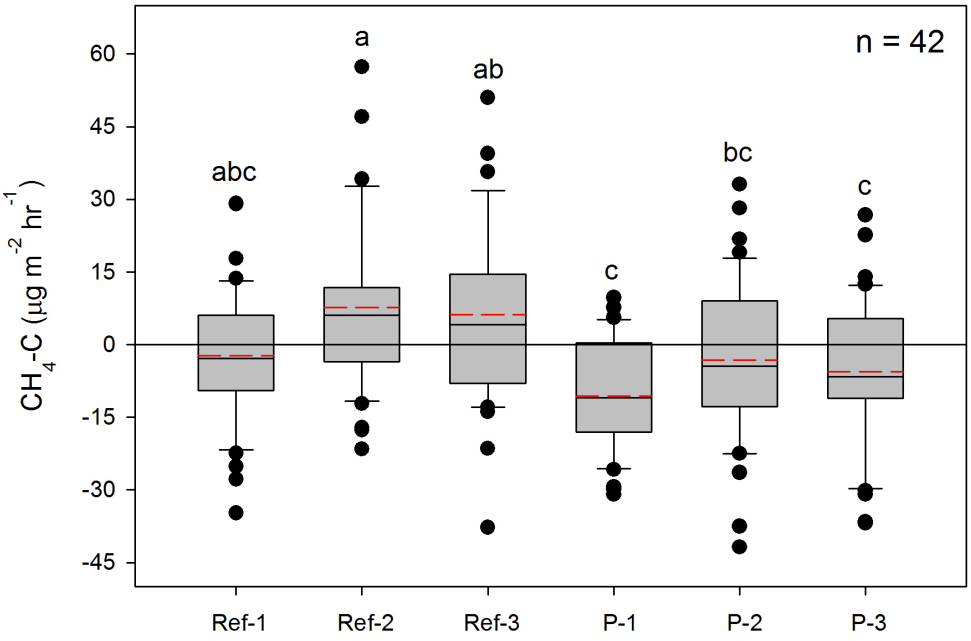

Fig. 6 Box whisker plots of CH_4 fluxes for three blocks with Reference and P treatments 1.5 years after the P addition; red dash lines indicate mean values; the small letters indicate the significance levels among the treatments and blocks.

Supplementary Materials

Phosphorus addition mitigates N_2O and CH_4 emissions in an N-saturated subtropical forest, SW China

Longfei Yu[1*], Yihao Wang[2, 3], Xiaoshan Zhang[3], Peter Dörsch[1], Jan Mulder[1]

[1]Department of Environmental Sciences, Norwegian University of Life Sciences, Postbox 5003, N-1432 Aas, Norway.

[2]Chongqing Academy of Forestry, 400036, Chongqing, China.

[3]Research Center for Eco-Environmental Sciences, Chinese Academy of Sciences, 100085, Beijing, China

[*]Correspondence: Longfei Yu, tel. +47 67231868, E-mail longfei.yu@nmbu.no

Phosphorus adsorption by soil

The required dose of P to stimulate significant increase in soil P concentration was determined based on sorption isotherms (Singh et al., 2005). The experiment was carried out with soils (triplicates mixed within each block as one sample) in the O/A, AB and B-horizons, from each block. Briefly, 1 g dry and sieved (2 mm) soil was added to 30 ml $CaCl_2$ solution with a gradient of initial PO_4^{3-} concentrations (0, 2.5, 5.0, 10.0, 20.0, 50.0 and 100 mg P L^{-1}). Next, the suspension was shaken for 24 h at 20 ºC. The P concentration was determined by colorimetric method (M&M) after centrifugation and filtration (0.45 μm). No P desorption was found in the zero-P treatments (only $CaCl_2$).

The results of P adsorption isotherms (Table S1 and Fig. S8) indicated medium sorption capacities in TSP soils (Singh et al., 2005), Based on P affinity constant and adsorption maxima, we chose an optimum P concentration of 1.0 mg L^{-1} for the P dose. Such dose is equivalent to 79.5 kg P ha^{-1} in TSP soil (0.3 g P kg^{-1} dw soil).

Table S1 P adsorption maximum, affinity constant and maximum buffering capacity obtained from Langmuir isotherms. The linear equation is C / (x/m) = 1 / (kb) + C / b; where C (mg P L^{-1}) is the equilibrium P concentration; x/m (mg P kg^{-1}) is the amount of P adsorbed per unit mass of adsorbent; k (L mg^{-1} P) is the P affinity constant; b (mg P kg^{-1}) is the P adsorption maximum.

		Adsorption maximum (b) (mg P kg^{-1})	P affinity constant (k) (L mg^{-1} P)	Maximum buffering capacity (mbc) (L kg^{-1})
	O/A	435	0.17	75
Block 1	AB	303	0.20	62
	B	278	1.00	277
	O/A	345	0.10	34
Block 2	AB	182	0.27	49
	B	278	0.24	65
	O/A	345	0.16	57
Block 3	AB	278	0.26	73
	B	357	0.28	99

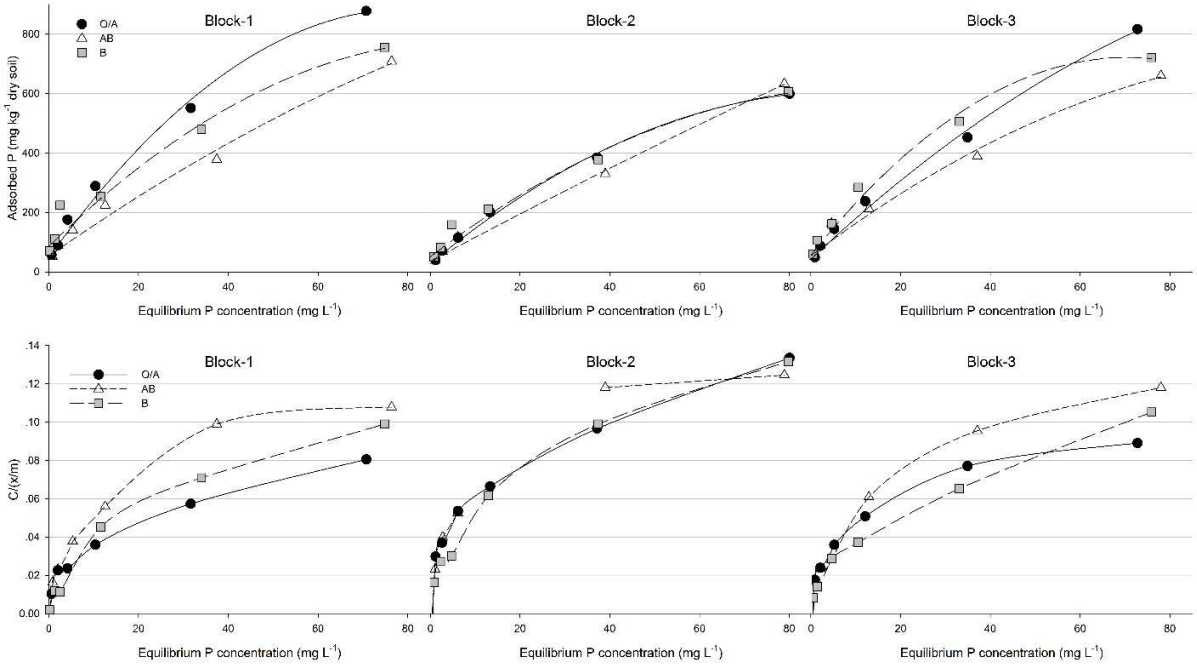

Fig. S1 Langmuir adsorption isotherms of soils from O/A, AB and B horizons in Block 1-3. The data were fitted to the Langmuir equation, after linearization.

Table S2 Half-yearly tree biomass, 500-needle weight and needle nutrient contents in Reference and P treatments[†]. Values are means and standard deviations (in brackets) (n = 9).

		500-needle g	Tree Biomass t ha^{-1}	Total C g kg^{-1}	Total N g kg^{-1}	Total P g kg^{-1}	C/N	N/P	K^+ g kg^{-1}	Mg^{2+} g kg^{-1}	Ca^{2+} g kg^{-1}
Nov. 2013	Ref	13.8 (1.8)	149 (11)	510 (9)	15.2 (0.8)	0.71 (0.04)	34 (2)	22 (1)	4.6 (0.8)	1.3 (0.2)	4.5 (1.3)
	P	12.5 (1.9)	131 (25)	517 (6)	14.7 (1.0)	0.73 (0.05)	35 (2)	20 (3)	4.7 (0.7)	1.4 (0.2)	5.3 (0.6)
Nov. 2014	Ref	13.8 (2.3)	148 (12)	551 (11)	14.9 (1.5)	0.88 (0.09)	37 (7)	17 (1)	6.6 (1.2)	1.6 (0.3)	7.8 (2.4)
	P	14.3 (2.3)	133 (27)	550 (9)	14.6 (1.1)	0.85 (0.11)	38 (4)	17 (1)	5.9 (0.9)	1.6 (0.4)	5.6 (3.1)
Feb. 2016	Ref	12.9 (2.3)	143 (8)	-[*]	-	-	-	-	-	-	-
	P	10.8 (2.4)	129 (29)	-	-	-	-	-	-	-	-

[†] P addition was conducted on 14/05/04

[*] Data were not available.

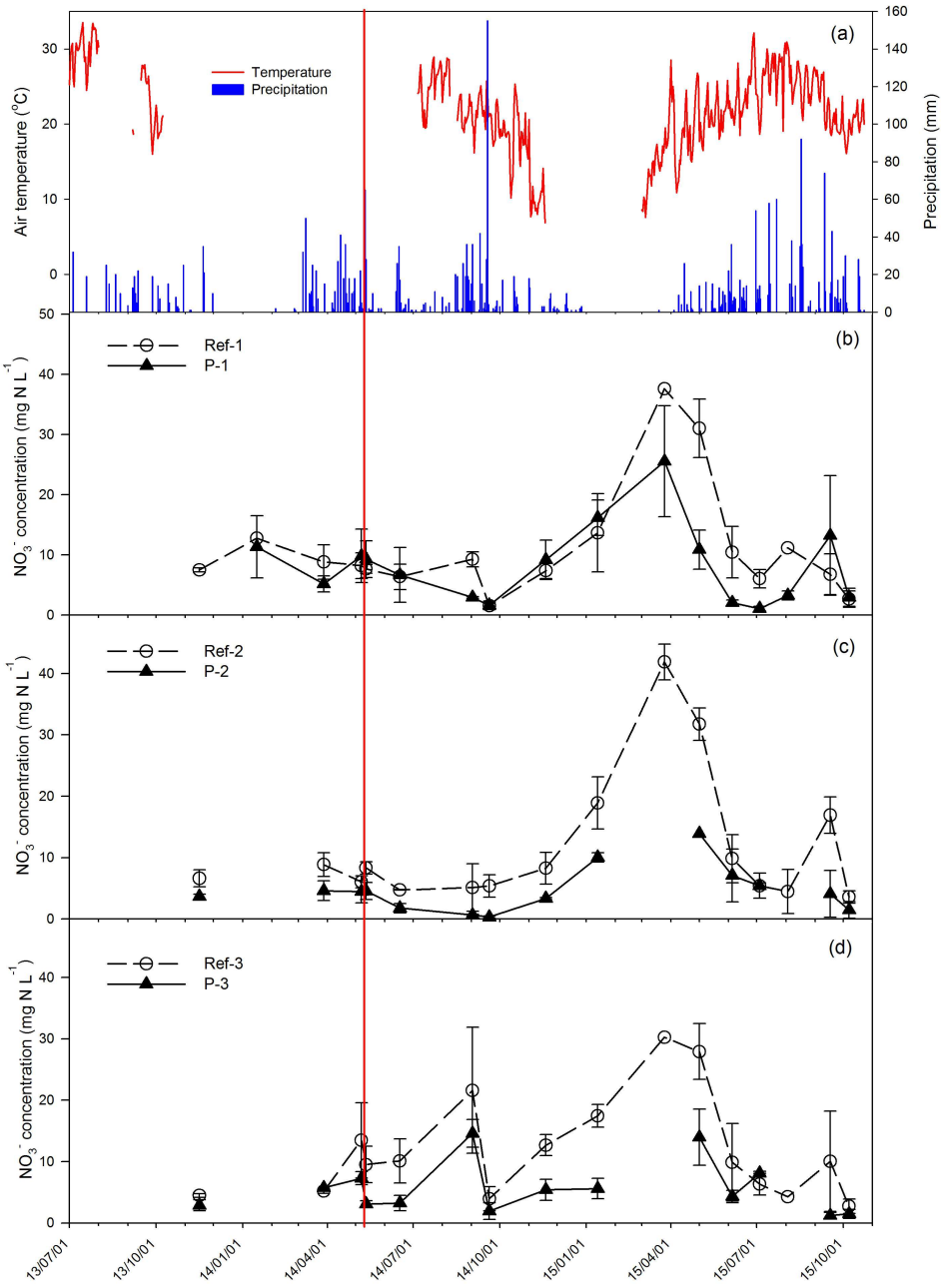

Fig. S2 Daily mean air temperature and precipitation (a), and monthly mean NO_3^- concentrations at the 5-cm soil depth for three blocks (b-d) with Reference and P treatments during two years; the red line refers to the date when P addition was conducted (for P treatments only).

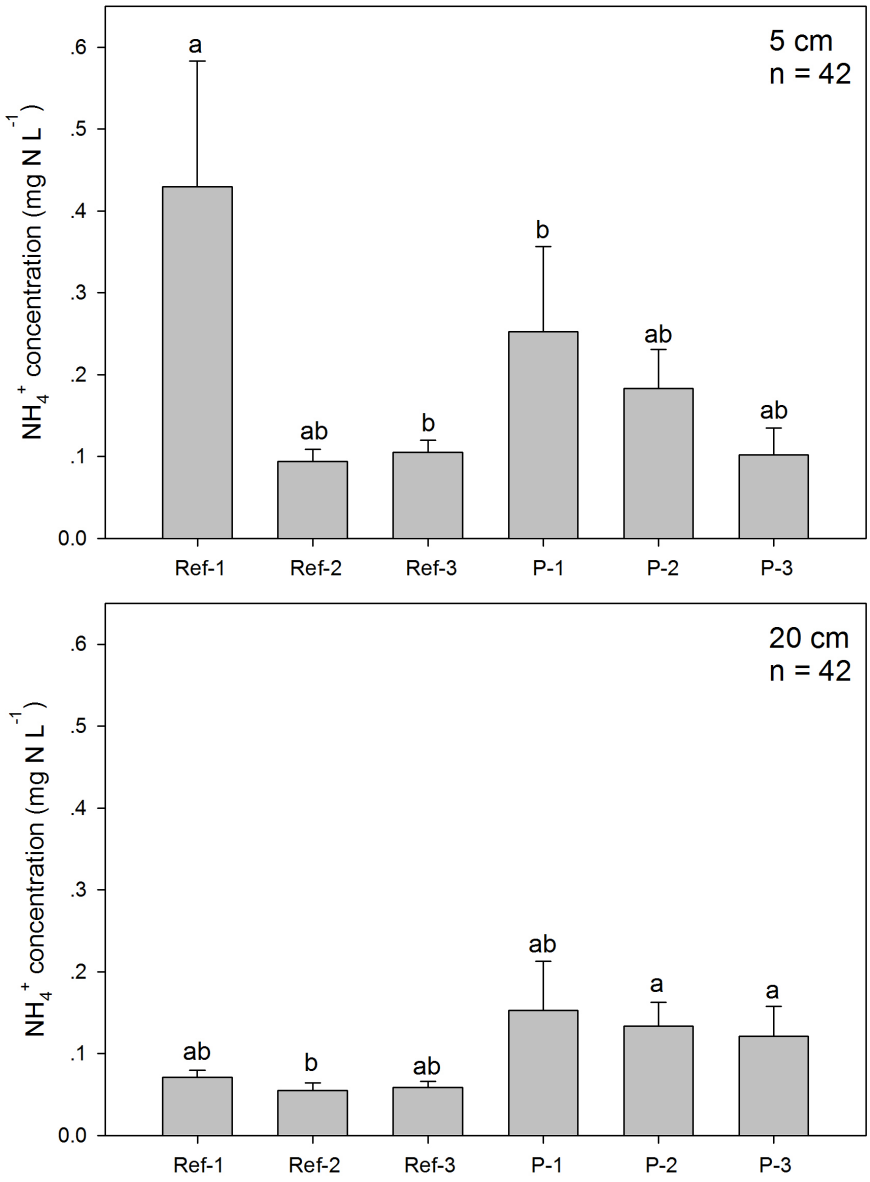

Fig. S3 Mean NH_4^+-N concentrations in soil water at 5 (a) and 20 (b) cm depths from three blocks with Reference and P treatments, 1.5 years after P addition; the small letters indicate the significance levels among the treatments and blocks.

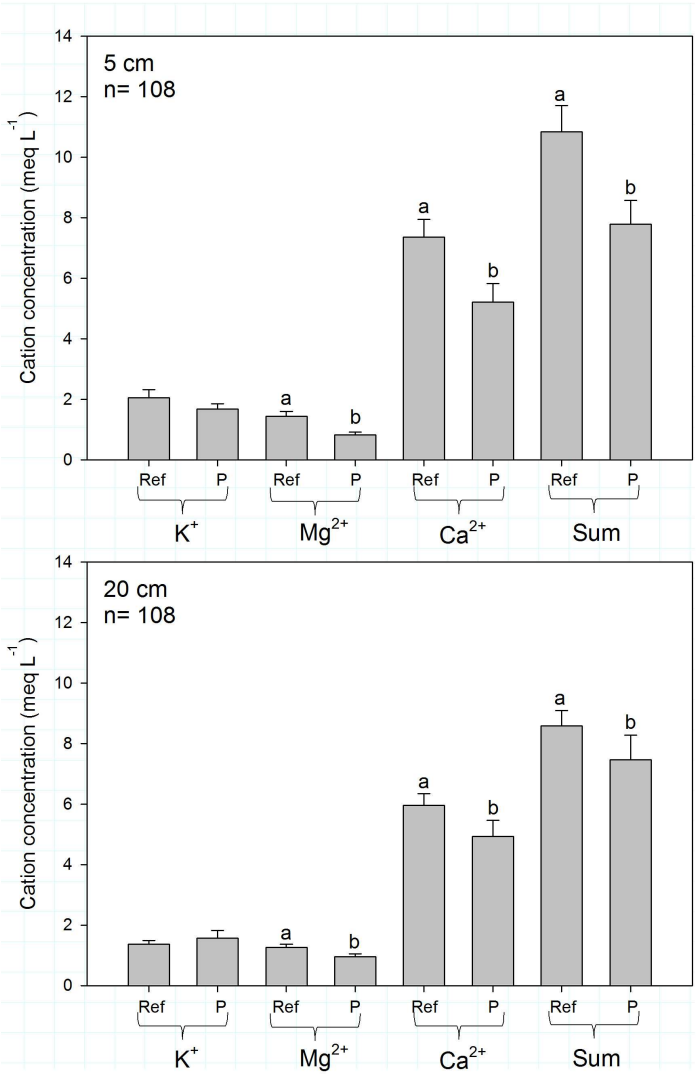

Fig. S4 Mean soil cation (K^+, Mg^{2+} and Ca^{2+}) concentrations in Reference and P treatments during 1.5 years after P addition

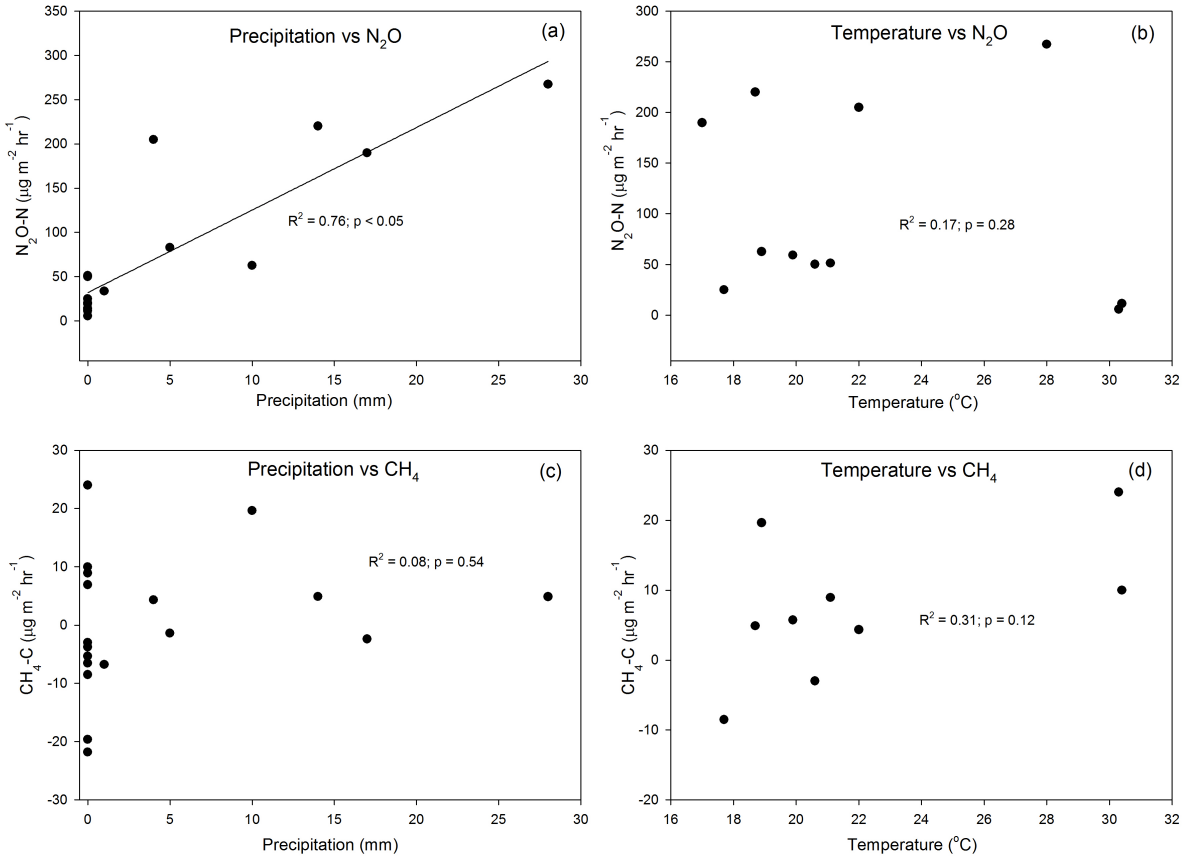

Fig. S5 Relationship between climatic factors (daily mean temperature and precipitation) and gas fluxes (mean monthly fluxes for N_2O (a&b) and CH_4 (c&d) from the References); due to temperature data missing from November 2013 to July 2014, fewer data points were presented in comparisons with temperature.

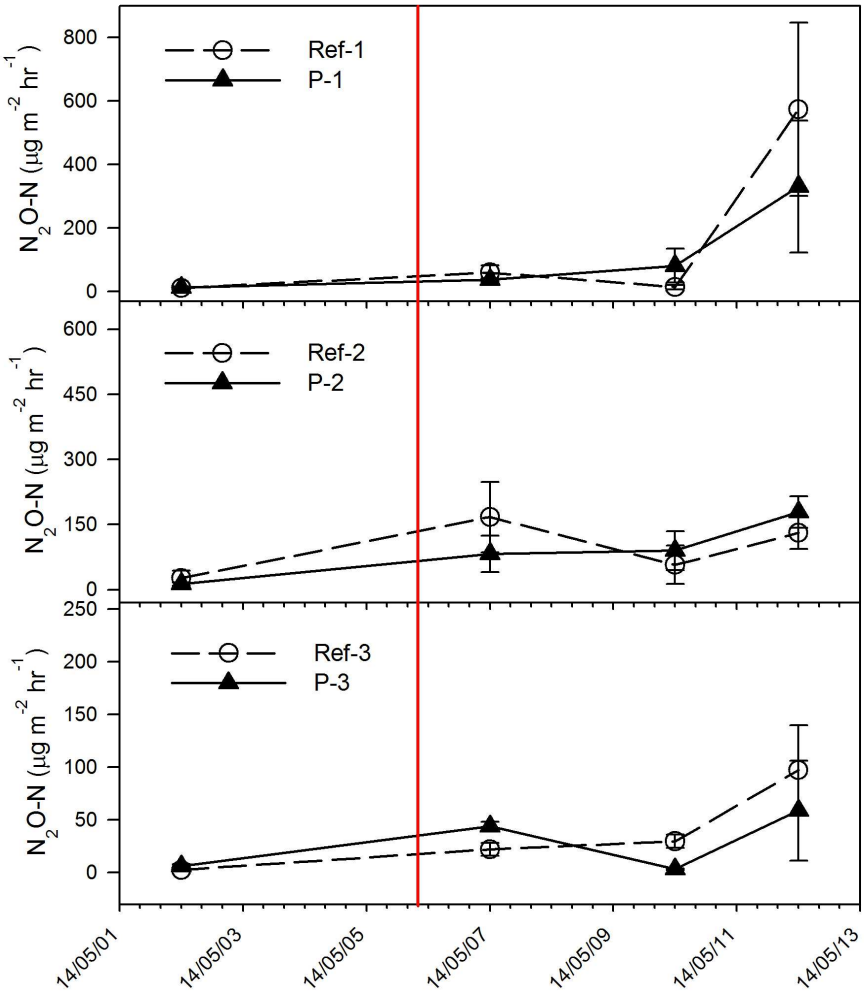

Fig. S6 Mean N_2O fluxes for three blocks in the Reference and P treatments during the 10 days before and after P application on 4 May 2014.

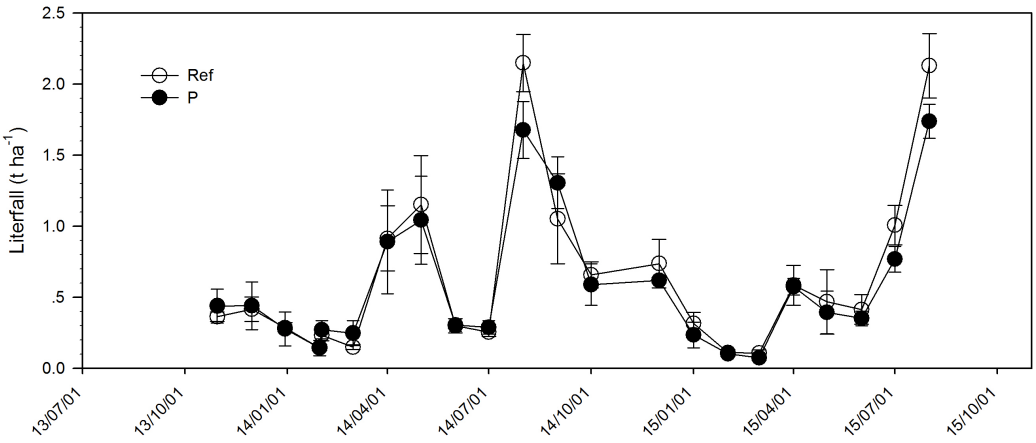

Fig. S7 Monthly litterfall for three blocks (a-c) with Reference and P treatments during two years.

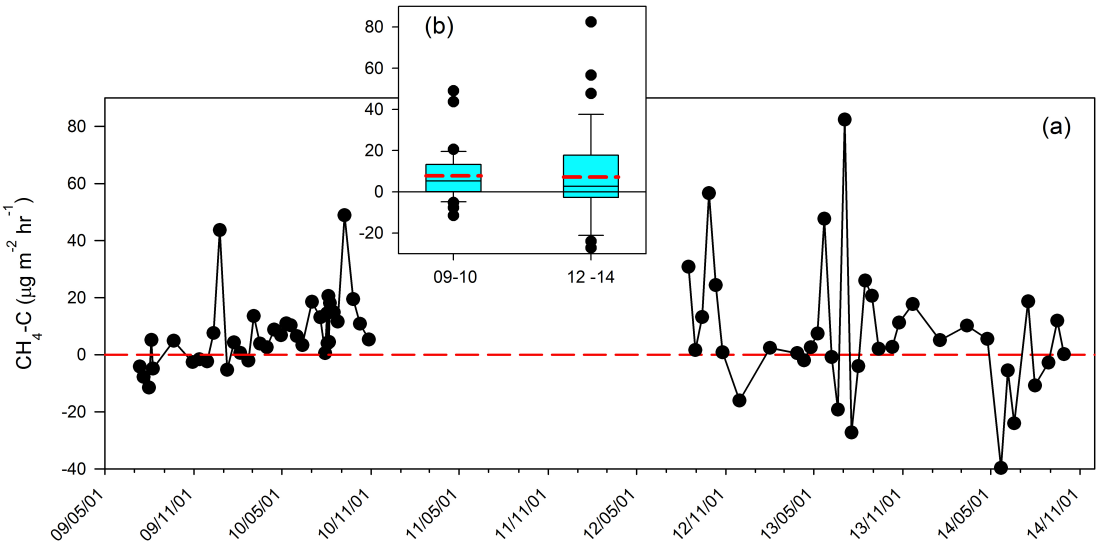

Fig. S8 (a) Temporal variations of CH_4 fluxes from 2009 to 2014 at TSP forest; red dash line refers to the zero flux; **(b)** Box whisker plots of mean CH_4 fluxes for 2009-2012 and 2012-2014 periods, respectively; red dash lines refer to the mean values. Data for long-term CH_4 fluxes were obtained from Zhu et al. (unpublished).

Paper V

Controlled induction of denitrification in *Pseudomonas aureofaciens*: a simplified denitrifier method for dual isotope analysis in NO_3^-

Jing Zhu, Longfei Yu, Lars R. Bakken, Pål Tore Mørkved, Jan Mulder, Peter Dörsch,

Manuscript

Controlled induction of denitrification in *Pseudomonas aureofaciens*: a simplified denitrifier method for dual isotope analysis in NO_3^-

Jing Zhu[1,3], Longfei Yu[1], Lars R. Bakken[1], Pål Tore Mørkved[2], Jan Mulder[1], Peter Dörsch[1]

[1] Department of Environmental Science, Norwegian University of Life Science, Box 5003, N-1432 Aas, Norway

[2] Department of Earth Science, University of Bergen, Box 7803, 5020 Bergen, Norway

[3] Department of Environment and Resources, Guangxi Normal University, 541004, Guilin, China

Running title: Simplified denitrifier method

E-mail addresses: zhu0773@126.com (Jing Zhu); longfei.yu@nmbu.no (Longfei Yu); lars.bakken@nmbu.no (Lars Reier Bakken); pal.morkved@uib.no (Pål Tore Mørkved); jan.mulder@nmbu.no (Jan Mulder); peter.doersch@nmbu.no (Peter Dörsch)

Corresponding author: Peter Dörsch, peter.doersch@nmbu.no, Tel. +47 67231836

Keywords: ^{18}O; ^{15}N; NO_3^-, *Pseudomonas aureofaciens*, *Paracoccus denitrificans*, denitrifier method

Abstract

Dual isotope signatures in NO_3^- ($\delta^{15}N$ and $\delta^{18}O$) are invaluable to constrain nitrogen transformation processes in nature. Biological conversion to nitrous oxide (N_2O) by denitrifiers lacking N_2O reductase ("denitrifier method") has become the method of choice for isolating NO_3^- from natural samples prior to ^{15}N and ^{18}O analysis. The success of the method depends on the ability of the culture to rapidly and quantitatively convert NO_3^- to N_2O, with little interference from non-sample NO_3^- and ^{18}O in water. We studied the transition from oxic to anoxic respiration in *Pseudomonas chlororaphis ss. aureofaciens* (ATCC 13985) grown oxically in complex medium (~7.5×10^8 cells ml^{-1}). When letting the culture turn anoxic in the presence of mM NO_3^-, nitric oxide (NO) accumulated to toxic levels, impairing denitrification. With µM NO_3^-, efficient conversion to N_2O depended on the presence of mM NH_4^+ in the medium. At higher cell densities, conversion efficiencies decreased, suggesting that the ability to express balanced denitrification in *P. aureofaciens* is growth dependent. We concluded that *P. aureofaciens* can induce balanced denitrification in NH_4^+-amended complex medium in the presence of small amounts of NO_3^-, typically processed by the denitrifier method, making anoxic preculturing with extraneous NO_3^- obsolete. Based on our results, we devise a simplified denitrifier method, which is fast (two days including oxic pre-culture and anoxic conversion) and does not require concentration of cells or removal of extraneous NO_3^- or N_2O. Background NO_3^- in the complex medium can be removed as N_2 by anoxic pre-incubation with *P. denitrificans*. The standard deviation for natural abundance was 0.1 - 0.3‰ for ^{15}N and 0.2 - 0.7‰ for ^{18}O. After correction, differences between measured and consensus $\delta^{15}N$ and $\delta^{18}O$ values of NO_3^- standards generally fell within the standard deviations of the measured values. We successfully tested the method for samples with low pH (pH=4) or high salinity (0.25 - 1M KCl) and found no cross-contamination when using $^{15}NH_4^+$-labelled NH_4NO_3.

1. Introduction

Nitrate (NO_3^-) is central to terrestrial and aquatic N cycling. The isotopic composition of both N and O in NO_3^- reflects the processes producing and consuming NO_3^-, be it during fertilizer production (e.g. Bateman and Kelly), chemical conversion in the atmosphere (Hastings et al., 2003), biological N cycling driven by nitrification and denitrification (Mariotti et al., 1981), assimilation (Waser et al., 1998), Anammox (Clark et al., 2008) or dissimilatory reduction to ammonium (DNRA) (McCready et al., 1983). The natural isotopic composition of NO_3^- thus provides insights into N cycling (e.g. Robinson, 2001; Ostrom et al., 2002; Dhondt et al., 2003; Barnes et al., 2008; Søvik and Mørkved, 2008; Otero et al., 2009; Yu et al., 2016), while ^{15}N-enriched NO_3^- is used to infer gross N cycling rates (Mary et al., 1998; Addy et al., 2002; Murphy et al., 2003; Rütting and Müller, 2007), to partition sources (Well et al., 2003; Mørkved et al., 2006; Zhu et al., 2013a) or to trace the fate of reactive nitrogen in the environment (Perakis and Hedin, 2001; Zak et al., 2004). Both approaches, natural abundance and ^{15}N labelling, require fast and reliable methods to isolate and convert NO_3^- to gaseous N, preferably N_2O because of its relative inertness, with minimum interference from non-sample N or O before isotopic analysis by isotope ratio mass spectrometry (IRMS) or other methods.

Four major approaches can be distinguished to isolate and convert NO_3^- to gaseous N: i) precipitation as silver, potassium or barium salt (Revesz et al., 1997; Silva et al., 2000; Huber et al., 2011) with subsequent combustion to N_2 for ^{15}N and CO for ^{18}O analysis; ii) chemical conversion of NO_3^- to ammonia (NH_3) with subsequent diffusion and combustion to N_2; no ^{18}O analysis is possible (Brooks et al., 1989); iii) chemical conversion of NO_3^- to nitrite (NO_2^-), using cadmium (Cd) or vanadium chloride (VCl_3), with subsequent reduction to N_2O by sodium azide (Stevens and Laughlin, 1994; McIlvin and Altabet, 2005; Lachouani et al., 2010) or hydroxylamine (Liu et al., 2014) and iv) biological conversion to N_2O by *nos*Z-deficient denitrifying bacteria lacking N_2O reductase (Christensen and Tiedje, 1988; Sigman et al., 2001; Casciotti et al., 2002; Mørkved et al., 2007; Rock and Ellen, 2007). The major advantages of the latter two approaches are their high selectivity and hence sensitivity (less than 0.1 µmol NO_3^- can be converted quantitatively) and the applicability to a range of sample matrices, such as sea water or soil extracts (Rock and Ellen, 2007). Compared to the chemical reduction by Cd or VCl_3 to NO_2^-, with

subsequent reduction to N_2O by azide or hydroxylamine, the denitrifier method involves no toxic chemical, and has therefore gained increasing popularity during recent years (Xue et al., 2010).

Pseudomonas chlororaphis and *Pseudomonas aureofaciens* (ATCC 13985, recently reclassified as a strain of *P. chlororaphis*) are the organism of choice for the quantitative conversion of NO_3^- to N_2O (Christensen and Tiedje, 1988; Sigman et al., 2001; Casciotti et al., 2002). Both strains possess the copper-type nitrite reductase NirK (Ye et al., 1991), but *P. aureofaciens* has been shown to exchange less oxygen with water during NO_2^- reduction, rendering it more suitable for the simultaneous analysis of ^{15}N and ^{18}O in NO_3^-. Since N and O isotopes in NO_3^- undergo kinetic fractionation during enzymatic conversion to N_2O, the denitrifier method relies on complete conversion of sample NO_3^- to N_2O. Further, the conversion should be rapid, and mediated by a dense *P. aureofaciens* culture, since *noz*-competent denitrifiers contained in the sample matrix may express N_2O reductase (N_2OR) during anoxic incubation, which would reduce some of the N_2O to N_2, thereby enriching the remaining N_2O isotopically. Accordingly, the method originally devised by Sigman et al. (2001) and Casciotti et al. (2002) uses concentrated cells of *P. aureofaciens* re-suspended in spent medium, which serves as an energy source during dissimilatory reduction of NO_3^- to N_2O. Denitrification is expressed during a lengthy period of preculturing in the presence of extraneous NO_3^-, during which cells deplete available oxygen and switch from oxic to anoxic respiration. This approach faces several challenges, which may compromise the assay. If the preculturing period is too short, consumption of extraneous NO_3^- will be incomplete in the spent medium and lead to large blank values. If the preculturing period is too long, growing *P. aureofaciens* cells are at risk to run out of electron acceptors (NO_3^-, NO_2^- and NO), which could impair their "fitness" to convert sample NO_3^- quantitatively to N_2O. In practice, it is difficult to monitor NO_3^- depletion during growth and induction of *P. aureofaciens*, unless incubation vessels allow aseptic and anoxic removal of aliquots for NO_3^- analysis. After denitrification is induced and NO_3^- is depleted, cells are harvested by centrifugation and re-suspended in spent medium from which the N_2O formed during anoxic growth has to be removed by He- or N_2-sparging. Together, this makes the denitrifier method a rather laborious method, with little possibility to evaluate the fitness of the working culture before using it for the conversion of known NO_3^- standards. Typically, 5 - 6 days are needed for pre-culturing and 1 day for cell concentration and N_2O The workflow for the method devised by Sigman et al. (2001) and Casciotti et al (2002) is shown in figure 1A.

Problems with the denitrifier method are reported occasionally, and typically attributed to loss of viability during culture storage or contamination of pre-cultures (Schauer, internet survey; Casciotti et al., 2002; Xue et al., 2010). Even though the method is widely used, conversion efficiencies and blank values are hardly ever reported, preventing any conclusion about the fitness of the anoxically induced strain and its conversion efficiency for NO_3^-.

The objective of the present study was to investigate the oxic-anoxic transition of growing *P. aureofaciens* in more detail by monitoring CO_2, O_2, NO, N_2O and N_2 kinetics under various conditions (type of medium, initial pO_2, cell density, pH, NO_3^- and NH_4^+ availability). The complete dissimilatory reduction of NO_3^- to N_2 (N_2O in the case of *P. aureofaciens*) via the intermediates NO_2^- and NO, relies on effective expression of the functional genes, and a balanced expression of nitrite- and nitric oxide reductase to avoid accumulation of nitrite (NO_2^-) and nitric oxide (NO) to toxic concentrations. Neither can be taken for granted when using cultured denitrifying organisms to convert NO_3^- to N_2O under anoxic conditions, as demonstrated for a variety of strains. For instance, a fast and complete removal of O_2 may entrap the cells in anoxia, without energy for synthesizing denitrification enzymes (Højberg et al., 1997). Stochastic expression of NO reductase, as demonstrated for *P. denitrificans* (Bergaust et al. 2011, Hassan et al 2014) can result in such entrapment for a fraction of the population, hence low initial denitrification rates by a minority of the cells. Robustly coordinated expression of NO_3^- and NO reductases is characteristic for some denitrifying strains (Hassan et al 2015), but not all. Bergaust et al. (2008) demonstrated that *Agrobacterium tumefaciens* accumulates NO to toxic levels (preventing further reduction to N_2O), if experiencing fast depletion of O_2. These phenomena must be taken into account as potential pitfalls when designing a routine to transform NO_3^- to N_2O for analytical purposes.

Based on the results of our study, we devise a modified "denitrifier method" with oxically grown *P. aureofaciens* that does not rely on induction of denitrification with extraneous NO_3^-. We build on previous modifications proposed by Mørkved et al., 2007) for *Pseudomonas chlororaphis* (ATCC 43928), who had shown that densely grown, anoxically induced cells of *Pseudomonas chlororaphis* could effectively and reliably convert 1 - 5 µg NO_3^- within a reasonable time span without pre-concentrating the cells. They also showed that by reducing the volume of the assay to a few millilitres, N_2O could be analysed without measurable fractionation directly from the

137 headspace of 120 ml serum bottles, without sparging the sample with He by means of a double
138 needle.

139 To address the problem with NO_3^- impurities often contained in complex media, we devise a simple
140 denitrifier method, i.e. NO_3^- conversion to N_2 by incubating the medium anoxically with
141 *Paracoccus denitrificans*, which allows producing large quantities of medium strongly reduced in
142 NO_3^-. We also characterized the tolerance of our simplified conversion assay to acidity and salt
143 content in different matrices. To evaluate the overall performance for ^{15}N and ^{18}O analyses, we
144 tested the method for a range of international NO_3^- standards (IAEA-N3, USGS32 and USGS34)
145 as well as for unknown standards and NO_3^- in natural samples provided by an international ring
146 test (Biasi et al., *in prep.*).
147

2. Materials and Methods

2.1 Bacterial strains and culture conditions

Two strains were used in this study, *Pseudomonas chlororaphis ss. aureofaciens* (ATCC 13985), which lacks N_2O reductase and *Paracoccus denitrificans* (ATCC 17741) which expresses all four functional denitrification enzymes (Bergaust et al., 2012). The strains were grown on ager plates with tryptic soy broth (TSB, 30g L^{-1}; amended with NH_4Cl, 20mM; KH_2PO_4, 36mM; Agar 15g L^{-1}). A single colony was picked and inoculated into 50 ml TSB medium (the same recipe but without agar, pH~7) and grown overnight. Aliquots of 1 ml culture were distributed into sterile 1.5 ml microtubes containing 0.2 ml of sterile glycerol and stored at -80 ºC until use. Before each experiment, a "starting culture" was prepared by inoculating one tube of either *P. aureofaciens* or *P. denitrificans* into 50 ml of fresh TSB medium or NO_3^--free TSB medium (see Ch. 2.3) (Fig. 1B) and grown aerobically while stirred at room temperature until turbidity developed. Before reaching stationary phase, each 1 ml of the aerobically grown culture containing 1.1 - 1.9×10^9 cells was distributed aseptically into 50 ml fresh TSB medium or NO_3^--free TSB medium to produce an oxic "working culture" (Fig. 1B). For each experiment described below, working culture was produced freshly.

2.2 Induction of denitrification in *P. aureofaciens* under different initial O_2 levels in the presence of ample NO_3^-

To evaluate how the rate of oxic-anoxic transition affects the induction of denitrification in *P. aureofaciens*, we set up an experiment with different initial O_2 concentrations. The higher the initial O_2 concentration, the more rapid the transition, as oxygen results in more oxic growth and hence greater cell numbers, depleting O_2 at a greater pace. Working cultures were prepared by inoculating 1 ml starting culture (1.1×10^9 cells ml^{-1}) into 15 ml sterile TSB amended with 10 mM NO_3^- (Casciotti et al., 2002) in autoclaved 120 ml bottles with magnetic stirrers. Each bottle was crimp-sealed with a butyl septum and the headspace was helium-washed by 5 cycles of evacuation and helium-filling (if not stated otherwise, the procedure of bottle sealing and He-washing is the same in all experiments). After releasing overpressure, three sets of flasks (triplicates) were adjusted with pure O_2 to 21, 10 and 5 vol% (equivalent to 57, 27 and 13.5 mmol L^{-1} O_2 in the headspace) and over-pressure was released. *P. aureofaciens* working culture (1 ml) was inoculated after O_2 concentrations were adjusted to provide equal starting conditions in all O_2 treatments. O_2

depletion and denitrification product accumulation (NO, N_2O) were monitored in the headspace every 2 h throughout 110 hours, while stirring the bottles constantly (400 rpm) at 20°C.

2.3 Removal of background NO_3^- from TSB

Complex media carry variable amounts of NO_2^- and NO_3^- which would interfere with the ^{15}N and ^{18}O of sample nitrate. To remove NO_3^- impurities, we inoculated freshly made, full-strength TSB medium with *P. denitrificans*, a denitrifier with a notoriously efficient N_2O reductase that reduces NO_3^- quantitatively to N_2 (Bergaust et al., 2012). To test conditions for efficient NO_3^- removal, we inoculated 50 ml TSB in 120 ml bottles with 1 ml of *P. denitrificans* grown oxically to either 3.7 or 9.3×10^8 cells ml^{-1}. Different amounts of O_2 (0, 0.5 and 2 ml in 70 ml He-headspace) were added, equivalent to 0, 0.42 and 1.67 mM O_2. Initial O_2 controls the oxic growth rate of *P. denitrificans* before turning the culture anoxic and had to be optimized to avoid over-growth, which would make it difficult to remove *P. denitrificans* cells once the NO_3- was removed from the medium. Bottles were incubated horizontally shaken for 6 days at room temperature after which they were amended with 20 mM NH_4^+ to replenish ammonium consumed during growth (see Ch. 2.4). Thereafter, *P. denitrificans* cells were removed by filtering the medium through a 0.22 µm filter using a peristaltic pump before autoclaving the medium. Residual NO_3^- was measured by a *P. aureofaciens* bioassay, inoculating 1 ml of 9.3×10^8 cells ml^{-1} into 40 ml *P. denitrificans*-treated medium and following N gas evolution every 1.9 h for 30 h. The resulting "NO_3-free" medium was used for subsequent experiments with *P. aurefaciens* and is henceforward termed *P. denitrificans* treated medium (short: TSB_{pd}). The efficiency of filtering and autoclaving used to remove residual *P. denitrificans* activity was verified by measuring N_2O production in anoxic TSB_{pd} blanks (no *P. aureofaciens* added) in the presence of 7 µmol fresh NO_3^- and 10 ml C_2H_2 in the headspace (to block N_2O reduction to N_2).

To produce TSB_{pd} in larger quantities, we tested medium pre-treatment with *P. denitrificans* in 500 ml Duran bottles (total volume of 620 ml). 500 ml TSB was inoculated with 10 ml *P. denitrificans* working culture (9.3×10^8 cells ml^{-1}), leaving a headspace of 110 ml with ambient air, equivalent to 2 ml O_2 for 50 ml TSB. The bottles were sealed air-tight using Teflon film and supported by several layers of plastic film around the screw cap. The bottles were incubated for 3 days standing upright on a horizontal shaker to prevent sedimentation before being amended with NH_4^+, filtered and autoclaved. The efficiency of NO_3^- removal and sterilization/cell removal was

checked as described above. Thereafter, the TSP_{pd} medium was portioned and frozen to -20°C. Producing TSB_{pd} in large batches has the advantage that medium specific ^{18}O exchange rates used for correction (see Ch. 2.7) can be determined for a large number of samples.

2.4 NH_4^+ assimilation and induction of denitrification at low NO_3^- concentrations

Preliminary experiments with *P. aureofaciens* working culture grown in TSB_{pd} showed that no balanced denitrification could be obtained in the presence of small, µM amounts of NO_3^-. To test whether depletion of NH_4^+ from the TSB medium during pre-treatment with *P. denitrificans* was the reason for *P. aureofaciens'* inability to induce balanced denitrification, we designed an experiment in which we compared the conversion efficiencies of *P. aurefaciens* grown in TSB_{pd} with and without 20 mM of NH_4^+ added before autoclaving. 1 ml of *P. aureofaciens* starting culture (9.3×10^8 cells ml^{-1}) was inoculated into 50 ml TSB_{pd} with and without NH_4^+ amendment. Both cultures were then incubated oxically for 3 - 5 hrs, to yield a working culture with a cell density of 5.6×10^8 cells ml^{-1}. 120 ml flasks with 2 ml solution, containing 0, 25, 50, 100, 150 and 200 nmol KNO_3 were capped and He-washed, to which each 2 ml of the working culture was added. NO and N_2O production were monitored every 1.7 hours for 24 hrs.

2.5 Effect of initial O_2 levels and cell densities of *P. aureofaciens* on complete conversion of NO_3^- to N_2O and its isotope effects

To find the best setup for a rapid and complete conversion of small amounts of NO_3^- to N_2O by oxically grown *P. aureofaciens* and to assess how well the isotopic composition of NO_3^- could be reproduced, we conducted experiments with international NO_3^- standards. Different volumes of *P. aureofaciens* start culture were inoculated into 50 ml TSB_{pd} and incubated aerobically for 3 - 5 h to yield working cultures with different cell densities, 5.6×10^8, 1.1×10^9 and 1.5×10^9 cells ml^{-1}. 0.5 ml of NO_3^- house standard, IAEA-N3, USGS32 and USGS34, each containing 100 nmol NO_3^- were added to sterile 120 ml bottles. The sample volume was augmented to 1 ml by adding 0.5 ml DI water or 0.5 ml ^{18}O-labelled water ($\delta^{18}O$=499.2‰). The latter treatment was used to determine ^{18}O exchange between NO_3^- and H_2O after isotope analysis. Bottles with 1 ml DI water (no NO_3^- addition) were used as blanks. The flasks were capped and He-washed as described After releasing the overpressure, half of the flasks received 0.2 ml pure O_2 (equivalent to 2.8 mM O_2 in liquid). The rationale of this was to test whether a small O_2 supplement would facilitate the induction of balanced denitrification with different cell densities by providing a small amount of

electron acceptor for generating energy during the induction of denitrification. Thereafter, 2 ml of working culture with different cell densities was injected to triplicate bottles, giving a total volume of 3 ml. Blank bottles (no NO_3^-) were set up with 5.6×10^8 cells ml^{-1} working culture only. NO and N_2O accumulation was monitored for 15 hours in blank bottles and bottles with house standard. All other bottles were incubated standing at room temperature. To stop *P. aurefaciens* activity after the conversion and to trap excess CO_2, 0.2 ml 10M NaOH was added after 15 hours (Casciotti et al., 2002). ^{15}N and ^{18}O of headspace N_2O was analysed by continuous-flow-IRMS within 5 days (Ch. 2.7).

2.6 Effect of acidity and KCl in sample matrix

We tested the effect of low pH and high salt concentrations, typical for soil extracts, on the ability of oxically grown *P. aureofaciens* to convert small samples of NO_3^- without prior induction of denitrification. 25 µM NO_3^- standards were prepared in triplicates in 4 ml DI water adjusted by 1M NaOH to pH 4 and in 4 ml 1, 0.5 and 0.25 M KCl solution. All solutions were prepared in 120 ml serum flasks, He-washed and inoculated with 2 ml *P. aureofaciens* working culture grown oxically in TSB_{pd} medium (cell density = 5.6×10^8 cells ml^{-1}). Sterile flasks with DI water, TSB_{pd} and KCl solution were used as blanks. NO and N_2O accumulation were monitored every 4 hrs for 36 hrs. ^{15}N and ^{18}O in N_2O was analysed within 5 days.

2.7 Incubation system and gas analyses

N-gas, CO_2 production and O_2 consumption were measured in constantly stirred (500 rpm) batch cultures using a robotized incubation system with automatic headspace analysis similar to that described by (Molstad et al., 2007), but with another gas chromatographic system (Model 7890A, Agilent, Santa Clara, CA, USA). The instrument setup and method are described in more detail in (Molstad et al., 2016) and (Zhu et al., 2013b). Gas production/consumption rates were calculated from concentration change, accounting for He-dilution and dissolution of gases in the medium by applying temperature-corrected Henry constants, assuming equilibrium between headspace and liquid.

Abundances of ^{15}N and ^{18}O in N_2O were analyzed by PreCon-GC-IRMS (Delta XP, Thermo Finnigan MAT, Bremen, Germany) directly from the headspace of the 120 ml bottles used for the conversion assay. Fractionation between headspace and liquid was considered negligible given the small volume of the liquid phase (4-6 ml). Three NO_3^- standards (IAEA-N3, USGS32 and

were included in triplicate into each batch for data correction. A N_2O house standard (4.64 ppm N_2O in He) was used for drift correction. Different amounts of DI Water enriched in ^{18}O ($\delta^{18}O$~900‰) were added to the medium and used to quantify ^{18}O exchange between NO_3^- and water.

2.7 Calculations

Isotopic abundances of ^{15}N and ^{18}O are expressed as $\delta^{15}N$ and $\delta^{18}O$ versus atmospheric N_2 and VSMOW, respectively. $\delta^{15}N$ values of NO_3^- were calibrated directly against the international standards IAEA N3, USGS 32 and USGS 34. The denitrifier method has four direct error sources for measured $\delta^{15}N$: i.) NO_3^- and N_2O blanks of the working culture, ii.) completeness of conversion, iii.) non-linearity of the raw ratios with sample size effect, causing a size-effect on measured isotope ratios in N_2O and iv.), instrument drift (Sigman, 2001). The latter was evaluated and corrected by including house standards (100 µmol KNO_3) between every 8th run. Assuming that the NO_3^- and N_2O-background (blank) is constant for every batch of medium, and the ^{15}N fractionation during the conversion is equal for internal standards and samples when processed in same amounts, the blank and the conversion error can be corrected for as long as the isotopic relationship between sample and standard values is linear. Therefore, the ^{15}N correction can be simplified by using a range of certified standards with sufficient spread in isotopic values. Correction of the $\delta^{18}O$ values has to consider in addition the fractionation of $\delta^{18}O$ during the conversion of NO_3^- to N_2O and the O-exchange between NO_3^-, NO_2^- or NO and H_2O during denitrification to N_2O (Casciotti et al., 2002). For this, two standards differing in $\delta^{18}O$ values (USGS-32: 25.7 ‰ and USGS-34: -27.9‰) were included in each batch, correcting for the combined effect of all error sources (Casciotti et al., 2002). This approach requires that equal amounts of NO_3^- are processed in standards and samples.

We applied the equation from (Stevens and Laughlin, 1994) to calculate atm% ^{15}N in N_2O from ^{15}N-enriched samples, to account for double-^{15}N substituted N_2O:

$$\mathrm{At\%}\,^{15}\mathrm{N}-\mathrm{N_2O} = 100({}^{45}R + 2 * {}^{46}R - {}^{17}R - 2 * {}^{18}R)/(2 + 2 * {}^{45}R + 2 * {}^{46}R)$$

where ^{45}R, ^{46}R, ^{17}R and ^{18}R stand for atom ratios of $^{45}N/^{44}N$, $^{46}N/^{44}N$, $^{17}O/^{16}O$ and $^{18}O/^{16}O$, respectively.

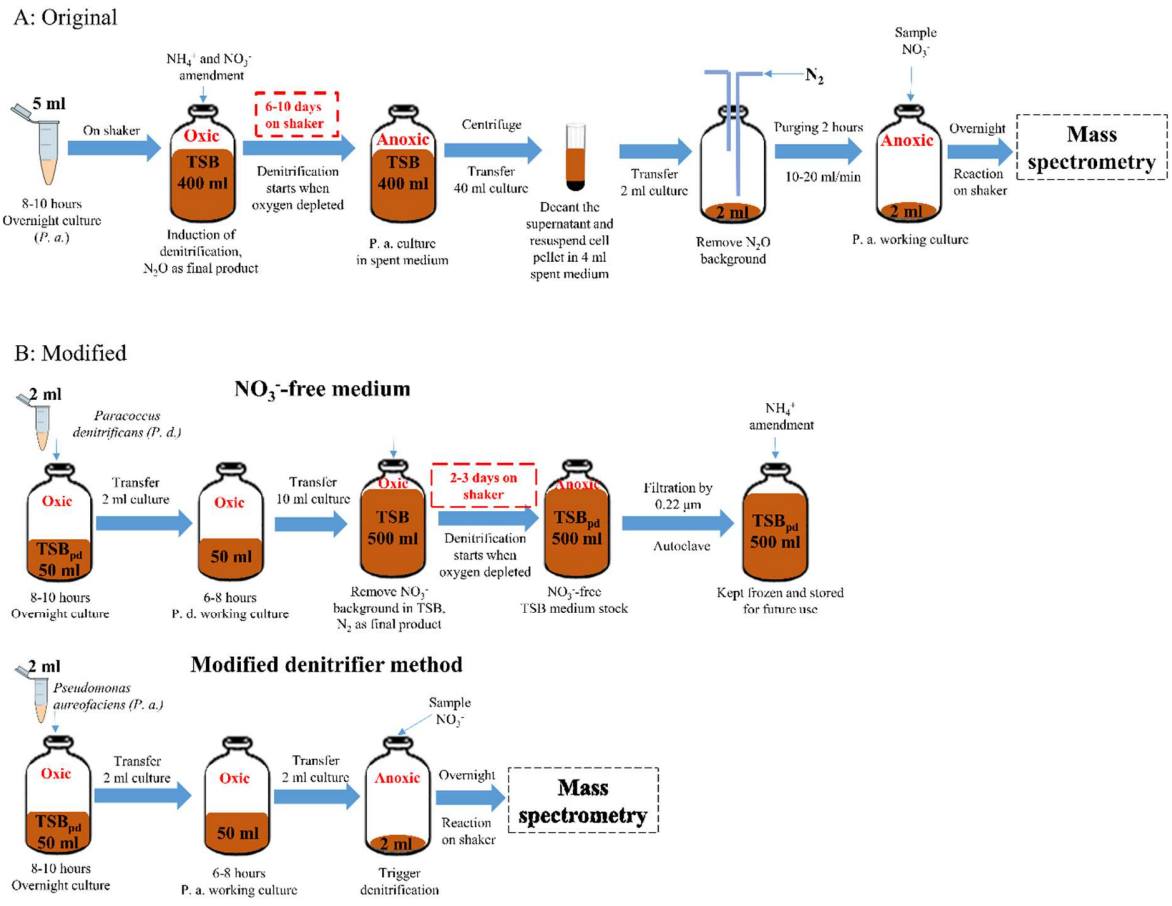

Figure 1. Work flow of the original denitrifier method (A) developed by Sigman et al. (2001) and Casciotti et al. (2002) and (B) of the modified denitrifier method (this study).

3. Results and Discussions

3.1 Induction of denitrification in *P. aureofaciens* in batch culture with different initial O_2 concentrations and ample NO_3^-

To test the effect of initial oxygen availability on the ability to induce balanced denitrification in *P. aureofaciens*, we prepared batch cultures with oxically grown cells inoculated to fresh, untreated TSB medium amended with 10 mM KNO_3. Before inoculation, headspace O_2 was adjusted to 21, 10 and 5 vol% O_2 under constant stirring (equivalent to 56.9, 27.1 and 13.5 mM O_2). O_2 depletion and NO and N_2O production were observed over 105 h (Fig. 2). The maximum O_2 consumption rate differed clearly with initial O_2 concentration and was greatest with 21 vol% (87.1 ± 2.4 µmol O_2 h^{-1} $bottle^{-1}$), intermediate with 10 vol% (45.9 ± 3.9) and smallest with 5 vol% initial O_2 (25.0 ± 1.1). With 21 vol% initial O_2, *P. aureofaciens* did not induce functional denitrification despite complete exhaustion of O_2 (Fig. 2A); 6.3% of the added N (150 µmol $bottle^{-1}$) accumulated as NO after 110 h of incubation, but no N_2O production was detected, indicating severe impairment of denitrification when switching the culture rapidly to anoxia. Induction of denitrification with 10 vol% initial O_2 converted more NO_3^- to gaseous N (52.1% of the added N accumulated as NO and 8.7% as N_2O-N, Fig. 2B), but NO accumulated to toxic concentration levels, likely preventing complete conversion of NO_3^- to N_2O. With 5 vol% initial O_2, maximum NO accumulation was < 0.1% of added NO_3^--N and 103.6 % was recovered as N_2O (Fig. 2B). The slightly higher amount of N recovered than added may be due to the unknown NO_3^- background in TSB medium, which was not removed in this experiment.

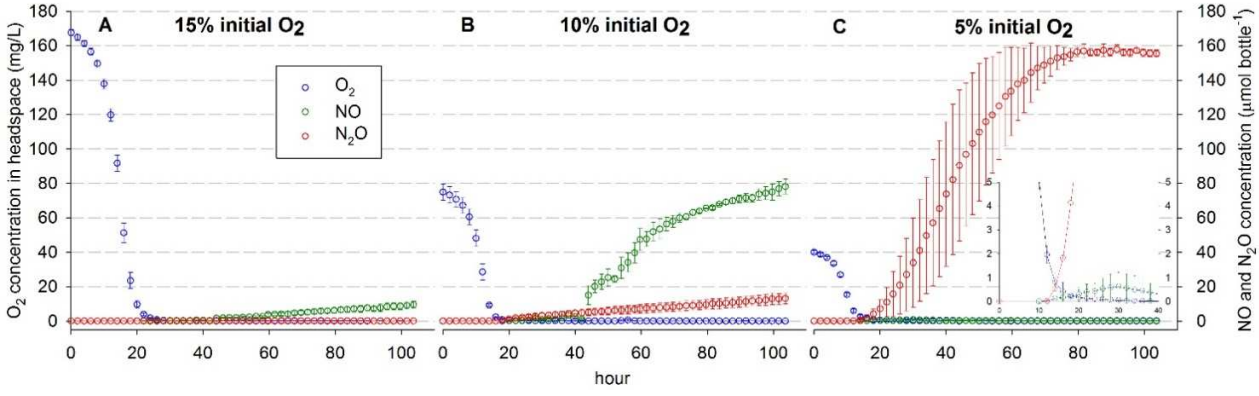

Figure 2: Kinetics of O_2 consumption and NO and N_2O production in oxically grown *P. aureofaciens* incubated with 21 (A), 10 (B) and 5 vol% (C) initial O_2 in headspace. Shown are

averages of 2 to 5 bottles; error bars are 1 SD. The insert in (C) shows the onset of NO and N_2O production with decline O_2 concentration in the headspace.

Unbalanced induction with uncontrolled accumulation of NO to micro-molar levels as found in our 10 vol% O_2 treatment (Fig. 2B) has been observed previously in batch experiments with the *nos*-deficient strain *Agrobacterium tumefaciens* and was attributed to rapid oxic-anoxic transition (Bergaust et al., 2008; Kampschreur et al., 2012). In the present experiment, the 10 vol% treatment accumulated 28.23 µM NO in the liquid, which is considered inhibitive for cellular growth (Zumft, 1997). In contrast, the 5 vol% treatment accumulated a maximum of 0.4 µM NO. Together, these results demonstrate that induction of denitrification in *P. aureofaciens* is highly sensitive to the pace at which O_2 depletes, resulting either in no induction (with 21 vol% initial O_2), unbalanced denitrification with uncontrolled NO production (10 vol% initial O_2) or well-balanced denitrification with complete conversion of NO_3^- to N_2O with little transient NO accumulation (5 vol% initial O_2). In the method of Sigman et al. (2001) and Casciotti et al. (2002), the velocity of this transition when growing the working culture is ultimately controlled by the volume ratio of culture to air in the headspace. Our results indicate that O_2 depletion rates exceeding 1.7 mM hr^{-1} (the rate observed in the 5 vol% treatment) may result in dysfunctional cultures. As shown in our 5 vol% treatment, successful induction is characterized by a simultaneous onset of NO and N_2O production when the O_2 concentration in the headspace falls below ~0.5 vol% (insert in Fig. 2C). In contrast, there was a significant delay in the onset of N_2O relative to NO accumulation in the treatments with higher initial O_2 concentrations, and NO production commenced at higher O_2 concentration. In summary, induction of balanced denitrification in *P. aureofaciens* in the presence of ample NO_3^- appears to rely on "slow" transition from oxic to anoxic respiration, which may be a challenge when preculturing *P. aureofaciens* in greater quantities with a given medium to headspace ratio. Too fast O_2 depletion during growth and induction of *P. aureofaciens* may thus be one reason for failure in producing a functional working culture *sensu* figure 1A. On the other hand, this opens for inducing denitrification in P. aureofaciens with little O_2 (as is present after He-washing) as oxic cell growth will be limited.

3.2 Removal of NO_3^- background from TSB medium

To test the feasibility of inducing anoxic respiration in an oxically grown *P. aureofaciens* working culture (Fig. 1B) with typically small amounts of sample NO_3^-, we had to strongly reduce the NO_3^- background in TSB. Freshly prepared TSB medium contains considerable amounts of NO_3^- (34.5 µM in the present case), which is similar in magnitude to the amount of expected sample NO_3^-. For this, we pre-treated the medium with *P. denitrificans* (an efficient denitrifier quantitatively converting NO_3^- to N_2) and tested NO_3^- removal with different initial O_2 concentrations and inoculum densities.

P. denitrificans efficiently removed NO_3^- from the medium under all conditions with initial headspace O_2 concentrations varying from 0 - 1.82 mM O_2 and inoculum densities from 3.7 to 9.3 $\times 10^8$ cells ml^{-1} (Tab. 1). Removal efficiencies varied between 96.8% - 98.8%, leaving 0.41-1.10 µM NO_3^- in the medium. Using 2 ml of the *P. denitrificans* treated TSB medium (henceforth called TSB_{pd}) for the conversion essay with *P. aureofaciens,* would introduce a blank value (non-sample NO_3^-) of 0.82 – 2.20 nmol which was deemed acceptable for sample sizes between 10 and 100 nmol NO_3^- (in 2 ml matrix) or 0.3 – 3 mg NO_3^- L^{-1}. For smaller concentrations, more solution could be processed.

To produce TSB_{pd} in greater batches, we tested the *P. denitrificans* pre-treatment in 500 ml Duran bottles and found that the residual NO_3^- was 0.49 µM NO_3^- (98.6% NO_3^- removal; Tab. 1), proving that the removal efficiency is reproducible independent of medium volume. This allowed us to produce TSB_{pd} in quantities that could be frozen in portions and used for growth of oxic *P. aureofaciens* working culture on demand (Fig. 1B).

To prevent interference by *P. denitrificans* remnants with *P. aureofaciens* growth, we filtered (0.22µm) the pre-treated medium prior to autoclaving. Controls without *P. aureofaciens* but added NO_3^- and C_2H_2 showed no measurable CO_2 or N_2O production over 90 h anoxic incubation (not shown), suggesting that *P. denitrificans* was successfully inactivated.

382 Table 1. NO_3^- removal from TSB medium by *P. denitrificans* using different cell densities and
383 initial O_2 concentration in closed flasks. The residual NO_3^- concentration was calculated from
384 N_2O production in the presence of acetylene. Given are single bottle values for 0% O_2 and mean
385 values ± SE for triplicate bottles with 0.5 and 2 ml O_2 in headspace

Volumes of medium and flasks	O_2 in headspace (ml)	Cell density of *P.d.* inoculum	Residual NO_3^- concentration in TSB_{pd}	NO_3^- removal efficiency compared to untreated TSB
		$\times 10^8$ cells ml^{-1}	µM	%
50 ml in 120 ml flask	0	3.7 (1 ml)	0.81	97.65%
	0	9.3 (1 ml)	0.41	98.81%
	0.5	3.7 (1 ml)	1.10 ± 0.14	96.8 ± 0.4%
	0.5	9.3 (1 ml)	0.64 ± 0.29	98.1 ± 0.8%
	2	3.7 (1 ml)	0.53 ± 0.06	98.4 ± 0.2%
	2	9.3 (1 ml)	0.79 ± 0.14	97.7 ± 0.4%
500 ml in 620 ml	110 ml air	9.3 (10 ml)	0.49 ± 0.04	98.6 ± 0.1%

386

387

388 **3.3 NH_4^+ assimilation during growth of *P. aureofaciens* and its effect on the ability to induce**
389 **denitrification at low NO_3^- concentrations**

390 A potential pitfall during the induction of denitrification in *P. aureofaciens* incubated with spent
391 medium depleted in NH_4^+, would be assimilation of a fraction of the NO_3^- present, since a
392 minimum of NH_4^+ is needed to repress the pathway for assimilatory reduction of NO_3^- (Siva Raju
393 et al., 1996; Bisen et al., 1991; Alef et al., 1985). To test this, we used *P. aureofaciens* grown
394 oxically in TSB_{pd} medium without added NH_4^+ ($TSB_{pd\text{-}NH4}$) and small amounts of NO_3^- (< 200
395 nmol). 2 ml of $TSB_{pd\text{-}NH4}$ working culture was added directly to 2 ml solution containing different
396 amounts of NO_3^- (0 - 200 nmol) in anoxic 120 ml flasks (no extra O_2 added) and N gas production
397 was followed for 26 hours at room temperature.

398

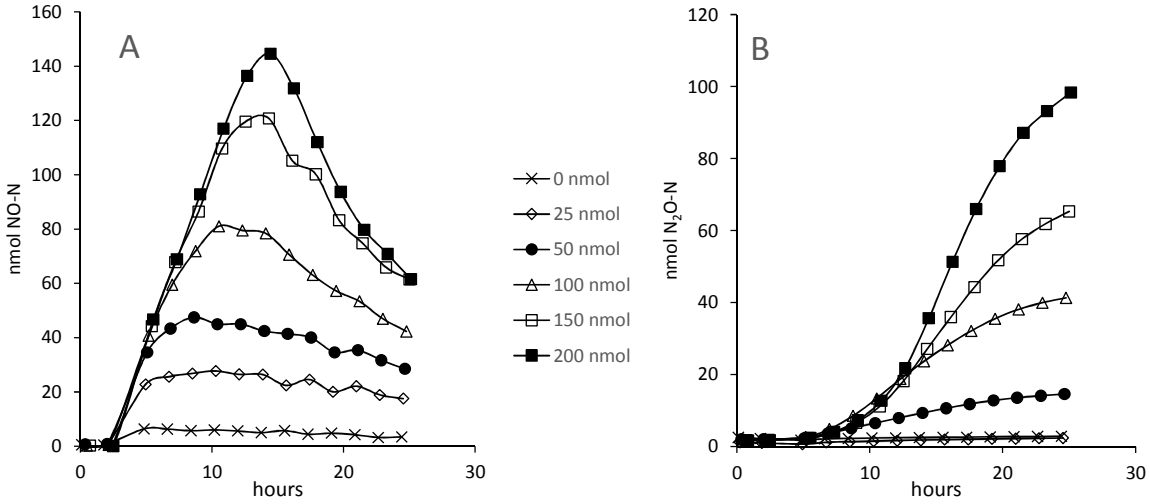

399

400 **Fig. 3** Kinetics of NO (A) and N_2O (B) production by *P. aureofaciens* in 0 – 200 nmol NO_3^-
401 amended TSB medium without added NH_4^+. Shown are results from single bottles. Note difference
402 in y-axis scales in figures A and B

403

404 Between 69 and 85% of the added NO_3- accumulated as NO (Fig. 3A), reaching its maximum
405 between 10 and 15 hours into the incubation, before starting to deplete and giving rise to N_2O
406 production (Fig. 3B). Unlike in the experiment with rapid switching from oxic to anoxic respiration
407 in the presence of mM NO_3^- (Ch. 3.1), which resulted in µM NO concentrations in the medium,
408 the nM molar concentrations observed here (up to 50 nM NO accumulated in the medium) cannot
409 have impaired denitrification. Between 87.9 and 94.2% of the added NO_3^- accumulated between
410 10 and 15 h, most of it as NO, however (Fig. 3A). The onset of N_2O accumulation was delayed
411 relatively to that of NO. At the end of the incubation, the proportion of added N recovered as
412 gaseous N (NO + N_2O) was clearly smaller than during maximum accumulation (Tab. 2),
413 suggesting that gaseous N was consumed by processes other than denitrification. This unexpected
414 loss of gaseous N amounted to between 9 and 23 nmol and increased with increasing N addition.
415 Nadeem et al. (2013) modelled NO chemistry in a closed 2-phase systems identical to that used
416 here, and showed that NO in the headspace is in equilibrium with NO_2^- in the solution. Thus, we
417 tentatively explain the missing N by NO_2^- assimilation during NH_4^+-limited growth of
418 *P. aureofaciens*. This would be consistent with the finding that the amount of N missing at the end

of the incubation increased with added N, since growth-dependent immobilization is expected to depend on the amount of electron acceptor (NO_3^-) in the system. The experiment was terminated after 26 hours, when not more than ~50% of the added N were recovered as N_2O, and we concluded that the requirement for rapid conversion to N_2O was not met with spent medium depleted in NH_4^+.

Tab. 2. Maximum recovery (%) of NO_3^- as NO and N_2O during incubation, the sum of recovered N at the end of the incubation (26 h), the share of added N recovered as N_2O and apparent N uptake, expressed as the difference of recovered NO+N_2O at maximum accumulation and at the end of incubation in TSB_{pd} medium without added NH_4^+ (Fig. 3)

Added NO_3^-	*Max. recovery as NO + N_2O-N during incubation*	*Recovery as NO + N_2O-N at end of incubation*	*Recovery as NO-N at end of experiment*	*Apparent N uptake*
nmol		%		nmol N $bottle^{-1}$
25	90.6	62.8	11.4	9.30
50	90.6	73.7	27.5	9.85
100	94.2	77.1	40.4	18.54
150	93.3	80.0	44.2	21.13
200	87.9	76.7	53.7	23.33

Based on the single bottle experiment with spent medium (Fig. 3), we performed a full experiment in triplicate with the same N additions, using TSB_{pd} medium that was amended with 20 mM NH_4^+ before establishing the working culture. In contrast to the incubations without added NH_4^+, NO_3^- was rapidly converted to N_2O, reaching recovery rates of 82 - 92% after 17 h and 90 - 100% after 36 h, independent of the amount of NO_3^- added (Fig. 4B and Tab. 3). N not recovered as N_2O by the end of the incubation was roughly matched by NO (Fig. 4A and Tab. 3). Unfortunately, due to instrument failure, no NO data are available before 17 h into the incubation (Fig. 4). The recovery of NO after >30 h of incubation suggests that *P. aureofaciens* is susceptible to incomplete NO reduction, a variable hardly ever measured when using the “denitrifier method” for converting NO_3^-. It is noteworthy that the N_2O kinetics indicated declining rates of NO reduction, which may

point at that the culture did not grow exponentially any longer. This prompted us to test the effect of culture age and initial O_2 concentration on the conversion of µM NO_3^- in NH_4^+-amended spent medium.

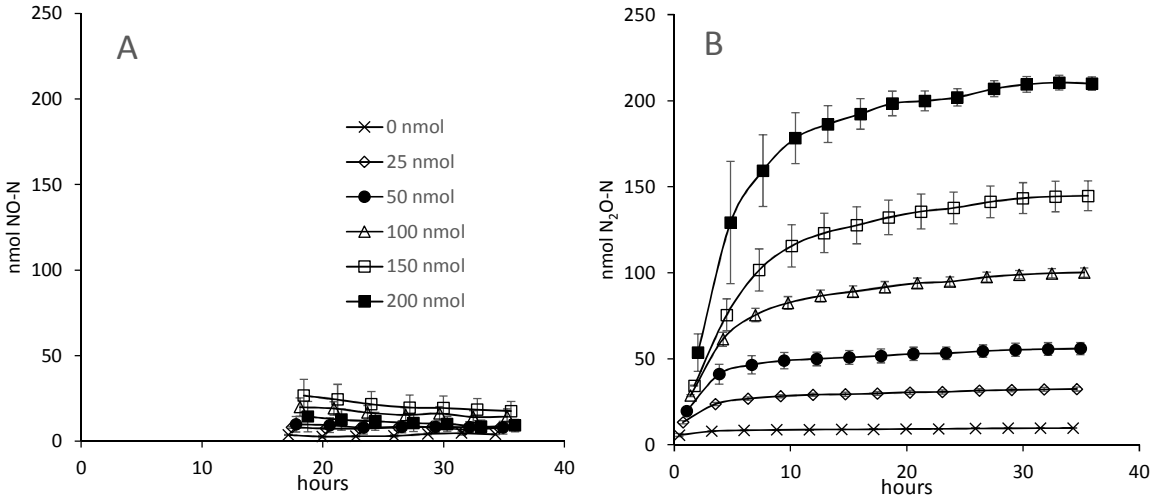

Fig. 4 Kinetics of NO (A) and N_2O (B) accumulation by *P. aureafaciens* in 0 – 200 nmol KNO_3 amended TSB_{pd} medium with added NH_4^+ (20 mM)

Table 3. Recovery of NO_3^- as N_2O after 25 hours incubation in NH_4^+ amended TSB_{pd}

added NO_3^-	*Recovery as N_2O-N after 17 hrs*	*Recovery as N_2O-N at end*	*Recovery as NO-N at end*
nmol		%	
25	83.3 (4.4)	90.9 (4.8)	15.2 (1.7)
50	85.4 (8.1)	92.3 (7.1)	7.9 (7.5)
100	82.6 (3.2)	90.4 (2.6)	10.4 (4.5)
150	82.1 (6.3)	90.0 (5.8)	9.1 (3.8)
200	94.7 (3.6)	100.1 (1.9)	2.6 (1.8)

3.4 Effect of initial O_2 concentration and cell density of the working culture

The effect of cell density in the working culture, which is equivalent to the growth stage, was tested with and without a small amount of O_2 (0.2 ml) added to the headspace after He-washing. In this experiment, we also analysed $\delta^{15}N$ and $\delta^{18}O$ of produced N_2O and determined the ^{18}O exchange. The two treatments with the lowest initial cell density (5.6×10^8 cells ml^{-1}) converted NO_3^- most rapidly, showing exponential N_2O accumulation (Fig. 5). Approximate mass balance was reached after 9-11 h. Oxygen added at the beginning of the assay had no significant effect on the conversion efficiency. Larger cell densities resulted in lower conversion efficiencies. Inspection of O_2 kinetics showed that bottles with denser inocula, taken from later growth stages of the working culture, were not able to completely deplete O_2 (not shown), which explains the incomplete conversion of NO_3^-. We therefore conclude that the working culture used for the conversion assay (Fig. 1B) should not exceed ~5×10^8 cells ml^{-1}.

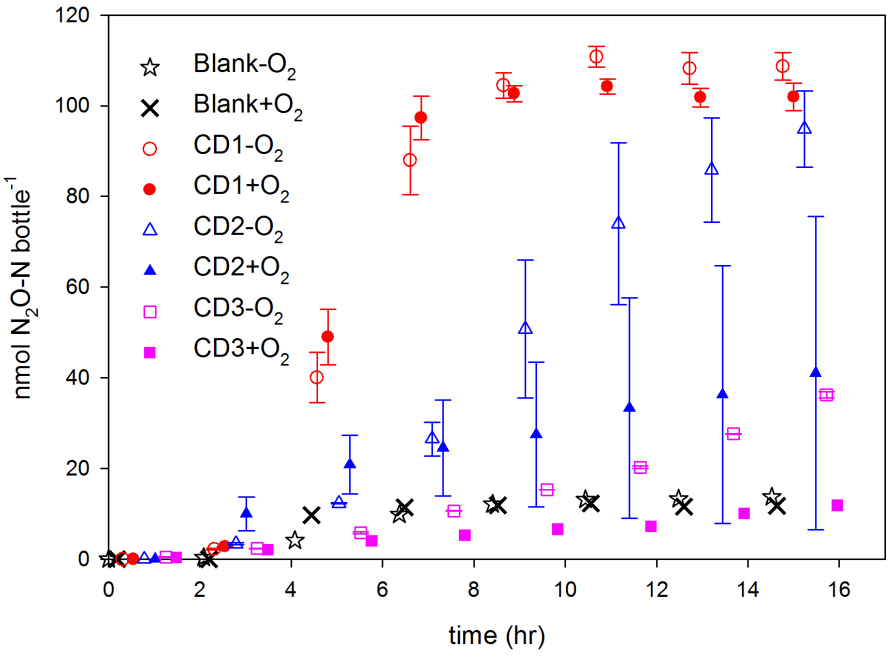

Figure 5. Kinetics of N_2O accumulation in anoxic NO_3^- conversion assays with oxically grown *P. aureofaciens*. All treatments were run in 50 ml NH_4^+ (20 mM) amended TSB_{pd} amended with 100 nmol KNO_3. Different initial O_2 additions to the He-washed headspace (-O_2: no O_2; +O_2: 0.2 ml) and cell densities (CD1, CD2, and CD3 refer to 5.6×10^8, 1.1×10^9, 1.5×10^9 cells ml^{-1}, respectively) were tested. Error bars are 1 SE.

The observed differences in conversion efficiency and recovery of N_2O (Fig. 5) did not affect the ^{15}N isotope abundance, as $\delta^{15}N$ values of NO_3^- standards were fairly well reproduced in all treatments (Tab. 4). However, SD values for the different $\delta^{15}N$ standards were smallest with the low initial cell density. This may be due to the faster growth of *P. aureofaciens* in bottles with smaller initial cell density, resulting in higher conversion rates and hence smaller isotopic fractionation (Fry et al. 1997). In contrast, $\delta^{18}O$ values varied greatly across treatments, but matched consensus values most closely in treatments with low initial cell density. Among the two treatments with low cell density (5.6×10^8 cells ml^{-1}), theoretical values were matched best and most reproducibly (i.e. with smallest SE) in treatments without added O_2.

Table 5 gives the values for ^{18}O exchange between NO_3^- and H_2O ("oxygen scrambling") during the conversion of NO_3^- to N_2O in the different treatments, calculated from treatments with heavy water. Scrambling was very large (~25 - 35%) with high initial cell densities, reflecting slower conversion of NO_3^- to N_2O via NO_2^- and NO, which increases the chance for ^{18}O being exchanged with water (Kool et al., 2011; Knöller et al., 2011). The values ^{18}O scrambling were markedly smaller and more constant in the treatment with the smallest cell density without O_2 addition (8.2 - 9.8%). Scrambling factors around 10% are in the range of those reported for *P. aureofaciens* by Casciotti et al. (2002). Our results suggest that constant scrambling factors are only valid for exponentially growing cultures of *P. aurefaciens*.

In summary, conversion of small amounts of NO_3^- to N_2O by oxically grown *P. aureofaciens*, with acceptable ^{18}O exchange, proceeded best when using moderate densities of exponentially growing cells and exposing them to sudden anoxia (no O_2 added). Under these conditions, differences between measured and consensus $\delta^{15}N$ and $\delta^{18}O$ values of NO_3^- standards (IAEA-N3, USGS-32 and USGS-34) were generally were less than 0.2‰ and 0.7‰, and standard deviations smaller than 0.3‰ and 1.0‰, respectively (Tab. 4).

Table 4. Raw and corrected $\delta^{15}N$ and $\delta^{18}O$ values for NO_3^- (international standards) measured in N_2O from *P. aurefaciens* assays with different initial O_2 levels ($-O_2$: no O_2 in headspace; $+O_2$: 0.2 ml O_2 in headspace) and cell densities. All conversion assays were run in triplicate

Standards	theoretical $\delta^{15}N$ (‰)	theoretical $\delta^{18}O$ (‰)	corrected $\delta^{15}N$ (‰)	SD	corrected $\delta^{18}O$ (‰)	SD
cell density = 5.6×10^8 cells ml^{-1}, $-O_2$						
N3-3	4.7	25.6	4.5	0.1	26.3	0.3
USGS-32	180	25.7	180.0	0.1	25.4	1.0
USGS-34	-1.8	-27.9	-1.6	0.3	-28.0	0.3
cell density = 5.6×10^8 cells ml^{-1}, $+O_2$						
N3-3	4.7	25.6	5.2	0.3	25.3	4.0
USGS-32	180	25.7	180.0	0.9	26.4	0.4
USGS-34	-1.8	-27.9	-2.2	0.3	-35.0	
cell density = 1.1×10^9 cells ml^{-1}, $-O_2$						
N3-3	4.7	25.6	4.6	0.8	30.5	1.8
USGS-32	180	25.7	180.0	1.2	19.5	3.3
USGS-34	-1.8	-27.9	-1.7	0.7	-26.6	0.2
cell density = 1.1×10^9 cells ml^{-1}, $+O_2$						
N3-3	4.7	25.6	3.3	2.1	29.3	2.0
USGS-32	180	25.7	179.9	5.5	15.6	
USGS-34	-1.8	-27.9	-0.3	0.7	-25.3	
cell density = 1.5×10^9 cells ml^{-1}, $-O_2$						
N3-3	4.7	25.6	4.4	0.6	30.0	
USGS-32	180	25.7	180.0	2.4	23.1	1.8
USGS-34	-1.8	-27.9	-1.6	0.1	-27.6	1.1
cell density = 1.5×10^9 cells ml^{-1}, $+O_2$						
N3-3	4.7	25.6	7.8	0.1	27.0	6.0
USGS-32	180	25.7	179.8	1.9	23.0	5.2
USGS-34	-1.8	-27.9	-3.6	5.0	-26.6	7.6

Table 5. ^{18}O-exchange rates (%) between NO_3^- with H_2O in *P. aureofaciens* conversion assays with 100 nmol KNO_3 and different initial O_2 levels ($-O_2$: no O_2 in headspace; $+O_2$: 0.2 ml O_2 in headspace) and initial cell densities

	IAEA-N3	USGS-32	USGS-34	avg	std
			%		
5.6×10^8 cells ml^{-1}, $-O_2$	9.0	9.8	8.2	9.0	0.8
5.6×10^8 cells ml^{-1}, $+O_2$	-0.5	21.0	9.0	9.8	10.7
1.1×10^9 cells ml^{-1}, $-O_2$	25.7	38.5	36.3	33.5	6.8
1.1×10^9 cells ml^{-1}, $+O_2$	15.1	35.4	32.9	27.8	11.1
1.5×10^9 cells ml^{-1}, $-O_2$	40.1	27.8	36.4	34.8	6.3
1.5×10^9 cells ml^{-1}, $+O_2$	19.5	33.9	19.3	24.3	8.4

3.5 Effect of acidity and salt concentration

The denitrifier method was originally developed with *P. chlororaphis* to isolate NO_3^- from seawater for isotope analysis (Sigman et al., 2001; Casciotti et al., 2002). Rock and Ellen (2007) and Mørkved et al (2007) confirmed that *P. chlororaphis* was well suited for soil extracts with a molarity of up to 1 M KCl. Another issue is the acidity present in extracts from acid soils, which could inhibit growth of *P. aureofaciens* and hence lead to incomplete conversion with high ^{18}O-scrambling. We tested both factors in an experiment converting NO_3^- house standards (100 nmol) in acidified (pH4) TSB_{pd} or with TSB_{pd} adjusted to 0, 0.25, 0.5 and 1M KCl.

Nitrate conversion to N_2O was rapid and complete within 5 - 9 h (Fig. 6). Conversion in pH 4 adjusted medium was only slightly delayed. There was no significant difference in N_2O kinetics in medium with 0.25 M and 0.5 M KCl. In contrast, the conversion in 1M KCl was significantly delayed and did not reach complete conversion before 21 h.

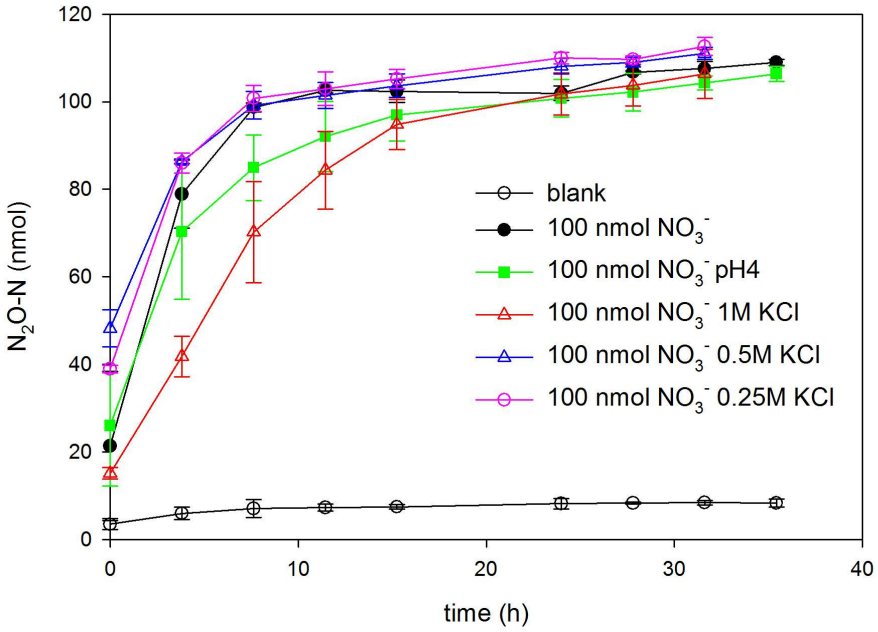

518

519 Figure 6. N_2O kinetics during conversion of 100 nmol KNO_3 in TSB_{pd} adjusted to pH4 or to
520 different salt concentrations. Error bars are 1 SE.

521

522 ^{15}N and ^{18}O signatures were not significantly affected by neither acidity nor 0.25 M KCl (Tab. 6).
523 However, with higher KCl concentrations (0.5 and 1M), $\delta^{15}N$ decreased, while $\delta^{18}O$ increased,
524 indicating incomplete conversion. This illustrates that the endpoints $\delta^{15}N$ and $\delta^{18}O$ are sensitive to
525 the growth conditions during conversion of NO_3^- to N_2O. We therefore recommend to avoid salt
526 concentrations > 0.25M, which means that KCl-extracts from soil should be diluted prior to
527 applying the method. In our assay, we used we used 2 ml sample, 2 ml working culture and 2 ml
528 additional DI water, yielding a dilution of 1:3. Greater dilutions could be used if the sample matrix
529 contains sufficient NO_3^-.

530

531

532

533

Table 6. ^{15}N and ^{18}O abundance of NO_3^- (house standard) in conversion assays adjusted to different pH values and with different molarities of KCl

House KNO_3	$\delta^{15}N$	SD	$\delta^{18}O$	SD
-	1.47	0.29	9.19	1.67
pH4	1.51	0.39	8.21	2.88
0.25M KCl	1.35	0.26	11.55	1.29
0.5M KCl	0.37	0.30	13.82	0.81
1M KCl	-1.58	1.06	19.04	3.29

3.6 Accuracy of the simplified denitrifier method applied to NO_3^- standards and natural samples

To evaluate the accuracy of our simplified denitrifier method with oxically grown *P. aurefaciens*, we applied the method to three sets of standards and natural samples provided by an international laboratory inter-comparison of N isotope techniques (Biasi et al., *in prep.*). The tested NO_3^- standards comprised one standard at natural abundance and five standards with approximate $\delta^{15}N$ values of ~0, ~10, ~30, ~1000 and ~5000. An additional NH_4NO_3 standard at natural abundance and ^{15}N-enriched NH_4^+ in addition to a ^{15}N-enriched amino acid was analysed to test for cross-contamination of NO_3^- during conversion. The environmental samples comprised natural river water (182 µM NO_3^-) and 0.5M K_2SO_4 extracts from an acid grassland soil (212 µM NO_3^-), acid forest soil (24 µM NO_3^-) and a neutral forest soil (91 µM NO_3^-). The $\delta^{15}N$ values obtained by our method overestimated "actual" values of KNO_3 standards by 1 - 2‰ at ^{15}N abundances below 30‰; by 10‰ at ~1000‰, and underestimated $\delta^{15}N$ by more than 300‰ when the standard was close to 5000‰. This suggests that our method works satisfactorily at close to ^{15}N natural abundance levels but not with NO_3^- strongly enriched in ^{15}N. ^{18}O abundances were not covered by the ring test. Denitrifier methods in general performed superior with respect to cross-contamination and our corrected $\delta^{15}N$ values for the environmental samples were close to those obtained by the original denitrifier method and other methods (micro-diffusion, chemical conversion to N_2O and N_2, EA-IRMS methods).

4. Summary

We studied the effect of oxic-anoxic transition on denitrification in oxically grown *P. aureofaciens* with respect to completeness, rapidness and ^{15}N and ^{18}O integrity of the NO_3^- conversion to N_2O. We found that oxically grown cells of *P. aureofaciens* can be used to convert small amounts of NO_3^- in various matrixes to N_2O for subsequent ^{15}N and ^{18}O analysis, if i) the background NO_3^- contained in the medium is depleted prior to growing the *P. aureofaciens* culture, ii) the medium is amended with additional NH_4^+ (to prevent immobilization of sample NO_3^- or denitrification intermediates in the conversion assay), iii) the "working culture" is kept in a stage of exponential growth, and iv) small inocula (cell densities) are used for the conversion assay. We converted absolute amounts of NO_3^- ranging from 25 to 200 nmol (in 2 ml), equivalent to NO_3^- concentrations between 50 and 400 µM. Based on our findings, we devise a novel *P. aurefaciens* method (Fig. 1B, Supplementary Material), in which denitrification is induced by He-washing of oxically grown cultures in the presence of sample NO_3^-, rather than induction with extraneous KNO_3. This abridges the time needed by a factor of ~4 relative to the original method (Fig. 1A). We tested our method successfully for in sample matrixes with low pH (pH=4) or high salinity (0.25 - 1M KCl) and applied it to natural samples (river waters, soil extracts).

Acknowledgements

JZ and LY thank the Norwegian Quota System and the China Scholarship Council (CSC), respectively, for their PhD scholarships. This work was supported by Norwegian Research Council projects 193725/S30 "N_2O emissions from N saturated subtropical forest in South China" and 209696/E10 "Forest in South China: an important sink for reactive nitrogen and a regional hotspot for N_2O?". We are grateful to Trygve Fredriksen and Dr. Shahid Nadeem for their technical assistance.

582 **Reference**

583 Addy, K., Kellogg, D.Q., Gold, A.J., Groffman, P.M., Ferendo, G., Sawyer, C., 2002. *In situ* push-
584 pull method to determine ground water denitrification in riparian zones. Journal of
585 Environmental Quality 31, 1017-1024.

586 Alef, K., Jackson, J.B., McEwan, A., Ferguson, S., 1985. The activities of two pathways of nitrate
587 reduction in *Rhodopseudomonas capsulata*. Archives of Microbiology 142, 403-408.

588 Barnes, R.T., Raymond, P.A., Casciotti, K.L., 2008. Dual isotope analyses indicate efficient
589 processing of atmospheric nitrate by forested watersheds in the northeastern US.
590 Biogeochemistry 90, 15-27.

591 Bateman, A.S., Kelly, S.D., 2007. Fertilizer nitrogen isotope signatures. Isotopes in Environmental
592 and Health Studies 43, 237-247.

593 Bergaust, L., Shapleigh, J., Frostegard, A., Bakken, L., 2008. Transcription and activities of NO_x
594 reductases in *Agrobacterium tumefaciens*: the influence of nitrate, nitrite and oxygen
595 availability. Environmental Microbiology 10, 3070-3081.

596 Bergaust, L., Bakken, L.R., Frostegard, Å., 2011. Denitrification Regulatory Phenotype, a new
597 term for the characterization of denitrifying bacteria. Biochem Soc Trans 39:207-212
598 doi:10.1042/BST0390207

599 Bergaust, L., van Spanning, R.J.M., Frostegård, Å., Bakken, L.R., 2012. Expression of nitrous
600 oxide reductase in *Paracoccus denitrificans* is regulated by oxygen and nitric oxide through
601 FnrP and NNR. Microbiology 158, 826-834.

602 Biasi, C., Jokinen, S., Prommer, J., Ambus, P., Dörsch, P., Halas, S., Granger, S., Van Nieuland,
603 K., Brüggemann, N., Voropaev, A., Zilberman, T., Jäntti, H., Trubnikova, T., Welti, N.,
604 Gebus, B., Czupyt, Z., Wanek, W., Challenges in measuring $\delta^{15}N$ in inorganic nitrogen
605 forms: results from a ring test comparing three measurement approaches show large
606 variation. *In preparation*

607 Bisen, P.S., Shanthy, S., 1991. Regulation of assimilatory nitrate reductase in the cyanobacterium
608 *Anabaena doliolum*. Current Microbiology 23, 239-244.

609 Brooks, P.D., Stark, J.M., McInteer, B.B., Preston, T., 1989. Diffusion method to prepare soil
610 extracts for automated N-15 analysis. Soil Science Society of America Journal 53, 1707-
611 1711.

612 Casciotti, K.L., Sigman, D.M., Hastings, M.G., Bohlke, J.K., Hilkert, A., 2002. Measurement of
613 the oxygen isotopic composition of nitrate in seawater and freshwater using the denitrifier
614 method. Analytical Chemistry 74, 4905-4912.

615 Christensen, S., Tiedje, J.M., 1988. Sub-parts-per-billion nitrate method: use of an N_2O-producing
616 denitrifier to convert NO_3^- or $^{15}NO_3^-$ to N_2O. Applied and Environmental Microbiology 54,
617 1409-1413.

618 Clark, I., Timlin, R., Bourbonnais, A., Jones, K., Lafleur, D., Wickens, K., 2008. Origin and fate
619 of industrial ammonium in anoxic ground water - ^{15}N evidence for anaerobic oxidation
620 (Anammox). Ground Water Monitoring and Remediation 28, 73-82.

Dhondt, K., Boeckx, P., Van Cleemput, O., Hofman, G., 2003. Quantifying nitrate retention processes in a riparian buffer zone using the natural abundance of N-15 in NO_3^-. Rapid Communications in Mass Spectrometry 17, 2597-2604.

Hassan, J., Bergaust, L., Wheat, D., Bakken, L.R., 2014. Low probability of initiating the *nir*S transcription explains the observed gas kinetics and growth of bacteria switching from aerobic respiration to denitrification. PLOS Comp Biol, doi:10.1371/journal.pcpi.1003933

Hassan, J., Bergaust, L., Qu, Z., Bakken, L.R., 2015. Transient accumulation of NO_2^- and N_2O during denitrification explained by assuming cell diversification by stochastic transcription of denitrification genes. PLOS Computational Biology, doi: 10.1371/journal.pcbi.1004621

Hastings, M.G., Sigman, D.M., Lipschultz, F., 2003. Isotopic evidence for source changes of nitrate in rain at Bermuda. Journal of Geophysical Research: Atmospheres 108, NO. D24, 4790, doi:10.1029/2003JD003789

Huber, B., Bernasconi, S.M., Luster, J., Pannatier, E.G., 2011. A new isolation procedure of nitrate from freshwater for nitrogen and oxygen isotope analysis. Rapid Communications in Mass Spectrometry 25, 3056-3062.

Kampschreur, M.J., Kleerebezem, R., Picioreanu, C., Bakken, L., Bergaust, L., de Vries, S., Jetten, M.S., van Loosdrecht, M.C., 2012. Metabolic modeling of denitrification in *Agrobacterium tumefaciens*: a tool to study inhibiting and activating compounds for the denitrification pathway. Frontiers in Microbiology 3, 370.

Knöller, K., Vogt, C., Haupt, M., Feisthauer, S., Richnow, H.H. Experimental investigation of nitrogen and oxygen isotope fractionation in nitrate and nitrite during denitrification. Biogeochemostry 103, 371-384

Kool, D.M., Wrage, N., Oenema, O., Van Kessel, C., Van Groeningen, J.W. Oxygen exchange with water alters the oxygen isotopic signature of nitrate in soil ecosystems. Soil Biology and Biochemistry 43, 1180-1185

Lachouani, P., Frank, A.H., Wanek, W., 2010. A suite of sensitive chemical methods to determine the delta N-15 of ammonium, nitrate and total dissolved N in soil extracts. Rapid Communications in Mass Spectrometry 24, 3615-3623.

Liu, D., Fang, Y., Tu, Y., Pan, Y., 2014. Chemical method for nitrogen isotopic analysis of ammonium at natural abundance. Anal Chem 86, 3787-3792.

Mariotti, A., Germon, J.C., Hubert, P., Kaiser, P., Letolle, R., Tardieux, A., Tardieux, P., 1981. Experimental determination of nitrogen kinetic isotope fractionation - some principles - illustration for the denitrifiation and nitrification processe. Plant and Soil 62, 413-430.

Mary, B., Recous, S., Robin, D., 1998. A model for calculating nitrogen fluxes in soil using ^{15}N tracing. Soil Biology and Biochemistry 30, 1963-1979.

McCready, R.G.L., Gould, W.D., Barendregt, R.W., 1983. Nitrogen isotope fractionation during the reduction of NO_3^- to NH_4^+ by *Desulfovibrio sp*. Canadian Journal of Microbiology 29, 231-234.

McIlvin, M.R., Altabet, M.A., 2005. Chemical conversion of nitrate and nitrite to nitrous oxide for nitrogen and oxygen isotopic analysis in freshwater and seawater. Analytical Chemistry 77, 5589-5595.

662 Molstad, L., Dörsch, P., Bakken, L.R., 2007. Robotized incubation system for monitoring gases
663 (O_2, NO, N_2O, N_2) in denitrifying cultures. Journal of Microbiological Methods 71, 202-211.

664 Molstad, L., Dörsch, P., Bakken, L.R., 2016. New improved robot for gas kinetics in batch
665 cultures, Research Gate, doi: 10.13140/RG.2.2.30688.07680.

666 Murphy, D.V., Recous, S., Stockdale, E.A., Fillery, I.R.P., Jensen, L.S., Hatch, D.J., Goulding,
667 K.W.T., 2003. Gross nitrogen fluxes in soil: Theory, measurement and application of N-15
668 pool dilution techniques. Advances in Agronomy, Vol 79 79, 69-118.

669 Mørkved, P.T., Dörsch, P., Henriksen, T.M., Bakken, L.R., 2006. N_2O emissions and product
670 ratios of nitrification and denitrification as affected by freezing and thawing. Soil Biology &
671 Biochemistry 38, 3411-3420.

672 Mørkved, P.T., Dörsch, P., Søvik, A.K., Bakken, L.R., 2007. Simplified preparation for the delta
673 N-15-analysis in soil NO_3^- by the denitrifier method. Soil Biology & Biochemistry 39, 1907-
674 1915.

675 Nadeem, S., Dorsch, P., Bakken, L.R., 2013. Autoxidation and acetylene-accelerated oxidation of
676 NO in a 2-phase system: Implications for the expression of denitrification in *ex situ*
677 experiments. Soil Biology & Biochemistry 57, 606-614.

678 Ostrom, N.E., Hedin, L.O., von Fischer, J.C., Robertson, G.P., 2002. Nitrogen transformations and
679 NO_3^- removal at a soil-stream interface: A stable isotope approach. Ecological Applications
680 12, 1027-1043.

681 Otero, N., Torrento, C., Soler, A., Mencio, A., Mas-Pla, J., 2009. Monitoring groundwater nitrate
682 attenuation in a regional system coupling hydrogeology with multi-isotopic methods: The
683 case of Plana de Vic (Osona, Spain). Agriculture Ecosystems & Environment 133, 103-113.

684 Perakis, S.S., Hedin, L.O., 2001. Fluxes and fates of nitrogen in soil of an unpolluted old-growth
685 temperate forest, southern Chile. Ecology 82, 2245-2260.

686 Revesz, K., Bohlke, J.K., Yoshinari, T., 1997. Determination of delta O-18 and delta N-15 in
687 nitrate. Analytical Chemistry 69, 4375-4380.

688 Robinson, D., 2001. delta N-15 as an integrator of the nitrogen cycle. Trends in Ecology &
689 Evolution 16, 153-162.

690 Rock, L., Ellen, B.H., 2007. Nitrogen-15 and oxygen-18 natural abundance of potassium chloride
691 extractable soil nitrate using the denitrifier method. Soil Science Society of America Journal
692 71, 355-361.

693 Rütting, T., Müller, C., 2007. ^{15}N tracing models with a Monte Carlo optimization procedure
694 provide new insights on gross N transformations in soils. Soil Biology and Biochemistry 39,
695 2351-2361.

696 Schauer, A., Bacterial Denitrifier Harvesting Strategy Survey. http://isolab.ess.washington.edu
697 /isolab/data-articles/bacterial-denitrifier-harvesting-strategy-survey

698 Sigman, D.M., Casciotti, K.L., Andreani, M., Barford, C., Galanter, M., Bohlke, J.K., 2001. A
699 bacterial method for the nitrogen isotopic analysis of nitrate in seawater and freshwater.
700 Analytical Chemistry 73, 4145-4153.

Silva, S.R., Kendall, C., Wilkison, D.H., Ziegler, A.C., Chang, C.C.Y., Avanzino, R.J., 2000. A new method for collection of nitrate from fresh water and the analysis of nitrogen and oxygen isotope ratios. Journal of Hydrology 228, 22-36.

Siva Raju, K., Sharma, N.D., Lodha, M.L., 1996. Inhibition of assimilatory nitrate uptake by ammonium ions in *Azorhizobium caulinodans* IRBG 46. Journal of Plant Biochemistry and Biotechnology 5, 119-121.

Stevens, R.J., Laughlin, R.J., 1994. Determining Nitrogen-15 in Nitrite or Nitrate by Producing Nitrous Oxide. Soil Science Society of America Journal 58, 1108-1116.

Søvik, A.K., Mørkved, P.T., 2008. Use of stable nitrogen isotope fractionation to estimate denitrification in small constructed wetlands treating agricultural runoff. Science of the Total Environment 392, 157-165.

Waser, N.A.D., Harrison, P.J., Nielsen, B., Calvert, S.E., Turpin, D.H., 1998. Nitrogen isotope fractionation during the uptake and assimilation of nitrate, nitrite, ammonium, and urea by a marine diatom. Limnology and Oceanography 43, 215-224.

Well, R., Augustin, J., Meyer, K., Myrold, D.D., 2003. Comparison of field and laboratory measurement of denitrification and N_2O production in the saturated zone of hydromorphic soils. Soil Biology & Biochemistry 35, 783-799.

Xue, D., De Baets, B., Botte, J., Vermeulen, J., Van Cleemput, O., Boeckx, P., 2010. Comparison of the silver nitrate and bacterial denitrification methods for the determination of nitrogen and oxygen isotope ratios of nitrate in surface water. Rapid Commun Mass Spectrom 24, 833-840.

Ye, R.W., Torosuarez, I., Tiedje, J.M., Averill, B.A., 1991. H_2O-O18 isotope exchange studies on the mechanism of reduction of nitric oxide and nitrite to nitrous oxide by denitrifying bacteria – eveidence for an electrophilic nitrosyl during reduction of nitric oxide. Journal of Biological Chemistry 266, 12848-12851.

Yu, L., Zhu, J., Mulder, J., Dörsch, P., 2016. Multi-year dual nitrate isotope signatures suggest that N-saturated subtropical forested catchments can act as robust N sinks. Global Change Biology, doi: 10.1111/gcb.13333.

Zak, D.R., Pregitzer, K.S., Holmes, W.E., Burton, A.J., Zogg, G.P., 2004. Anthropogenic N deposition and the fate of NO_3^--N15 in a northern hardwood ecosystem. Biogeochemistry 69, 143-157.

Zhu, J., Mulder, J., Bakken, L., Dörsch, P., 2013a. The importance of denitrification for N_2O emissions from an N-saturated forest in SW China: results from *in situ* N-15 labeling experiments. Biogeochemistry 116, 103-117.

Zhu, J., Mulder, J., Solheimslid, S.O., Dörsch, P., 2013b. Functional traits of denitrification in a subtropical forest catchment in China with high atmogenic N deposition. Soil Biology and Biochemistry 57, 577-586.

Zumft, W.G., 1997. Cell biology and molecular basis of denitrification. Microbiology and Molecular Biology Reviews 61, 533-616.

Supplemtary Materials

Controlled induction of denitrification in *Pseudomonas aureofaciens*: a simplified denitrifier method for dual isotope analysis in NO_3^-

Jing Zhu[1,3], Longfei Yu[1], Lars R. Bakken[1], Pål Tore Mørkved[2], Jan Mulder[1], Peter Dörsch[1]

Production of NO_3^- free TSB medium (Fig. 1B, upper panel)

Paracoccus denitrificans is inoculated into sterile medium (30 g TSB/l; 20mM NH_4Cl; 36mM KH_2PO_4, pH ~7) and grown aerobically overnight while stirring at room temperature. This results in a starting culture of *P. denitrificans* of which 2 ml are inoculated into a 120 ml flask with 50 ml TSB for growing the working culture aerobically for 8-10 h. This results in a cell number of 1.9 – 5.6 × 10^8 cells ml^{-1}. Each 10 ml of the working culture is inoculated into five 0.5 L Duran bottles filled with 0.5 L sterile TSB medium. The screw cap is closed and additionally sealed with parafilm to prevent O_2 leakage into the bottle during shaking. The culture is incubated while shaking horizontally for 2 - 3 days at room temperature, thus creating anoxic conditions and completely removing traces of NO_3^- from the TSB medium. Next, the medium is filtered aseptically (0.22 µm sterile filter) to remove *P. denitrificans* cells and amended with 0.53g NH_4Cl (20 mM NH_4^+) before being autoclaved. The *P. denitrificans* treated NO_3^--free TSB medium (TSB_{pd}) is frozen for future use.

The modified denitrifier method (Fig. 1B, lower panel)

TSB_{pd} is thawed and inoculated with *Pseudomonas aureofaciens* and incubated aerobically overnight while stirring at room temperature to create a starting culture. To create a working culture, 2 ml of the starting culture is inoculated into a 120 ml flask with 50 ml TSB_{pd} and grown aerobically for about 6-8 h while stirring at room temperature to reach a cell density of 5.6 – 9.3 × 10^8 cells ml^{-1}. Up to 4 ml of either samples or KNO_3 standards containing 20 - 100 nmol NO_3^- is added to an autoclaved empty 120 ml flask. Each flask is crimp-sealed with butyl septa and the headspace is washed with helium (5 subsequent cycles of evacuation and He-filling). Overpressure is released and 2 ml *P. aureofaciens* working culture is added. The flasks are incubated for at least 12 h to denitrify NO_3^- quantitatively to N_2O at room temperature while shaking. Prior to the analysis of $\delta^{15}N$ and $\delta^{18}O$ in N_2O directly from the headspace, 0.1 - 0.2 ml 10 M NaOH is added to the flasks to stop reaction and to trap excess CO_2 (Casciotti et al., 2002).